

RARE-EARTH SOIL HORIZON MARKERS TO DETERMINE
THE SHORT-TERM ACCRETION IN
LOUISIANA MARSHES

A Thesis

Submitted to the Graduate Faculty of the
Louisiana State University and
Agricultural and Mechanical College
in partial fulfillment of the
requirements for the degree of
Master of Science

in the

Nuclear Science Center

by

Daniel Lee Van Gent

B.S., University of California at Davis, 1980

May 1988

ACKNOWLEDGEMENTS

This study was funded in part by a grant from the Minerals Management Service (MMS), New Orleans, LA, through the Coastal Ecology Institute at LSU, Contract No.14-12-0001-30252. Additional support was provided by the Nuclear Science Center at LSU, Texas A&M University Nuclear Science Center at College Station, TX, the Nuclear Science Center at Oregon State University, and the University of California Los Alamos National Laboratory at Los Alamos, NM. Texas A&M University (John Krohn), Oregon State University (Mike Conrady and Dr. Art Johnson), and Los Alamos National Laboratory (Keith Abel and Merle Bunker) facilities were utilized to activate 80%, 10%, and 10%, respectively, of the soil samples through the Reactor Sharing Program, sponsored by the U.S. Department of Energy.

I wish to express my gratitude to Dr. R. Eugene Turner for allocating the funding which put me through the M.S. Graduate Program here at LSU and, of course, Dr. Ronald M. Knaus for procuring the funds.

Dr. Knaus has been instrumental in providing guidance and suggestions which largely directed the course of my thinking throughout this study. I have vastly enjoyed my sojourn with this unique individual. It is rare to find the qualities of an avid naturalist, physical scientist, and compassionate human being in one person. Although he technically was the teacher and I the student, I

believe our relationship transcended the usual bounds of that artificial construct of the academic world. I look forward to many more years of continuing professional interaction and personal friendship with him.

Many others contributed to the work presented in this thesis, including Dr. Donald Cahoon who provided invaluable field support and welcomed comic relief during some very difficult and even dangerous field excursions. LUMCON (Louisiana Universities Marine Consortium) provided lodging on many of the field trips as well as the very capable assistance of Wilton Delaune whose phenomenal navigational abilities and boating skills were indispensable. Many thanks to Scott Brown, Firozeh Eftekhari, Kiffin Luce, Greg King, Michael Scott, and Steve Harrell for literally thousands of hours of tireless and nearly 100% accurate data entry and organization. Richard Teague is a computer wizard without whose skills I would never have been able to bring this study to its logical conclusion. Very special thanks are due Mrs. Yvonne Thomas for her patient instruction in the art of wordprocessing, and for going to bat for me twice when red tape prevented me from receiving my monthly paycheck.

The special friendship and support of several people has been an integral part of my experience here in Louisiana. My heartfelt thanks are given to Kiffin Luce and Rodney and Lynn Blanchard for their personal friendship and many hours of thoroughly enjoyable companionship. Their kindness and concern for me will not be forgotten. Allan Showler, who was responsible for talking me into

leaving California to come to Louisiana, shall not go unpunished. However, I remain his loyal and devoted friend, and I hope that our paths soon cross again where I will delight in sharing in further mischief and misadventure with him.

Finally, I wish to express as best as I am able my feelings of devotion and honor towards my parents, Daniel L. Van Gent, Sr. and Charolette Joy Van Gent. There is no man on earth whom I respect more than my father. Although he was not "college educated," he is one of the most intelligent men I have known, and I hope that a small portion of his intellectual and athletic abilities has rubbed off on me. Throughout my life, my mother has patiently guided me in the understanding of patience, compassion, and love. Once again, I hope that a measure of those qualities has been imparted to me. Both of these wonderful individuals will continue to provide inspiration for me in the years to come.

TABLE OF CONTENTS

	<u>PAGE</u>
ACKNOWLEDGEMENTS.....	ii
TABLE OF CONTENTS.....	v
LIST OF TABLES.....	viii
LIST OF FIGURES.....	ix
ABSTRACT.....	xii
CHAPTER 1	
INTRODUCTION.....	15
CHAPTER 2	
SURFACE DISTURBANCE PHENOMENA.....	15
Bioturbation.....	15
Class I disturbance.....	22
Class II disturbance.....	23
CHAPTER 3	
GEOGRAPICAL LOCATIONS.....	29
Study regions.....	29
MMS study sites.....	29
Geographical locations and experimental design of MMS sites.....	32
Additional sites.....	35
Cameron Parish sites.....	35
St. John The Baptist Parish sites.....	42
Lafourche Parish sites.....	45
Terrebonne Parish sites.....	52
Experimental design.....	52

	<u>PAGE</u>
CHAPTER 4	
MATERIALS AND METHODS.....	55
Choice of marker.....	55
Preparation of marker.....	57
Application of marker.....	58
Sampling of marker.....	59
Sample preparation and neutron irradiation.....	62
Standard preparation.....	74
Data reduction.....	76
Core data analysis: Scheme I (Modal analysis)...	77
Core data analysis: Scheme II (Dynamic analysis).	84
CHAPTER 5	
RESULTS.....	95
Initial data processing.....	95
Modal analysis.....	101
Lafourche Parish study site.....	110
Waterway analysis.....	113
Terrebonne study site.....	122
Waterway analysis.....	128
Cameron study site.....	136
Other study sites.....	142
Dynamic analysis.....	142
Comparison of INAA and clay marker methodology..	154
CHAPTER 6	
DISCUSSION.....	158

	<u>PAGE</u>
Lafourche at Leeville.....	159
Terrebonne.....	159
Cameron.....	160
Other study areas.....	160
Statistical resolving power.....	161
Modal analysis vs. dynamic analysis.....	163
INAA vs. Clay methodology.....	165
Accretion as a transport process.....	168
Process signatures.....	178
 CHAPTER 7	
CONCLUSION.....	179
REFERENCES CITED.....	182
APPENDICES.....	189
A- MARKER DISTRIBUTION GRAPHS.....	190
B- COST ANALYSIS.....	227

LIST OF TABLES

<u>Table</u>	<u>PAGE</u>
5.1. Example of Lotus 1-2-3 Spreadsheet program used for spectral data reduction.....	96
5.2. Tabulated results of accretion depth as determined by modal analysis for all MMS sites and the additional sites.....	104
5.3. Accretion rate summary.....	109
5.4. Dynamic analysis parameters.....	146
5.5. Comparison of accretion determined by INAA vs. feldspar clay.....	152
6.1. Predicted statistical resolution of the INAA technique.....	162

LIST OF FIGURES

<u>Figure</u>	<u>PAGE</u>
1.1	Mississippi River deltaic plain..... 4
1.2	Land loss in Mississippi River deltaic plain..... 6
2.1	Schematic of the single mixing-layer model..... 27
3.1	Study areas..... 31
3.2	Boardwalk design utilized at Lafourche study area..... 34
3.3	Rockefeller Wildlife Refuge study area..... 37
3.4	MMS control study site at Cameron study area..... 39
3.5	MMS canal study site at Cameron study area..... 41
3.6	Lac Des Allemands study area..... 44
3.7	Lafourche at Fourchon study area..... 47
3.8	MMS Lafourche at Leeville study area..... 49
3.9	Cocodrie study area..... 51
3.10	MMS Terrebonne study area..... 54
4.1	Cryogenic coring device schematic..... 61
4.2	Sequence of procedures leading to detection of the rare earth horizon markers in the vertical soil profile..... 64
4.3	Continuation of Figure 4.2..... 66
4.4	The pneumatic transfer system at Oregon State University..... 69
4.5	The pneumatic tranfer system at Los Alamos Laboratories..... 71
4.6	The neutron activation scheme for the rare earth tracer, dysprosium..... 73
4.7	Idealized classification scheme applied to observed marker distributions..... 79

4.8	Observed marker distributions which demonstrate the utility of the idealized classification scheme.....	81
4.9	A computer model generated series of theoretical marker distributions.....	88-93
4.10	A computer model generated series of theoretical marker distributions.....	88-93
5.1	Typical activated Dy gamma ray spectral data.....	100
5.2	Marker distribution graph resulting from spectral data reduction.....	103
5.3	Marker distributions found at the Lafourche at Leeville natural waterway distance transect.....	112
5.4	Accretion depth summary at the Lafourche at Leeville natural and canal waterway distance transects.....	115
5.5	Accretion depth summary for 50 m plots at the Lafourche at Leeville study sites.....	118
5.6	Accretion depth summary for 50 m plots at the Lafourche at Leeville study sites.....	121
5.7	Marker distributions found at the Terrebonne natural distance transect.....	124
5.8	Marker distributions found at the Terrebonne pipeline canal distance transect.....	127
5.9	Six-month accretion depth summary at the Terrebonne natural and canal distance transects.....	130
5.10	One-year accretion depth summary at the Terrebonne natural and canal distance transects.....	132
5.11	Six-month and one-year accretion depth summary at eight different 50 m locations at the Terrebonne study area.....	135
5.12	Marker distributions found at Cameron natural waterway sites.....	138
5.13	Six-month accretion summary at six different 50 m locations at the Cameron study area.....	141
5.14	Characteristic Lac Des Allemands marker distribution.....	144

	<u>PAGE</u>
5.15 Observed marker distribution and matched computer model generated marker distribution.....	148
5.16 Scattergram of weighted depth vs. modal depth.....	151
5.17 Scattergrams of clay and rare earth paired individual accretion values.....	156
6.1 Demonstration of the possible barrier effect caused by the clay horizon.....	167
6.2 Marker distributions which demonstrate the "process sig- nature" concept.....	173
6.3 Marker distributions which demonstrate the "process sig- nature" concept.....	175
6.4 Marker distributions which demonstrate the "process sig- nature" concept.....	177

ABSTRACT

An accurate assessment of wetland surface accretion processes requires unique and innovative methodologies. Visible soil horizon markers such as glitter, ground glass, and feldspar clay have traditionally been utilized for determination of short-term (6 mo.- 2 yr.) accretion rates while radioisotopes such as ^{137}Cs and ^{210}Pb have been relied upon for determination of long-term (10 yr.- 100 yr.) accretion rates. Stable tracers (rare earth elements) were utilized as an alternate method for the assessment of accretion processes over a period of 6 months to 2 years in the investigation reported here. In contrast to visible horizon marker methodology, the stable tracer methodology is suitable for an entirely quantitative treatment, whereas the visible marker technique is at best semiquantitative. Results from this study confirm that the first few centimeters of the marsh surface is dynamic (in nature) and a gaussian diffusion coefficient can be estimated which adequately accounts for physical and biological mixing. Application of a single mixing-layer model derived from the general diffusion-advection equation to the observed data point to the complex nature of the surface accretion process. Interpretation of results without due consideration of the interaction between surface mixing and sedimentation components are likely to yield biased estimates of short-term and, possibly, long-term accretion rates. Site-specific influences (such as levees and impoundments) may affect the observed stable tracer distribution

in the vertical soil profile. Such distributions appear to be characteristic of local regions and could possibly be utilized as a site index predictor of marshland viability.

CHAPTER 1
INTRODUCTION

The Louisiana coastal zone is of enormous importance as a state, national, and international, renewable resource. It is estimated that Louisiana coastal wetlands comprise 41% of the U.S. total of wetlands (Craig et al., 1979). Currently, there are 50,000 square km of marshland in the southern Louisiana coastal zone. This land is a resource which has been estimated to be worth between \$20,000 and \$30,000 per hectare based on the marsh's ability to filter pollutants from water, fix carbon, and produce fish and fur (Turner, 1987). This figure does not represent the value of the land to indigenous human populations in terms of land and homes. Nearly 90% of commercially harvested fish spend an obligate part of their life cycle in the marsh and the estuarine and Gulf waters interact in such a way that a delicate balance of salinity conducive to the formation and continuance of 470,000 hectare of oyster reefs is maintained. The Gulf of Mexico fishing industry is worth \$500,000,000 annually. The harvest of Gulf shrimp amounts to \$400,000,000 comprising a total of nearly \$1,000,000,000 representing 28% of the national fisheries harvest.

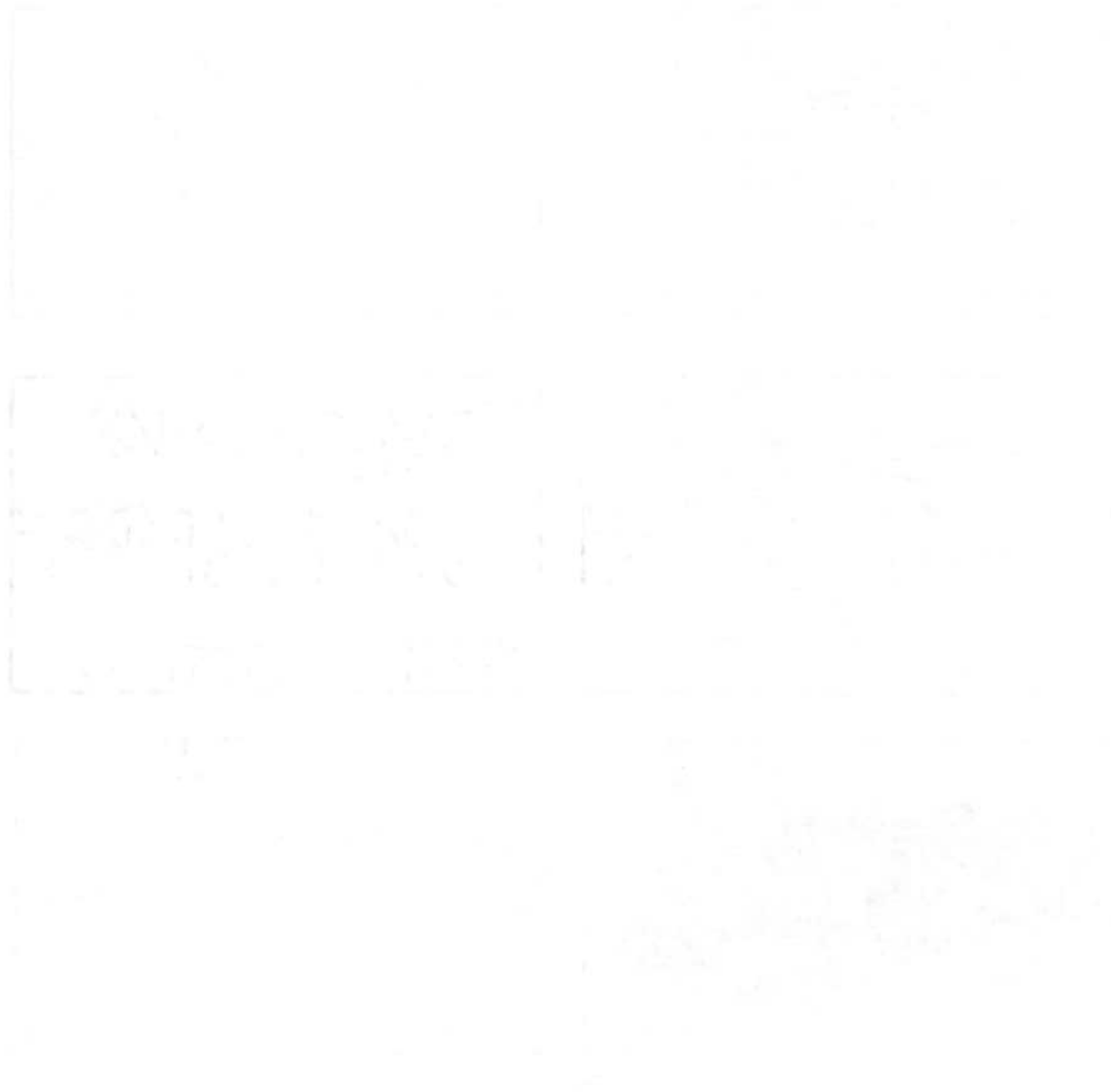
For the last few decades, it has become apparent that the wetlands in southern Louisiana are rapidly deteriorating. Many areas have become open water, and the coastline is shifting inland.

Land loss problem

For many thousands of years, the Mississippi River has forged and followed its own course. Major course changes have occurred approximately every 1,000 years, causing some areas of land to build while others deteriorated (Coleman and Gagliano, 1964). After each course change, the process of new delta lobe formation occurs. Net coastal land gain in the Mississippi Deltaic Plain has historically been between four and five square km per year. During the building phase, the River forms a delta out into shallow shelf areas until its course becomes long, tortuous, and hydrologically inefficient. The increased inefficiency over time stems from the net decrease of elevational change and greater resistance to outflow of the discharge into the Gulf. Another major course change is then likely to occur so that the River follows a steeper and more efficient route to the Gulf. Consequently, there is a switching or changing of the location of the delta. This process has led to a series of delta lobes in various states of abandonment (Figure 1.1). The most recently abandoned deltaic lobe, being no longer fed by riverine sediment supply, slowly breaks up due to unopposed erosional forces and compaction and subsidence of soft sediments.

This natural system has been drastically altered during the last 100 years by man's successful attempts to control the course of the Mississippi River. The result of this containment appears to be the equivalent of a catastrophic natural event in terms of a geological time scale. The consequence of flood control efforts is an accelerated loss of southern Louisiana coastal wetlands, estimated to

Figure 1.1. Major delta lobes that have constructed the Holocene Mississippi River deltaic plain. From Turner, 1987.



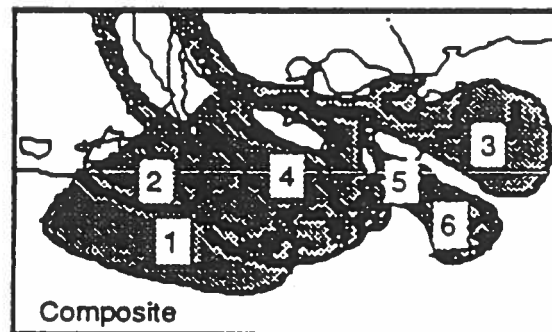
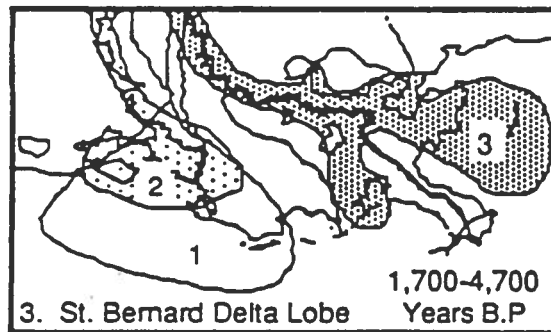
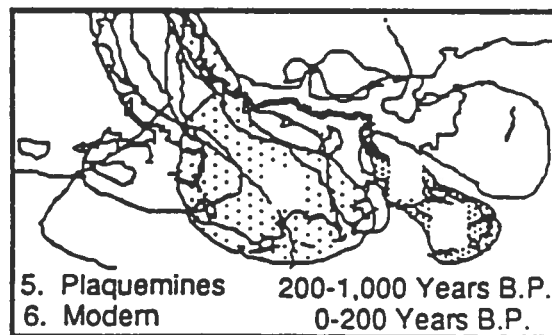
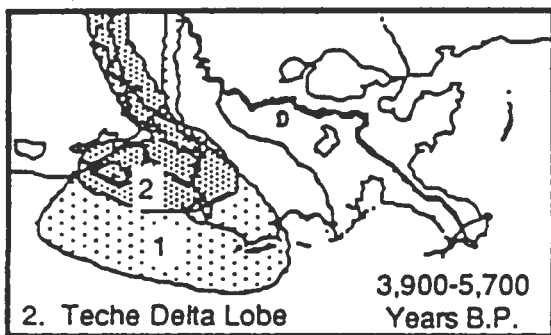
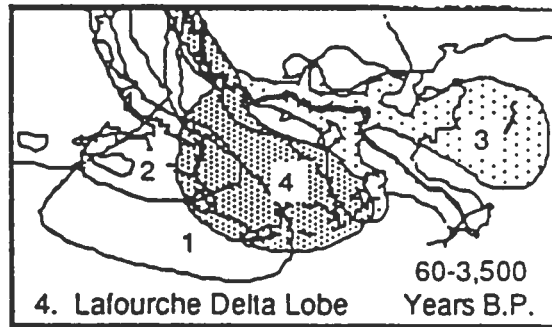
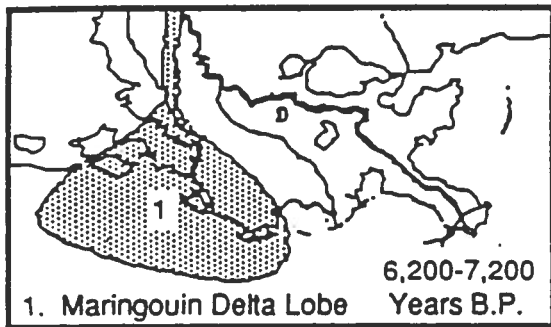
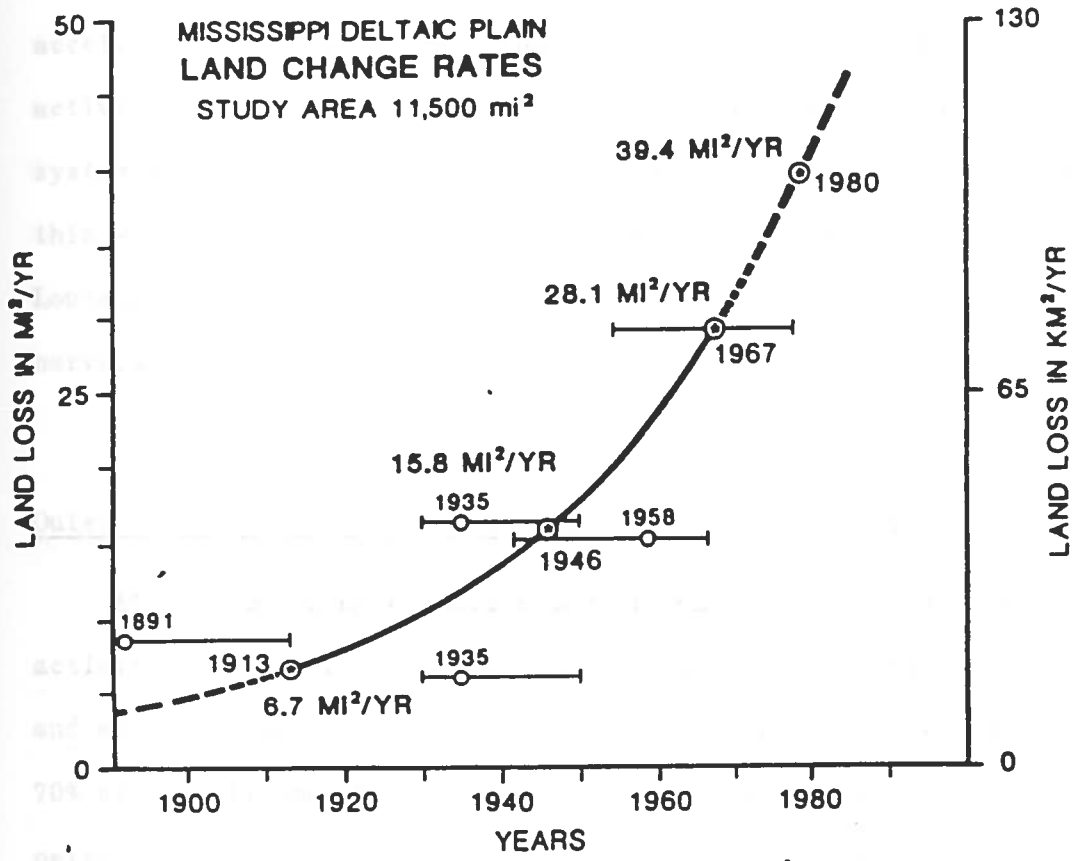


Figure 1.2. Acceleration of land loss rates in the Mississippi River deltaic plain. From Turner, 1985.



be occurring at an annual rate of 100 square km or 40 square miles (Gagliano et al., 1981). Figure 1.2 demonstrates graphically the magnitude of the loss that is occurring in the Mississippi River Deltaic Plain. The figure also shows that the rate of land loss is accelerating. It is evident that unless emergency mitigational activities are enacted, the major portion of the Louisiana wetlands system will be lost, most likely beyond retrieval. Needless to say, this will be devastating to the economy and well-being of not only Louisiana, but also the Gulf states which share in the rich fisheries harvest.

Outer Continental Shelf Oil and Gas Development Activities

At the beginning of this study, it was hypothesized that activities connected with offshore drilling and petroleum transport and egress through the marsh greatly aggravated landloss. More than 70% of the oil and 90% of the gas resulting from U.S. coastal petroleum mining continue to come from offshore Louisiana, move through it, and enter the industrial processing plants supplying the entire country (Turner et al. 1986). However, a multidisciplinary study which includes the work reported in this thesis, *Causes of Wetland Loss in the Coastal Central Gulf of Mexico* (Turner et al. 1987), yielded mixed results. For the most part, the scientific working group of the referenced study was unable to demonstrate statistically significant effects caused by pipeline and navigational canals directly connected with the Outer Continental Shelf developmental activities. It appears that the major causal mechanism

for net land loss is the discontinuance of sediment supply related to control of the Mississippi River and perhaps to the decrease of Riverbed load since the 1950's (Kesel, 1987). Therefore, it appears that the question of the impact of man-made canals and pipelines on the marsh is moot. Restorative efforts would probably best be spent on immediate resumption of sediment supply to the sediment-poor areas of southern Louisiana marshes. This thesis was done to develop a novel technique to assess the supposed impact of Outer Continental Shelf Oil and Gas Development activities on the sediment supply of Louisiana coastal wetlands.

Criteria for marsh restoration efforts

Currently, very little is known about site specific assessment which would allow one to gauge the status of marsh under study for evidence of adverse anthropogenic impact. It seems likely that there are three general categories that are applicable to the classification of the majority of marsh types along Louisiana's coastline:

1. Areas that are to some degree adaptive to erosional-subsidence processes.
2. Sensitive areas that are marginally adaptive to erosional-subsidence processes. Such areas would probably be detrimentally affected by minor changes in coastal and marshland exploitation.
3. Areas that, because of either natural or anthropogenic impacts, are beyond the help of current technologies or economic priorities.

It appears that there are a number of complex local processes which ultimately influence the status of a site as categorized above. The most important of these processes are sedimentation, accretion, aggradation, erosion, subsidence, submergence, accumulation, and deposition.

These processes are interconnected and related in ways that make their respective effects difficult to partition and delineate from one another. The terms which are most relevant to the work developed in this thesis are defined below for the sake of clarity and useful reference. Often, many of these terms are used interchangeably and without distinction by those working in this field, which results in ambiguities for the uninitiated or casual reader. It is especially important that a distinction be made between sedimentation and accretion for the clarity and understanding of the concepts developed in this thesis.

Sedimentation is defined here as the matter, both allochthonous (originating from an outside source) and *in situ*, both inorganic and organic, which settles onto the surface of the marsh soil profile. This particular matter may or may not be eventually incorporated into the vertical soil profile. The medium for its transport is the estuarine or freshwater system (Turner, 1987).

Accretion is defined here as the net positive building process which occurs at the marsh soil-water interface regardless of the incoming sediment supply (Turner, 1987). This does not imply that sediment supply is not a component of the upward building process, but it does imply that the biological component of the marsh system, both

plant and animal, contributes significantly to the upward building process as defined here. Implicit in this definition is the likelihood that the accreting surface of the marsh is composed of a structural matrix which is different from that of the individual sedimentary components settling onto the marsh surface. Possibly, a helpful analogy is that of the difference between the structural nature of water and ice. Both are composed of the same substance, but the intrinsic molecular structuring of each is completely dissimilar which results in striking differences in macroscopic properties and appearance. Likewise, the accreting surface is composed of sediment components, but the structural matrix resulting from the mixture and biological reworking of those sediment components is quite different from that of the individual sediment components if considered separately.

The attempts to build models of marsh accretion have usually concentrated on mature marshes and assume that the marsh is in equilibrium with its tidal inundation regime. Letzsh and Frey (1980) noted that rates of accretion decrease with increased marsh maturity and stability. However, these approaches are of little value when applied to the Louisiana wetland system since the majority of the system is not at equilibrium, but is rapidly deteriorating. In addition, few studies of marsh accretion distinguish between contributions of organic and inorganic sediment. Of these, Harrison and Bloom (1977) identify their highest organic matter contents in those marsh soils where total sedimentation rates are lowest, and much lower organic contents are found in areas with higher total

sedimentation. The relation between organic and inorganic sedimentation, and its interplay with accretion processes is quite complex.

Erosion is defined here as the process by which the particulate matter and solutes is carried away from a given site by physical forces such as wave action and water flux across the marsh surface.

Subsidence is defined here as the downward movement of the marsh surface due to compaction of sediment and settling of deltaic plates, and is irrespective of sea level changes due to tidal surges or eustatic sea level rise. Subsidence occurs at a more or less constant rate over time, and is affected by sedimentation and accretion processes. The greater the load of accreted material, the greater the subsidence (because of compaction) at a given site. However, sedimentation and accretion amounts are not used to calculate subsidence rates. Subsidence refers only to downward movement of marshland.

Submergence as used here is as defined by Delaune and Patrick (1978). This is the downward movement of marshland as determined by tide gauges in a given area. Submergence is directly influenced by subsidence and eustatic sea level changes. Thus, this empirical observation is directly observable from tide gauges. It is noteworthy that accretion does not influence tidal gauge altitude, and therefore, accretion is not measurable using empirical observations gathered from tide gauges.

The above defined terms are the major factors which influence the status of the particular wetland system under consideration. The

terms accumulation and deposition will not be used in this thesis because of the ambiguity and misapplication associated with usage over the years. The work developed in the following chapters was applied to the measurement and quantification of the accretion process.

Methods available for accretion measurement

Currently, there are a number of methods to estimate accretion rates. One of the most common is the visible marker technique. This technique employs a material that is easily identified and delineated in marsh soil. A number of materials has been used. Brick dust has been successfully used as an artificial horizon marker in previous sedimentation studies (Stearns and MacCreary, 1957; Richard, 1978). Ground glass, glitter, and powdered metals have also been used (Baumann, 1980). More recently, white feldspar clay has been the marker of choice because of its high visibility in contrast with marsh soil. Other desirable characteristics are similar density as compared to marsh soil (not subject to sinkage in highly inorganic salt marsh soils), ease of preparation, uniform particle size, and low cost. (Baumann, 1980; Cahoon, 1986). Two disadvantages of the white feldspar marker are the inapplicability to freshwater systems because of low density soil and high water velocities in freshwater marsh systems (Baumann, 1980). Another possible disadvantage of this marker is the fact that it is very unlikely to behave in a manner analogous to that of the new-forming soil, and therefore, it may bias the accretion or sedimentation estimates. The visible marker is usually applicable only to short-term studies because of the small plot size,

and the difficulty of locating the plot site long after it is established.

Another type of horizon is the "fortuitous" marker. Often, a catastrophic event such as a forest fire (Davis, 1964), meteor impact (Glass, 1969), or nuclear incident or accident such as weapons testing (Delaune and Patrick, 1978) provides a layer of material in the soil profile such as charcoal, microscopic glass shards, or radionuclides, respectively. If the time of the event is known, an estimation of accretion rate can be determined by dividing the dimension of the layer of sediment accreted above the horizon by the time which has elapsed since the event. The markers which are the result of natural processes of a noncatastrophic nature are more common. Examples of this type are pollen horizons (Davis, 1964), ^{210}Pb , and ^{14}C .

The most commonly used method for determination of 20-30 years time averaged accretion rates is that developed by Delaune and Patrick (1978). This entails the location and measurement of the fall-out radioactive ^{137}Cs deposited in the soil profile during the years of prolific atmospheric testing of nuclear weapons. Advantages of this method are the widespread occurrence of the radionuclide and the ability to measure long-term accretion rates (20 to 30 yr).

A disadvantage of ^{137}Cs method is that the method is applicable only for assessment of long-term accretion rates, which may have little significance in terms of surface accretion processes. Another disadvantage is the relatively short 30 year half-life of ^{137}Cs . In a few decades, it probably will not be detectible.

Stable tracer

The thrust of this thesis is the use of stable, activable tracers in the establishment of an artificial soil horizon. Advantages of this technique are that the marker can be applied to large areas (100 of square meters), there is no introduction of radioactivity into the environment (Knaus, 1976), the short-term and long-term accretion rates can be measured, and the material transport of particulate matter within the soil profile can be followed both vertically and, possibly, laterally. Knaus and Van Gent (1987) have demonstrated the feasibility of using the rare earth elements dysprosium (Dy) and samarium (Sm) for determination of accretion rates over 6-month and 1-year periods. They were able to demonstrate that short-term accretion rates can be measured in freshwater systems (Knaus, 1987). Apparently, this is the first successful attempt recorded to date.

Disadvantages of the stable tracer technique are that the method of analysis is relatively expensive (Appendix B), the researcher is unable to locate the tracer *in situ* (Knaus, 1987), the tracer can reach saturation levels in the soil matrix, and it is possible that low pH and high salinity levels may influence the intrinsic mobility and solubility of the tracer *in situ*.

Evidence indicates that the tracer is generally applicable to all situations found in southern Louisiana wetland systems. The body of this thesis supports the utility of this method.

CHAPTER 2

SURFACE DISTURBANCE PHENOMENA

Stirring and mixing of soil by biological organisms is of concern and deserves consideration when an accurate assessment of short-term accretion rates is attempted. It is quite possible that bioturbation may affect the accuracy with which the exact position of the marker in the soil profile can be determined.

Bioturbation

Bioturbation is the biogenic vertical or horizontal disturbance of any medium, especially soil. This phenomenon is of concern especially when an artificial soil horizon is relied upon for accurate assessment of short-term and perhaps long-term accretion rates. Relatively little is known about the nature of and extent to which bioturbation affects the surface and shallow subsurface sediments of saline, brackish, and freshwater marshes.

It is intuitively obvious that macrofauna, such as fishes, snakes, alligators, birds, and mammals, are capable of stirring up surface and subsurface sediments. However, it is not at all clear how somewhat smaller more numerous, and less mobile macrofauna such as crustaceans, molluscs, insects, and certain polychaetes affect the wetland soil profile. Likewise, the meiofauna indigenous to Louisiana marshes and swamps such as nematodes, smaller polychaetes, oligochaetes and copepods are present in large population densities,

ranging from 5,000 to 50,000 organisms per cm^2 (Fleeger, 1985). Since the literature is sparse concerning wetland bioturbation, it is necessary to examine studies pertaining to biogenic surface disturbance in marine and freshwater benthic systems.

Charles Darwin (1881) was possibly the first scientist to realize that the burrowing and feeding behavior of soil organisms significantly affects geological processes such as sedimentation and layering. Darwin noted that earthworms reworked and "stirred" the vertical soil profile. Dapples (1942) observed that marine sediment in areas with large benthic animal populations was ingested many times before it is buried beneath the range of the organisms. He also noted that this reworking reduced sediment grain size and consequently increased the possibility of dissolution or mechanical removal of sediment by water currents. Of greater relevance to artificial soil horizon methodologies, he noted that bedding had probably been destroyed by burrowing organisms if lamination was absent in sediments. If bedding was observed under conditions where burrowing organisms were numerous, the rate of sedimentation exceeded the rate at which organisms worked the sediments. Moore and Scuton (1957), from a study of sediment structures in 2000 cores taken off the Mississippi Delta and the central Texas coast, found mottled and irregular sediment lamination, presumably a result of benthic organisms and possibly the filling of burrows by material different from that of the proximal sediment. Subsequent tank experiments tended to verify this hypothesis, and a generalized sequence describing the effects on sediment structures by increased degrees of

mixing was formed. The researchers concluded that regularly layered sediment would be transformed into irregularly layered sediment, distinctly mottled sediment, indistinctly mottled sediment, and finally, homogenous sediment as the duration and intensity of biological activity increased. Davis (1967) noted that two horizons of charcoal which were the result of severe fires around four lakes in Maine were definitely mixed, and were actually found deeper in the sediment profiles with considerable mixing. The effects of bioturbation on pollen horizons found in the same lakes was much less noticeable presumably because the pollen phases into the lake sediment continuously, whereas charcoal from a fire is essentially an instantaneous input event or "pulse." Glass (1969) determined that the observed distributions of microtektites, which are small glassy objects between 20 μm and 1 mm resulting from meteor impacts, found off the Ivory Coast within the dispersal zone were related in a general way to the amount of burrowing evident in the cores. Cullen (1973), characterized the surface tracks of hermit crabs (Eupagurus) as "lebensspuren" and observed that carefully protected lebensspuren gradually disappeared when the aquarium tanks containing them were left undisturbed. Under carefully controlled conditions, it was determined that the erasure of lebensspuren was caused by meiofaunal activity. This was indicative of extensive bioturbation on a microscopic scale and demonstrated that very tiny organisms play a significant role in disturbing surface sediments.

The same type of mixing phenomenon has been observed by those working with radionuclides in sediment profiles. Eddington and

Robbins (1976) noted that in many cases, the ^{210}Pb and ^{137}Cs distributions in cores taken from the bathos of Lake Michigan showed vertical mixing which they hypothesized was due to bioturbation and microturbulence. This phenomenon had the effect of distributing the radionuclides deeper into the vertical sediment profile than would be expected in undisturbed sediments. Robbins et al. (1977) concluded that regular-homogenous biogenic mixing of nuclides within lake bottom sediments in the Great Lakes could be represented as a diffusional process model and that an eddy diffusion coefficient adequately accounted for observed distributions of ^{210}Pb and ^{137}Cs in Lake Huron. They also determined that in comparison with bioturbation, molecular diffusion is of minor importance in the post-depositional mobility of ^{210}Pb and ^{137}Cs . Robbins (1982) concluded that bioturbation is an important process influencing the observed radioactivity and heavy metal profiles of recent sediments of the North American Great Lakes. He produced a quantitative steady-state mixing model which accounted for the observed distributions.

A review of the literature available describing bioturbation in wetland systems yields few studies, and those which are available deal with bioturbation qualitatively. Basan and Frey (1977) noted that among studies of salt marshes, three areas of investigation have been neglected: (1) substantive classification of marsh habitats, (2) documentation of characteristic salt marsh traces ("fossil" burrows, lebensspuren, etc.), and (3) discrimination between marsh ichnocoenoses (biological process producing a characteristic pattern of fossil traces). The investigators studied salt marshes near Sapelo

Island, Georgia. Using a series of transects, they developed a habitat classification which included creek banks, low-marsh environments predominately vegetated by Spartina alterniflora (oyster grass) which is the dominant marsh plant in most Louisiana salt marshes, high-marsh environments which consist of mature stable marsh which ultimately develops into chenier plains, transitional marshes which are the gradational zones between low marshes and high marshes, and barrens which are areas within the marsh that are devoid of vegetation. Five salient points were brought out in their study:

1. Creek banks:

Bioerosion and mass-wasting are prominent. At or immediately below the level of the creek bank vegetation, the substrate is riddled by extensive burrow systems of fiddler crabs. A consequential weakening and undermining of the upper slope of the creek bank results in large clasts of mud which either slump or tumble down to the lower slope of the creek bank. This mud is often incorporated into the contemporaneous sediments of the lower slope of the creek bank which produces a characteristic "chaotic bedding". Visible sedimentary structures include distinct, contorted to planar, intercalated laminae of clay, silt, and sand.

2. Low-marsh environments:

Active roots of S. alterniflora, which may penetrate the substrate to depths of at least 1 m, together with abundant burrowing fiddler crabs, derange or obliterate the depositional fabric (i.e.

destroy distinct layering of sediments). Ponded areas are common locally, although all are intergradational biologically and are similar sedimentologically. Mussels are widely distributed, removing suspended sediment from the water during tidal inundation and depositing much of the material as faecal pellets and pseudofaeces. The mussels thus gradually construct low but conspicuous small mounds of sediment, and their byssal threads help bind the deposits in place. Crabs and burrowing polychaetes are especially abundant, but bioturbation is less intense here than at the creek bank environment. Uca pugnax, the most abundant of the fiddler crabs observed by the investigators, was determined to be present at a density of 111 per square meter.

3. High-marsh environments:

High-marsh environments are divided by ecologists on the basis of plant zonation. Sedimentologically, these areas are extremely similar, typically consisting of slightly muddy to nearly pure sand. Normal marine deposition ordinarily is limited to high spring-tide level. This deposition is distinctive, and accounts for the extremely uniform elevation of high-marsh surfaces in general. Cores reveal areas of discontinuous, thinly laminated sand and silt, much less persistent and distinct than laminations in creek banks. Most deposits are sparsely to intensely bioturbated by plant roots and fiddler crabs.

4. Transitional marsh environments:

These areas represent the midpoint between lower, muddier, more densely vegetated substrates and higher, sandier, less vegetated zones. Ecologically, it is a minor ecotone, where the ranges of low-marsh and high-marsh organisms overlap. This environment is difficult to characterize because of the varying degrees of overlap.

5. Barrens:

Barrens are typically found near the terrestrial margins of marshes. Sediment composition and physical sedimentary structures in barrens are essentially the same as those in otherwise comparable vegetated habitats; desiccation cracks are abundant locally in mud barrens. Biogenic structures are conspicuously different, however. Root mottling is either relict or absent. Numerous crabs feed upon the surface, thoroughly reworking the uppermost layer of sediments, but do not as commonly burrow there.

The above observations may be applicable to Louisiana marshes, particularly salt marshes, which are similar with but not identical to salt marshes found in Georgia. For instance, Uca longisignalis is the dominant fiddler crab found in coastal Louisiana marshes, and Georgia marshes are fairly stable while Louisiana coastal marshes are rapidly eroding and are not in equilibrium with their tidal inundation regimen. Georgia marshes are composed of layers of different and distinguishable sediment types, whereas Louisiana marshes are composed of homogenous silt-like sediment which possess no distinguishing characteristics. However, the descriptions of creek banks and

low-marsh environments are generally compatible with the corresponding habitats found in Louisiana coastal marshes.

It seems likely that there is enough information available to justify an *a priori* qualitative scheme which may serve to facilitate and explain anticipated marker-sediment discontinuities which may arise during the course of this study. Therefore, the following general classification scheme is presented here for the first time:

Class I disturbance

- Description- Macroscopic disruption of marker-sediment continuity.
- Spatial structure- Biogenic; trails, burrows, nests, tracks, footprints, shells, rooting paths, etc.
- Geophysical; erosion holes, trenasses, breaches, etc.
- Spatial distribution- 2- or 3-dimensional, patchy, random, highly variable occurrence. Depth may extend to over 1 m.
- Observed direct effect- Sample core overlaps with disruption. Completely unintelligible convolution of marker in sediment profile.
- Observed indirect effect- Sample core proximal to disruptional area.
- Possible uniform marker-sediment discontinuity resulting from dislodgement, and redistribution of marker into sample area adjacent to disruption. Significant interference with determination of location of original marker layer not anticipated.
- Critical period- Marker horizon will be subject to Class I disturbances for several months to years. Crabs and plant rooting extend to

vertical depths over 1 m.

Causative agents - Macroflora rooting, various marsh grasses and plants. Macrofauna such as reptiles, burrowing and nest building mammals, burrowing and feeding crustaceans, foraging snails, birds, and possibly Homo sapiens. Physical surface turbulence due to storm and tidal surges, erosional processes.

Class II disturbance

Description- Microscopic disruption of marker-sediment continuity.

Spatial structure- Biogenic; shallow subsurface zone of mixing.

Geophysical; shallow subsurface zone of mixing

Spatial distribution- 2- or 3-dimensional uniform distribution. Intensity may vary locally, with possible patchy areas of high and low intensity disturbance correlated with meiofaunal and microfaunal population densities.

Observed direct effect- Uniform blurring and blending of marker horizon with vertical sediment profile. Possibly quantifiable uncertainty as to the location of the marker in the vertical soil profile.

Observed indirect effect- Reworking of sediment and marker by indigenous organisms may lead to resuspension and redeposition of marker material in soil profile above original marker layer. Original marker should be discernible by virtue of greater quantity.

Critical period- Marker horizon will be subject to Class II disturbances for a period of a few months to one year, depending

upon the local sediment rate and depth of oxygenated zone. The oxygenated zone drops off rapidly in coastal marshes (Fleeger, 1985).

Causative agents- Various microfauna and meiofauna. Nematodes, polychaetes, oligochaetes, and copepods are known to be present in high population densities in Louisiana marshes (Fleeger, 1985).

Physical microturbulence such as vibration, non-laminar surface water movement.

It does not seem likely that a quantitative treatment of Class I disturbances would be possible because of the large-scale disruption of the soil profile. Sample cores intersecting a Class I disturbance area would not contain any useful information concerning accretion or mixing rates. A random mixing of the marker with the sediment would be evident and unrevealing. However, Class II disturbance would not necessarily yield nonutilizable data. Since this type of disturbance is homogenous in nature, it would presumably affect the soil profile uniformly in any system containing micro- to meiofauna and flora. Depending on the intensity of this type of bioturbation, the observed marker distributions would range from minimal disturbance to possibly severe disturbance. The greater the intensity of the disturbance, the more uncertainty related to the original position of the horizon marker.

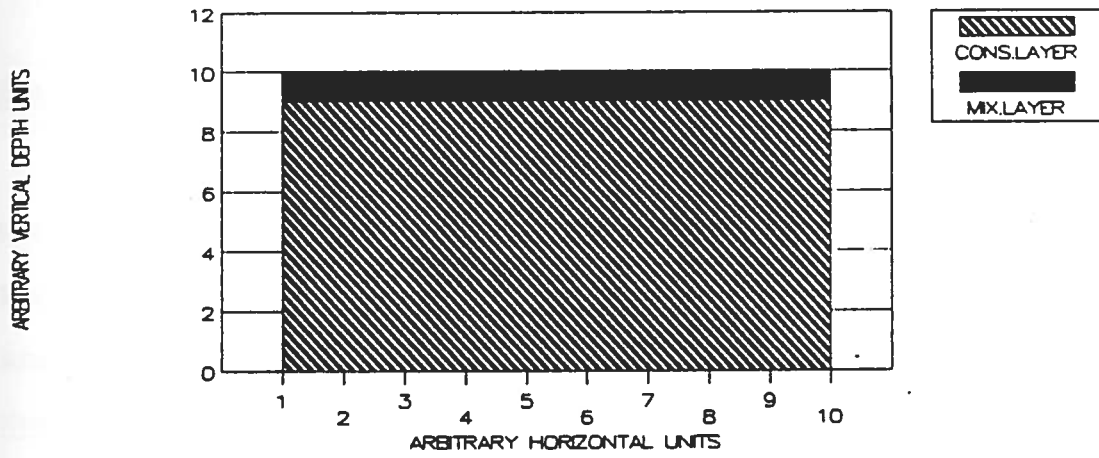
Several researchers have attempted to quantify the type of mixing described here as Class II. Goldberg and Koide (1962) introduced a

mathematical mixing model with the assumption of steady state mixing conditions to explain observed concentration profiles of thorium and ionium in deep-sea sediments. They assumed a single mixing layer with a constant or uniform rate of mixing and a consolidated non-mixing layer boundary beneath the upper mixing layer (Figure 2.1). Using this model, Goldberg and Koide concluded that mixing could explain the observed distributions of ionium and thorium, but they did not attempt to evaluate mixing rates or sedimentation rates. Berger and Heath (1968) assumed complete mixing of a layer of depth L so that any input of material would result in an entirely homogenous concentration of the input-material with subsequent propagation of the input-material into the non-mixing layer without disturbance. Others have reported similar models with the primary assumption of complete and homogenous mixing in the single mixing layer (Robbins and Edgington 1975, Robbins 1982, Christensen 1982).

Guinasso and Schink (1975) produced a model which is more general and applicable to a wider variety of situations than the models which assume homogenous mixing in the mixing-layer. Their model allows for differential rates of mixing and sedimentation. The mixing assumed in their model is gaussian in nature, meaning that the input-material diffuses away from its original theoretical one-dimensional distribution (which can be thought of as the mean) into a two dimensional distribution which is exactly analogous to the normal or gaussian distribution. The sedimentation rate is combined with the gaussian diffusion coefficient to express the G parameter. The G parameter determines the shape of the distribution of input-material.

Figure 2.1. Single mixing-layer schematic. The mixing layer is depicted at the top of the graph and the consolidated non-mixing layer is the cross-hatched region beneath the mixing layer. An input material must propagate vertically through the mixing layer before passing into the consolidated layer. The hypothetical soil surface is at an arbitrary depth of 10 and soil depth increase in the downward direction.

*SINGLE MIXING-LAYER MODEL
SCHEMATIC*



This model is explained further in Chapter 4.

Study 1

A...

Nuclea...

Resour...

Minerals

Study/W...

(Camer...

sites H...

Refuge...

At the W...

conjur...

accumu...

feldsp...

utilize...

radio...

analog...

applic...

to 1...

long...

MS 810

CHAPTER 3
GEOGRAPHICAL LOCATIONS

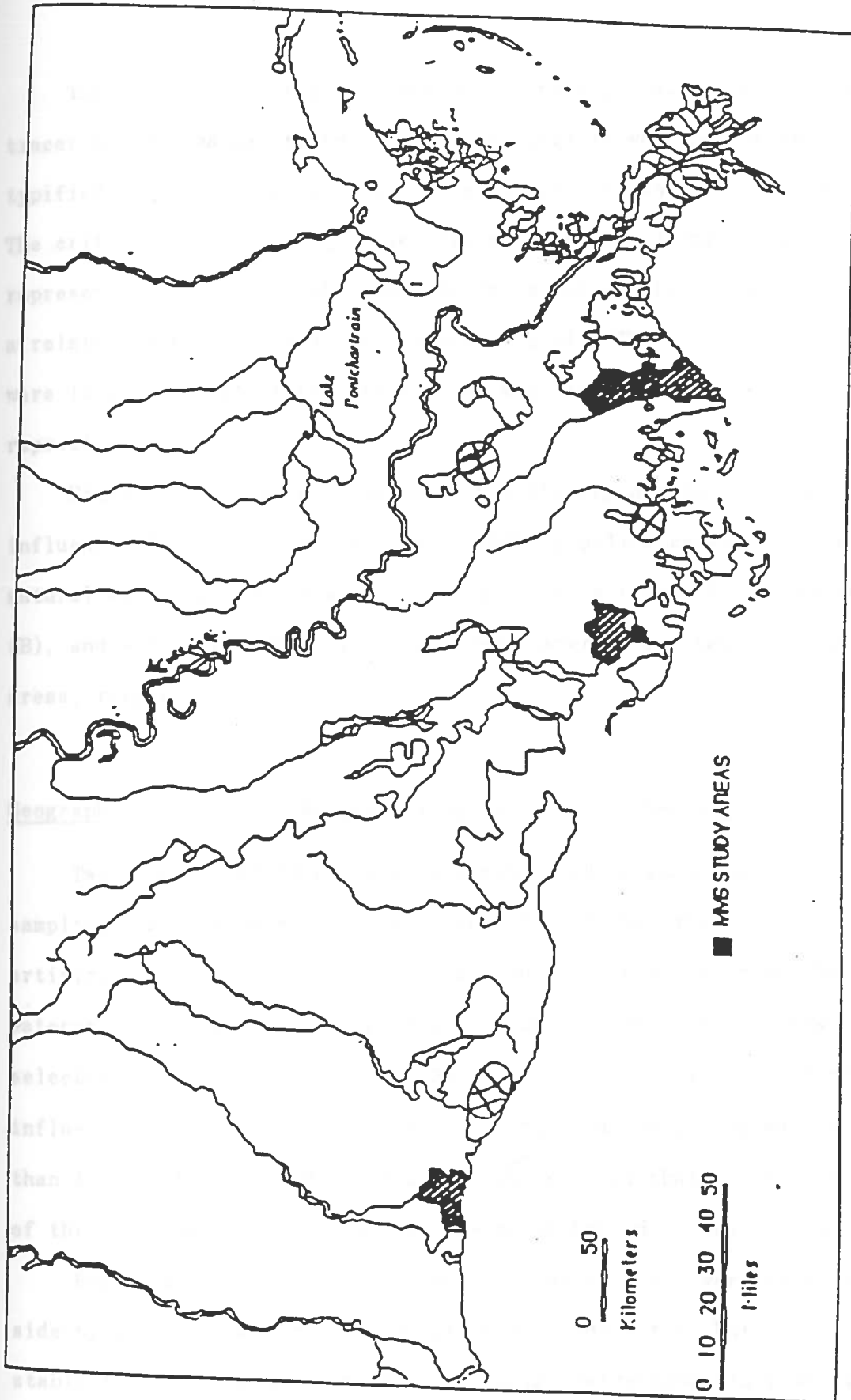
Study regions

A portion of this study was a cooperative effort between the Nuclear Science Center OF L.S.U and the Department of Wetland Resources of Louisiana State University supported by a grant from the Minerals Management Service (MMS, Contract No.14-12-0001-30252. OCS Study/MMS 87-0119). Figure 3.1 differentiates the 3 MMS study sites (Cameron, Lafourche at Leeville , and Terrebonne) from 4 additional sites (Lac Des Allemands, Lafourche at Fourchon, Rockefeller Wildlife Refuge, and Cocodrie) which were established prior to the MMS study. At the MMS site locations, two alternate techniques were employed in conjunction with the stable tracer technique for assessment of accumulation rates. One of these alternate techniques utilized feldspar clay as a visible horizon marker. The other technique utilized ^{137}Cs deposited during the years of atmospheric testing as a radiotracer horizon marker. The visible marker technique is somewhat analogous to the stable tracer technique in that both methods are applicable for measurements of short-term accumulation rates (6 months to 1 year). The radiotracer method is more useful for evaluation of long-term accumulation rates.

MMS study sites

Figure 3.1. The Minerals Management Service study sites (shaded) and feasibility study areas (circled). From left to right, the MMS study areas are Cameron, Terrebonne, and Lafourche at Leeville. From left to right, the feasibility study areas are Rockefeller Wildlife Refuge, Cocodrie, Lac Des Allemands, and Lafourche at Fourchon.

Source: Cahoon et al., 1987.



The experimental regions chosen for the application of the stable tracer horizon marker technique were selected in wetlands which typified a spectrum of habitats representative of southern Louisiana. The criterion used for region selection was sedimentological province, representing a recently abandoned delta, an older abandoned delta and a relatively stable chenier plane environment. These study regions were located in Lafourche, Terrebonne, and Cameron parishes, respectively.

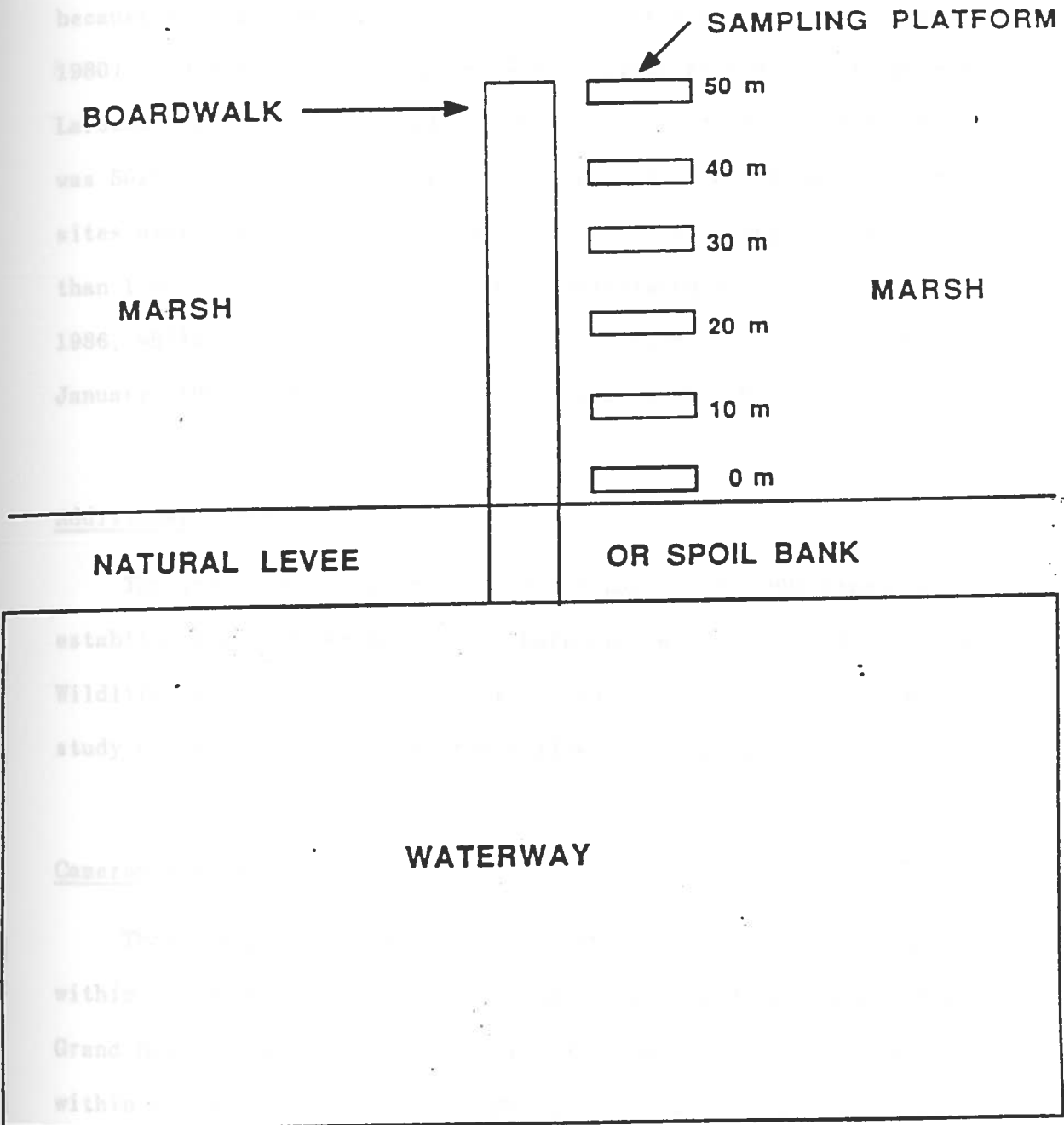
Sites of study were selected within the regions to test the influence of outer continental shelf (OCS) pipeline canals (C), and natural waterways (N) on accretion processes in fresh (F), brackish (B), and saline (S) marshes (Terrebonne, Cameron, and Lafourche study areas, respectively).

Geographical locations and experimental design of MMS sites

Two types of field plots were established in each region: (1) sampling stations 50 m inland from the edge of the natural or artificial levee; and, (2) transects running perpendicular to the waterway for 50 m inland (Figure 3.2). The distance of 50 m was selected because Hatton et al. (1983) demonstrated that the lateral influence of the streamside levee on vertical accumulation was less than 50 m in Barataria Bay. Thus, it was ensured that the full effect of the levee and its influence on the marsh behind it was encountered.

Both stable tracer and clay horizon marker plots were established side-by-side at the Cameron and Lafourche study sites, but only the stable tracer technique was utilized in the Terrebonne study sites

Figure 3.2. Boardwalk design used in the Lafourche at Leeville study area. Both rare earth and clay horizons were employed at these sites. The distance of 0 m is placed where the marsh behind the levee or spoil bank is not visibly distinguishable from the marsh at 50 m. From Cahoon and Turner, 1987.



because of the unsuitability of clay in freshwater marshes (Baumann, 1980). In all, 88 white-clay marker horizons were established in the Lafourche study area, and 24 at the Cameron study area. Each of these was 50x50 cm. The stable tracer was applied to nearly all of the same sites over the entire plot area, often times covering an area greater than 1 ha. The Lafourche plots were established during June and July, 1986, while the Cameron plots were established in November, 1986, and January, 1987. The Terrebonne plots were established in June, 1986.

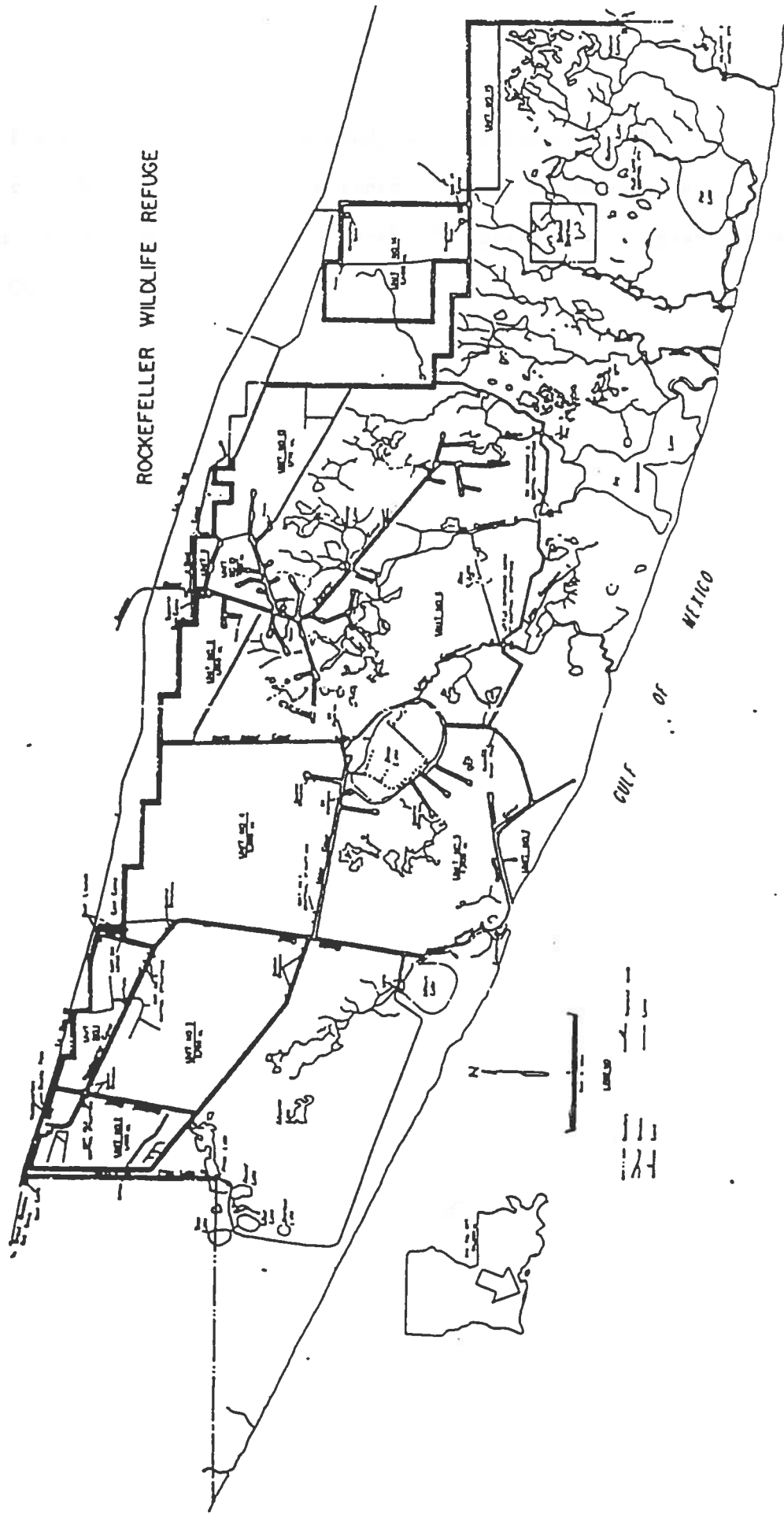
Additional sites

The additional sites which were not part of the MMS study were established at Lac Des Allemands, Lafourche at Fourchon, Rockefeller Wildlife Refuge, and Cocodrie. All study areas including the MMS study areas are described in the following paragraphs.

Cameron Parish sites

Three geographical locations in Cameron Parish included two sites within the Rockefeller Wildlife Refuge (Figure 3.3) and a site near Grand Bayou, Lake Calcasieu (Figures 3.4 and 3.5). The two sites within the Rockefeller Wildlife Refuge (not part of the MMS study) were treated with tracer in February 1984 (Ronald M. Knaus, 1987, personal communication) and the control (natural) site at Grand Bayou (MMS) , Lake Calcasieu, was treated in November 1987. The other sites at Lake Calcasieu were treated in January 1987. The two-month difference in treatment dates reflects navigational problems

Figure 3.3. Rockefeller Wildlife Refuge. Marker was applied at Price Lake and Superior Canal. Source: Louisiana State Department of Wildlife and Fisheries.

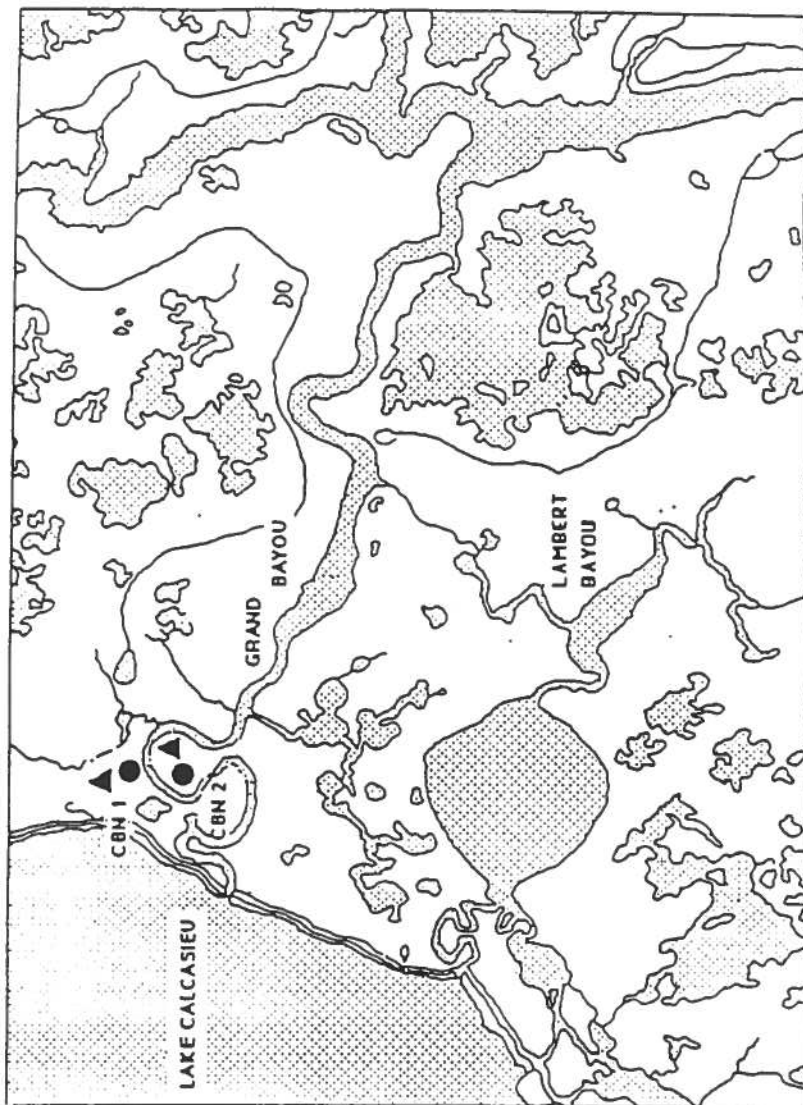


ROCKEFELLER WILDLIFE REFUGE

GULF OF MEXICO

Figure 3.4. MMS control study site at Cameron. CBN 1 and CBN 2 were considered to be controls since they are situated on a natural bayou. Both clay (Δ) and rare earth (O) horizons were established. From Cahoon et al., 1987.

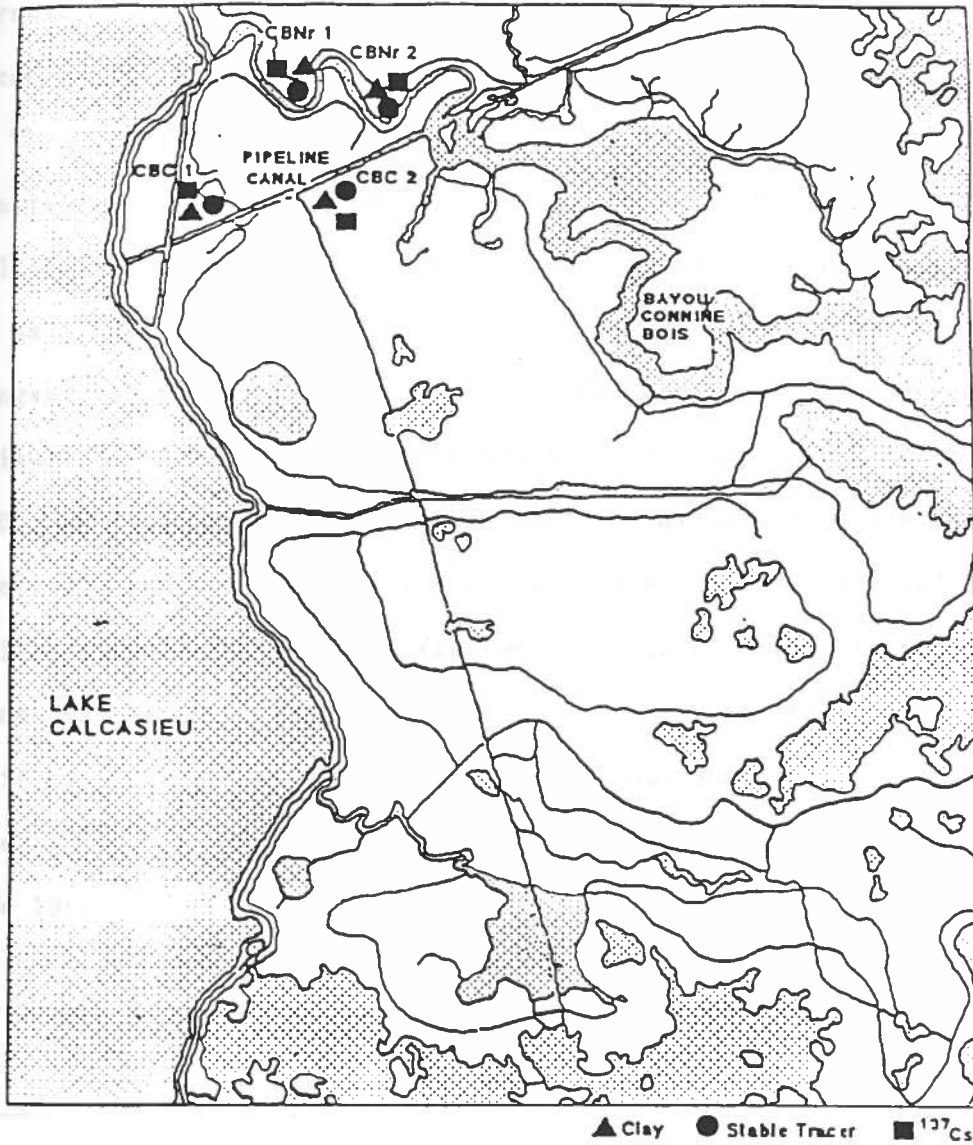
FL
STB 60
ON & PL
horizon



▲ Clay ● Stable Tracer

Figure 3.5. MMS canal study site at Cameron. CBNr 1 and CBNr 2 are on natural waterways but flow is restricted. CBC 1 and CBC 2 are on a pipeline canal. Clay (Δ), rare earth (O), and ^{137}Cs (\square) horizons. Source: Cahoon et al., 1987.

exper
encoun
The
char
by c
to a
drill
the
area
cbv
198
110
rap
sho
er
tak
Jun
St
one-
the
1986
All



experienced in November when unexpectedly low water levels were encountered.

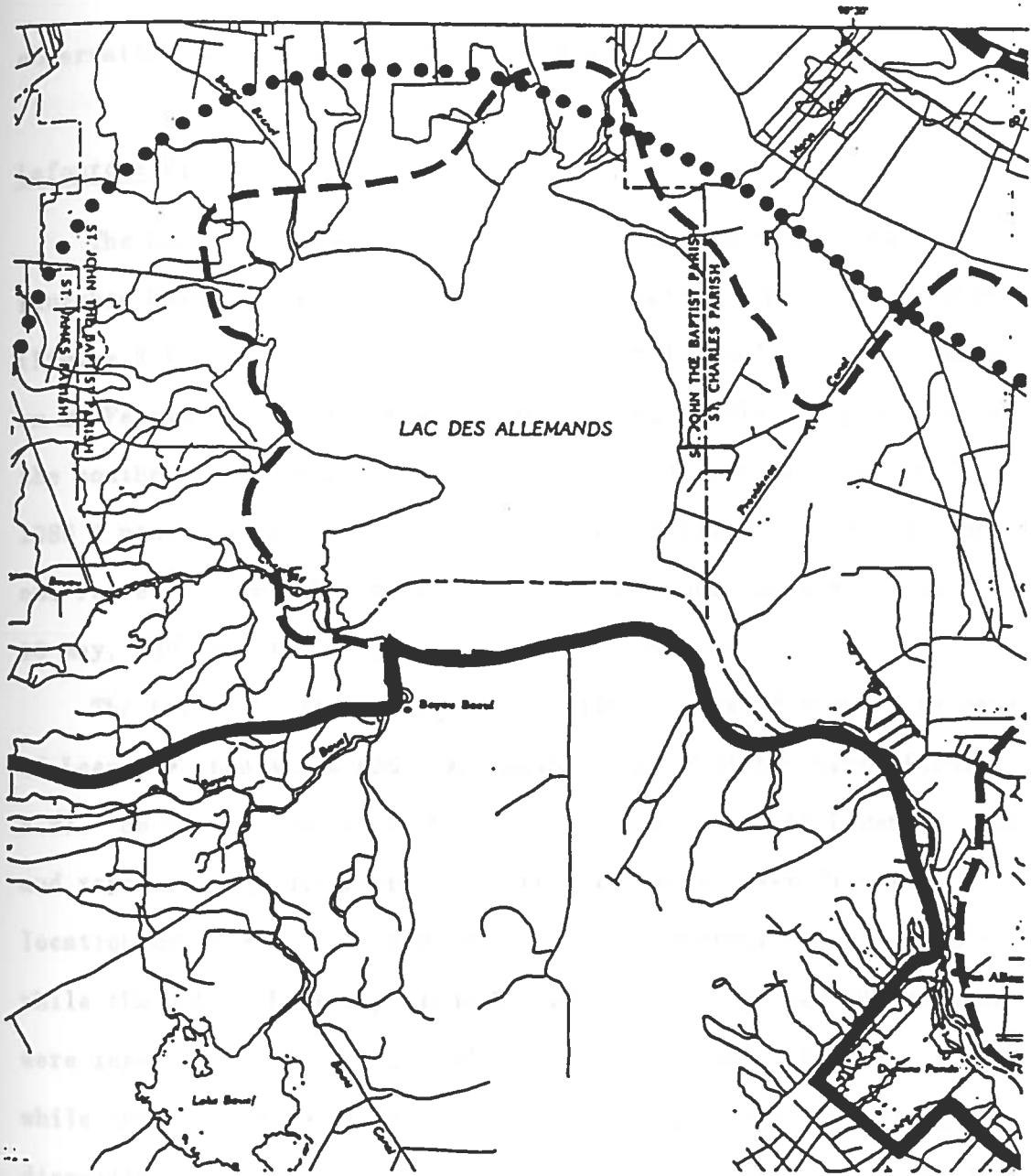
The Price Lake location in Rockefeller Wildlife Refuge is characterized by freshwater plants, although it is entirely surrounded by canals containing salt to brackish water.

The superior canal site is about 15 km to the east of Price Lake in a recently truncated canal just off Superior Canal. This defunct drilling site was chosen for study since it had been closed off from the salt water canal by an earthen barrier for the purposes of a water management experiment in 1982. The Dy-Sm marker was in place in an obviously freshwater habitat for about a year, when, in about February 1985, the comings and goings of an abundant alligator population literally eroded a breach through the barrier. The artificial pond rapidly became brackish, the freshwater flora died, and the alligators abandoned the immediate area. Two cores were taken from the breached artificial pond in March of 1985. Since that sampling, two cores were taken from this site and three from the Price Lake site on the date 17 June 1986.

St. John The Baptist Parish sites

In the freshwater habitat of Lac Des Allemands a series of six one-year cores were analysed prior to the work presented in this thesis. (Figure 3.6). The cores taken during the current study in 1986 represent 2 year sampling data (Table 5.3). The Lac Des Allemands study site is the northern-most area of Louisiana under

Figure 3.6. Lac Des Allemands feasibility study area. Study sites not shown. Source: U.S. Department of the Interior, Mississippi Deltaic Plain Region Ecological Atlas, 1981. FWS/OBS-81/16, Map A8.



observation, and is a fresh water lake habitat.

Lafourche Parish sites

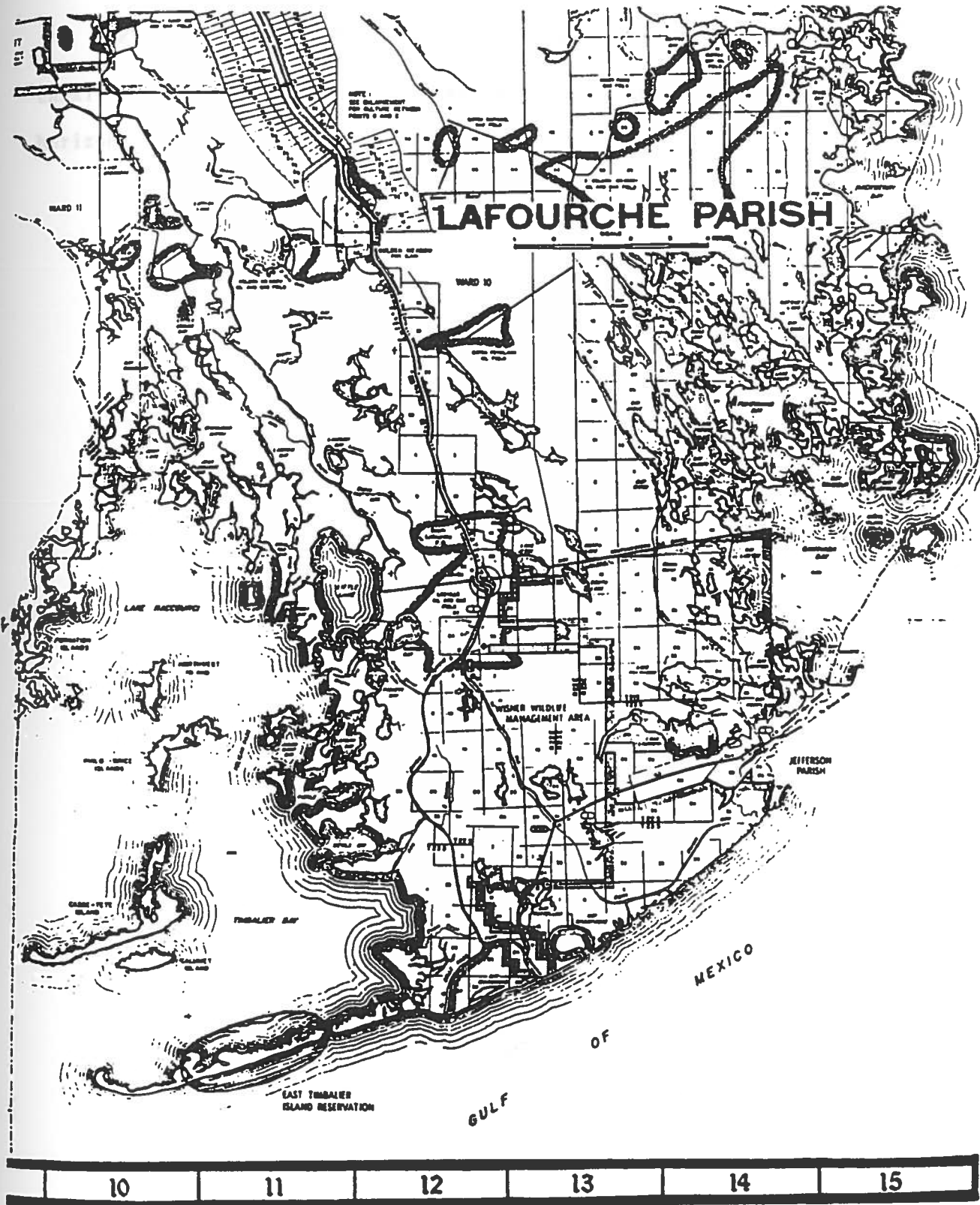
The Lafourche study area at Fourchon is located 5 km east of the Fourchon Camp, the Louisiana Universities Marine Consortium (LUMCON) (Figure 3.7). Three cores were taken prior to application of marker on 20 February, 1986 to establish background levels of Dy and Sm in the southern Louisiana environs. Three cores were taken on 21 June, 1986 4 months after the establishment of the artificial horizon marker and represent 6 month samples. Three additional cores were taken on 13 May, 1987 and these represent one-year samples.

The Lafourche study area at Leeville is located about 7 km east of Leeville, Louisiana and 7 km north of the Fourchon Camp (Figure 3.8). Seven cores were taken from this location on 12 December, 1987 and represent 6-month samples. Five cores were taken from this location on 13 May, 1987 and two of these represent 6-month samples while the other three represent 1 year samples. An additional 9 cores were taken on 11 June, 1987 and 5 of these represent 6-month data while the other 4 represent one year data. Once again, there is a disparity between plot establishment dates *and* sample dates due to logistical problems. Which are the dates of site establishment and sample collection are summarized for the sake of clarity in Table 5.3.

The Cocodrie study site is located within 2 km of the Cocodrie LUMCON station (Figure 3.9). This site consists of two plots, one of which was vandalized and ruined before samples could be taken. Three cores were taken from the remaining plot on 11 November, 1986 which

Figure 3.7. Lafourche at Fourchon feasibility study area. Source:
Gail's Bait Shop, Leeville, LA.





10	11	12	13	14	15
----	----	----	----	----	----

Figure 3.8. Lafourche at Leeville study area. Natural (LSN) and canal (LSC) sites with clay (Δ), rare earth (O), and ^{137}Cs (\square) horizons. Source: Cahoon et al., 1987.

Figure 1
LONDON

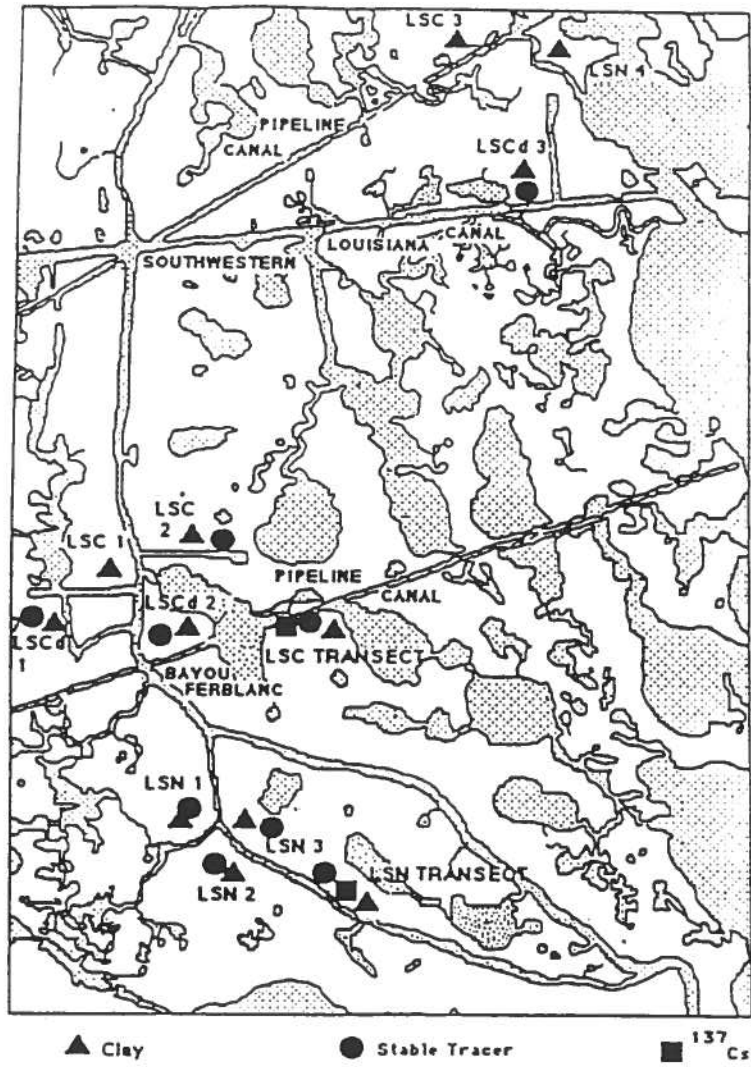
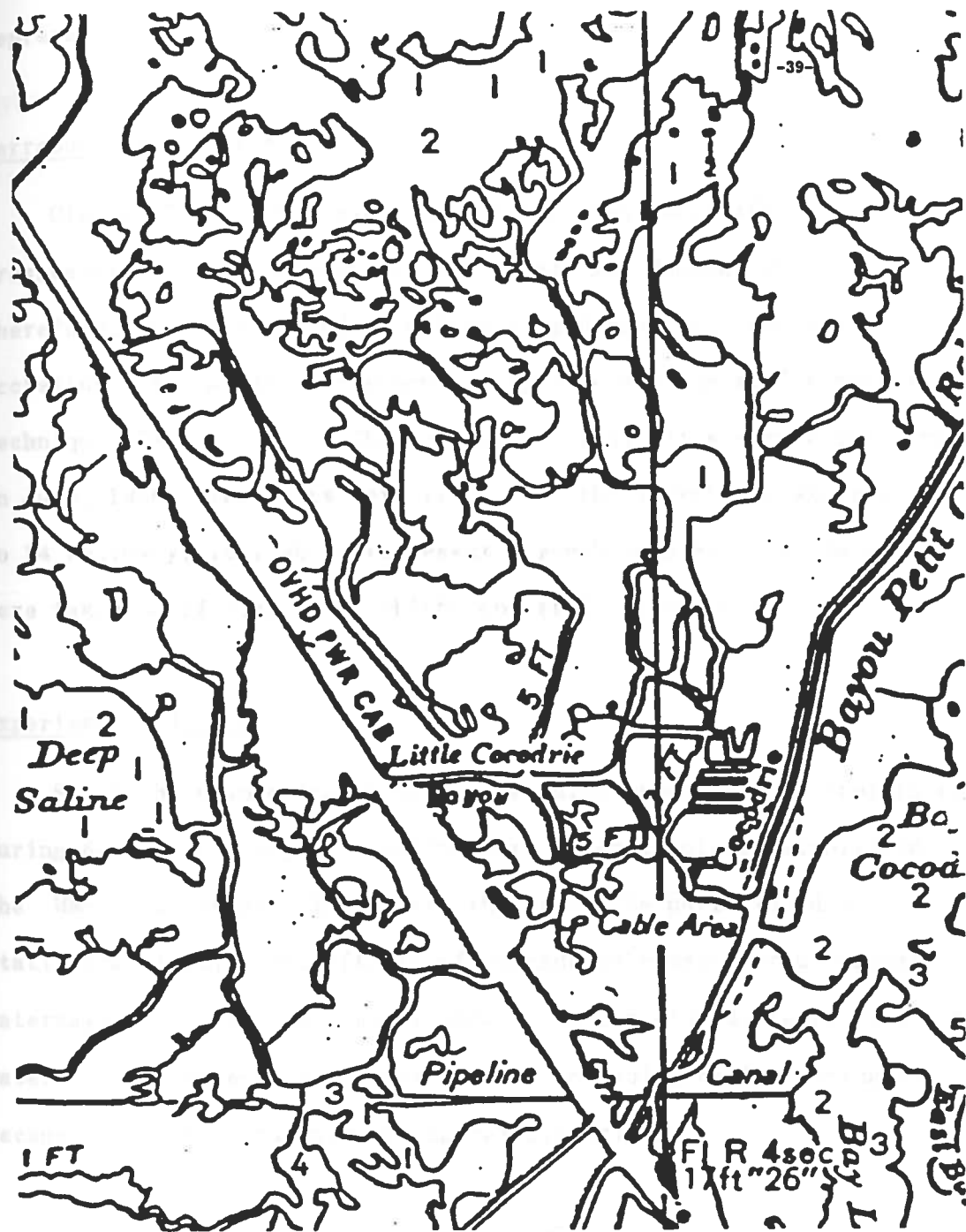


Figure 3.9. Cocodrie feasibility study area. Source: Cocodrie LUMCON (Louisiana Universities Marine Consortium).





represent 6-month samples.

Terrebonne Parish sites

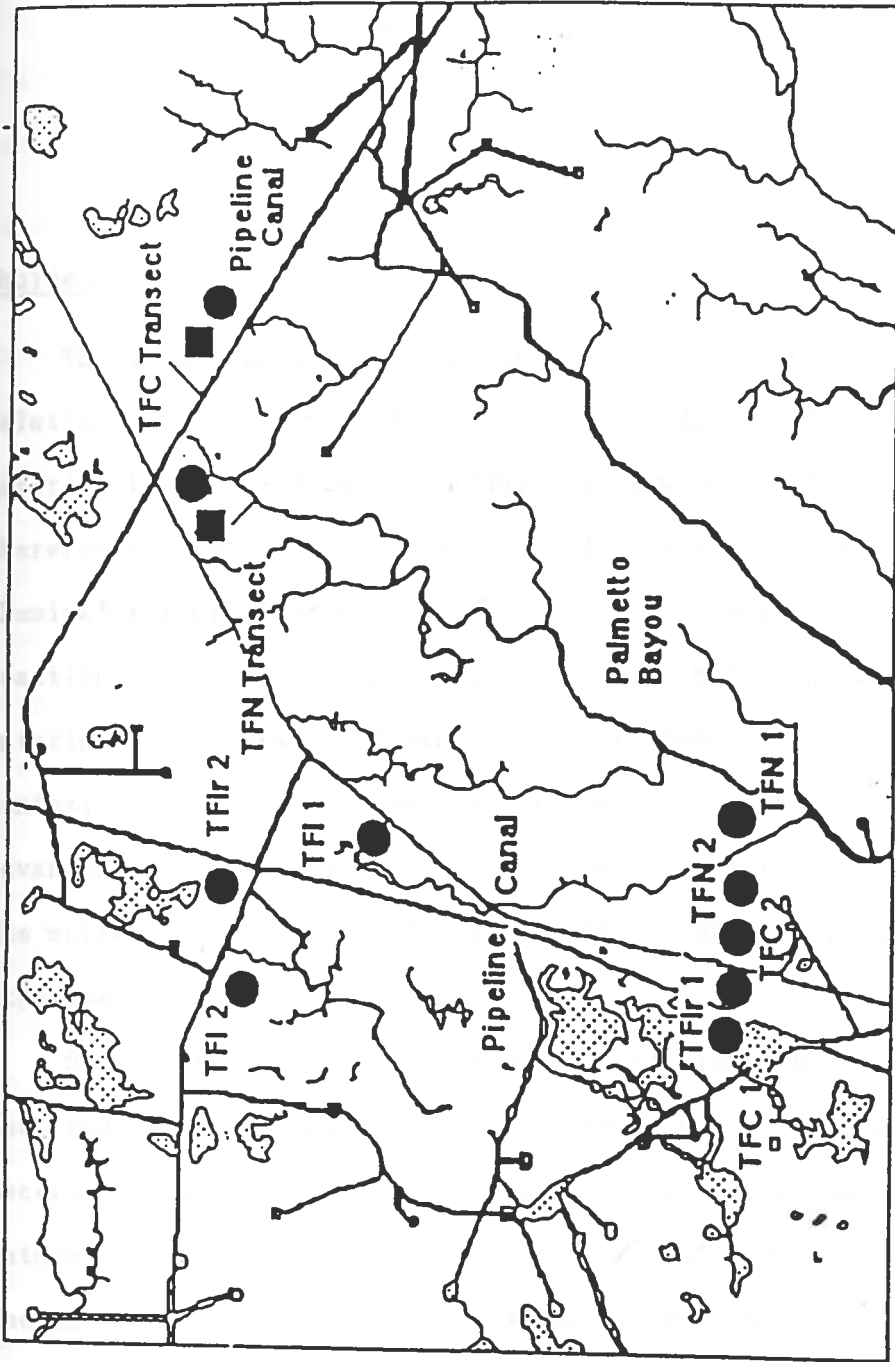
Clay soil horizon markers have not proved successful in freshwater habitats (Baumann et al., 1984, and Baumann 1980). Therefore, the sole method of determining 6 month and one year accretion rates at the Terrebonne study site was the stable marker technique (Figure 3.10). The Terrebonne study sites were established in June, 1986. Ten cores were taken from the Terrebonne study plots on 14 February, 1987 which represent 6-month samples. Twelve cores were taken on 24 June, 1987 which represent 1-year data.

Experimental design

Since the stable tracer method is quite expensive, no replicates during 6-month and 1-year sampling were taken at plots established in the MMS study areas. The effect that could be partitioned by statistical testing was effects of manmade waterways versus natural waterways within the same study areas. Testing for differences due to waterway type between study areas would be biologically meaningless because of geophysical and ecological disparities.

Figure 3.10. MMS Terrebonne study area. Natural (TFN), canal (TFC), impounded (TFI), and impounded restricted flow (TFIr). Rare earth (O) and ^{137}Cs (□) horizons. Source: Cahoon et al., 1987.





● Stable Tracer ■ ¹³⁷Cs

CHAPTER 4
MATERIALS AND METHODS

Choice of marker

The stable tracer must be biologically nonessential, in a relatively inert form, and inexpensive. A biological nonessential material is unlikely to be scavenged by living organisms and will therefore not be subject to mobility due to biogenic transport. A chemically inert material will be unlikely to participate in redox reactions or other chemical reactions which might increase the material's mobility. Additionally, inert materials are usually nontoxic to biological organisms at low concentration levels. The advantages of relative low cost are obvious. The lower the cost of the material, the greater the area that can be treated and followed experimentally.

Since neutron activation was the analytical method of choice for the study presented in this thesis, certain nuclear properties were necessary. The isotopic stable tracer must have a reasonably high natural isotopic abundance and a high thermal neutron cross-section. The amount of the stable tracer which can be converted to a detectible radionuclide in a given amount of time in a neutron bombardment chamber is directly related to natural isotopic abundance and thermal

neutron cross-section. The following relationship describes the kinetics of the neutron bombardment reaction:

$$A = \phi N \sigma (1 - e^{-\lambda t_1}) (e^{-\lambda t_2}) \quad (\text{Eq. 4.1})$$

where A is the activity in disintegrations per second (dps) of the neutron produced radionuclide in the sample, ϕ is the neutron flux in neutrons $\text{cm}^{-2} \cdot \text{sec}^{-1}$, N is the number of atoms of the activable stable isotope in the sample, σ is the thermal neutron cross-section in barns, λ is the decay constant of the neutron produced radionuclide per second, t_1 is the amount of time the sample is subjected to neutron bombardment in seconds, and t_2 is the time elapsed after the end of bombardment (EOB) in seconds. Increases in ϕ , N , or σ will result in greater activity after a given time of neutron bombardment. Large isotopic abundance results in large N . The thermal neutron cross-section (σ) can be thought of as the probability of a neutron which passes through a sample actually interacting with a nucleus of the activable stable isotope and producing the activation product radionuclide. Thermal neutron cross-section is an intrinsic nuclear property that cannot be manipulated which necessitates the selection of a stable activable isotope with a reasonably high cross-section. The neutron-activated radionuclide must have an adequately intense and energetic gamma ray emission for ease of quantitative detection as well as possess a half-life sufficiently long for gamma ray analysis, post neutron bombardment (Knaus and Curry, 1979). Certain rare earth elements possess the above qualities and are ideal for large-scale environmental studies involving field applications where radiotracers

would be prohibited (Knaus and El-Fawaris, 1981). The rare earth elements selected for this research were dysprosium (Dy) and samarium (Sm) because they meet all of the criteria specified and they have been successfully utilized in feasibility studies (Knaus, 1987).

Preparation of marker

Kilogram quantities of each rare earth element were obtained as the soluble nitrate (95% purity) and as the insoluble oxide (89% purity) from *Research Chemicals, NUCOR Corporation, Phoenix, Arizona*. Because of their lower cost, the large-scale application necessary for this study required the use of the oxides rather than nitrates. 1000 gm of each oxide was slowly added to 1500 ml of hot concentrated nitric acid (119^o centigrade) in a 3 liter beaker with a magnetic stirrer. Extreme caution must be exercised during this procedure because the dissolution of the oxides in acid is highly exothermic, and the potential for an explosive reaction is high. The nitric acid must be hot because the oxide will not dissolve in the acid until a temperature over 80^o centigrade is reached (If the oxide is heaped in cold nitric acid and the mixture is heated, a spectacular explosion will result). After dissolution of the oxide, the mixture was allowed to cool and 500 ml was added. This entire procedure was repeated several times so that and the resulting mixtures of each rare earth were poured into a single container which resulted in a total of 22 liters of solution containing a concentration of each rare earth of

approximately 0.15 gm per ml.

Application of marker

Measured amounts of the highly acidified Dy-Sm nitrate mixture described above in the "Preparation of marker" section, were diluted with marsh water present at the site of isotope application and applied to the surface of the experimental plots by a CO₂ driven spray apparatus, typically used for herbicide and insecticide applications. The diluted marker exits the four nozzels of the spray boom as a fine mist which evenly covered the marsh surface. Marsh vegetation was unavoidably sprayed during this procedure. Knowing the area covered by the spray and the concentration of the mixture, a minimum of 100 ug of each rare earth metal as the trivalent cation was applied per cm² of marsh surface. The lower limit of sensitivity of the INAA technique for Dy and Sm in environmental matrices has been determined to be approximately 0.10 ug per sample. In most cases, the soil of the plots was covered by a layer of water which is typically present during the summer months because of prevailing conditions of atmospheric high pressure over the Gulf of Mexico waters. Upon contact of the water-diluted tracer spray with the surface waters of the marsh, an increase in pH caused a milky white precipitate to form which extends through the water column and settles onto the soil surface. It is reasonable to assume that in the salt-water marshes, the form of the marker in the soil is either sorbed ion or insoluble carbonate or hydroxide precipitate. The pH of salt and brackish waters is between 8.0 and 8.5. The pH of fresh water marshes is usually more acidic in

comparison to that found in saline and brackish marshes.

Sampling of marker

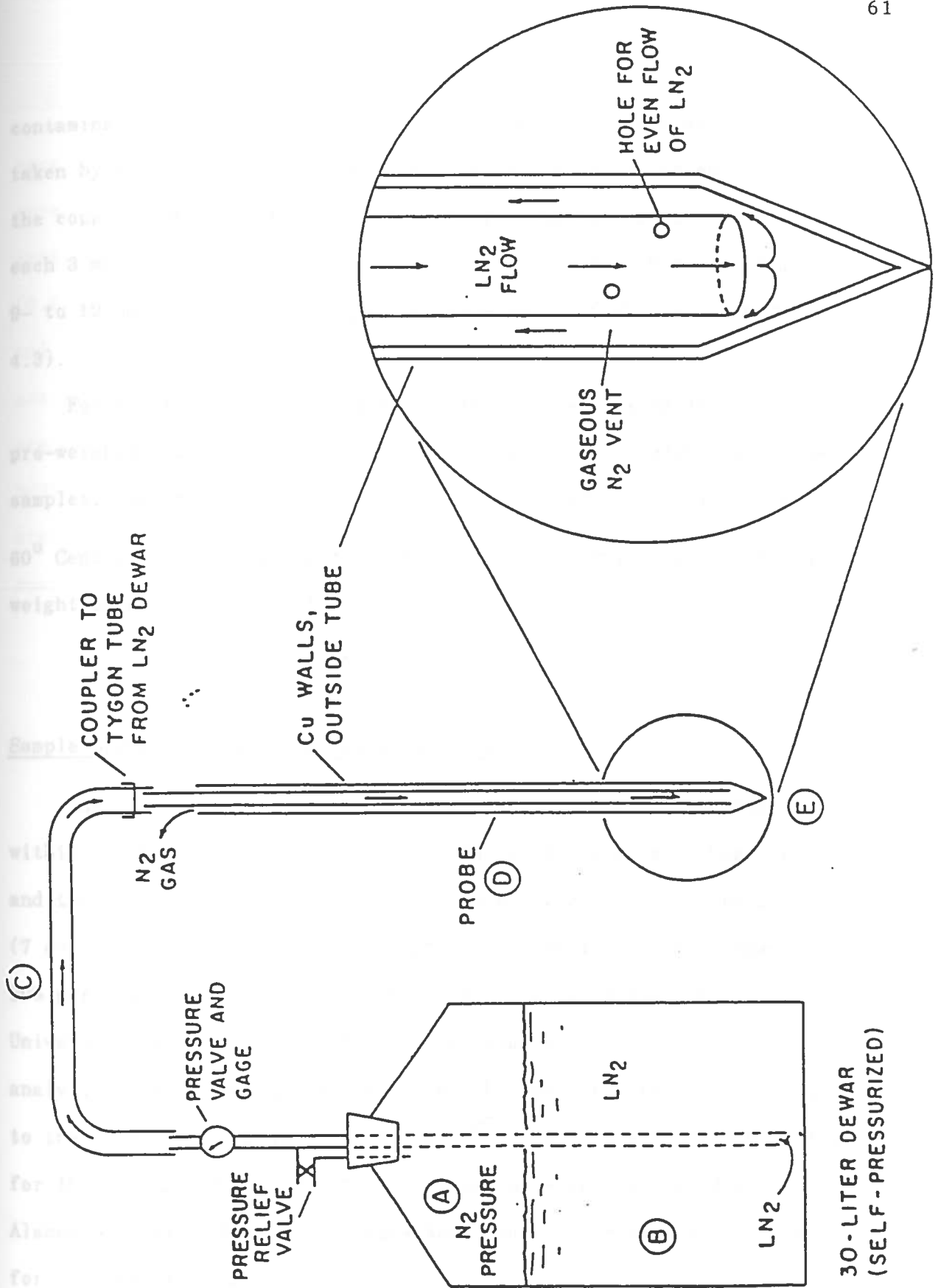
Recent sediment accumulations are often loose, flocculent material that is nearly impossible to sample if the stratigraphy of the sample is to be preserved. In order to overcome this problem, a cryogenic coring device has been developed (Knaus, 1986) that freezes the core *in situ* (Figure 4.1). The frozen core was extracted from the sediment, placed in an ice chest containing dry ice, and transported back to the lab for sectioning. The sequence of procedures leading to numerical results is a lengthy one (Figures 4.2 and 4.3). In the laboratory, the frozen core was prepared for sectioning by scraping off loose, angular debris projecting from the core in order to produce a smooth vertical surface of frozen mud and organic detritus. This scraping step assured that the samples to be taken from the core were not contaminated by melt water that occasionally flows from the ice above the water-sediment interface onto the outer surface of the core.

The core was sectioned with a razor blade serially beginning at the water-sediment interface along its length. In this study, the core was usually sectioned in 3-mm intervals (5-mm interval for one-year Terrebonne Parish cores). The 3-mm sections seem to be the smallest sizes that can be cut without an unreasonable increase in time and cost. After the ten 3-mm sections were cut, a careful measurement was made to assure that the sum of the ten sections was, indeed, equal to a total of 30 mm. Because of the possibility of

Figure 4.1. Cryogenic coring device. From Knaus, 1986.

© 1986 by the American Society of Civil Engineers
All rights reserved. No part of this publication may be reproduced, stored in a retrieval system, or transmitted, in any form or by any means, electronic, mechanical, photocopying, recording, or by any information storage and retrieval system, without the prior written permission of the American Society of Civil Engineers, 1801 Alexander Bell Drive, Reston, VA 20191.





30-LITER DEWAR
(SELF-PRESSURIZED)

contamination of the copper coring device, a further precaution was taken by not collecting a 3-mm section close to the outer surface of the copper probe (Figure 4.1). The observed marker concentrations in each 3 mm cut segment were reported at the midpoint. For example, the 9- to 12-mm section datum is plotted at a depth of 10.5 mm (Figure 4.3).

For wet weights, the 3-mm serial sections were weighed in pre-weighed 2/27th-dram (0.2 cc) polyethylene vials (polyvials). The samples, typically 0.1 g (wet weight) were placed in a drying oven at 60° Centigrade overnight and reweighed to obtain dry weights. The dry weight of a 3-mm section is about 0.01 g.

Sample preparation and neutron irradiation

The dried samples were heat-sealed in the polyvials and placed within 2/5th-dram (1.5cc) polyvials. These, in turn, were heat-sealed and two of these 2/5th-dram polyvials were encapsulated in one 2-dram (7 cc) polyvial for neutron irradiation (Figure 4.2). Approximately 80% percent of the samples were irradiated at the Texas A & M University Reactor Facility for instrumental neutron activation analysis (INAA). Approximately 10% of the samples were irradiated at to the Oregon State University Radiation Center TRIGA Reactor Facility for INAA (Figure 4.4) and 10% of the samples were irradiated at Los Alamos National Laboratory's Omega West Reactor Facility in New Mexico for INAA(Figure 4.5).

At each reactor site, samples and standards were irradiated with

Figure 4.2. Sequence of procedures leading to detection of the rare earth horizon markers in the vertical soil profile. Cryogenic core is taken from marsh site to laboratory where it is sectioned vertically by 3 mm increments. Each cut segment is placed in a 2/27 (0.2 ml) dram ploy vial, dried, and weighed. This vial is heat sealed and encapsulated in a 2/5 dram (7 ml) poly vial. Two of these vials are placed in a 2 dram vial and transported to a reactor where they are subjected to neutron bombardment. After neutron activation, the 2/27 dram vial is removed and placed in a clean 2/5 dram vial. The vial is then placed in a GeLi detection system, and the gamma ray spectrum is generated.



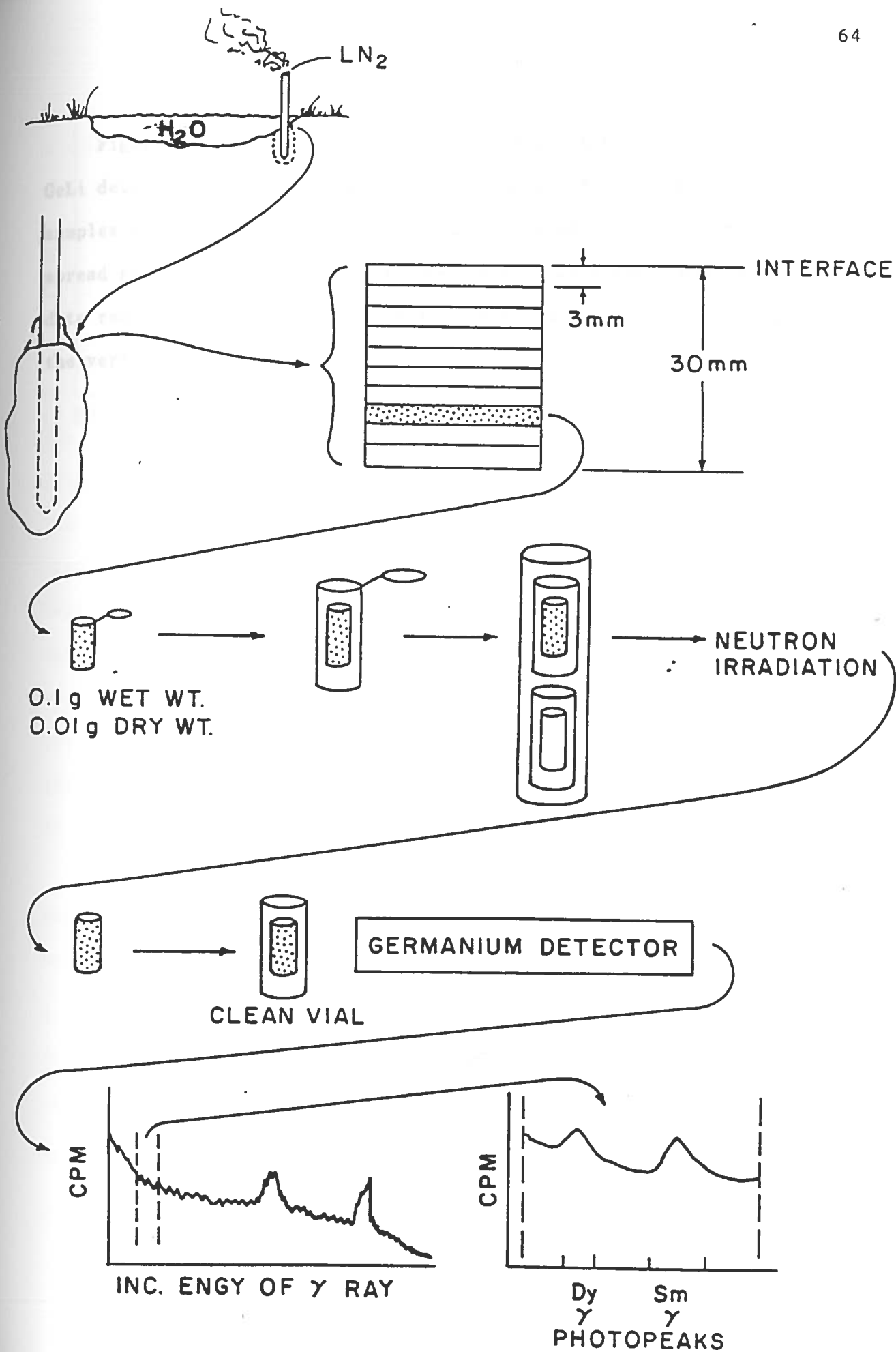
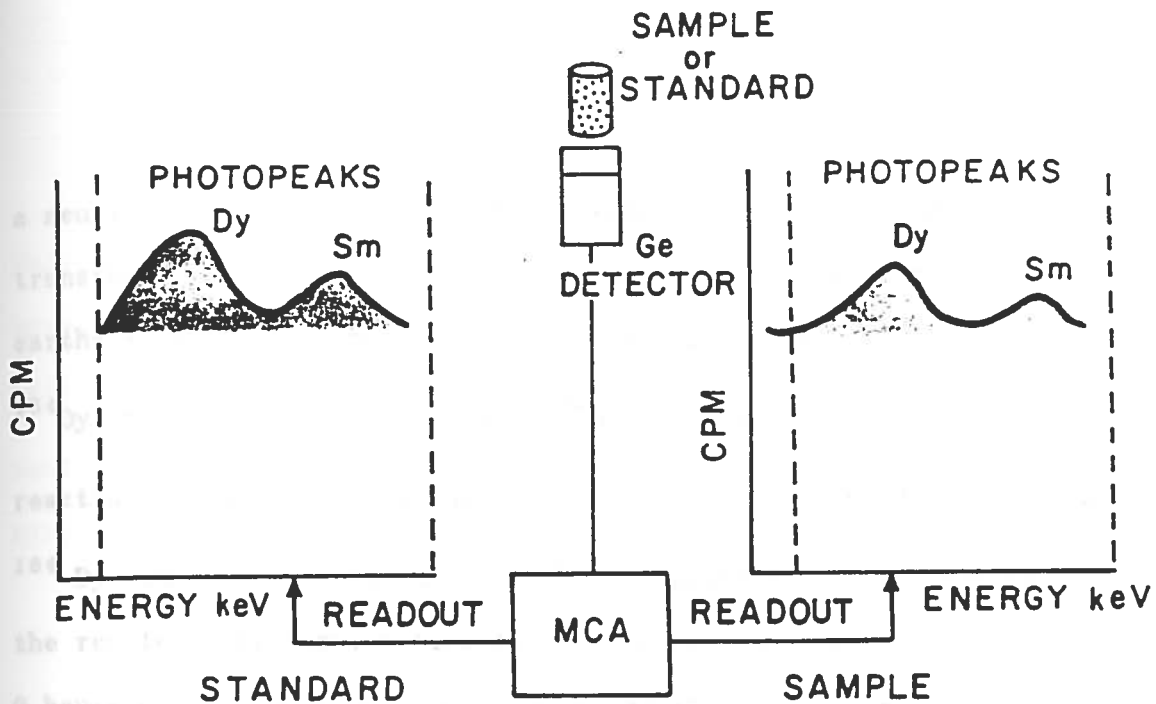
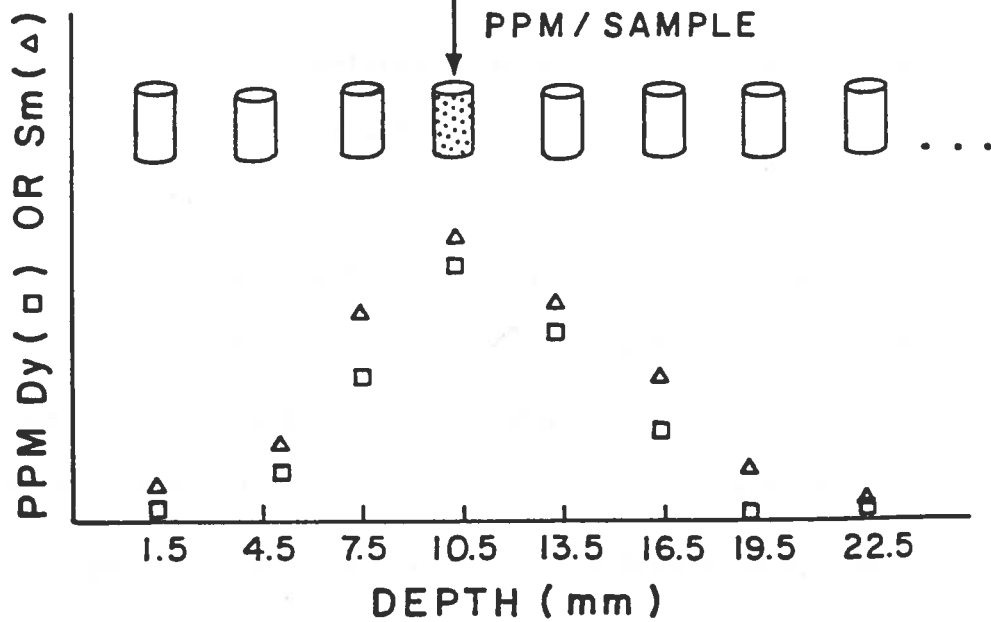
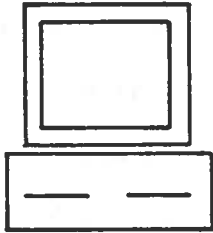


Figure 4.3. Continuation of process shown in Figure 4.2. The GeLi detector system generates the gamma ray spectra for both soil samples and standards which are subsequently read into an electronic spread sheet data base. The data base program performs a number of data reductions which result in the observed marker distribution in the vertical soil profile.



LOTUS 1-2-3 DATA BASE

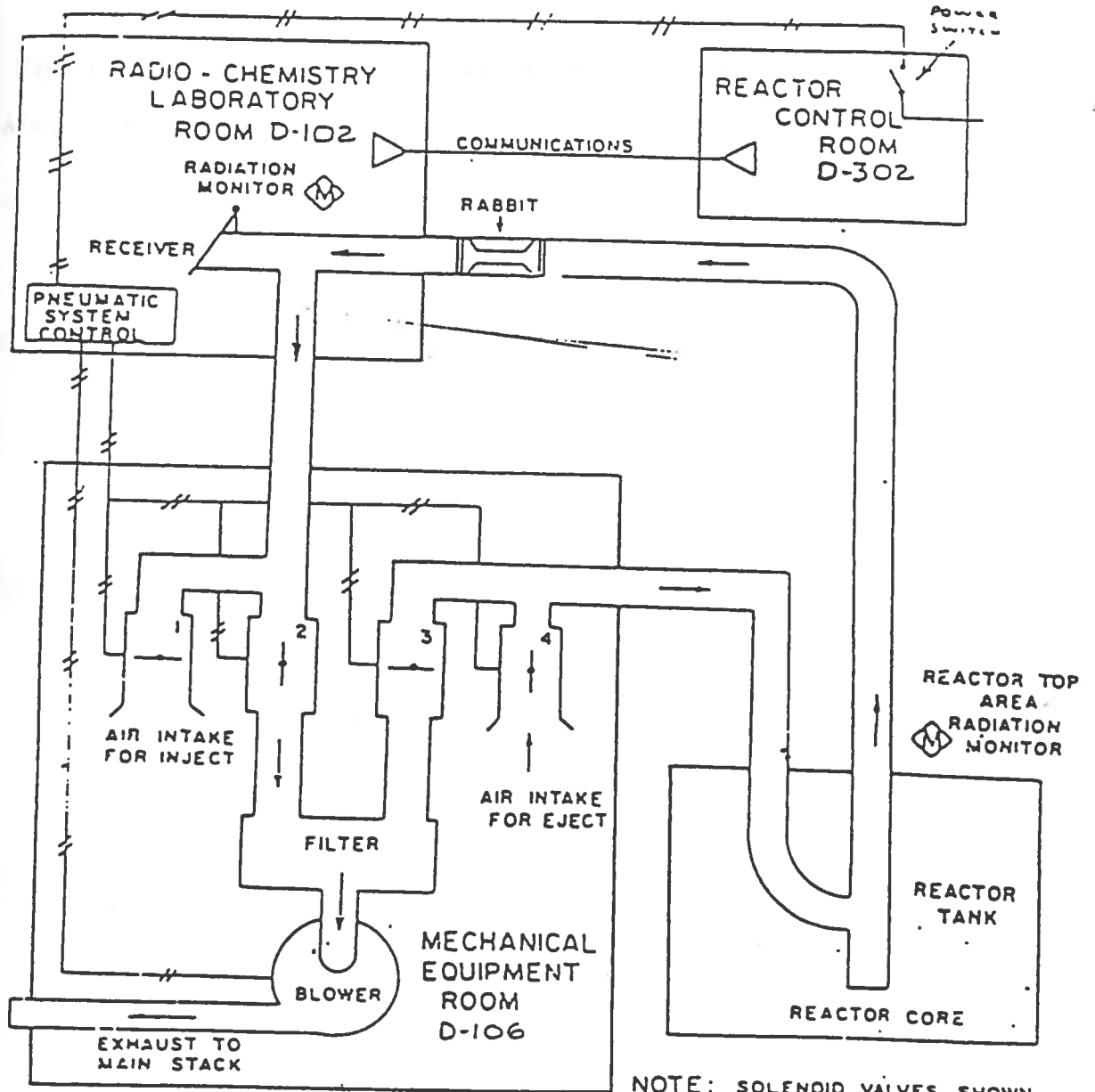


MARKER DEPTH : 10.5 mm

a neutron flux of 10^{13} neutrons \cdot cm $^{-2}$ \cdot sec $^{-1}$ for 2-3 min via a pneumatic transfer system. The neutron bombardment reaction for both rare earths is a neutron absorption and prompt gamma reaction to transmute ^{164}Dy to ^{165}Dy (Figure 4.6) and ^{152}Sm to ^{153}Sm (i.e., the (n, γ) reaction). The isotopic abundances of the stable naturally occurring ^{164}Dy and ^{152}Sm are 28.1% and 26.7%, respectively. Upon removal from the reactor, the samples were allowed to radioactively decay at least 2 hours before counting. The reason for this time delay is to allow the sample to decrease to radiation levels low enough so that the deadtime of the GeLi detector system is not greater than 10%. Deadtime refers to the amount of time the detector system is unable to detect an impinging radiation event because of the finite amount of time required for electrons in the detector matrix excited by a previous radiation interaction to return to ground state. As deadtime increases, the efficiency of the detection system decreases (Wang, Willis, and Loveland, 1975).

The delayed gammas characteristic of the activated rare-earths were detected by means of a GeLi detector interfaced with a multichannel analyzer. Analysis for the 0.0947 MeV gamma ray of the 2.33-h ^{165}Dy was performed within 5 h, post neutron bombardment. Analysis of the same sample for the 0.1032 MeV gamma ray of the 46.7-h ^{153}Sm was performed 48 to 100 h, post bombardment. The combination of the two tracers is an internal verification of the data and also overcomes the possible interference with ^{165}Dy detection of the 15-h

Figure 4.4. The pneumatic transfer system at Oregon State University showing the tube in which the rabbits travel and the air blowing mechanics. Rabbit is ejected under pressure from Radio-chemistry Laboratory to reactor core where it is subjected to a neutron flux of approximately 10^{13} neutrons \cdot cm $^{-2}\cdot$ sec $^{-1}$ for 2-3 minutes.



NOTE: SOLENOID VALVES SHOWN IN DE-ENERGIZED POSITION

PNEUMATIC TRANSFER SYSTEM SCHEMATIC

Figure 4.5. Schematic showing the automated pneumatic system at Los Alamos National Laboratory.



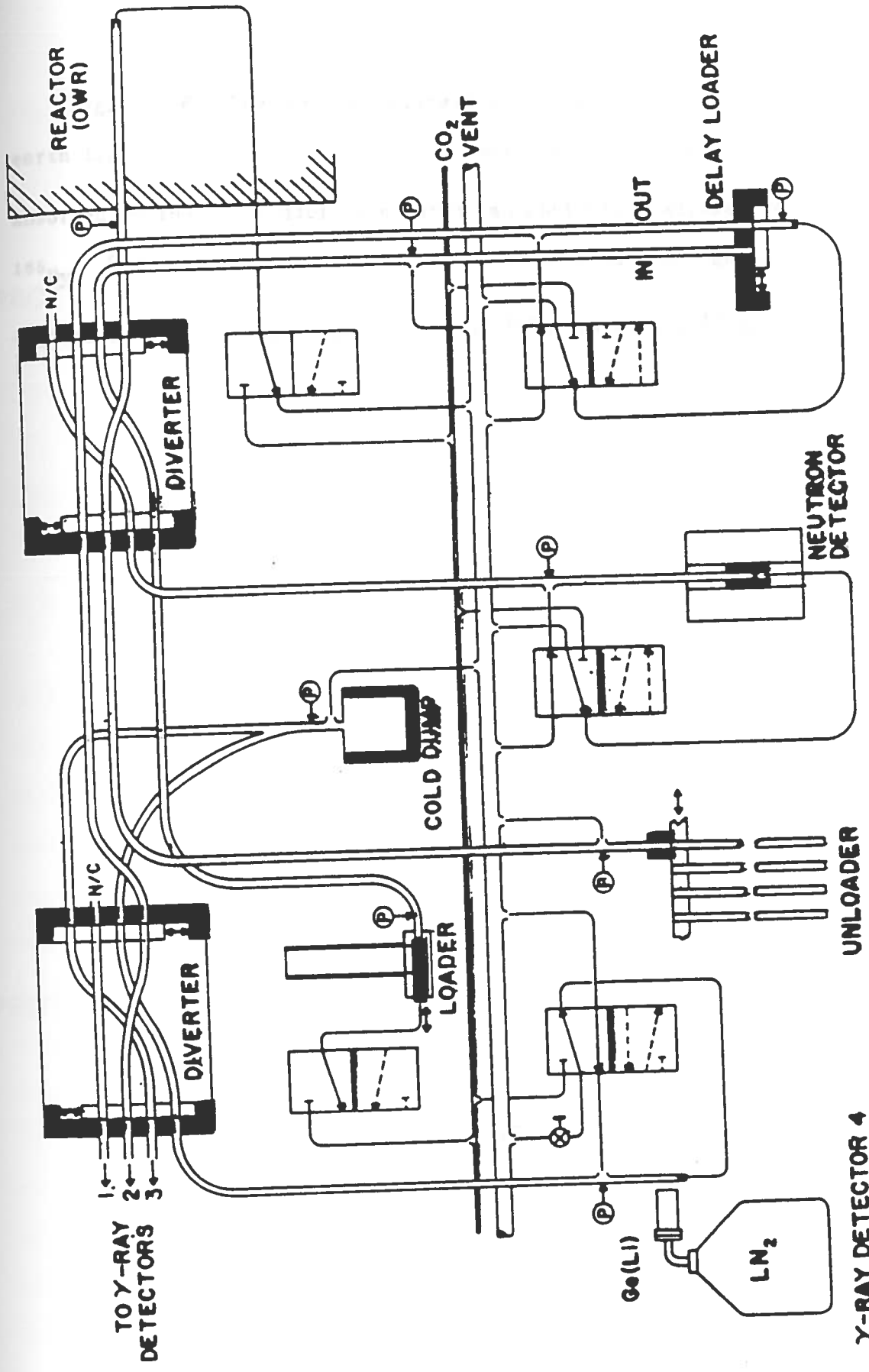
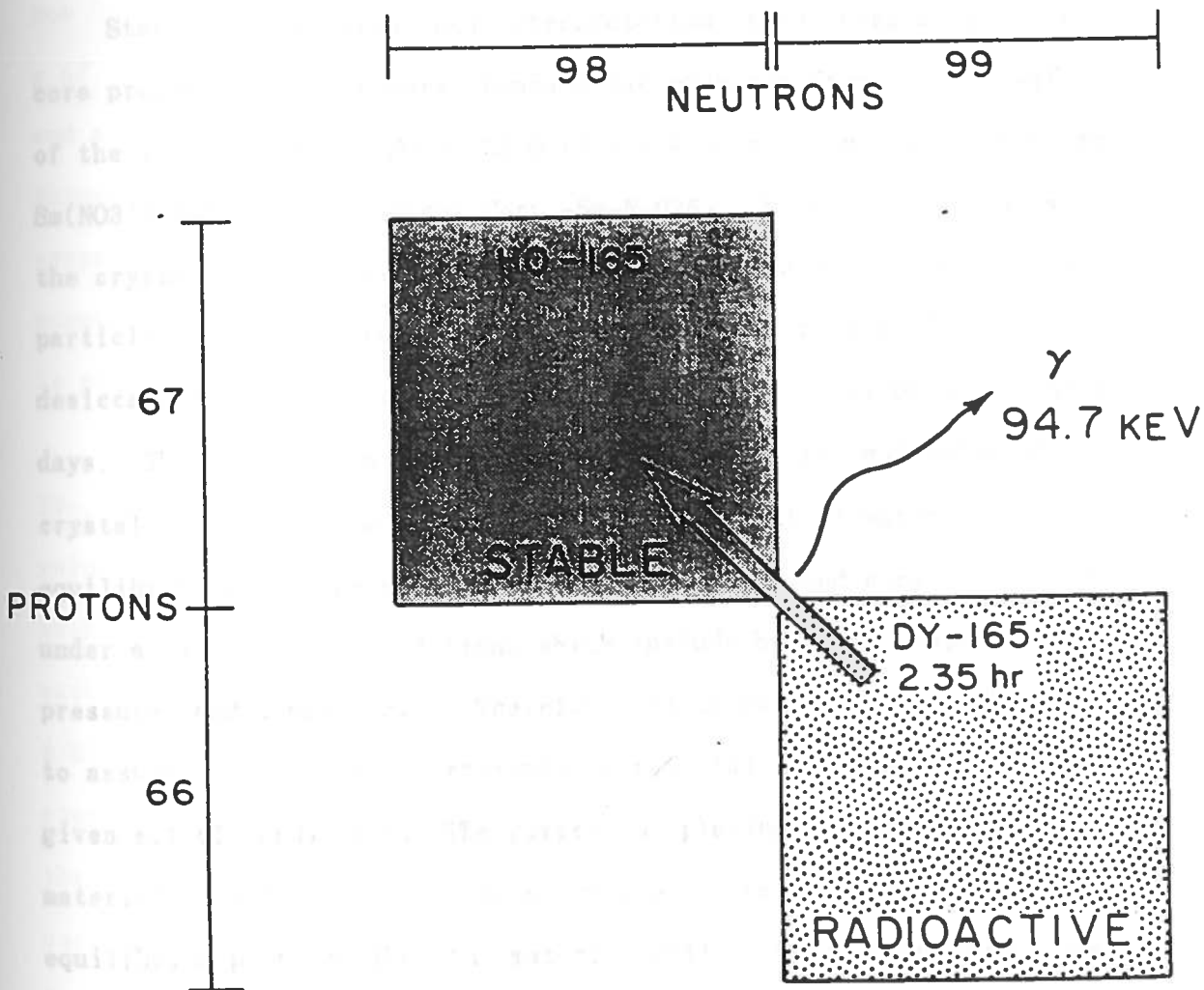
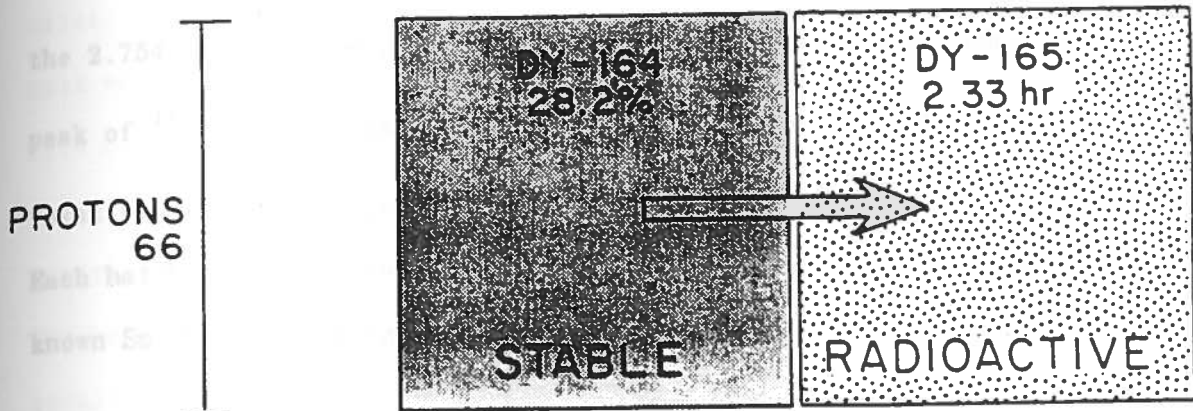


Figure 4.6. The neutron activation scheme is shown for the rare earth tracer, dysprosium (DY). A thermal neutron (top drawing) is absorbed by the ^{164}Dy nucleus creating an unstable (radioactive) atom, ^{165}Dy . Beta decay results in the emission of a 94.7 keV gamma photon (bottom drawing) and a transmutation of ^{165}Dy to stable ^{165}Ho .

NEUTRON ACTIVATION OF DYSPROSIUM



GAMMA RAY EMISSION

^{24}Na in samples high in sodium content. If the Compton continuum of the 2.754 and 1.369 MeV ^{24}Na peaks masks the short-lived gamma ray peak of ^{165}Dy , the gamma ray peak of the long-lived ^{153}Sm will grow relative to the ^{24}Na peak after multiple half-lives of ^{24}Na pass. Each batch of irradiated marsh samples was accompanied by standards of known Sm, Dy, and Na content.

Standard preparation

Standard preparation and interpretation is an integral part of core processing. A primary standard was prepared from nitrate salts of the rare earths, $\text{Dy}(\text{NO}_3)_3 \cdot 5\text{H}_2\text{O}$ (Stock #-Nucor Corp.-Dy-N-3-010) and $\text{Sm}(\text{NO}_3)_3 \cdot 6\text{H}_2\text{O}$ (Stock #-Nucor Corp.-Sm-N-026). Each of these salts in the crystalline form was ground with a mortar and pestle to a uniform particle size. Quantities of this preparation were placed in a CaCl_2 desiccator and the system was allowed to come to equilibrium for seven days. The water which forms an integral part of the molecular or crystal structure of a solid is classed as essential water. An equilibrium always exists between hydrated solid and anhydrous solid under a given set of conditions which include humidity, vapor pressure, and temperature. Therefore, it is not technically correct to assume that all of the crystalline material is hydrated under any given set of conditions. The purpose of placing the crystalline material in a desiccator is to allow the system to move to a stable equilibrium point so that the material will be homogeneous with respect to distribution of hydrated and anhydrous forms (Skoog and West 1969).

After 7 days, it was assumed that stable equilibrium conditions exist. At this point, 0.2699 g of the Dy salt and 0.2956 g of the Sm salt were weighed and placed in the same 1000-ml volumetric flask. Five ml of technical grade 16N HCl was added and the flask was brought up to volume with tap water. The acidic environment overcomes the tendency of the Dy and Sm to form hydroxide and carbonate precipitates. Tap water was used instead of distilled water for the reason that the resulting standard would be more similar to the matrices found in environmental samples. The resulting mixed primary standard was 100 ppm Dy and Sm, $\pm 10\%$. At the time of preparation, four samples of 1.5 g of each of the Dy and Sm salts were placed in crucibles for ignition and subsequent gravimetric analysis. The primary standard was used throughout the study. In this way, every separate data set is comparable to all others. Therefore, even though exact values of the standards may not be determined, the relative comparison of data sets is precise.

For the preparation of the secondary standards for INAA, 1-, 2-, 10-, an 20-ml aliquots of the primary standard were placed in 100-ml volumetric flasks. The secondary standards were brought up to volume with tap water after adding 1 ml of 16N HCl. An aliquot of 0.1 ml of each of the four secondary standards was pipetted into four 2/27th-dram (0.2ml) polyvials to make 0.1, 0.2, 1.0, and 2.0 μg standards. A reagent blank was prepared along with the standards in the same manner. Standards and reagent blanks were dried along with core samples and encapsulated for neutron irradiation as described in the "Sample preparation and neutron irradiation" section of this

chapter.

Data reduction

Spectral data are received from the reactor facility on a computer printout. There are two separate printouts for each sample vial representing gamma ray emissions detected from Dy-165 and Sm-153. By visual inspection two separate 10- to 12- channel portions of the 4000 channel spectrum are partitioned for analysis for the Dy and Sm photopeaks. These sections of the data represent the characteristic photopeaks of the tracers, which are usually Gaussian in nature (Figure 5.1).

Once the photopeak has been chosen, the data is loaded on a Lotus 1-2-3 spreadsheet (Table 5.1). The data base is then subjected to a number of calculations in which the net photopeak area for both Dy and Sm is determined (Covell, 1959), decay corrected, and reported as net cpm. This process is applied to both standards and samples. Once the cpm per ug of Dy and Sm in the series of standards has been determined, a least squares regression analysis is carried out, with ug Dy or Sm as the independent variable and net cpm as the dependent variable. The regression analysis on the standards includes a linear, logarithmic, exponential, and power curve fit. In nearly every case, the power curve gives the best correlation coefficient, and the best goodness of fit. The power curve fit is in the form $Y = B_0X^{B_1}$, where Y is cpm and X is ug of Dy and Sm. In this generalized form, if B_1 approaches 1, then the relationship between marker and cpm is a linear one. If B_1 departs significantly from 1,

then a nonlinear relationship is implied (Steel and Torrie, 1980). Usually, the relationship is significantly nonlinear. From this regression equation, cpm per sample is converted to ug of Dy or Sm, and this value is ultimately converted to ppm of Dy and Sm in the soil sample.

A 99% confidence interval for background levels of Dy and Sm in marsh soil samples has previously been determined using a Student's t -distribution (Steel and Torrie, 1980, p. 65). This background interval is subtracted from all values determined by the method described in this section of the thesis. This provides a method whereby random noise can effectively be partitioned from real signal.

Core data analysis: Scheme I (Modal analysis)

The types of distributions of the stable tracer horizon markers varies greatly among and within the experimental sites. Two classification schemes for the various types of distribution of marker have been developed for this study.

The first classification scheme is depicted in Figure 4.7 and observed marker distributions which are representative of this classification are shown in Figure 4.8. A Type I distribution is the ideal finding, where the marker is located unequivocally in a single 3-mm section of the core. Therefore, the mode and mean are identical and it is the center of the 3-mm section containing the marker that is reported for the depth. Eighteen percent of the cores sampled in this study are categorized as a Type I class.

A Type II distribution is divided into two subclasses: Type II A

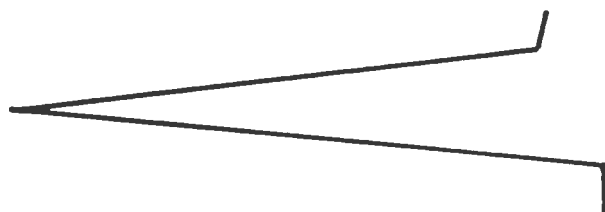
Figure 4.7. Idealized classification scheme applied to observed marker distributions.

TYPE I

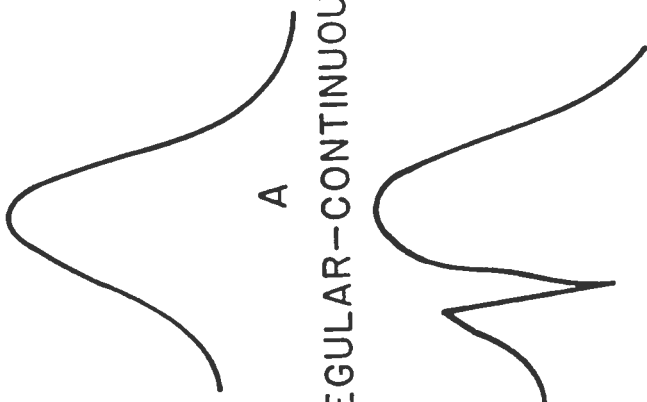
TYPE II

TYPE III

TYPE IV -- TYPE V



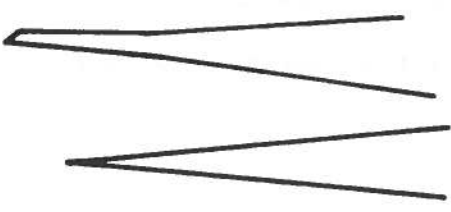
DISCRETE



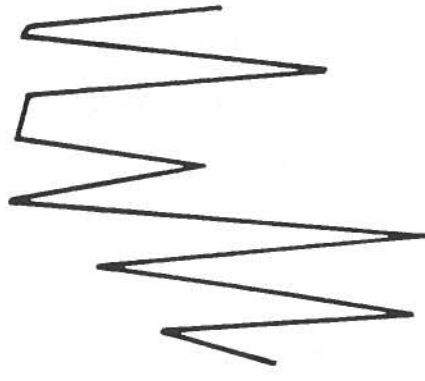
REGULAR--CONTINUOUS

B

IRREGULAR--CONTINUOUS



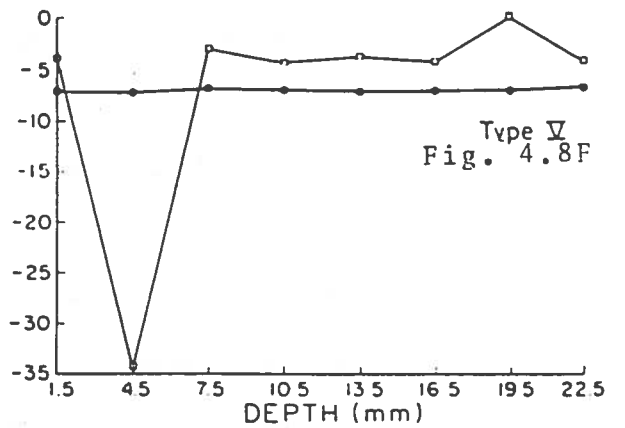
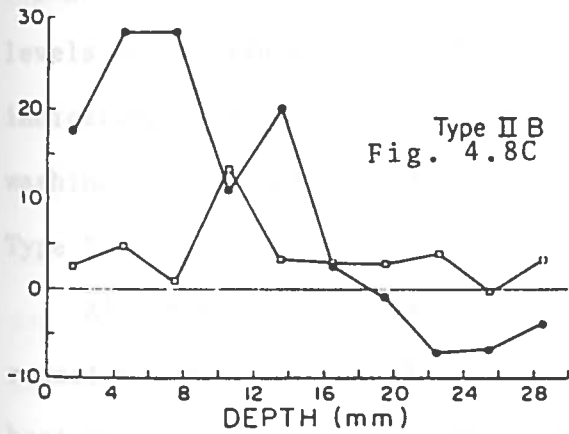
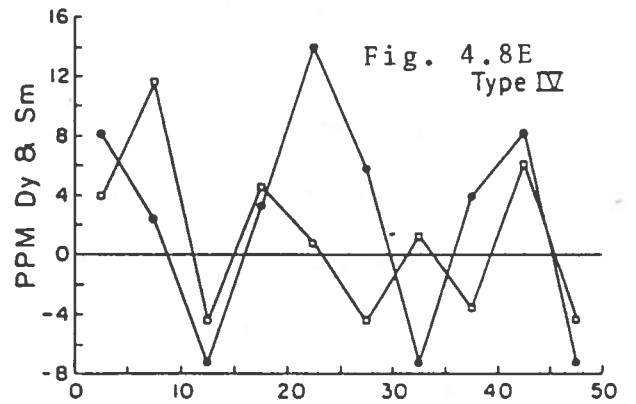
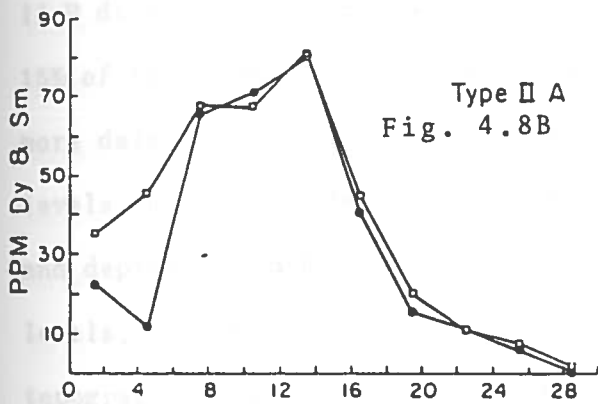
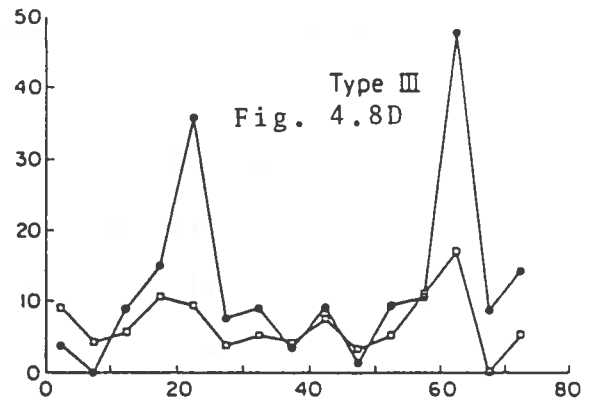
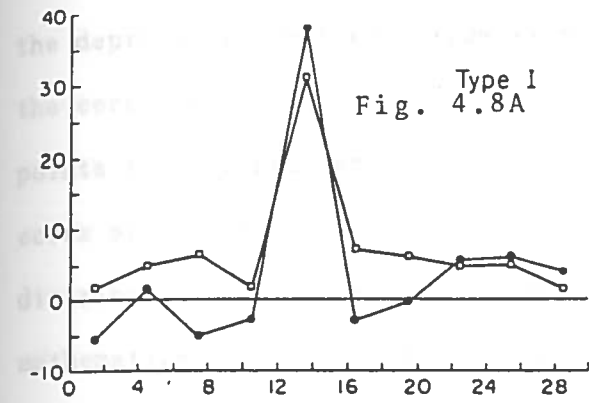
BIMODAL



CONFLUENT NONSENSE

Figure 4.8A-F. Observed marker distributions which demonstrate the utility of the classification scheme. Figure 4.8A shows a Type I discrete marker distribution, Figure 4.8B shows a Type IIA regular-continuous distribution, Figure 4.8C shows a Type IIB irregular-continuous distribution, Figure 4.8D shows a Type III bimodal distribution, Figure 4.8E shows a Type IV uninterpretable distribution above background levels, and Figure 4.8F shows a core which contains no marker above background levels. A negative ppm value indicates how far below the upper limit of the 99% confidence interval for background levels of Dy and Sm the datum is.

DISTRIBUTION OF Dy & Sm



○ PPM Dy
● PPM Sm

and Type II B. Type II A approximates a Gaussian distribution and the data can be fitted to an idealized binomial with the mean reported as the depth of the marker. Type II A distributions account for 42% of the cores sampled. Type II B is like Type II A, but has one or two points that do not easily fit the binomial. The depths of type II B cores are reported as the idealized binomial means of the distributions unless visual inspection leads one to believe that the mathematically determined mean is biased from the actual mean. Type II B distributions account for 9% of the cores. Type III accounts for 15% of the cores sampled, depicting two distinct peaks where two or more data points between the peaks register at or near background levels for the stable tracers. Type IV accounts for 8% of the cores and depicts a random distribution of the tracer above background levels, indicating either macro scale mixing, or uneven marsh surface topography where the sample was taken. Type V is like type IV, but levels of the tracer are within the expected background range, indicating a "miss" (unable to accurately relocate plot) or the washing away of marked sediments. Twenty percent of the cores are Type V.

All of the above core data are subjected to three separate reductions reported in Table 5.2. The first analysis is a binomial best fit model (Steel and Torrie, 1980, p. 524) A binomial distribution is fitted to the individual data points using a computer program which iterates to a best fit using a chi-squared goodness of fit criterion. The mean depth is calculated from the idealized binomial curve generated from the data points. If the distribution is

Type III, the binomial is fit to each distribution separately, and the mean of the peak with the greatest depth is reported.

The second data reduction technique is a visual inspection and selection of the depth at which the "apparent mode" occurs. The apparent mode is that point on the graph (tracer abundance vs. depth of tracer) which would probably be the data point with the greatest concentration if no "marker wash-in" occurred. Marker wash-in is a phenomenon which has been observed by others working with trace substances in the soil profile, particularly ^{137}Cs (Miller and Heit, 1986). It seems plausible that excess marker unavoidably sorbed to marsh vegetation during the application process may wash onto the surface of the treated experimental plots well after the original treatment or that annual vegetative dieback contributes sorbed marker to the marsh surface. In 85% of the cores analyzed, the apparent mode and the real mode are one and the same.

The third reduction is visual inspection and selection of the "break-point." The break-point is the depth at which the sharpest drop-off of marker occurs (the greatest negative change in slope). There is reason to believe that the break-point is biologically meaningful in at least some of the cores sampled and represents the depth at which biological mixing ceases to be a significant factor in tracer pulse distortion. This is based on the model presented in the next section of this thesis. In 50% of the cores analyzed, the depth at which the apparent mode and the breakpoint occur is identical.

Core data analysis: Scheme II (Dynamic analysis)

A mathematical model first developed by Guinasso and Schink (1975) is adapted as the framework for the second classification scheme. In general, the model describes the behavior of a "conservative" tracer pulse as it propagates through a biological mixing layer into more stable layers of sediment below. A conservative tracer is used here in the sense that it is non-radioactive, chemically stable, and biologically inert. The analytical form of the model is derived from the general diffusion-advection equation:

$$\frac{\delta c}{\delta t} = D \frac{\delta^2 c}{\delta x^2} - v \frac{\delta c}{\delta x} \quad (\text{Eq. 4.2})$$

where: $c(x,t)$ is the concentration of tracer (dimensionless), D is the eddy diffusion coefficient ($\text{cm}^2 \cdot \text{yr}^{-1}$), v is the sedimentation rate, x is depth from the surface increasing downward (cm) and t is time (yr). The paper by Guinasso and Schink (1975) gives an excellent treatment of the derivation of the analytical solution (Eq. 4.3) from Eq. 4.2. The reader is referred to that paper for further detail which is beyond the scope of this thesis. The rigorous form of the analytical solution is as follows:

$$c(x^*, t^*) = \exp\left(\frac{x^*}{2G} - \frac{t^*}{4G}\right) \cdot \sum_{n=1}^{\infty} \left(\frac{1}{\beta_n} \left(\cos \alpha_n x^* + \frac{1}{2G\alpha_n} \sin \alpha_n x^* \right) \cdot \exp(-G\alpha_n^2 t^*) \right) \quad (\text{Eq. 4.3})$$

where: $\alpha_n - (1/(4G^2)) - (\alpha_n/G) \cot \alpha_n = 0$ (Eq. 4.4)

$\beta_n = 1/2 + \frac{1}{2G\alpha_n^2} + \frac{1}{8G^2\alpha_n^2}$ (Eq. 4.5)

In the above equation, x^* is a dimensionless relative depth unit, t^* is a dimensionless relative time unit, and G is a dimensionless mixing parameter defined by the following variables:

$$G = \frac{D}{LV} \quad (\text{Eq. 4.6})$$

where D is the eddy diffusion coefficient ($\text{cm}^2 \cdot \text{yr}^{-1}$) and represents the gaussian mixing analog, L is the depth of the mixing layer (cm), and V is the sedimentation velocity ($\text{cm} \cdot \text{yr}^{-1}$). The above model is derived in detail from first principle partial differential equations in the paper by Guinasso and Schink (1975) and an excellent explanation given of the concepts involved in detail. It is not possible to give an in-depth treatment of the model here because of time and space limitations, and it is really beyond the scope of this thesis. However, a practical application without undue complexities is presented in the following paragraphs.

The model (Eq. 4.3) is largely dependent on the magnitude of the G parameter. As the G parameter increases in magnitude, both σ (the standard deviation) and the kurtosis (skewness) of the original marker pulse will also increase in magnitude with depth and time. The degree of kurtosis is of primary importance in this model since it implies deviation of the visible mode from the actual depth of deposition. Kurtosis does not begin to occur until the mode of the original tracer

pulse passes through the biological mixing layer (Fig. 4.9A-B). It is important to note that even though D may be large (representing a high rate of biological mixing), little distortion will be seen if the sedimentation velocity is high (Eq. 4.6). Conversely, even if D is small (representing a low rate of biological mixing), large distortion will be seen if sedimentation velocity is also relatively low.

The above model (Eq. 4.3) implies that there is complete ambiguity in the interpretation of a given distribution of tracer with depth. For instance, if one does not have estimates for D and L , V cannot be ascertained. As the model is thus far presented, it seems to suggest intractable problems in determination of sedimentation rates.

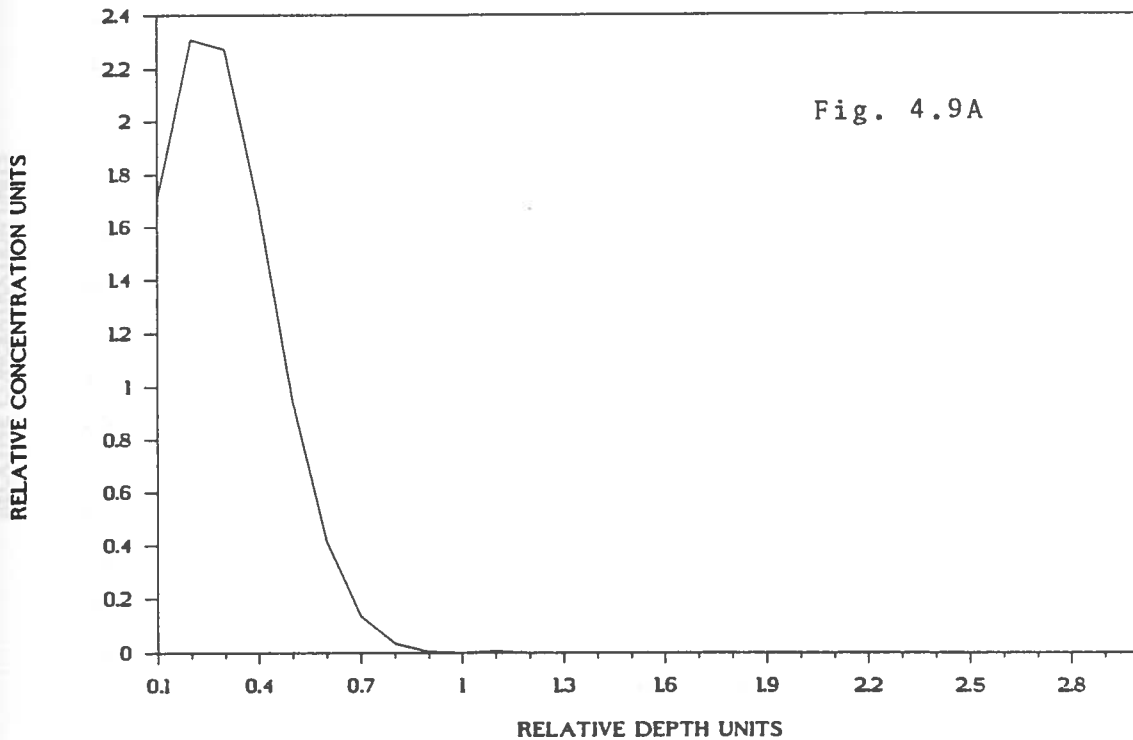
However, it can be mathematically demonstrated that the *weighted mean depth* is always equal to $V \cdot T$, or the weighted mean depth is where we would expect to find the initial impulse concentration if no mixing took place (Guinasso and Schink, 1975). This value represents the actual sedimentation.

A series of figures (Fig. 4.9A-F and 4.10A-F) demonstrate the behavior of the original marker pulse with time under two different mixing conditions, $G = 0.10$ and $G = 0.30$. The biological mixing in the 4.9A-F figures is 3 times less than that in the 4.10A-F figures. As time progresses, one can see that the system with the largest mixing parameter tends to spread more, and in the final graphs of the series (Fig. 4.9F and Fig. 4.10F), it can be seen that the two modes are markedly displaced from one another, even though there is identical sedimentation velocity, mixing depth, and time. What is actually occurring in terms of the model is that as G approaches 10,

Figure 4.9A-F and 4.10A-F. A computer model generated series of marker distributions. The 4.9A-F series shows a marker pulse moving through a soil profile with nominal mixing ($G=0.1$). The 4.10A-F series corresponds directly with the 4.9A-F series except that the marker pulse is moving through a soil profile with moderate mixing ($G=0.30$). Note the greater distortion of the marker distribution and greater bias away from the actual sedimentation (time is equivalent to sedimentation) in the 4.10A-F series. Relative depth units are on the x-axis and relative concentration units are on the y-axis. The area under the curve of concentration vs. depth of each tracer at any time after $t=0.0$ is unity (1.0).

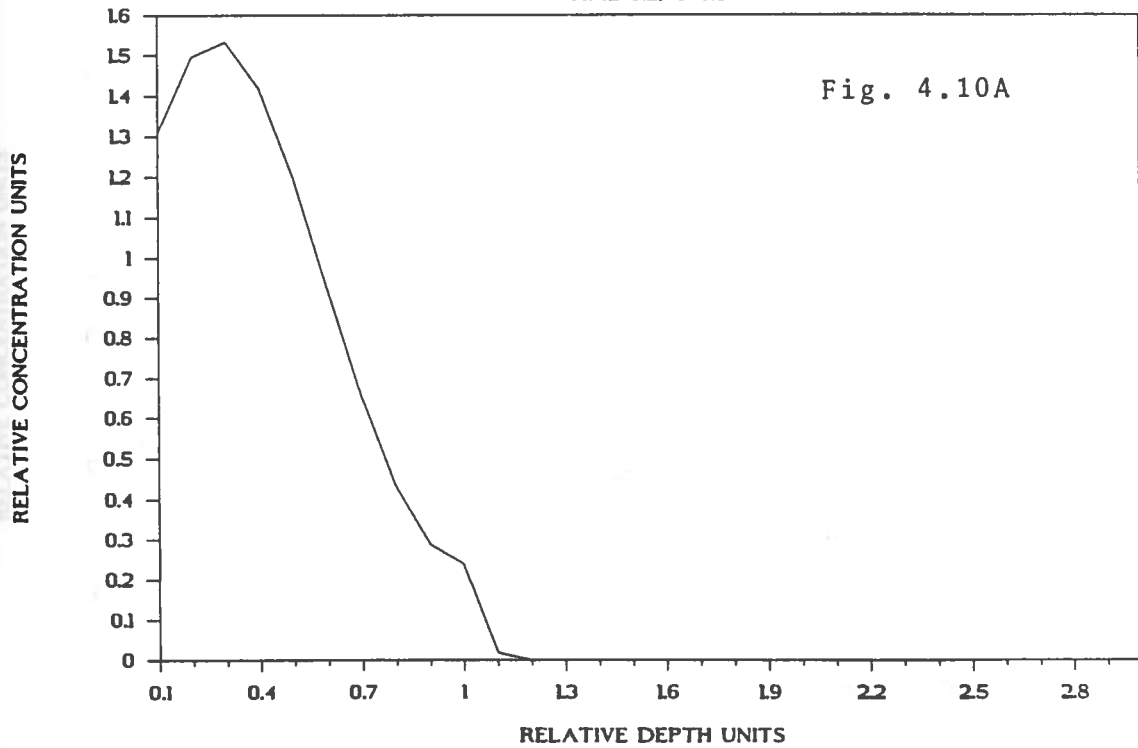
CONCENTRATION vs. DEPTH

TIME-0.2 G-0.1



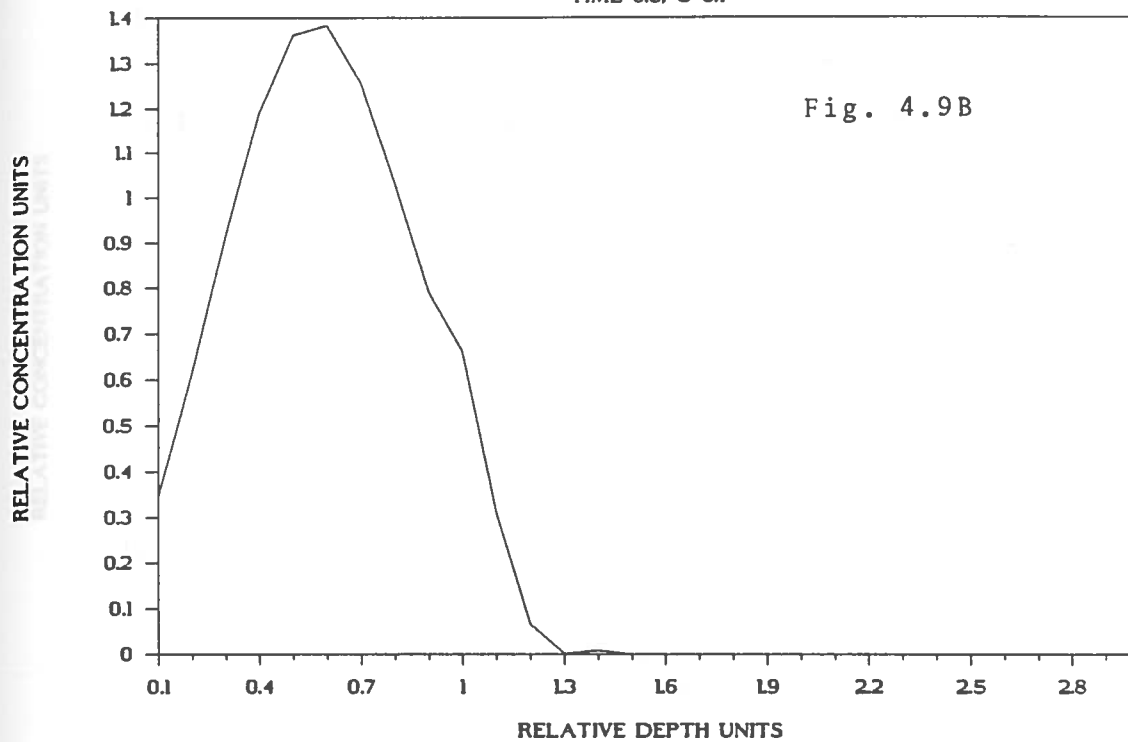
CONCENTRATION vs. DEPTH

TIME-0.2 G-0.3



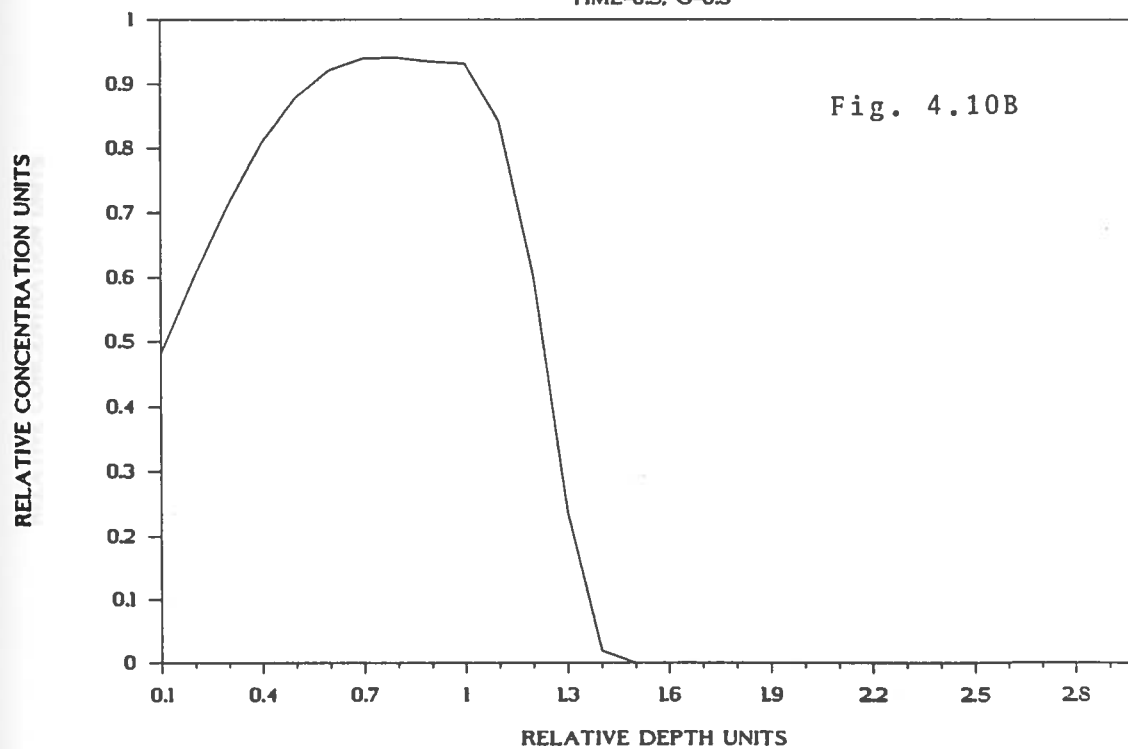
CONCENTRATION vs. DEPTH

TIME-0.5, G-0.1



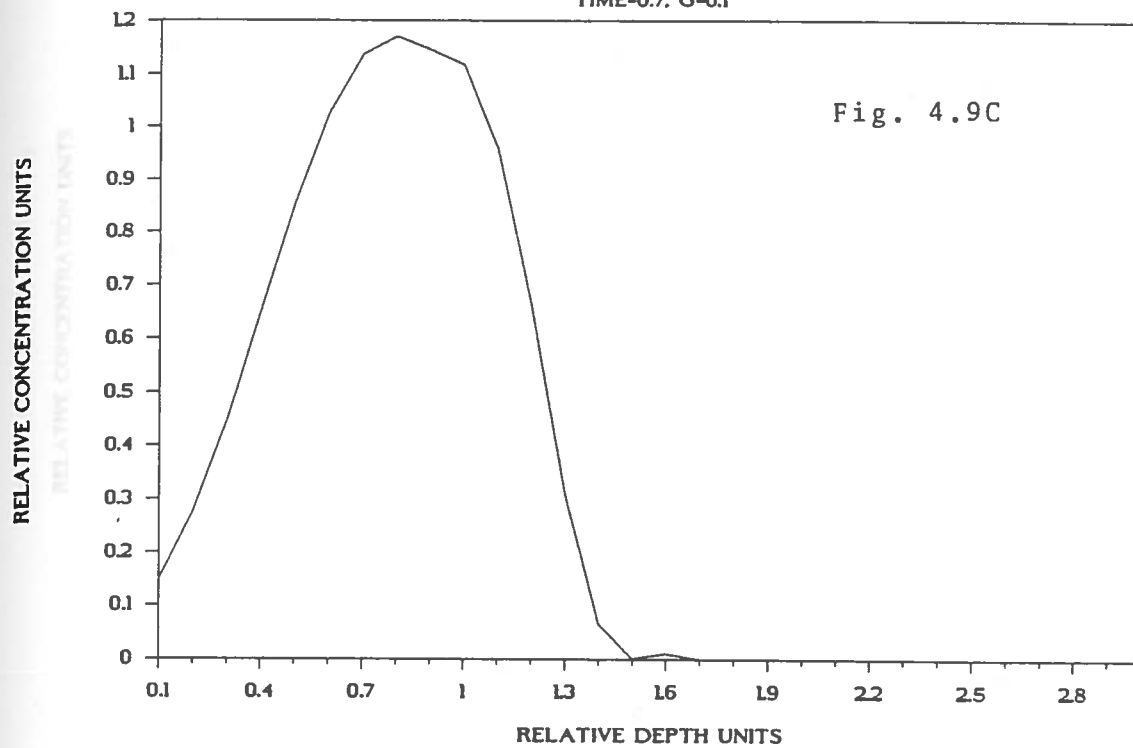
CONCENTRATION vs. DEPTH

TIME-0.5, G-0.3



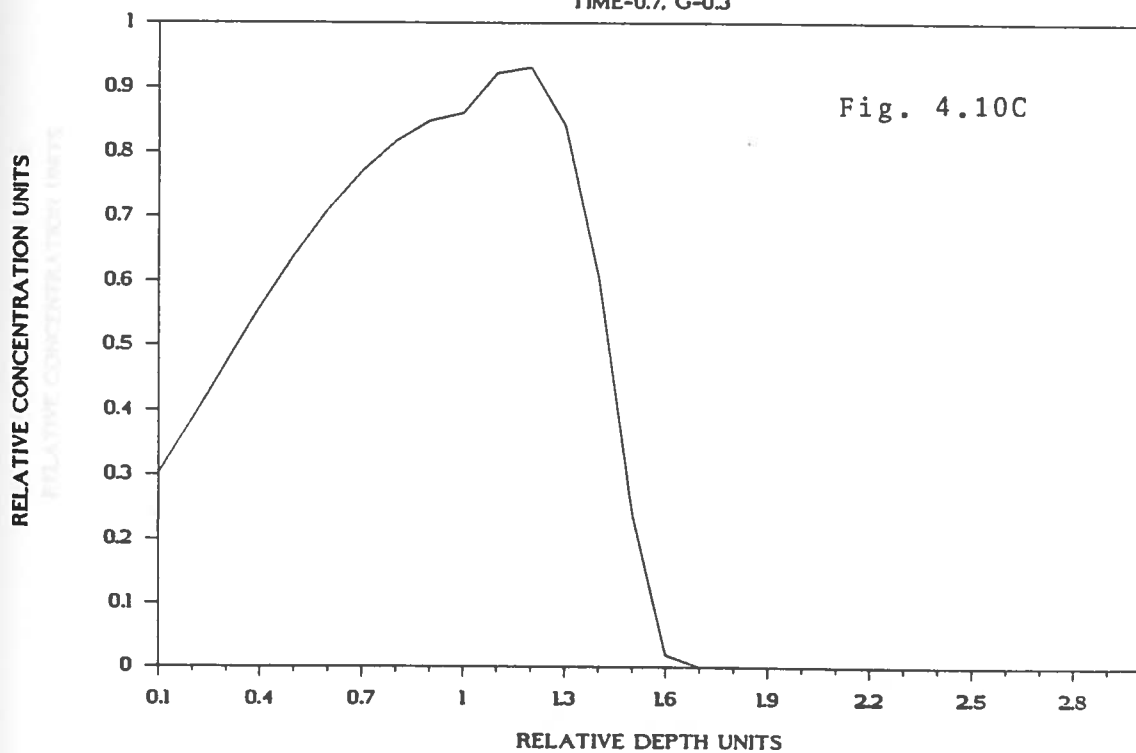
CONCENTRATION vs. DEPTH

TIME-0.7, G-0.1



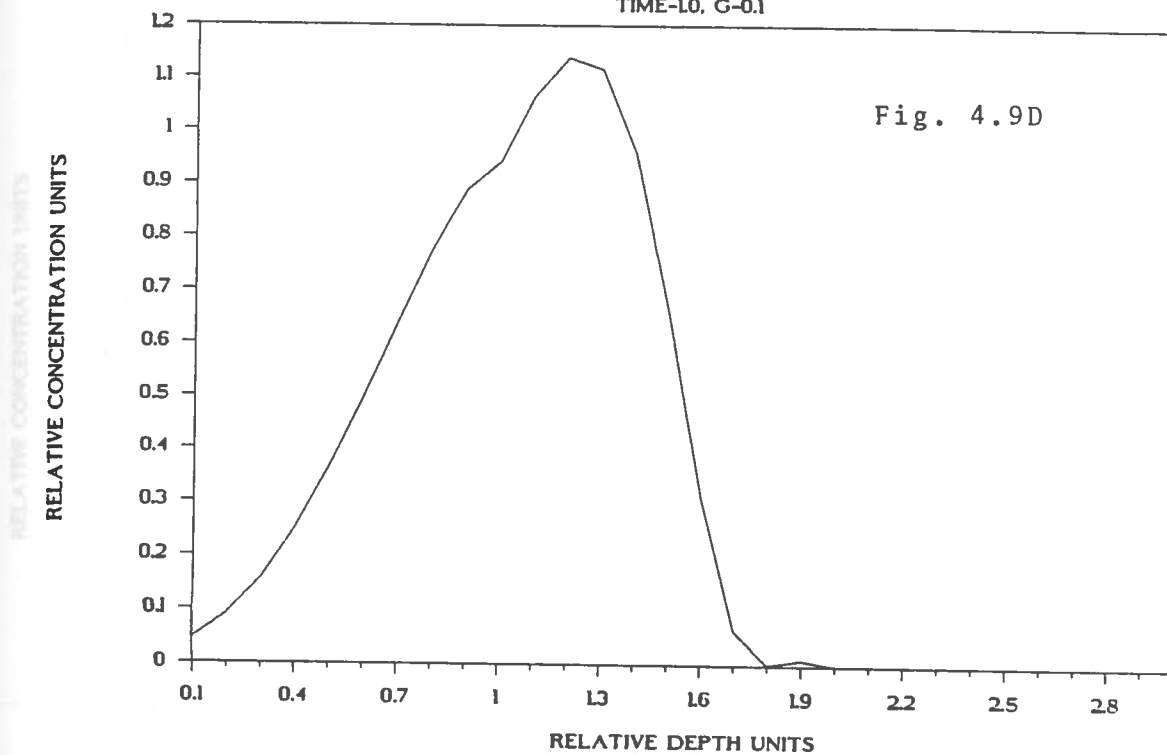
CONCENTRATION vs. DEPTH

TIME-0.7, G-0.3



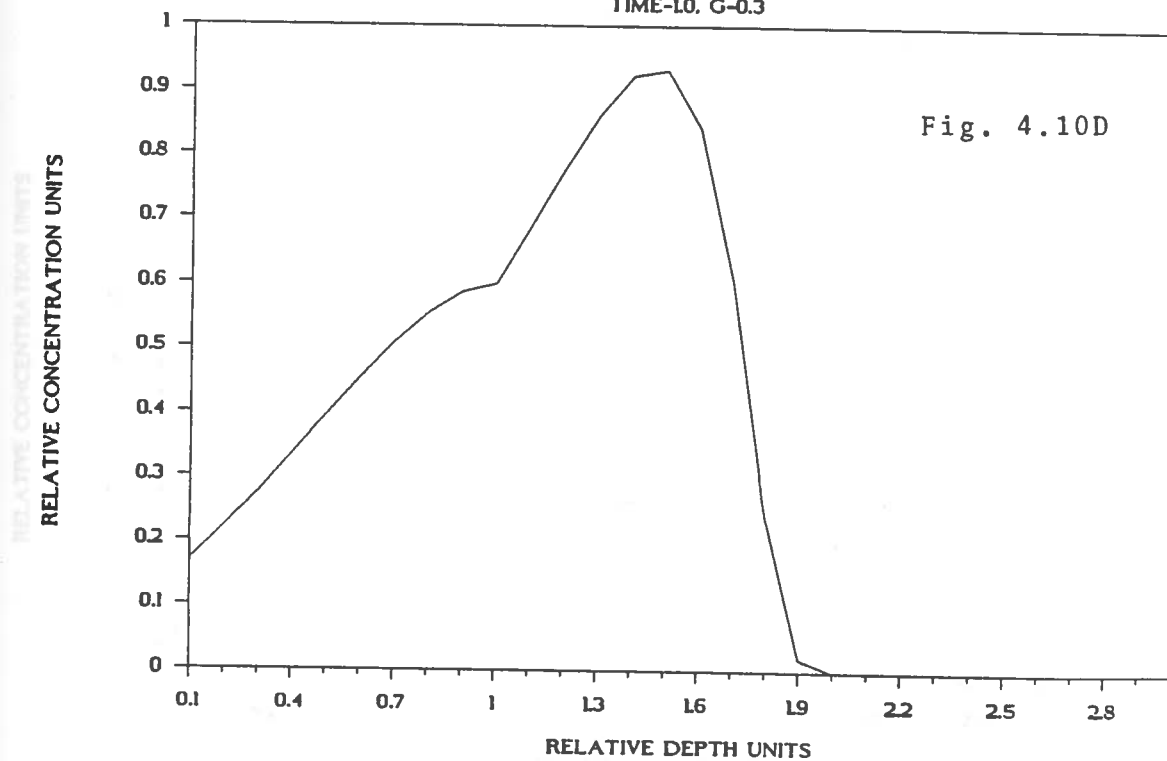
CONCENTRATION vs. DEPTH

TIME-10, G-0.1



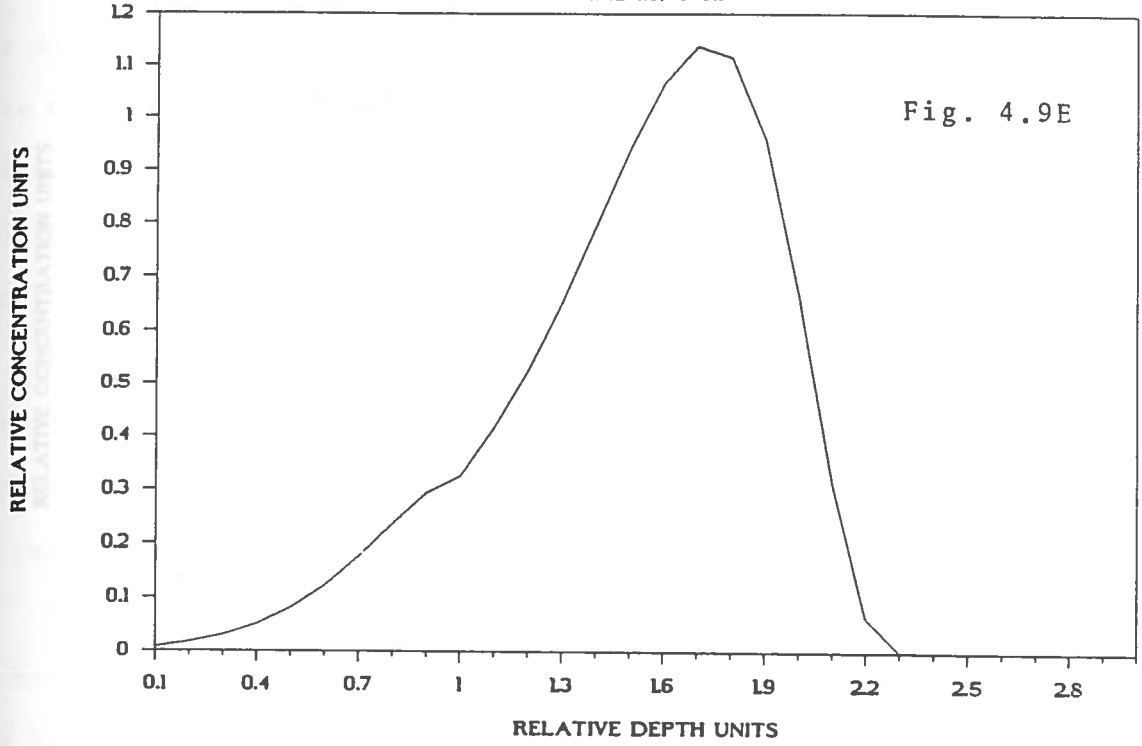
CONCENTRATION vs. DEPTH

TIME-10, G-0.3



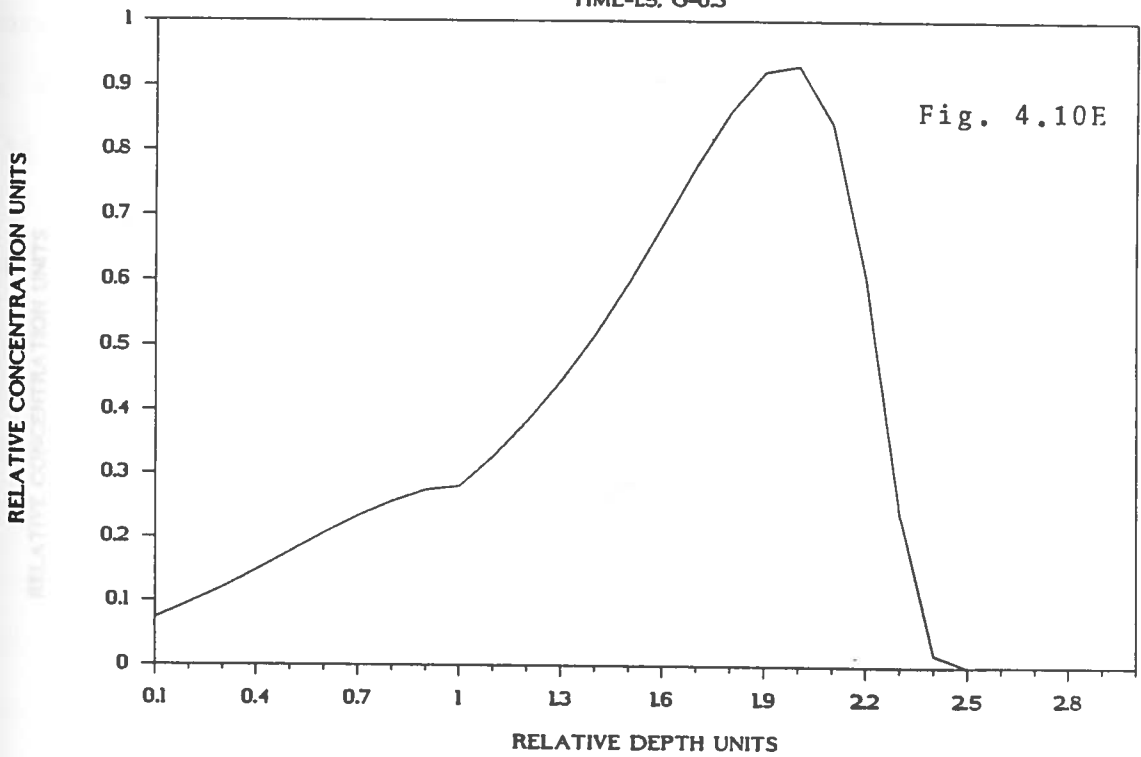
CONCENTRATION vs. DEPTH

TIME-1.5, G-0.1



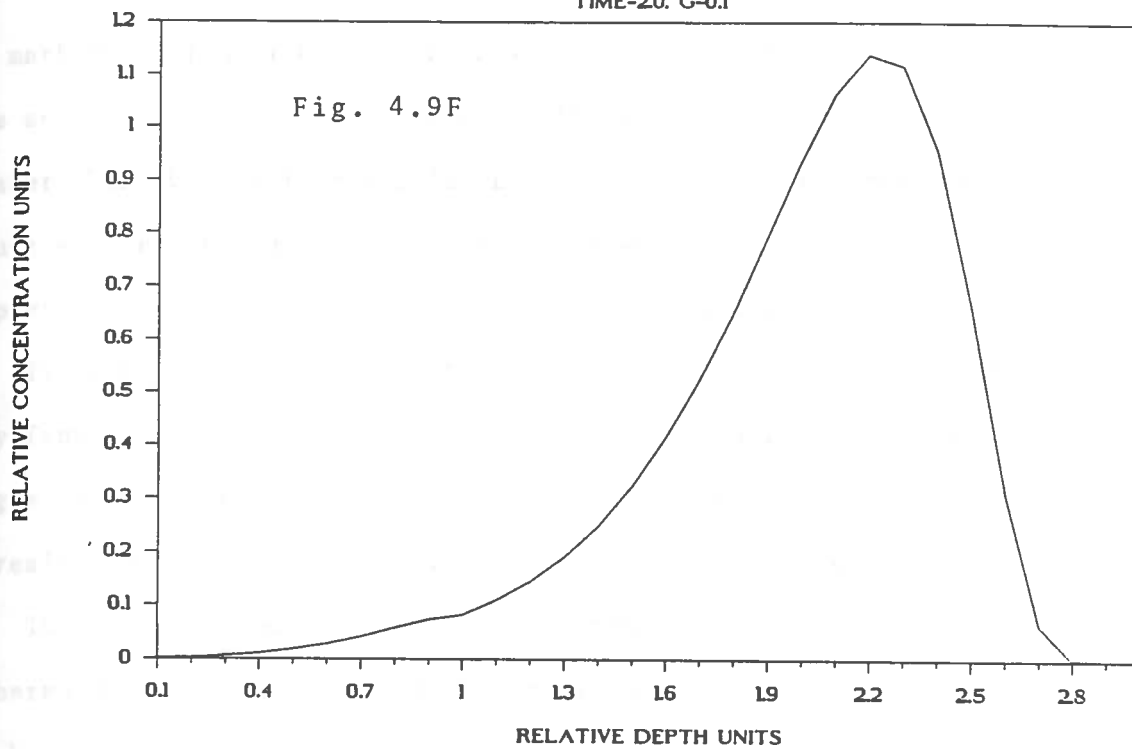
CONCENTRATION vs. DEPTH

TIME-1.5, G-0.3



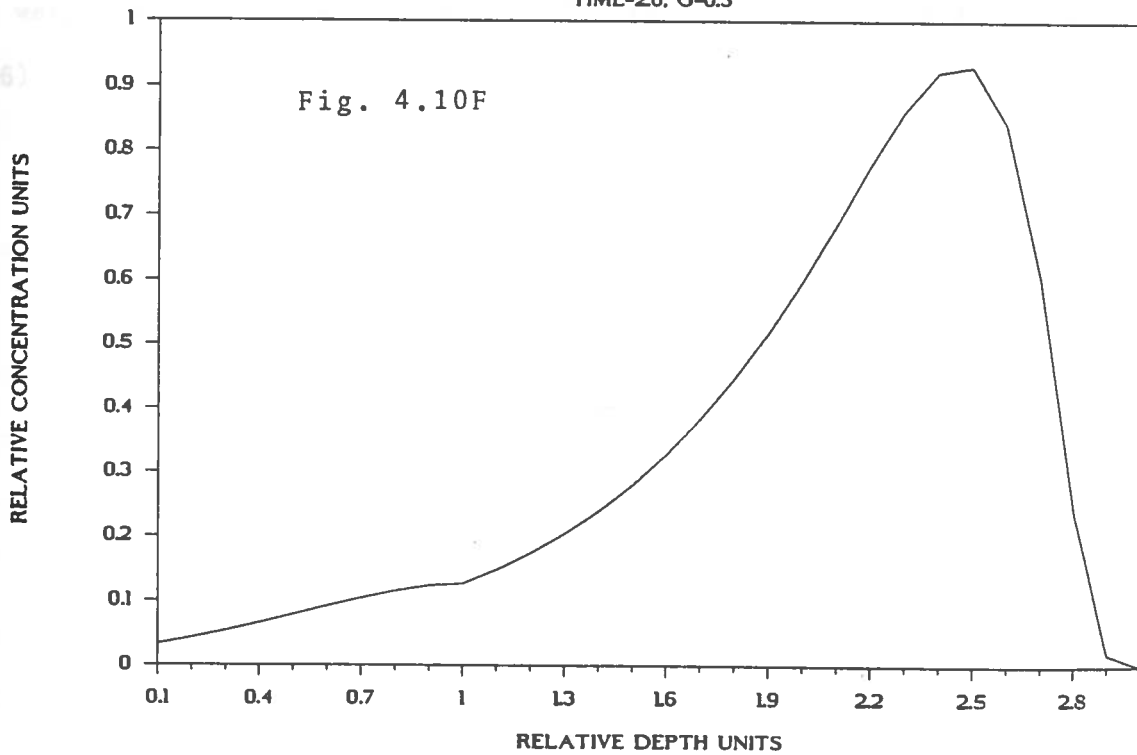
CONCENTRATION vs. DEPTH

TIME-20. G-01



CONCENTRATION vs. DEPTH

TIME-20. G-03



the marker distribution becomes less and less gaussian in nature and more and more exponential in nature with increasing time. When G is greater than 10, the tracer pulse essentially loses its gaussian nature and becomes purely exponential. When this is the case, complete homogeneity of the tracer in the mixing layer occurs.

It seems counterintuitive that the mode of the tracer can move away from its original "position" in the soil profile. The single mixing-layer model has serious implications if it has a basis in reality where wetland accretion processes are concerned.

The model as represented above was applied to the actual data gathered during this study. Marker distributions were reclassified on the basis of the " G " parameter as determined by visual goodness of fit application of the model (Fig. 5.15). Furthermore, depths of accretion were determined using the weighted mean depth criterion mentioned above. The depths as determined by the two techniques (modal analysis vs. weighted depth) were contrasted and compared (Table 5.4 and Figure 5.16).

CHAPTER 5

RESULTS

Initial data processing

The following results are examples taken from the large body of samples collected during this study. It is impractical to present and discuss each of the 71 cores collected and analysed. A graphic representation of each core can be found in Appendix A. Table 5.1 is a copy of a representative spreadsheet which shows how data for an individual core are processed. The core which is represented in table 5.1 comes from a sampling at Leeville, LA on 15 Dec. 1986. In this core, 12-3 mm segments were sectioned, dried and weighed. The depth for each sample was considered to be intermediate in each 3 mm section, so that the first 3 mm segment represents a depth of 1.5 mm. Only the dysprosium spectral data are shown. The energy window which was selected for the detection of the gamma photon of interest is 90.40 keV to 98.39 keV with the centroid occurring at 94.7 keV. Figure 5.1 shows the spectral peaks of the first 4-3 mm segments. The spreadsheet program calculates the Compton continuum level, subtracts it from the photopeak area, yielding net photopeak area. This area is corrected for decay back to the end of neutron activation. The corrected cpm is converted to μg of Dy after a least squares regression analysis is run on the standards which are usually 0.1, 0.2, 1.0, and 2.0 μg of Dy. The value in μg Dy is then divided by the

Table 5.1- Data exactly as it is tabulated on the Lotus 123 Spreadsheet program used for spectral data reduction.

LEEB86-12/15/86

TAMU PORTION OF LEEVILLE 12/15/86

*- ASTERISK MEANS A VALUE MUST BE ENTERED INTO RESPECTIVE CELL

SAMPLE NAME*	CORES SITE-3E.// LSN 2(50-M)				
	5-1	5-2	5-3	5-4	5-5
SAMPLE NUMBER*					
WT. EMPTY VIAL (GM)*	0.2912	0.2912	0.2989	0.2984	0.3004
WT VIAL + SAMPLE (GM)*	0.3057	0.3038	0.3208	0.3227	0.33
NET SAMPLE WEIGHT (GM)	0.0145	0.0126	0.0219	0.0243	0.0296
DEPTH (MM)*	1.5	4.5	7.5	10.5	13.5
†	5-1	5-2	5-3	5-4	5-5
1RST CHAN. DY (COUNTS)*	544	399	828	954	1839
LAST CHAN. DY (COUNTS)*	571	398	799	949	2327
COUNT TIME DY (MIN)*	3	3	3	3	3
ELAPSED TIME DY (MIN)*	372	378	325	332	321
†	5-1	5-2	5-3	5-4	5-5
1RST CHAN. SM (COUNTS)*	474	450	384	1571	555
LAST CHAN. SM (COUNTS)*	406	393	649	3850	467
COUNT TIME SM (MIN)*	5	5	5	5	5
ELAPSED TIME SM (MIN)*	8492	7244	3199	4546	7228
†	5-1	5-2	5-3	5-4	5-5
† CHAN. DY	16	16	16	16	16
† CHAN. SM	14	14	14	14	14
INTEGRAL DY (TOTAL COUNTS)	13901	10805	22126	25363	63934
INTEGRAL SM (TOTAL COUNTS)	22650	24114	16025	96034	28085
DECAY CORR. DY (CPM)	10496.61	9615.134	15207.85	17523.24	8142.185
DECAY CORR. SM (CPM)	26939.28	21852.33	3879.937	35760.20	25014.26
CALCULATED ug DY	7.587469	6.880536	11.47183	13.43560	5.716146
CALCULATED ug SM	8.329563	6.932084	1.520952	10.68002	7.804889
PPM DY	523.2737	546.0743	523.8279	552.9054	193.1130
PPM SM	574.4526	550.1654	69.44990	439.5071	263.6787
BACKGND CORR. PPM DY	518.8737	541.6743	519.4279	548.5054	188.7130
BACKGND CORR. PPM SM	567.2526	542.9654	62.24990	432.3071	256.4787

Dysprosium counts	5-1	5-2	5-3	5-4	5-5
Arbitrary chan. †					
1	544	399	828	954	1839
2	533	418	842	973	2061
3	582	420	903	978	2421
4	677	486	947	1176	3003
5	754	583	1238	1458	3768
6	951	674	1574	1836	5140
7	1292	1009	2119	2312	6677
8	1545	1244	2449	2846	7733
9	1511	1265	2607	2921	7642
10	1352	1117	2228	2534	6159
11	1061	853	1603	1906	4489
12	778	594	1313	1457	3486
13	648	510	1024	1178	2648
14	546	437	863	988	2388
15	556	398	789	897	2153
16	571	398	799	949	2327

Table 5.1 continued

LEEB86-12/15/86

TAMU PORTION OF LEEVILLE 12/15/86

*-- ASTERISK MEANS A VALUE MUST BE ENTERED INTO RESPECTIVE CELL

SAMPLE NAME*	5-6	5-7	5-8	5-9	5-10
SAMPLE NUMBER*					
WT. EMPTY VIAL (GM)*	0.2989	0.2939	0.3004	0.2904	0.294
WT VIAL + SAMPLE (GM)*	0.4078	0.3887	0.405	0.3626	0.3156
NET SAMPLE WEIGHT (GM)	0.1089	0.0948	0.1046	0.0722	0.0216
DEPTH (MM)*	16.5	19.5	22.5	25.5	28.5
†	5-6	5-7	5-8	5-9	5-10
1RST CHAN. DY (COUNTS)*	1390	1164	1094	4100	819
LAST CHAN. DY (COUNTS)*	1337	1222	1158	3979	838
COUNT TIME DY (MIN)*	3	3	3	3	3
ELAPSED TIME DY (MIN)*	329	371	376	233	287
†	5-6	5-7	5-8	5-9	5-10
1RST CHAN. SM (COUNTS)*	554	392	286	189	129
LAST CHAN. SM (COUNTS)*	450	328	211	196	123
COUNT TIME SM (MIN)*	5	5	5	5	5
ELAPSED TIME SM (MIN)*	7219	8609	8576	7157	7170
†	5-6	5-7	5-8	5-9	5-10
‡ CHAN. DY	16	16	16	16	16
‡ CHAN. SM	14	14	14	14	14
INTEGRAL DY (TOTAL COUNTS)	27894	23215	20682	84592	19989
INTEGRAL SM (TOTAL COUNTS)	24711	18608	11054	7696	5098
DECAY CORR. DY (CPM)	10349.55	8653.948	5730.653	1954.065	1513.375
DECAY CORR. SM (CPM)	21085.65	22816.46	12634.86	5872.572	3927.656
CALCULATED ug DY	7.469037	6.118163	3.863890	1.164191	0.875523
CALCULATED ug SM	6.718192	7.199764	4.286200	2.188148	1.537355
PPM DY	68.58620	64.53758	36.93967	16.12453	40.53350
PPM SM	61.69138	75.94687	40.97705	30.30676	71.17388
BACKGND CORR. PPM DY	64.18620	60.13758	32.53967	11.72453	36.13350
BACKGND CORR. PPM SM	54.49138	68.74687	33.77705	23.10676	63.97388

Dysprosium counts Arbitrary chan. †	5-6	5-7	5-8	5-9	5-10
1	1390	1164	1094	4100	819
2	1381	1158	1099	4352	810
3	1442	1170	1100	4912	861
4	1519	1291	1206	5651	1068
5	1664	1451	1239	6394	1212
6	1960	1519	1337	7183	1516
7	2291	1869	1523	7394	1776
8	2490	2002	1616	7201	2066
9	2465	1963	1627	6533	2089
10	2231	1854	1471	5706	1692
11	1881	1589	1404	4942	1418
12	1677	1380	1376	4399	1104
13	1403	1286	1171	4016	1028
14	1454	1151	1133	3958	848
15	1309	1146	1128	3872	844
16	1337	1222	1158	3979	838

Table 5.1 continued

LEEB86-12/15/86

TAMU PORTION OF LEEVILLE 12/15/86

*- ASTERISK MEANS A VALUE MUST BE ENTERED INTO RESPECTIVE CELL

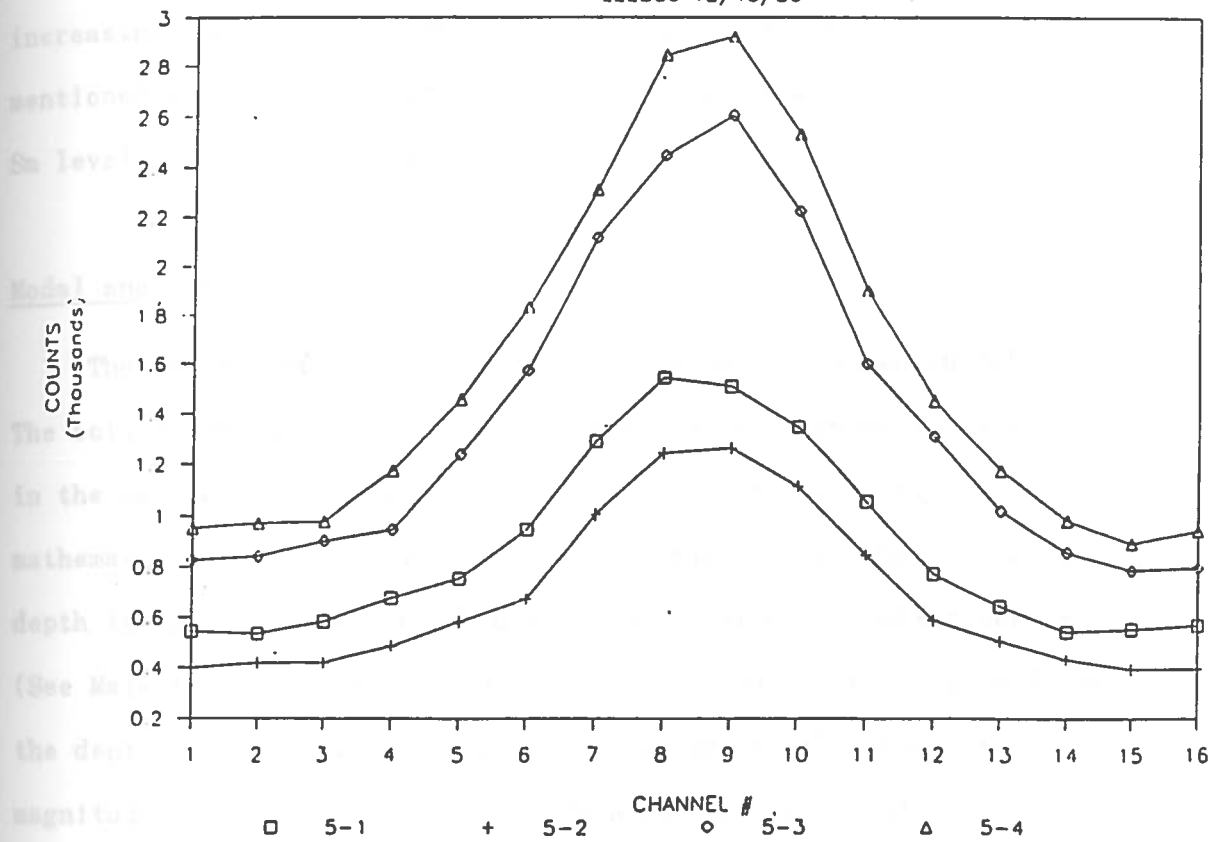
SAMPLE NAME*	5-11	5-12	BL.
SAMPLE NUMBER*			
WT. EMPTY VIAL (GM)*	0.3001	0.2993	0.2975
WT VIAL + SAMPLE (GM)*	0.3094	0.3161	0.2978
NET SAMPLE WEIGHT (GM)	0.0093	0.0168	0.0003
DEPTH (MM)*	31.5	34.5	39
†	5-11	5-12	5-13
1RST CHAN. DY (COUNTS)*	131	232	50
LAST CHAN. DY (COUNTS)*	137	234	29
COUNT TIME DY (MIN)*	3	3	3
ELAPSED TIME DY (MIN)*	367	375	209
†	5-11	5-12	5-13
1RST CHAN. SM (COUNTS)*	34	35	9
LAST CHAN. SM (COUNTS)*	33	31	10
COUNT TIME SM (MIN)*	5	5	5
ELAPSED TIME SM (MIN)*	7136	8549	7185
†	5-11	5-12	5-13
† CHAN. DY	16	16	16
† CHAN. SM	14	15	15
INTEGRAL DY (TOTAL COUNTS)	2265	3897	617
INTEGRAL SM (TOTAL COUNTS)	951	733	197
DECAY CORR. DY (CPM)	248.7447	361.4746	-1.30377
DECAY CORR. SM (CPM)	563.0707	394.3345	64.44297
CALCULATED ug DY	0.116921	0.177371	ERR
CALCULATED ug SM	0.279579	0.204526	0.041725
PPM DY	12.57216	10.55783	ERR
PPM SM	30.06227	12.17422	139.0834
BACKGND CORR. PPM DY	8.172167	6.157839	-4.4
BACKGND CORR. PPM SM	22.86227	4.974222	131.8834

Dysprosium counts	5-11	5-12	5-13
Arbitrary chan. †			
1	131	232	50
2	128	232	33
3	135	237	36
4	144	248	35
5	149	234	45
6	125	216	40
7	130	251	39
8	163	261	47
9	148	232	44
10	164	256	46
11	153	266	39
12	137	238	42
13	143	259	33
14	146	250	37
15	132	251	22
16	137	234	29

Figure 5.1. Typical gamma ray spectral data from 4 segments of a core. This data is adjusted for Compton continuum and converted to counts per minute (cpm), decay corrected back to the end of activation, compared to reference standards, and reported as ppm Dy present at the particular depth in the soil profile.

SPECTRAL DATA DY

LEEB86 12/15/86



dry weight of the sample segment to determine ppm Dy. The 99% confidence interval for background levels of Dy is automatically subtracted from this value which is then graphed on the y-axis against increasing depth on the x-axis (Figure 5.2). The entire process mentioned above is also carried out for analysis and determination of Sm levels in the soil sample.

Modal analysis

The summary of the extensive core analysis is shown in Table 5.2. The soil graphs which were used for this summary appear in Appendix A in the same order they appear in Table 5.2. The binomial depth is the mathematically determined mean depth and the mode is that point or depth in the core where the highest concentration of marker occurs (See Materials and Methods, *Core data; modal analysis*). The mode is the depth on the soil graph which corresponds to the greatest magnitude in ppm Dy or Sm. The breakpoint is that point at which the greatest negative slope occurs in the marker distribution. It was often difficult to determine this point with accuracy and it is therefore somewhat subjective and open to interpretation. It should be noted that the breakpoint did not appear to be of any biological or physical significance and is included here for reference only. The class refers to the classification scheme presented in Chapter 4 of this thesis in the *Modal analysis* section. The average modes is an average of the two modes represented by Dy and Sm. Occasionally, the mode of the observed distribution of Dy was different than that of the observed Sm distribution.

Figure 5.2. The final result of spectral data reduction is the marker distribution graph. Increasing depth is shown on the x-axis and marker concentration (Dy and Sm) on the y-axis.

DISTRIBUTION OF DY & SM

LEEB86 (LSN-2 (50-M)) 12/15/86

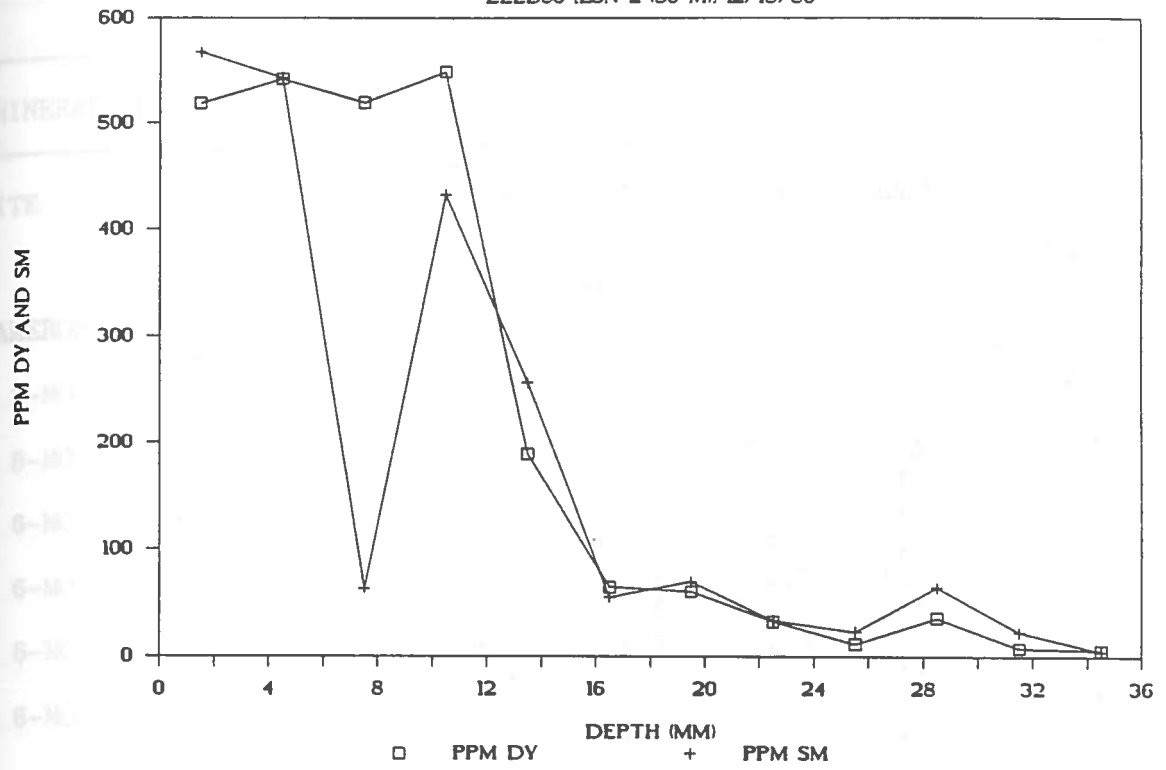


Table 5.2- Results from 6-month and 1-yr cores for MMS study sites and variable times for other sites. The text contains an explanation of the headings used below.

MINERALS MANAGEMENT SERVICE STUDY						
SITE		BINOM.	MODE	BREAK PT.	CLASS	AVG. MODES
		DEPTH(MM)				
		DY SM	DY SM	DY SM	DY SM	DY & SM (mm/yr)
CAMERON						(mm/6 mo.)
	7/8/87					
8-MO	CBN 1	11.8	7.5	7.5	IIA	5.6
		11.2	7.5	7.5	IIA	
8-MO	CBN-2-S	10.0	13.5	13.5	IIA	10.1
		9.7	13.5	13.5	IIA	
6-MO	CBNr 1	7.3	7.5	7.5	I	7.5
		7.3	7.5	7.5	I	
6-MO	CBNr 2	9.0	1.5	1.5	IIA	1.5
		8.7	1.5	1.5	IIA	
6-MO	CBC 1	9.1	1.5	1.5	IIA	1.5
		8.9	1.5	1.5	IIA	
6-MO	CBC 2	10.1	4.5	4.5	I	4.5
		9.8	4.5	4.5	I	
LEEVILLE						(mm/6 mo.)
	12/15/86					
6-MO	LSC TRANS. (0-M)	N/A	1.5	1.5	I	1.5
		N/A	1.5	1.5	I	
6-MO	LSC TRAN(BRG)15M	-	-	-	V	-
		-	-	-	V	
6-MO	LSC TRAN(STRM)35	-	-	-	V	-
		-	-	-	V	
6-MO	LSN 1	5.7	7.5	7.5	I	7.5
		6.2	7.5	7.5	I	
6-MO	LSN 2	8.5	10.5	10.5	IIA	10.5
		8.6	10.5	10.5	IIB	
6-MO	LSN 3	8.2	4.5	13.5	IIA	4.5
		8.6	4.5	4.5	IIA	
6-MO	LSCd 2	11.0	7.5	10.5	IIA	7.5
		11.3	7.5	7.5	IIA	
	5/13/87 & 6/11/87					
6-MO	LSN TRAN (0-M)JU	9.1	7.5	10.5	IIA	7.5
		9.1	7.5	10.5	IIA	
6-MO	LSN TRAN(10-M)JU	10.7	13.5	10.5	IIA	13.5
		10.7	13.5	10.5	IIA	
6-MO	LSN TRAN(30-M)JU	9.2	7.5	7.5	IIA	6.0
		10.3	4.5	4.5	IIB	
6-MO	LSN TRAN(50-M)JU	10.6	7.5	7.5	IIA	7.5
		7.0	7.5	7.5	IIA	
6-MO	LSCd 3 (50-M) JU	9.8	7.5	10.5	IIA	7.5
		9.8	7.5	10.5	IIA	
6-MO	LSC 2 WEST MAY	7.5	7.5	-	IIA	7.5
		7.5	7.5	-	IIA	
6-MO	LSC 2 EAST MAY	4.6	4.5	4.5	I	4.5
		6.2	4.5	4.5	IIA	

Table 5.2 continued

MINERALS MANAGEMENT SERVICE STUDY						
SITE	BINOM. DEPTH(MM)	MODE	BREAK PT.	CLASS	AVG. MODES	
					DY SM	DY & SM (mm/yr) (mm/yr)
1-YR	LSC TR(0-M)M CAN	N/A	16.5	16.5	III	16.5
		N/A	16.5	16.5	III	
1-YR	LSC TRAN(20-M)JU	9.9	16.5	10.5	IIA	16.5
		9.9	16.5	10.5	IIA	
1-YR	LSC TRAN(30-M)JU	9.2	16.5	7.5	IIB	15.0
		9.2	13.5	7.5	IIB	
1-YR	LSC TRAN(50-M)JU	10.3	16.5	10.5	I	16.5
		10.3	16.5	10.5	I	
1-YR	LSN 1 MAY	11.0	13.5	7.5	IIA	13.5
		10.4	13.5	7.5	IIA	
1-YR	LSN 2 MAY	5.9	7.5	7.5	IIA	7.5
		5.7	7.5	4.0	IIA	
1-YR	LSN 3 MAY	7.8	4.5	4.5	IIA	4.5
		7.9	4.5	4.5	IIA	
TERREBONNE (mm/6 mo.)						
6-MO	2/14/87 TFN TRANS (0-M)C	18.4	19.5	19.5	IIB	18.0
		16.5	16.5	16.5	IIA	
6-MO	TFN TRANS (25-M)	-	-	-	V	-
		-	-	-	V	
6-MO	TFN TRANS (50-M)	20.7	19.5	23.5	IIA	19.5
		-	-	-	V	
6-MO	TFC TRANS (0-M)	14.5	13.5	13.5	I	13.5
		17.2	13.5	13.5	I	
6-MO	TFC TRANS (25-M)	5.9	4.5	4.5	I	4.5
		-	-	-	V	
6-MO	TFC TRANS (50-M)	11.1	10.5	17.5	I	9.0
		7.0	7.5	10.5	IIB	
6-MO	TFN-2-50M WEST	15.9	25.5	25.5	IIA	25.5
		15.9	25.5	25.5	IIA	
6-MO	TFN-1-50M EAST	11.5	13.5	13.5	IIA	13.5
		11.6	13.5	13.5	IIA	
6-MO	TFN-1-50M EST CO	-	-	-	N/A	-
		-	-	-	N/A	
6-MO	TFN-1-50M TYPHA	-	19.5	-	III	19.5
		-	-	-	V	
(mm/yr)						
1-YR	6/24/87 TFN TRANS (0-M)	N/A	42.5	7.5	III	42.5
		N/A	42.5	7.5	III	

Table 5.2 continued

SITE		MINERALS MANAGEMENT SERVICE STUDY					AVG. MODES
		BINOM. DEPTH(MM)	MODE	BREAK PT.	CLASS	DY & SM (mm/yr)	
		DY SM	DY SM	DY SM	DY SM		
1-YR	TFN TRANS (25-M)	-	-	-	V	32.5	
		32.5	32.5	-	IIA		
1-YR	TFN TRANS (50-M)	N/A	47.5	37.5	I	47.5	
		N/A	47.5	22.5	III		
1-YR	TFC TRANS (0-M)	23.4	22.5	22.5	IIA	19.2	
		15.1	N/A	2.5	IIA		
1-YR	TFC TRANS (25-M)	-	-	-	V	32.5	
		N/A	32.5	-	III		
1-YR	TFC TRANS (50-M)	27.2	27.5	27.5	IIA	24.1	
		21.0	-	-	IV		
1-YR	TFN-1-50M EAST	N/A	32.5	22.5	I	35.0	
		N/A	37.5	37.5	III		
1-YR	TFN-2-50M WEST	24.9	27.5	27.5	I	25.5	
		26.5	N/A	-	IV		
TERREBONNE							
	6/24/87						
1-YR	TFI-1-50M	22.3	7.5	17.5	IV	22.1	
		22.0	22.5	22.5	IV		
1-YR	TFI-2-50M	-	-	-	-	-	
		-	-	-	-		
1-YR	TFC-1-50M	21.1	7.5	27.5	IIA	20.0	
		19.6	7.5	27.5	IIA		
1-YR	TFI _r -1-50M TYPHA	27.8	12.5	12.5	IIA	26.0	
		24.4	42.5	37.5	IIB		

Table 5.2 continued

SITE	BINOM. DEPTH(MM)	MODE	BREAK PT.	CLASS	AVG. MODES
	DY SM	DY SM	DY SM	DY SM	DY & SM (mm/yr)
COCODRIE					
11/8/86					
COC1(PLNK-7)	12.1	10.5	10.5	IIA	10.5
	11.7	4.5	4.5	IIA	
COC2(NEXT PLNK-7)	14.6	13.5	16.5	IIA	10.5
	14.2	10.5	10.5	IIA	
CO3ELBPLK-BY-PLK	15.5	7.5	19.5	IIA	7.5
	15.8	4.5	13.5	IIA	
FOURCHON					
2/20/86					
FOU REP1(BKGD)	-	-	-	V	
	-	-	-	V	
FOU REP2(BKGD)	-	-	-	V	
	-	-	-	V	
FOU REP3(BKGD)	-	-	-	V	
	-	-	-	V	
6/21/86					
FOU1(SAM 1)	-	-	-	IV	-
	-	-	-	IV	
FOU2(SAM 2)	20.0	16.5	16.5	IIA	7.5
	13.1	7.5	7.5	IIA	
FOU3(SAM 3)	16.4	1.5	13.5	IIA	7.5
	12.8	7.5	7.5	IIA	
5/13/87					
FOU87EDG COL-2	13.7	10.5	13.5	IIA	9.0
	15.8	7.5	7.5	IIA	
FOU87H2O DEEP PR	15.3	7.5	7.5	IIA	7.5
	12.8	7.5	7.5	IIA	
FOU87 ST.PROBE	-	-	-	V	
	-	-	-	V	
LAC DES ALLEMANDS					
8/8/86					
LAC1 S-3(LS-1)	-	-	-	III	32.5
	27.3	32.5	32.5	III	
LAC1B S-3(LS-1)	-	-	-	III	
	60.1	52.5	72.5	III	
LAC N/F S-3(LS-2)	-	-	-	IV	57.5
	-	57.5	57.5	IIB	
LAC2 S-2(1)	22.3	17.5	17.5	III	62.5
	22.3	17.5	17.5	III	
LAC2B S-2(1)	56.7	62.5	62.5		
	56.7	62.5	62.5		

Table 5.2 continued

SITE	BINOM.	MODE			BREAK PT.	CLASS	AVG. MODES
	DEPTH(MM)	DY SM	DY SM	DY SM	DY SM	DY SM	DY & SM (mm/yr)
LAC3A S-2(2)		28.7	37.5	37.5	37.5	III	57.5
		28.7	37.5	37.5	37.5	III	
LAC3B S-2(2)		50.4	52.5	52.5	52.5		
		50.4	62.5	62.5	62.5		
LAC4A S-3(3)RS.		26.5	32.5	32.5	32.5	III	42.5
		26.5	-	-	-	IV	
LAC4B S-3(RS)		49.1	32.5	32.5	32.5	III	
		49.1	-	-	-	IV	
ROCKEFELLER							
6/17/86							
ROC1 SU.CANAL S-		28.5	22.5	22.5	22.5	IIA	22.5
		24.8	2.5	37.5	37.5	IV	
ROC2 SU.CANAL S-		17.1	12.5	12.5	12.5	IIA	12.5
		27.8	-	-	-	IV	
ROC3 PRICE LAK S		30.1	-	-	-	IV	22.5
		22.6	22.5	22.5	22.5	IIA	
ROC4 PRICE LAK S		16.9	2.5	2.5	2.5	III	17.5
		20.7	17.5	17.5	17.5	IIA	
ROC5 PRICE LAK S		10.1	12.5	12.5	12.5	IIA	12.5
		26.8	12.5	12.5	12.5	IIB	

Table 5.3 Location and recent sediment accretion rates for marshland habitats (natural and disturbed) in Louisiana as determined by rare earth soil horizon markers and instrumental neutron activation analysis. Data from Rockefeller Refuge, Lac Des Allemands, Port Fourchon, and Cocodrie are included for comparison. Data below the line drawn above Leeville are from the MMS study. From Knaus (1987).

Geographic Location	Water Salinity ^a (collection interval)	Date, Marker placement (mo/yr)	6-mo		Yearly samples (n)	Yearly accretion (cm)	Yearly range (cm)
			samples (n)	range (cm)			
Rockefeller Wildlife Refuge							
a) Price Lake	Fresh, perched above salt	2/84	--	--	3	0.75	0.54-0.96
b) Superior Canal ^b	Fresh to brackish	2/84	--	--	2	0.75	0.54-0.96
Lac Des Allemands	Fresh (5/84-3/85) (5/84-6/86)	5/84	--	--	11 (6) (5)	2.67 (2.8) (2.52) ^c	1.20-4.70 (1.20-4.70) (1.45-2.80)
Cocodrie	Salt	4/86	3	0.95			0.75-1.05
Lafourche Parish							
a) Fourchon	Salt	2/86	2	1.12	2	0.66	0.60-0.72
b) Leeville	Salt (6/86-12/86) ^d (12/86-6/87) ^d	6/86	11 (4) (7)	0.76 (0.75) (0.77)	7	1.29	0.60-1.72 (0.45-1.35) (0.45-1.05) (0.45-1.35)
Terrebonne Parish	Fresh	6/86	8	1.42	11	2.97	1.95-4.75
Cameron Parish	Brackish (11/87-5/87) ^e (11/87-7/87) ^e	1/87	6 (4) (2)	0.51 (0.38) (0.79)	10	0.84	0.3-1.95 (0.15-0.75) (0.56-1.01)

^a Marsh type based on dominant vegetation type (Cowardin et al., 1979)

^b Earthen barrier breached to salt water, February 1985

^c The 2-yr accumulation was 5.04 cm; the 1-year accretion is obtained by dividing 5.04 cm by 2 years

^d The 6-month samples analyzed from Lafourche Parish were comprised of 4 samples, collected 12/86 and 7 samples collected 6/87, which were from 7 different sites than the first 4 sites

^e Four 6-month samples from Plum Bayou; two 8-month values from Grand Bayou were pro-rated to 6-month accumulation period

Lafourche Parish study site

Six-month accretion was measured at four distances along a boardwalk system at the Lafourche salt-water transect, which is perpendicular to a natural waterway (see Fig. 3.2). The distances into the marsh were 0.0, 10.0, 30.0, and 50.0 meters. The marker distributions found at each of these distances are shown in figures 5.3A-D. Note that each of these distributions can be classified as falling into the general category of Type II (See Materials and Methods, *Core data analysis*).

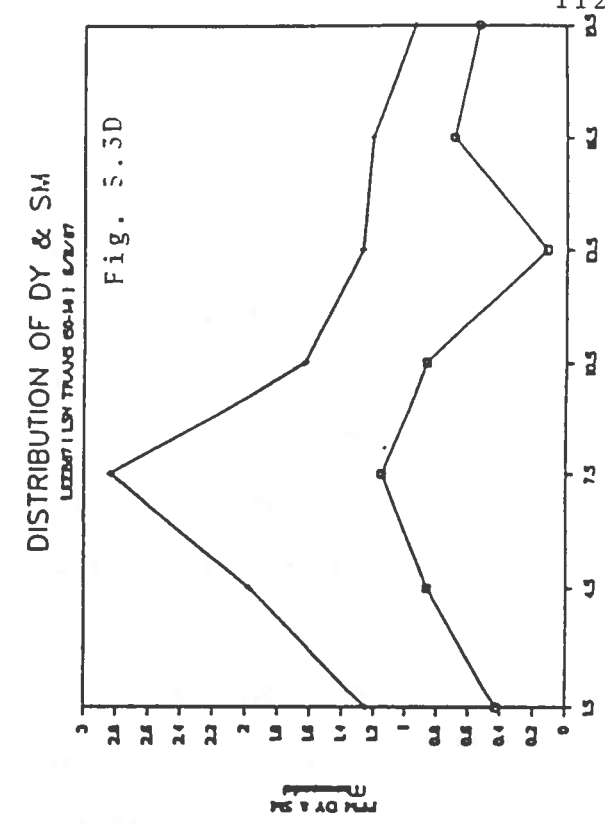
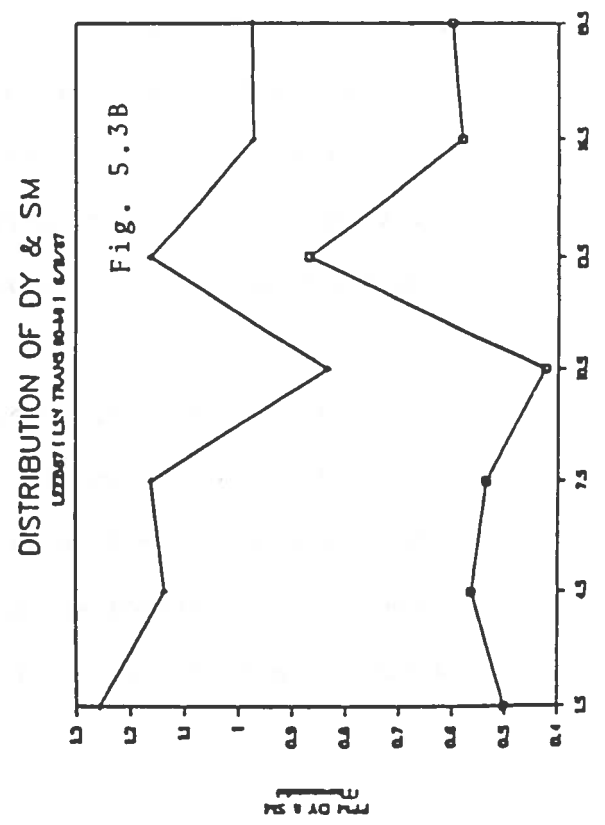
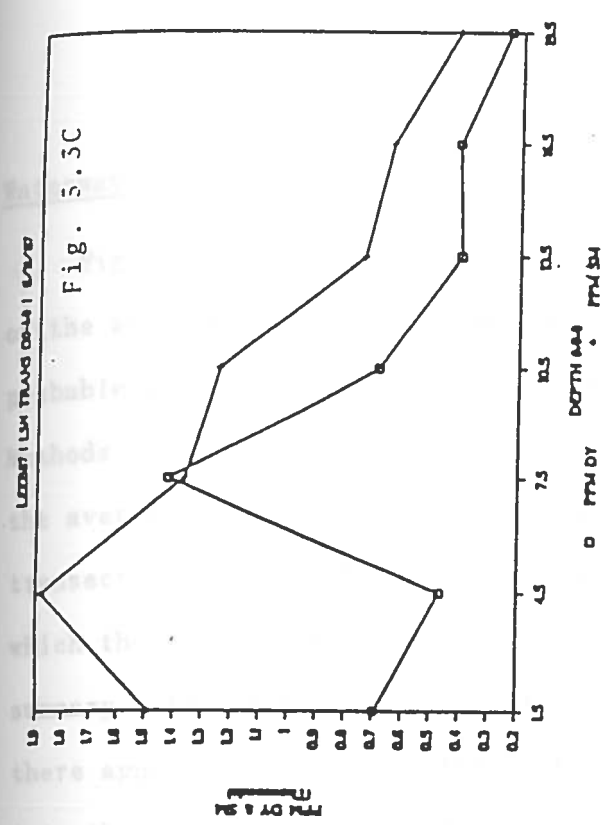
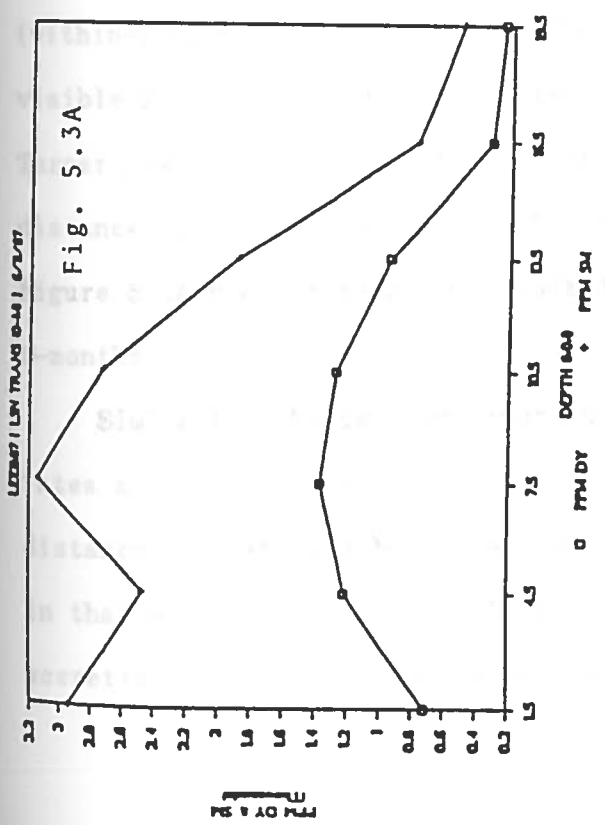
Figure 5.3A has a binomial depth of 10.7mm for both the Dy and Sm distribution. The mode occurs at a depth of 7.5mm for both Dy and Sm. The breakpoint occurs at 10.5mm for both Dy and Sm.

Figure 5.3B yields a binomial depth of 10.7mm for both Dy and Sm, and a mode of 13.5mm for both Dy and Sm. The Sm mode is an apparent mode. The breakpoint for both markers occurs at a depth of 7.5mm.

Figure 5.3C has a binomial depth of 7.5mm for Dy and 10.3mm for Sm. The mode for Dy occurs at 7.5mm and the mode for Sm occurs at 4.5mm. The breakpoint for Dy is at 7.5mm and that for Sm occurs at 4.5mm.

The data in Figure 5.3D yield a binomial depth of 10.6mm and 7.0mm for Dy and Sm respectively. The mode for both markers occurs at 7.5mm. The breakpoint occurs at 7.5mm.

Figure 5.3A-D. Marker distributions found at the Lafourche at Leeville natural transect distances into the marsh from the waterway of 0 m (Fig. 5.3A), 10 m (Fig. 5.3B), 30 m (Fig. 5.3C), and 50 m (Fig. 5.3D).



Waterway analysis

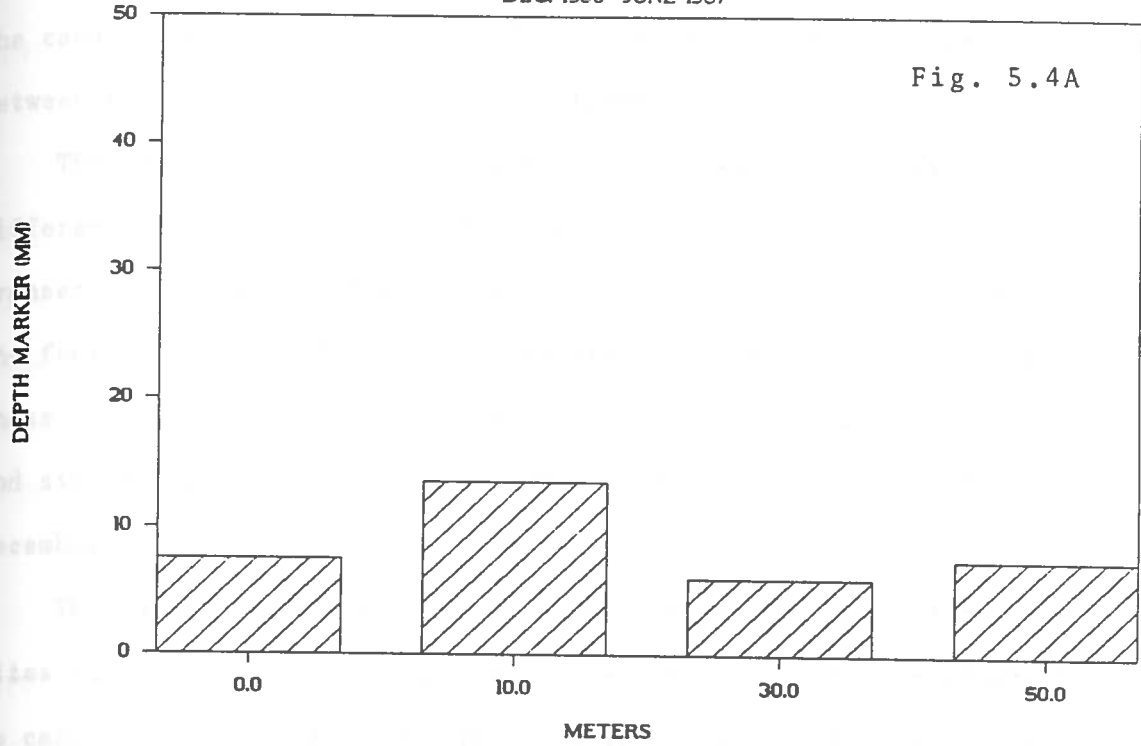
Figure 5.4A is a bar graph summary of the average depth for each of the above cores. The average depth is determined as the most probable position of the marker in the sampled core (See Materials and Methods, *Core data analysis*). Figure 5.4B is the bar graph summary of the average depth which was determined for cores taken from the canal transect site at Lafourche. The graphs of marker distributions from which these values were determined are found in Appendix A and the summary data are in Table 5.2. In both cases, it is notable that there appears to be no observable trend of accretion with distance into the marsh. This cannot be demonstrated statistically since replicate samples at each of the distances were not taken because of the time and expense involved. However, if it is assumed that there is no difference with distance into the marsh, it is possible to estimate a mean and variance in the particular plot (within-plot-variance). It was demonstrated by co-workers using the visible marker technique at the same sites and times (Cahoon and Turner, 1987) that there was no statistically significant trend with distance into the marsh at any of the transects. Thus, the data in Figure 5.4A yield a mean and standard deviation of $8.6 \text{ mm} \pm 3.3 \text{ mm}$ per 6-months.

Similarly, the data in Figure 5.4B show the 1-year accretion rates at the canal transect site. If no difference of accretion with distance into the marsh is assumed, a mean with a standard deviation in that plot of $16.1 \text{ mm} \pm 0.75 \text{ mm}$ per year is obtained. Since 6-month accretion was obtained at the natural site and one-year accretion at

Figure 5.4A-B. Accretion depth as determined by modal analysis at the Lafourche (Leeville) natural and canal distance transects (LSN and LSC) at 6 months and 1 year, respectively. The bars represent average values of the modes for the highest concentrations of the rare earth markers with depth.

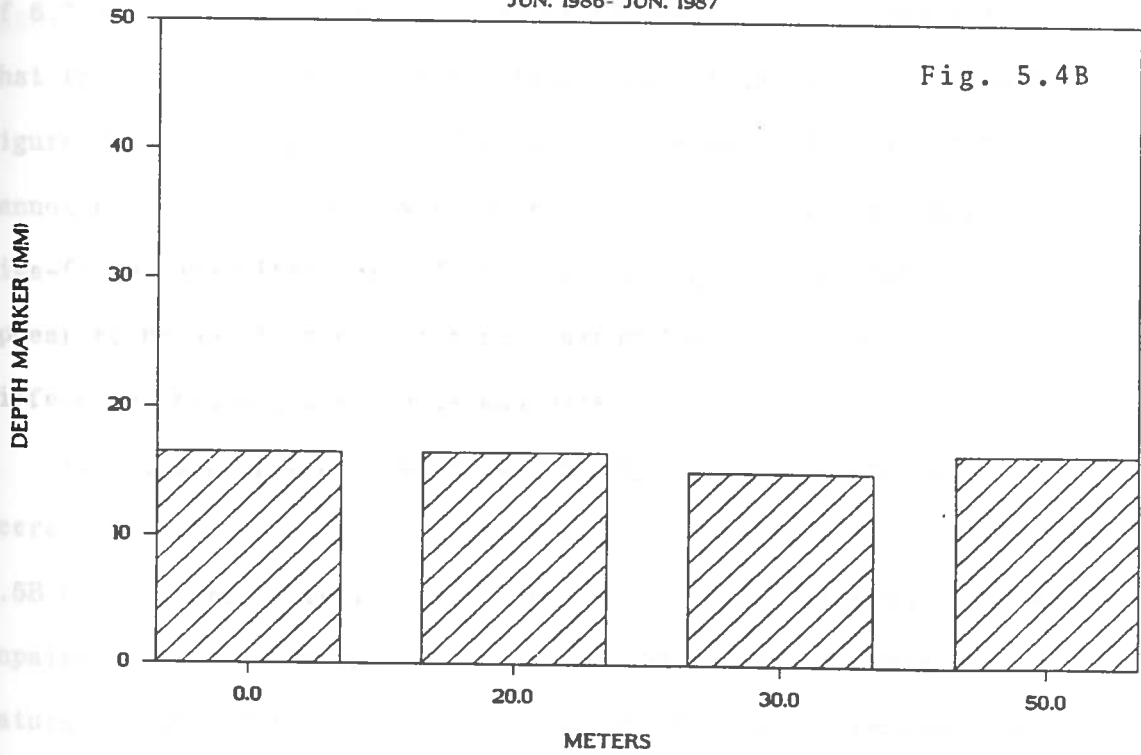
LEEVILLE NATURAL TRANSECT (6 MO.)

DEC. 1986- JUNE 1987



LEEVILLE CANAL TRANSECT (1 YR.)

JUN. 1986- JUN. 1987



the canal sites, it is not possible to make a meaningful comparison between the two different treatments (Canal vs. Natural).

The data in Figure 5.5A show 6-month accretion rates at 4 different sites, each located 50 m into the marsh. These are *not* transect data. Three of the sites were off natural waterways, while the fourth site was off a canal. No replicates were made at any of these sites. Combining the 3 natural 50 m sites yields a mean value and standard deviation of $7.5 \text{ mm} \pm 2.5 \text{ mm}$ during the 6-month June to December interval.

The data in Figure 5.5B show the 6-month accretion at 4 different sites located 50 m into the marsh. Three of the sites were adjacent to canal waterways, while the fourth site was adjacent to a natural waterway. No replicate cores were taken at any of the sites. Combining the 3 canal 50 m sites yields a mean and standard deviation of $6.7 \text{ mm} \pm 1.5 \text{ mm}$ during the 6-month December to June interval. Note that the LSN 50 m transect datum from Figure 5.4A is also recorded in Figure 5.5B for comparison. The data from Figures 5.5A and 5.5B cannot be compared directly because their respective 6-month accretion time-frames are different. It is interesting to note that there appear to be no visible differences among these sites and no differences between treatments and dates.

If the assumption is made that there is no difference of accretion with distance into the marsh, the data in Figures 5.4A and 5.5B (cores were collected at the same time) can be tested using an unpaired *t*-test. Testing for a significant difference between the natural treatment (n=4) of Figure 5.4A and the canal treatment of

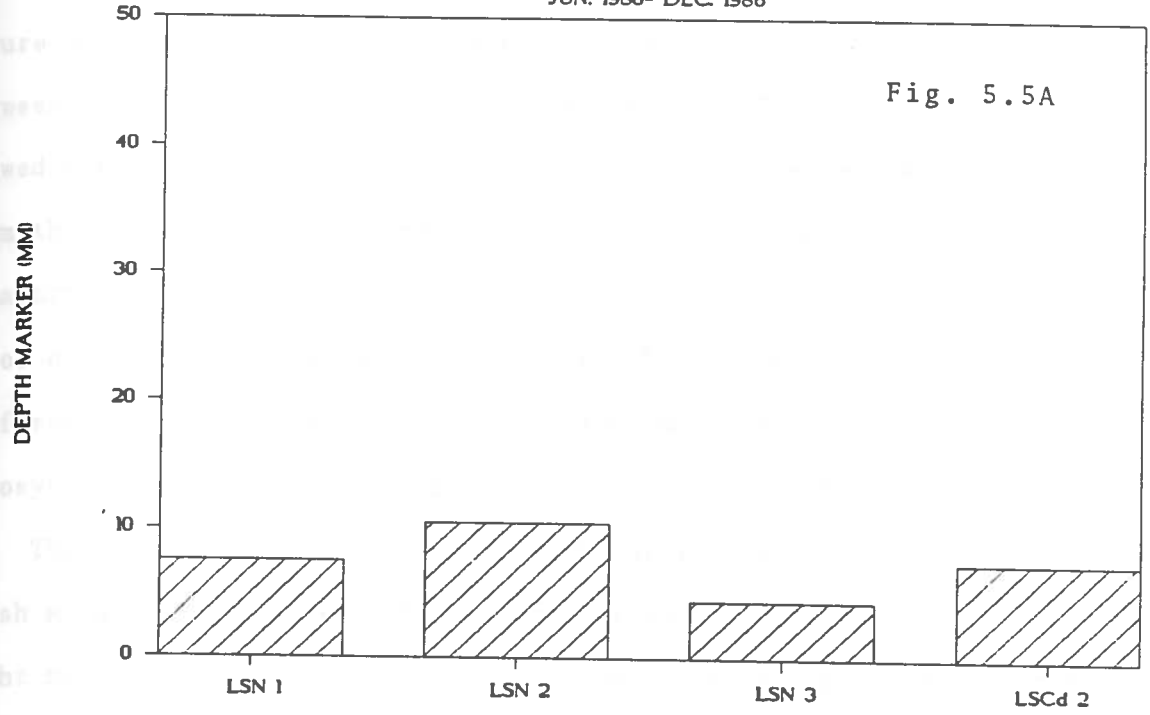
Figure 5.5A-B

Figure 5.5A. Accretion depth as determined by modal analysis for Lafourche (Leeville) at 4 different plots 50 m into the marsh, perpendicular to salt-water waterways. The bars represent average values of the modes for the highest concentration of the rare earth markers with depth. The 6-month accretion period was from June 1986 to December 1986.

Figure 5.5B. Accretion depth as determined by modal analysis for Lafourche (Leeville) at four different locations, 50 m into the marsh, perpendicular to salt-water waterways. The bars represent average values of the modes for the highest concentration of the rare earth markers with depth. The 6-month accretion period was from December 1986 to June 1987.

LEEVILLE 50-M DATA (6 MO.)

JUN. 1986- DEC. 1986



LEEVILLE 50-M DATA (6 MO.)

DEC. 1986- JUN. 1987

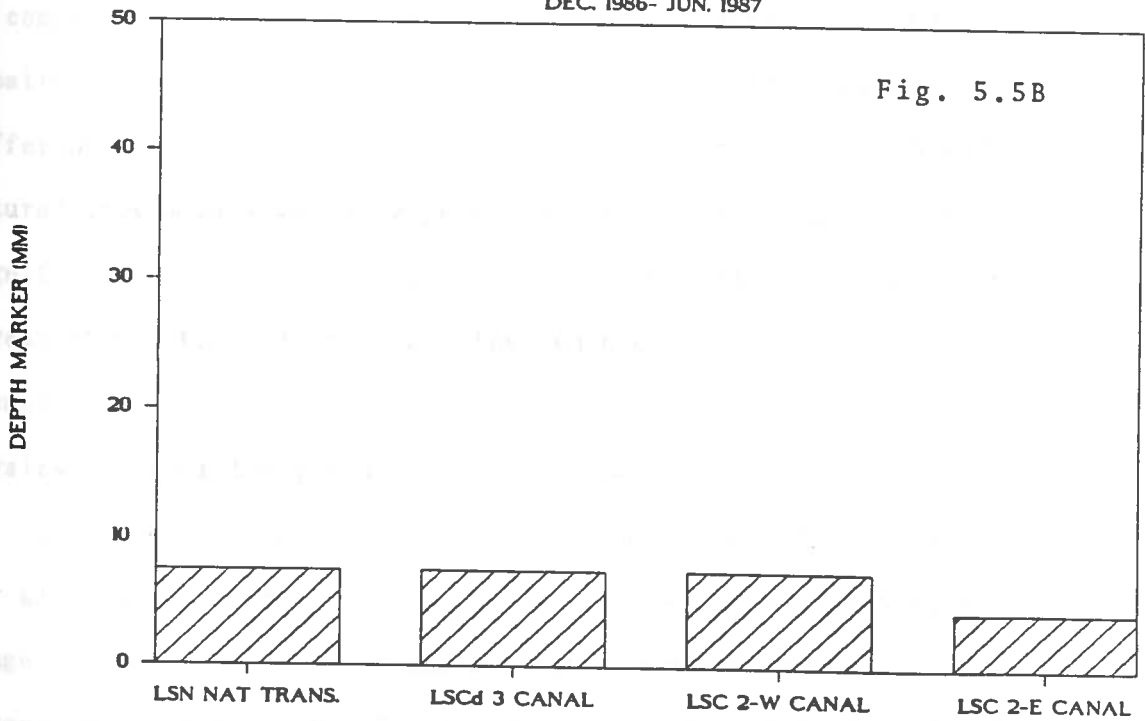


Figure 5.5B (n=3) reveals that there is no significant difference between these treatments at 6 months ($P \geq 0.41$). This test should be viewed with caution since the natural treatment cores were all taken from the *same* plot (natural transect site), whereas the canal treatment cores were each taken at *different* plots. The argument in favor of this procedure is that the effect being tested here is the difference between canal and natural sites, and a site specific idiosyncrasy is assumed to be unimportant or irrelevant.

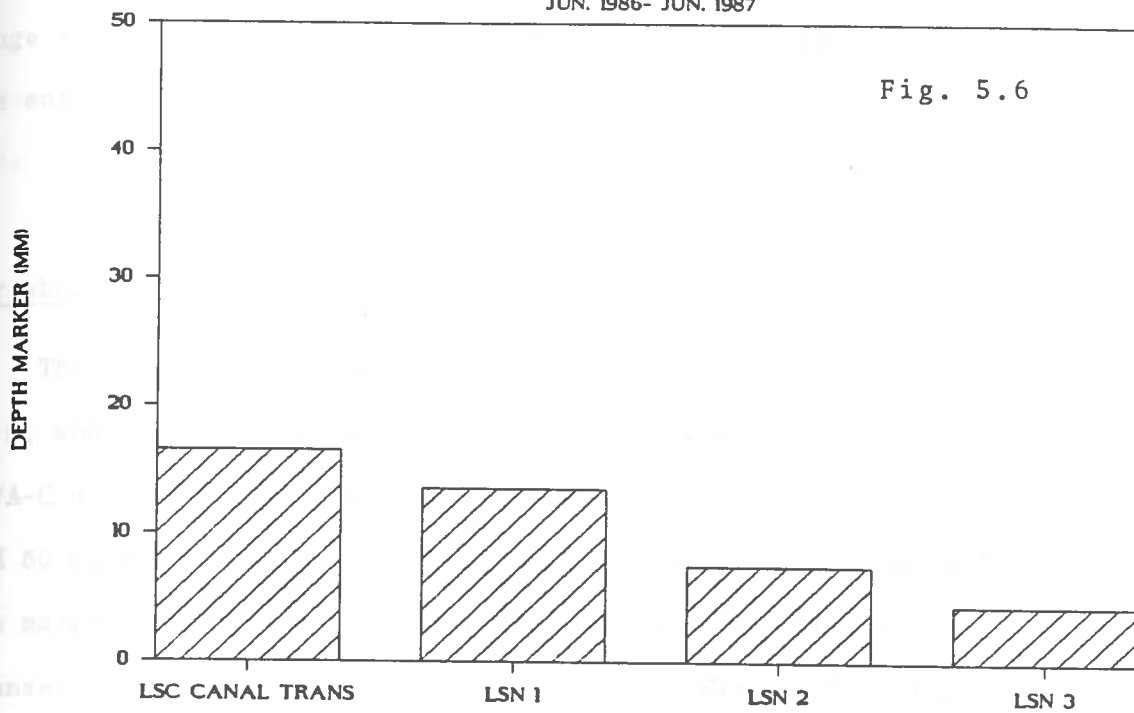
The data in Figure 5.6 show one-year accretion at 50 m into the marsh at 4 separate sites. Visual inspection suggests that there might be a difference between the one canal site and the three natural sites, but this cannot be stated definitely when there is no estimate of variance at each individual site. Note that the LSC 50 m transect datum from Figure 5.4B is also recorded in Figure 5.6 for comparison. By comparing the one-year accretion data in Figures 5.4B and 5.6, an unpaired *t*-test can be applied testing only for significant differences between the canal treatment (n=4) of Figure 5.4B and the natural treatment (n=3) of Figure 5.6. The canal treatment showed significantly higher accretion versus the natural stream treatment at 1 year ($P \leq 0.02$). Again, this test should be viewed with caution because of the problem of within-plot-samples being compared with physically separated plots.

The grand mean and standard deviation at the Lafourche study site for all 6-month data (11 cores, Table 5.3) is 7.6 mm \pm 2.6 mm with a range of 4.5-11.3 mm. The grand mean and standard deviation for all 1-year data (seven cores, Table 5.3) is 12.9 mm \pm 4.9 mm. with a

Figure 5.6. Accretion depth as determined by modal analysis at Lafourche (Leeville) at four different locations, 50 m into the marsh, perpendicular to salt-water waterways. The bars represent average values of the modes for the highest concentrations of the rare earth markers with depth.

LEEVILLE 50-M DATA (1 YR.)

JUN. 1986- JUN. 1987



range of 4.5 mm-16.5 mm. These means are probably representative of the entire Lafourche study area.

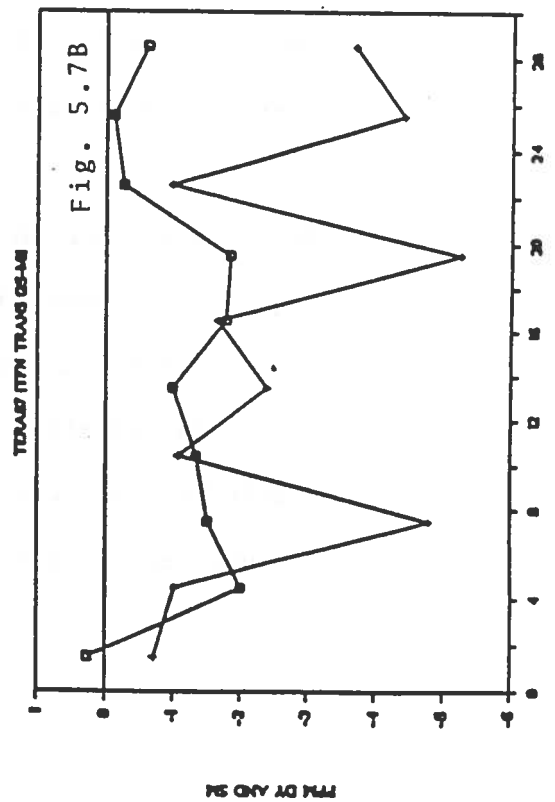
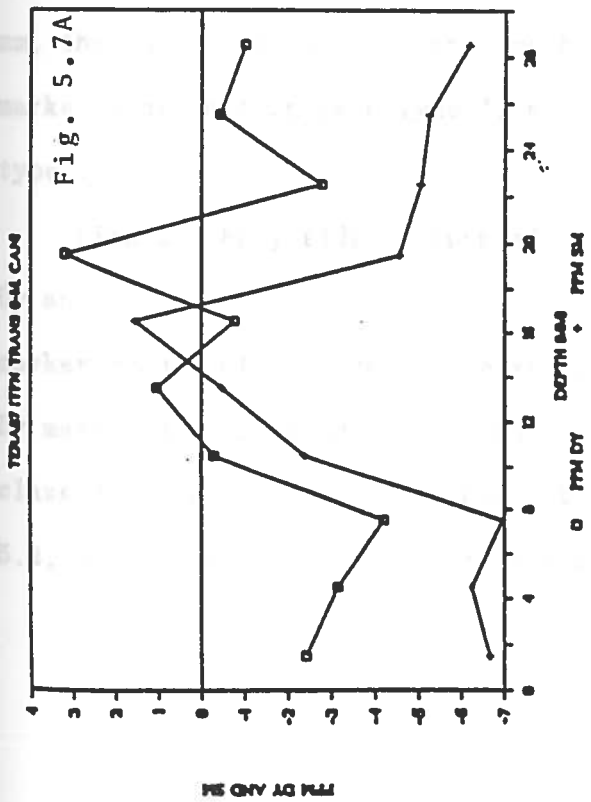
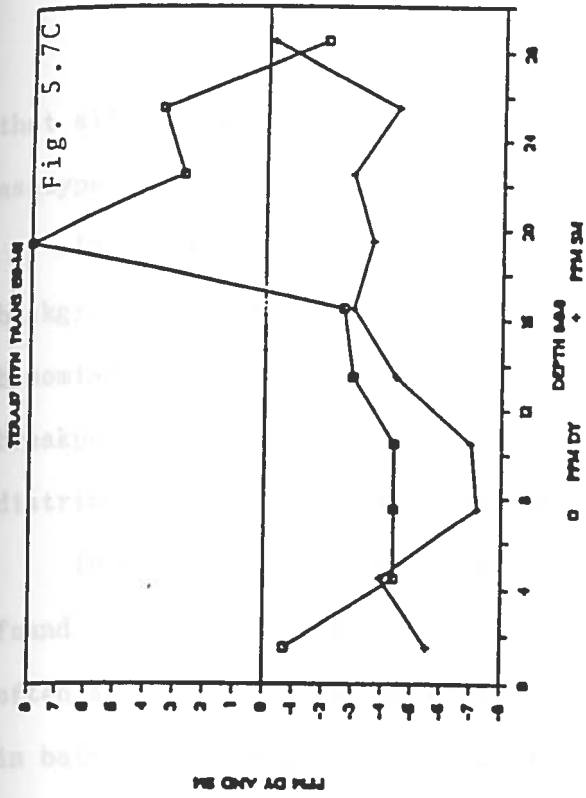
Terrebonne study site

The 6-month accretion was measured at three distances of 0.0 m, 25 m, and 50 m at both the natural and canal transect sites. Figures 5.7A-C are the marker distributions found at each distance (0 m, 25 m, and 50 m) within the natural transect plot, while Figures 5.8A-C show the marker distributions found at each distance within the canal transect plot. Note that the distribution in Figures 5.7A was obtained using a beer can coring technique used to sample visible clay marker by Cahoon and Turner (1987). The cryogenic core at that distance missed the plot, so the can core is accepted as a representative sample at the 0 m transect distance.

Figure 5.7A has a binomial depth of 18.4 mm and 16.5 mm for the Dy and Sm distribution, respectively. The mode for the Dy distribution occurs at 19.5 mm and at 16.5 mm for the Sm distribution. The breakpoint occurs at 19.5 mm and 16.5 mm for the Dy and Sm distribution, respectively. The distributions observed in this core fall within the general classification scheme as a type II.

Figure 5.7B represents the data obtained at 25 m into the marsh at the natural transect. Note that no marker was observed above the 99% confidence interval. This is indicative of a "miss", meaning that either the plot was not accurately relocated or that the marker has been washed away. A "miss" does not imply that the accretion rate at

Figure 5.7A-C. Marker distributions found at the Terrebonne natural transect distances into the marsh of 0 m (Fig. 5.7A), 25 m (Fig. 5.7B), and 50 m (Fig. 5.7C).



that site is zero. The distribution observed in this core is classed as type V, below background.

In Figure 5.7C, the Dy marker distribution is well above background, whereas the Sm marker distribution is not detectible. The binomial depth for Dy is 20.7 mm. The mode occurs at 19.5 mm and the breakpoint occurs at 23.5 mm. The Dy marker is in a class II distribution, whereas the Sm marker is in a class V distribution.

In Figure 5.8A, a very discrete distribution of both markers is found. This sort of distribution is classified as type I. This was often seen at the levee or stream bank sites during the entire study in both fresh and brackish marshes. A binomial depth of 14.5 mm and 17.2 mm is obtained for the Dy and Sm marker distributions, respectively. The mode occurs at 13.5 mm for both markers. The breakpoint for both markers occurs at 13.5 mm.

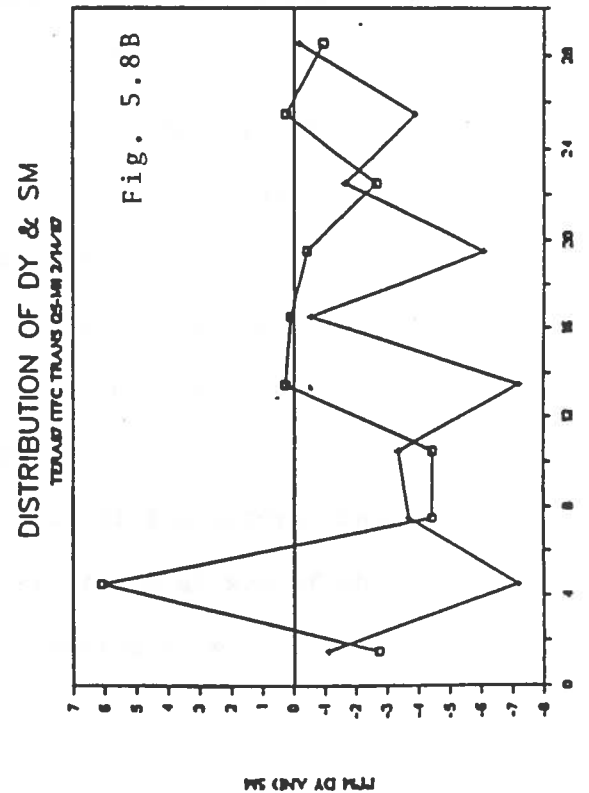
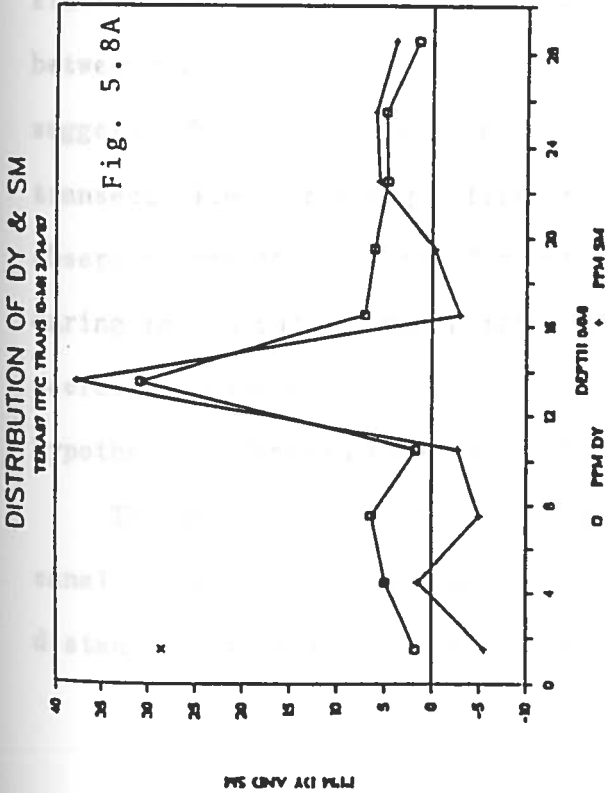
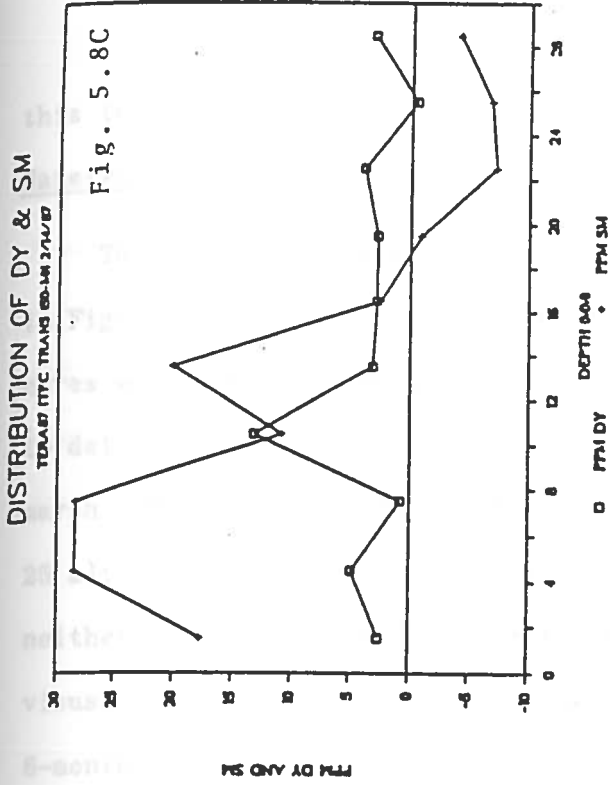
Figure 5.8B evidences only Dy as being above background, whereas the Sm is not above background. The binomial depth for Dy is at 5.9 mm, the mode is at 4.5 mm, and the breakpoint is at 4.5 mm. The Dy marker distribution is a type I, and the Sm marker distribution is a type V.

Figure 5.8C yields a binomial depth of 11.1 mm and 7.0mm for the Dy and Sm marker distributions, respectively. The mode for the Dy marker occurs at 10.5 mm, while the mode for Sm occurs at 7.5 mm. The Dy marker distribution is a class I while the Sm distribution is a class IIB. All of the above distributions are summarized in Table 5.2, as well as those which are not shown in the Results section of

Figure 5.8A-C. Marker distributions found at the Terrebonne pipeline canal transect distances into the marsh of 0 m (Fig. 5.8A), 25 m (Fig. 5.8B), and 50 m (Fig. 5.8C).

DISTRIBUTION OF BY & SM
RESULTS FROM MARK DISTR

DISTRIBUTION OF BY & SM
RESULTS FROM MARK DISTR



this thesis.

Waterway analysis

The 6-month accretion at the natural and canal sites are reported in Figure 5.9 for ease of comparison. Because no replicate cryogenic cores were taken at any of the transect distances, it is not possible to determine any significant accretion trend with distance into the marsh. No value is reported for the 25 m natural transect core (TFN 25 m); this finding does not imply zero accretion but, rather, that neither marker was found. Figure 5.9 as well as Figure 5.10 reveal no visual trends of accretion with distance into the marsh after a 6-month and a 1-year interval for both the canal and natural sites. It is likely that there is no trend of accretion with distance into the marsh within the 6-month time frame of these data.

The natural and canal transect sites were established and sampled at the same times, but because the TFN 50 m datum is missing, a 2-site statistical comparison cannot be done for detection of differences between natural and canal effects. However, a visual inspection suggests that slightly more accretion is occurring at the natural transect site. This suggestion is given more credence when one observes that the 0 m and 50 m natural site data both increased by 60% during the second six-month interval. Taking 40% of the 1-year accretion value of TFN 25 m (32.5 mm from Figure 3.16) yields a hypothetical 6-month accretion value of 13.5 mm.

The data in Figure 5.10 show 1-year accretion at the natural and canal transects. Because no replicate cores were taken at any of the distances into the marsh, it is not possible to determine any

Figure 5.9. Six-month accretion (mm) as determined by modal analysis measure at three distances (m) along two transects in freshwater habitats at the Terrebonne study area. One transect was located perpendicular to a natural waterway (left-hand diagonal bars), and the other perpendicular to a canal waterway (right-hand crosshatch bars). No marker was found in the 25 m core at the natural transect location.

TERREBONNE NAT. vs. CANAL TRANS (6 MO.)

JULY 1986- FEB. 1987

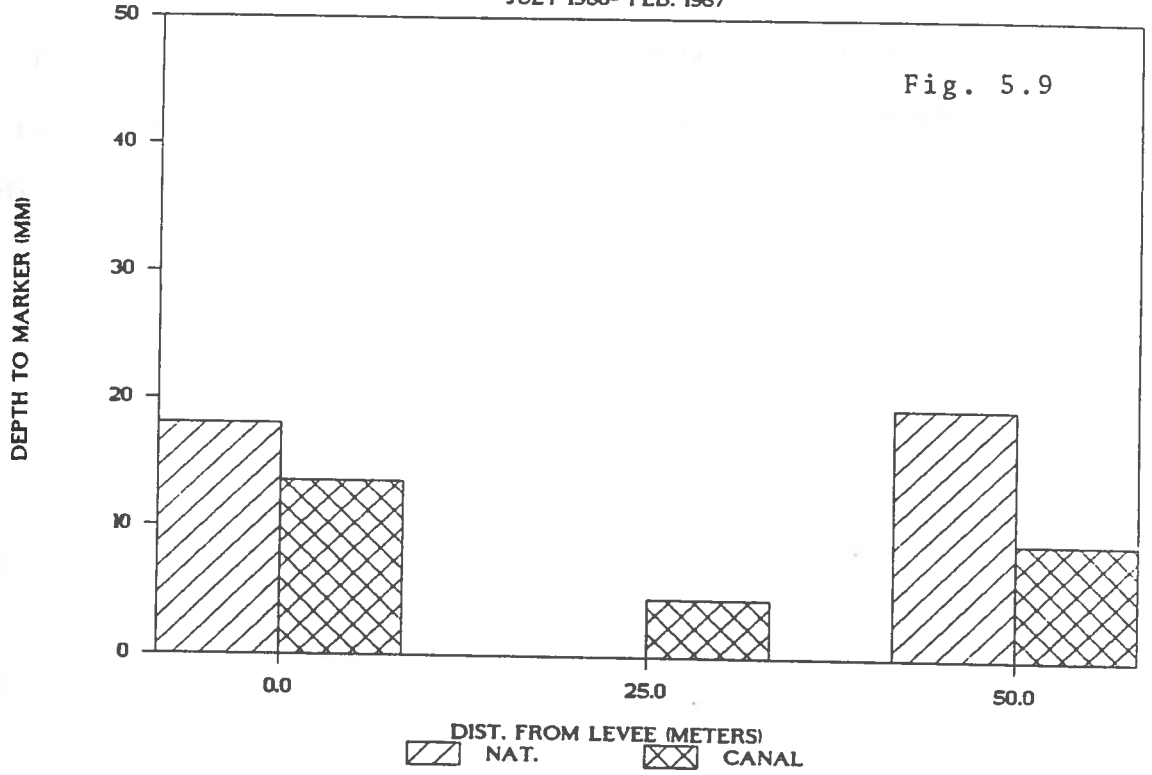
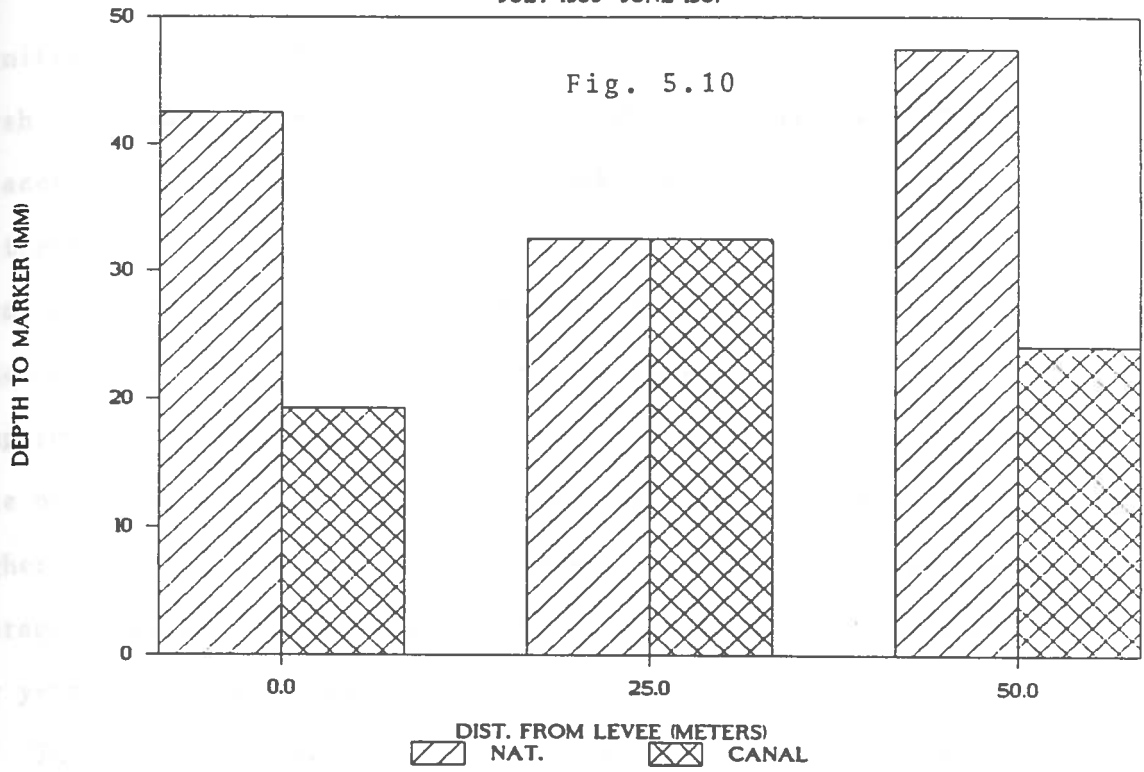


Figure 5.10. One-year accretion (mm) measured at three distances (m) at the same Terrebonne natural and canal transect sites as depicted in Fig. 5.9.

TERREBONNE NAT. vs. CANAL TRANS (1 YR.)

JULY 1986- JUNE 1987



significant trend of accretion with distance from the bank into the marsh. A visual inspection of Figure 5.10 reveals little difference in accretion with distance into the marsh. It is likely that there is no trend of accretion at either of the sites within the 1-year time frame of this study. Because the natural and canal one-year transect sites were established and sampled at the same time, they can be compared as replicates for the two habitats. The overall accretion rate of the three combined natural transect sites is significantly higher ($P \leq 0.01$) than the three combined canal transect sites; the average being 40.8 mm per year at the natural transect, versus 25.3 mm per year at the canal transect.

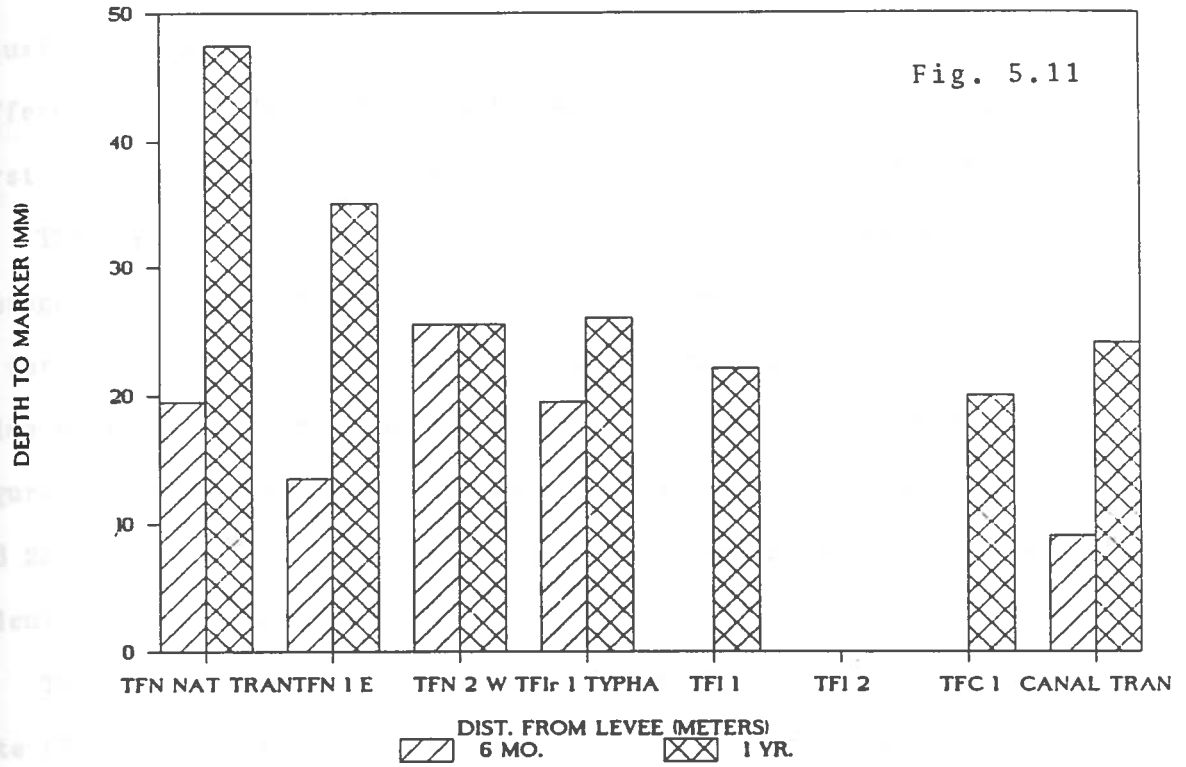
The data in Figure 5.11 show the 6-month and the 1-year accretion at 8 locations at natural bayous and canal sites, 50 m into the marsh. The data from TFC and TFN 50 m transect sites (for both 6 months and 1 year) are taken from Figures 5.9 and 5.10. No significant trend is found among sites or among natural, canal, and impoundment-influenced sites. The marker at the impoundment-influenced site, TFI-2, one-year, was not found in the core, and the lack of a value reported in Figure 5.11 does not imply a zero accretion rate. No six-month cores were taken at the TFC-1 and TFI-2 sites.

A statistical comparison of the 50 m data at six months and the 50 m data at one year shown in Figure 5.11 can be made. An unpaired *t*-test (six-month cores, $n=5$; 1-year cores, $n=7$) demonstrated a significantly higher accretion level at 1 year versus 6 months ($P \leq 0.05$). This result was expected. A *t*-test was also performed to determine whether 1-year accretion rates were greater than 6-month

Figure 5.11. Six-month (left-hand diagonal bars) and one-year (right-hand cross-hatch bars) accretion (mm) measured at eight different locations, 50 m into the marsh, perpendicular to freshwater waterways at the Terrebonne study area. The six-month and one-year values for the natural transect (TFN-Nat Tran) and canal transect (TFC-Canal Tran) at 50 m were taken from Figures 5.9 and 5.10, respectively, for comparison.

TERREBONNE 50 M DATA (6 MO. & 1 YR.)

JULY 1986- JUNE 1987



adjusted to 1-year accretion rates. There was no significant difference ($P \geq 0.35$). This result implies that accretion during the first 6-month period was the same for the second 6-month period.

The overall accretion rates of the combined 50-m data show an average accretion of 18.0 mm for 6 months and an average rate of 28.6 mm for 1 year (excluding the TFI-2). The difference in the average value of 18.0 and 28.6 mm accretion rates calculated from the data in Figure 5.11 and in the accretion values reported in Table 5.3 (14.2 and 29.7) results from the inclusion of the 0 and 25 m cores in the calculations of values for Table 3.2.

The grand mean and standard deviation at the Terrebonne study site (Table 5.3) for all the 6-month data (eight cores) is $15.3 \text{ mm} \pm 6.6 \text{ mm}$ with a range of 4.5–26.0 mm. The grand mean and standard deviation for all the 1-year data (eleven cores) is $29.7 \text{ mm} \pm 9.2 \text{ mm}$ with a range of 19.5–47.5 mm. These means are probably representative of the Terrebonne study area.

Cameron study site

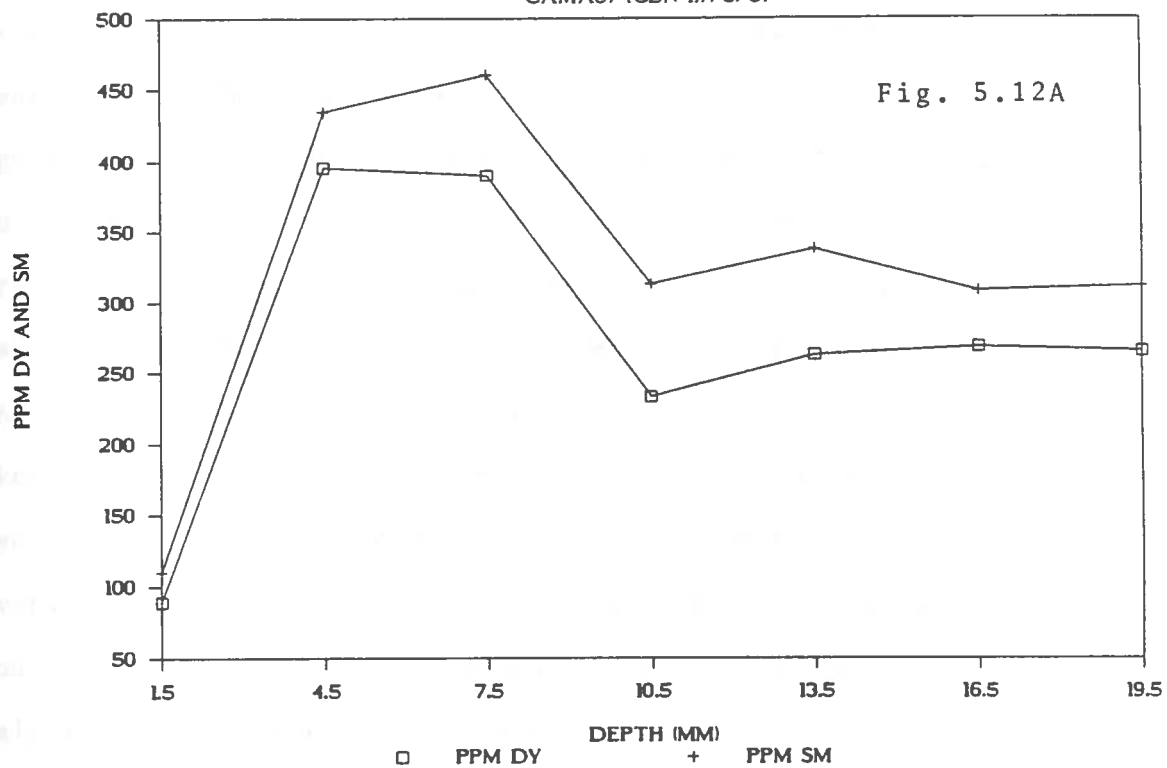
Distance transects were not utilized in the Cameron study area. All plots are 50 m from the waterway into the marsh. Figures 5.12A–B represent marker distributions found at the control sites (CBN-1 and CBN-2). These two sites are depicted in Figure 3.4 of Chapter 3 of this thesis.

The marker distribution in Figure 5.12A has a binomial depth of 11.8 mm and 11.2 mm for the Dy and Sm distributions, respectively.

Figure 5.12A-B. Marker distributions found at the Cameron natural sites. These sites are 50 m into the marsh perpendicular to the adjacent brackishwater waterways.

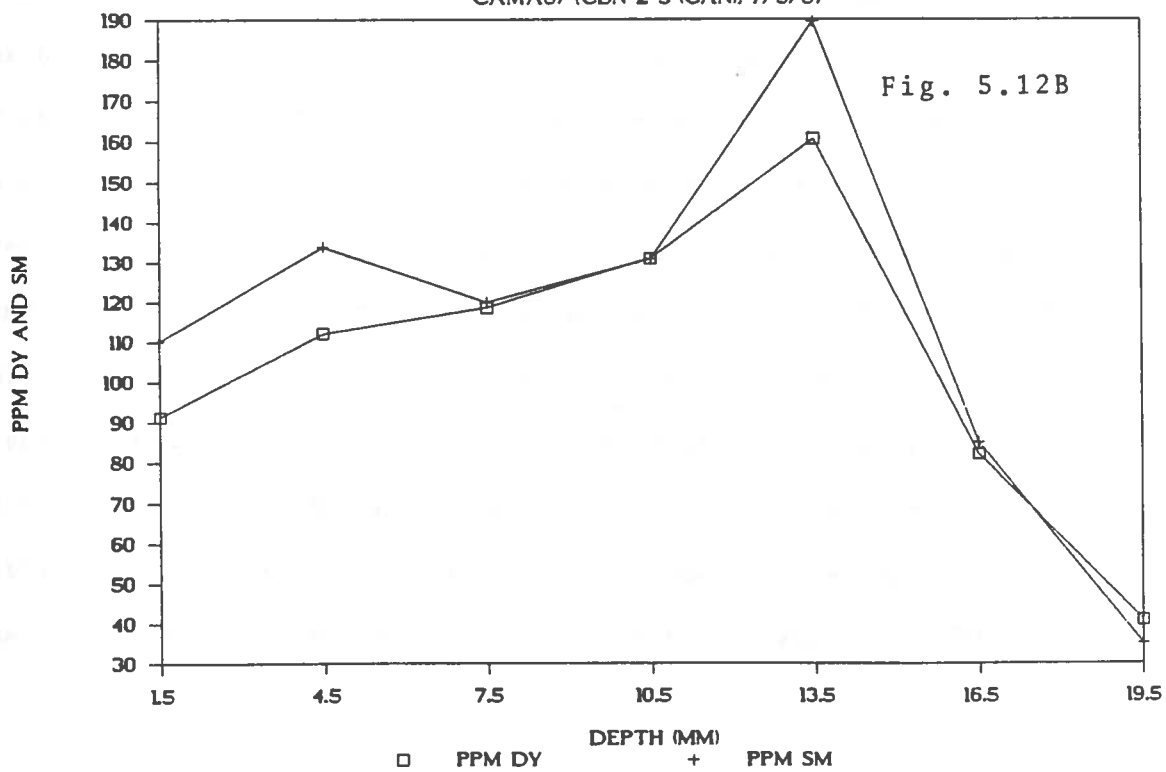
DISTRIBUTION OF DY & SM

CAMA87 (CBN 117/8/87)



DISTRIBUTION OF DY & SM

CAMA87 (CBN-2-S (CAN)) 7/8/87



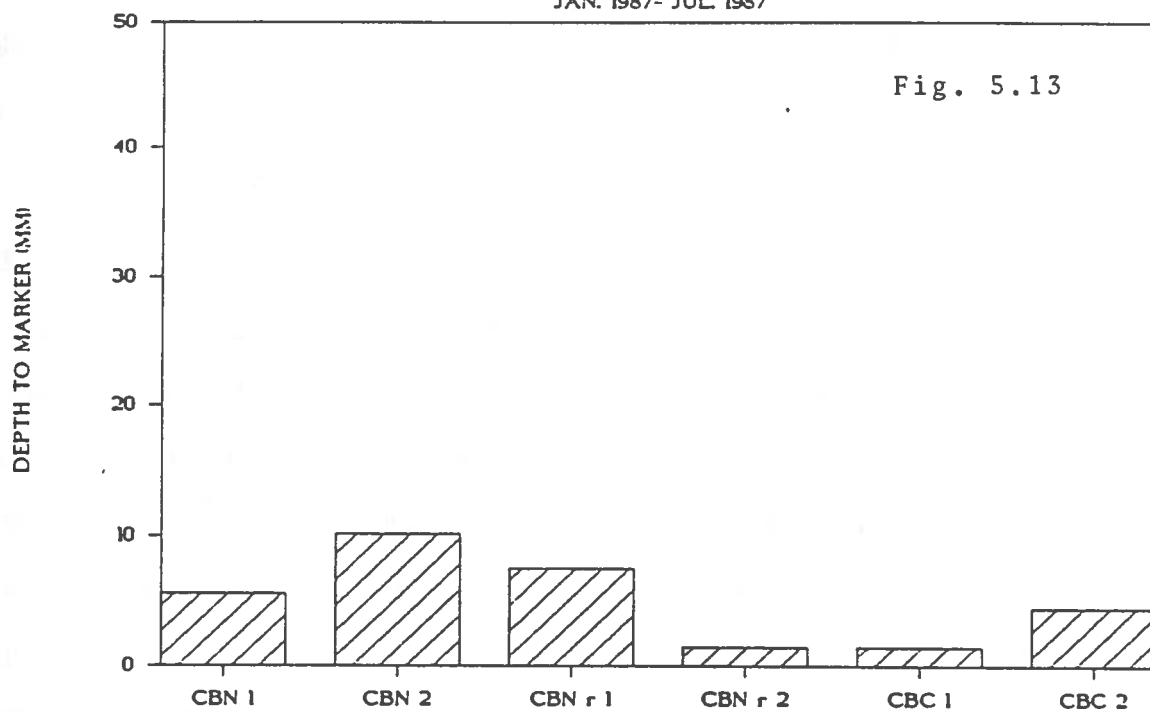
The mode occurs at 7.5 mm for both of the marker distributions. The breakpoint for the Dy distribution occurs at 7.5 mm for both markers. Figure 5.12B has a binomial depth of 10.0 mm for the Dy distribution and 9.7 for the Sm distribution. The mode occurs at 13.5 mm for both marker distributions. The breakpoint occurs 13.5 mm for both marker distributions. Both Figures represent marker distributions in Class IIA. It should be noted that the core represented in Figure 3.19 was taken by the can boring method used by Cahoon and Turner (1987). The cryogenic coring device was not used at the CBN-2 site because of adverse weather conditions. All other cores taken at the Cameron study site were taken by the cryogenic coring device and the core data analysis results are listed in table 5.2.

Figure 5.13 is a graphical representation of the depth found at all Cameron plots. Two of the sites (CBN 1 and CBN 2) were marked with rare earths 8 months prior to sampling. The data in Table 5.2 has been pro-rated to 6-months for the sake of comparison with the four 6-month sites (CBNr-1 and -2, and CBC 1 and 2). The mean value for the 6 cores is 5.1 mm accretion per six months. If the 6 cores are divided into two general collection area data (shown in parentheses in Table 5.2), the two cores taken near the unchanneled Grand Bayou (CBN 1 and CBN 2) show an accretion rate of 7.9 mm per 6 months, while the 4 cores, taken 5 km north of Grand Bayou in a recently leveed area along the eastern shore of Calcasieu Lake, show 3.8 mm accretion in six months. This may be indicative of a restriction of the source of sediment to the marsh as a result of the construction of the levee system 2 years prior to sampling. This

Figure 5.13. Six-month accretion (mm) measured at six different locations, 50 m into the marsh, perpendicular to brackish waterways at the Cameron study area. The bars represent modes for the highest concentrations of the rare earth markers with depth.

CAMERON 50-M DATA (6 MO.)

JAN. 1987- JUL. 1987



result cannot be demonstrated statistically because of the low sample number and because of the slightly differing time frames of application of marker.

Other study sites

Additional study sites are those that were not officially included in the MMS study. Dates of sampling and results of modal analysis are included in Table 5.2 as well as study area summary data in Table 5.3. These sites are Cocodrie, Fourchon camp, Lac Des Allemands, and Rockefeller Wildlife Refuge. It is noteworthy that samples taken from the Lac Des Allemands study site showed a distinct bimodal distribution of marker (Figure 5.14). The mode of the distribution which is deepest in the soil profile is used for the depth determination. In the case of Figure 3.21, this mode is found at 62.5 mm. The binomial depth occurs at 56.7 mm for both the Dy and Sm distribution. Possible explanations for this type of marker distribution (Type III) are found in the discussion chapter of this thesis.

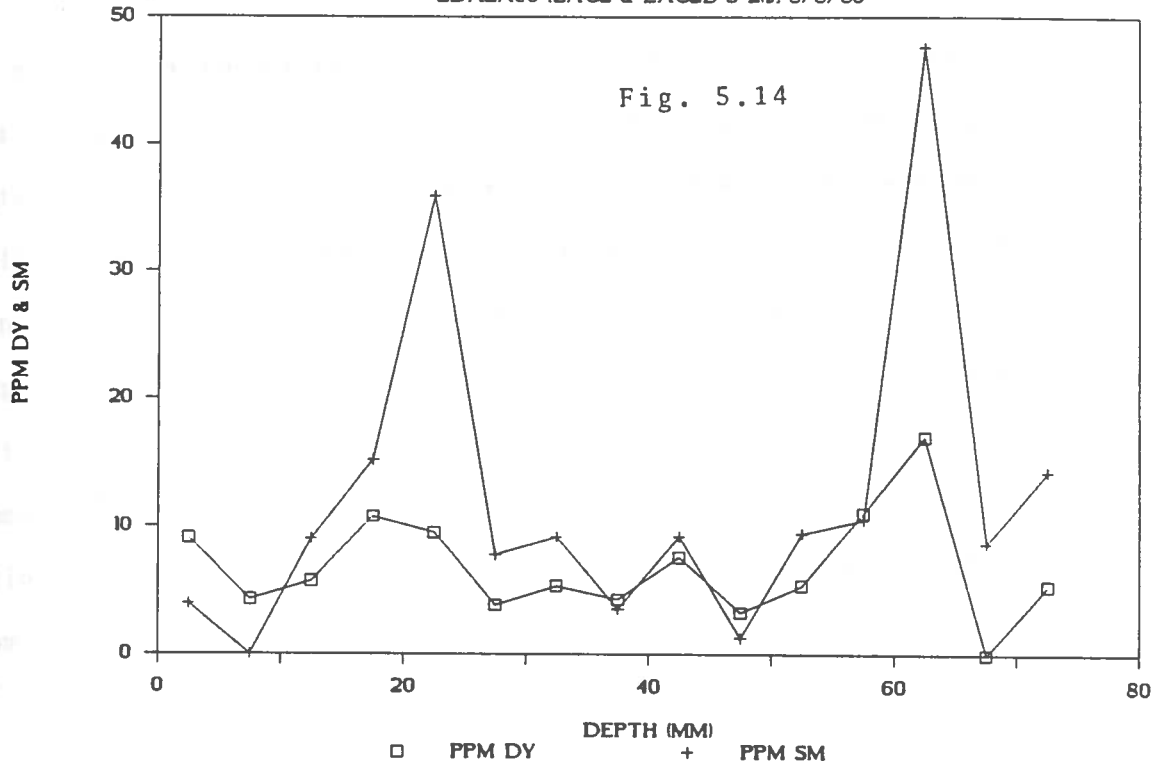
Dynamic Analysis

The dynamic analysis of the data is based on the model developed by Guinasso and Schink (1975) which is discussed in Chapter 4 of this thesis and is applied below. A semi-quantitative application of the model is presented here as a basis for future work. A more rigorous treatment of the data is not possible at this time because of

Figure 5.14. A bimodal marker distribution from the Lac Des Allemands study area which seems to be characteristic of that area.

DISTRIBUTION OF DY & SM

LDA2A86 (LAC2 & LAC2B S-21) 8/8/86



the complicated nature of developing a mathematically sound basis for best fit of observed data to theoretical predictions of the model (This problem is currently being addressed, but will not be ready for application by thesis deadline). Therefore, the G parameter, weighted mean depth, and mixing layer thickness have been estimated by visual inspection of appropriate marker distributions. Appropriate marker distributions are those which visually fit the model very well. A summation of this data as well as an estimate of the coefficient of mixing (D) appear in Table 5.4. The coefficient of mixing is obtained from the relationship:

$$G = \frac{D}{LV}$$

where G is the mixing parameter, D is the gaussian mixing coefficient analog, V is the sedimentation velocity, or in this case, accretion rate, and L is the mixing depth. This model is developed in Chapter 4 of this thesis in the section *Dynamic analysis*.

Visual fit to the optimum G parameter is accomplished by comparing observed marker distributions with computer model generated distributions. Figure 5.15A-B represents an example of the visual evaluation of best fit. The observed marker distribution appears in Figure 5.14A. The model generated distribution of G=2.0 and time=0.5 (6 months) appears in Figure 5.15B. The "shoulder" effect is apparent in both figures. The shoulder is biologically meaningful in that the point at which it branches off is probably the zone of bioturbation. This bioturbation can be represented by a gaussian mixing coefficient

Table 5.4- Dynamic analysis parameters.

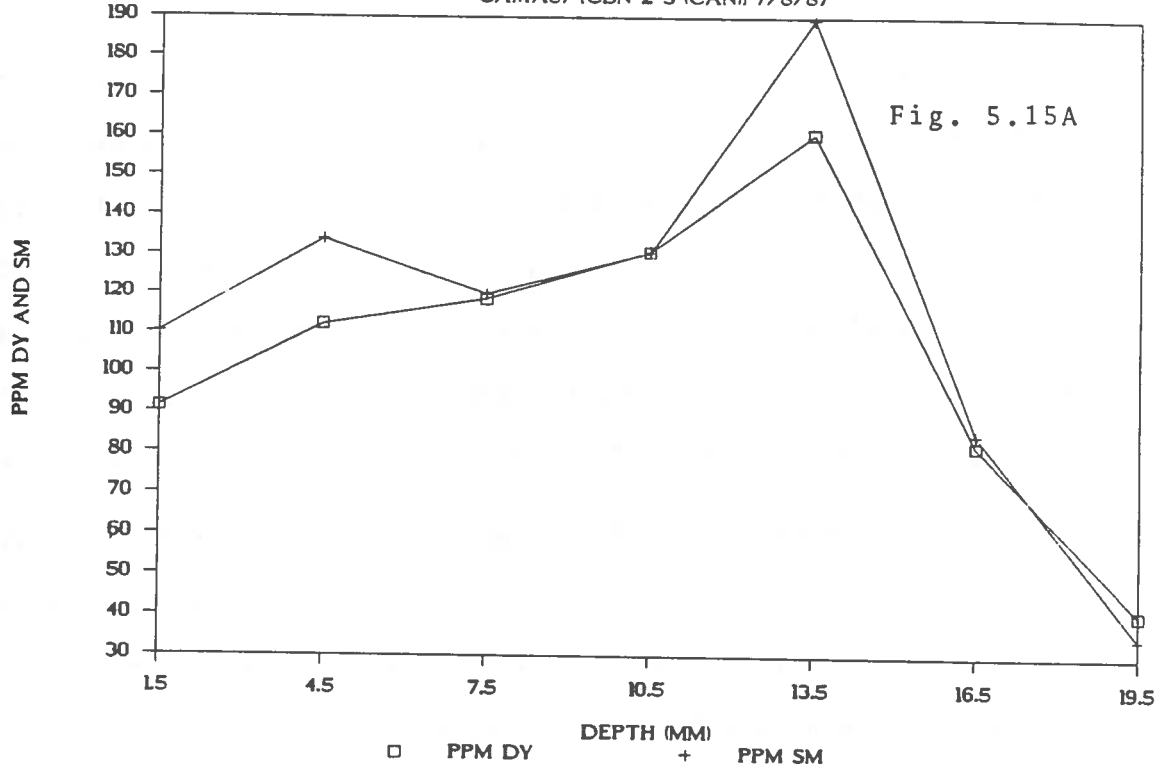
DYNAMIC ANALYSIS PARAMETERS

SITE		WEIGHTED DEPTH(CM)	MODAL DEPTH(CM)	G	V (CM/YR)	L (CM)	D (CM ² /YR)
CAMERON							
8-MO	7/8/87 CBN-S-2	1.50	2.03	2.00	1.50	1.05	3.18
6-MO	CBC 2	0.90	0.90	0.10	0.90	0.75	0.68
LEEVILLE							
6-MO	12/15/86 LSN 2	1.60	2.05	3.00	1.60	1.10	5.28
6-MO	LSN 3	0.90	0.90	0.10	0.90	1.00	0.09
6-MO	LSCd 2	0.80	1.50	3.00	0.80	1.00	2.40
6-MO	5/13/87 & 6/11/87 LSN 0-M	1.20	1.50	1.00	1.20	1.60	1.92
6-MO	LSN 10-M	2.14	2.70	2.00	2.14	1.05	4.49
6-MO	LSN 30-M	1.20	1.20	0.70	1.20	1.05	0.88
1-YR	LSC 40-M	1.03	1.50	4.00	1.03	1.65	6.80
1-YR	LSN 1	1.04	1.35	0.70	1.04	1.05	1.09
1-YR	LSN 2	0.59	0.75	2.00	0.59	0.75	0.88
1-YR	LSN 3	0.45	0.45	0.30	0.45	1.05	0.14
TERREBONNE							
6-MO	2/14/87 TFN 0-M	2.40	2.60	0.30	2.40	2.00	2.04
6-MO	TFN 50-M	4.14	3.90	0.70	4.14	1.60	9.28
6-MO	TFC 0-M	2.70	2.70	0.01	2.70	1.05	0.03
6-MO	TFN-1-50M	2.30	2.70	0.30	2.30	1.05	0.72
1-YR	6/24/87 TFN-2-50M	2.49	2.55	1.00	2.49	2.25	5.60

Figure 5.15A-B. A representative example of the visual comparison technique utilized to pair observed marker distributions with theoretical distributions generated from the single mixing layer model of Guinasso and Schink, 1975. Fig. 5.15A depicts the observed marker distribution, and Fig. 5.15B depicts the computer generated best match ($G=2.0$).

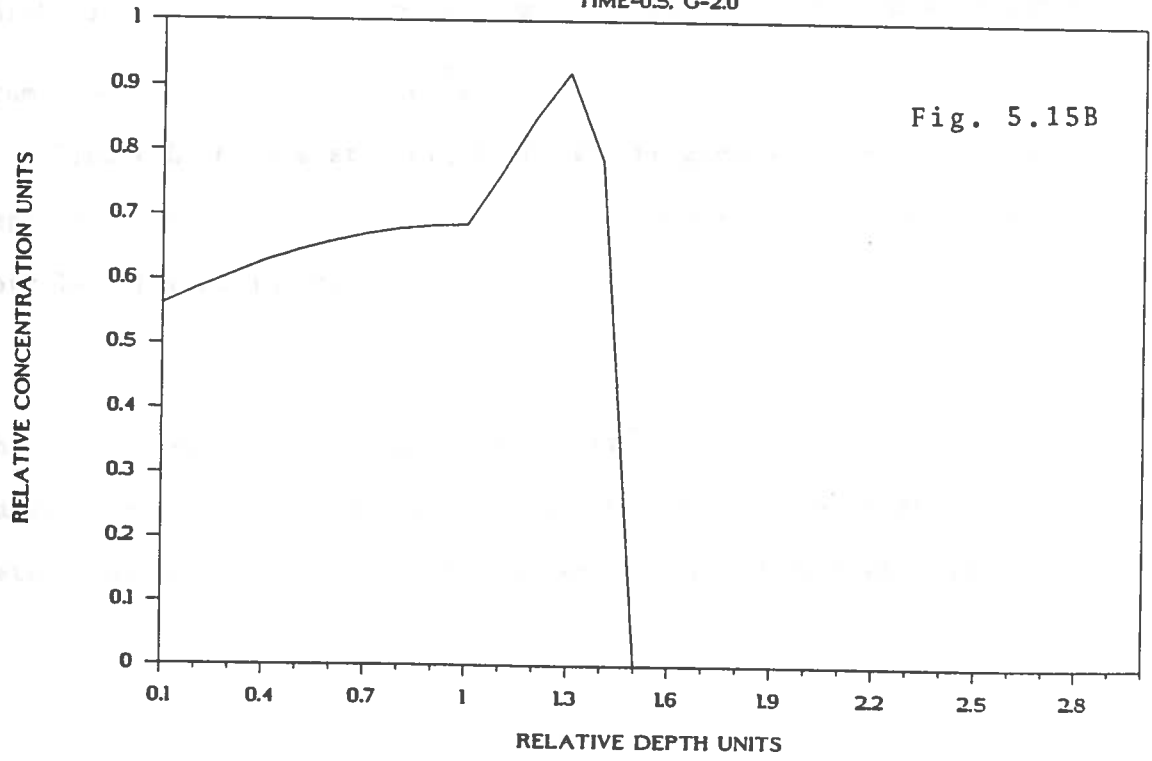
DISTRIBUTION OF DY & SM

CAMA87 (CBN-2-S (CAN)) 7/8/87



CONCENTRATION vs. DEPTH

TIME-0.5, G-2.0



if the bioturbation is Class II in nature (see Chapter 2, this thesis) which it appears to be in Figure 5.15A. Thus, visual inspection of Figure 5.14A reveals that the mixing layer depth (L) is approximately 1.05 cm, the weighted depth (the imaginary line which divides the marker inventory 50/50) occurs at 1.01 cm which when prorated to 12 months is 1.50 cm which is also the sedimentation velocity (V). Since G, V, and L are known, one can solve for D which in this case equals a diffusion coefficient of $3.18 \text{ cm}^2 \cdot \text{yr}^{-1}$. These values are shown in the first row of Table 5.4.

The 6-month samples are adjusted to yearly accretion rates for both the modal depth and the weighted depth. The G parameter, which is dimensionless, ranges from 0.01 to 4.00. The weighted mean depth ranges from $0.45 \text{ cm} \cdot \text{year}^{-1}$ to $4.14 \text{ cm} \cdot \text{yr}^{-1}$. The thickness of the mixing layer ranges from 0.75 cm to 2.25 cm. In the salt marshes, the thickness varies little from 1.0 cm. The coefficient of mixing varies from $0.03 \text{ cm}^2 \cdot \text{yr}^{-1}$ to $9.28 \text{ cm}^2 \cdot \text{yr}^{-1}$.

Figure 5.16 is a scattergram of the weighted depth vs. the modal depth as found in Table 5.4. Correlation analysis yields a linear correlation equation of:

$$y = (.92)x + 0.36 ; r^2 = .96$$

The y-intercept departs significantly from 0.0 ($p \leq 0.01$). This suggests that there is a bias between the two methods of accretion determination, the modal depth consistently yielding higher values.

Figure 5.16. A scattergram of weighted depth (cm) on the x-axis plotted against modal depth (cm) on the y-axis. The y-intercept departs significantly from 0.0 ($p \leq 0.05$) suggesting that the bias associated with accretion determination by modal analysis is high on the average by 0.36 cm (the y-intercept).

MODAL DEPTH VS. WEIGHTED DEPTH

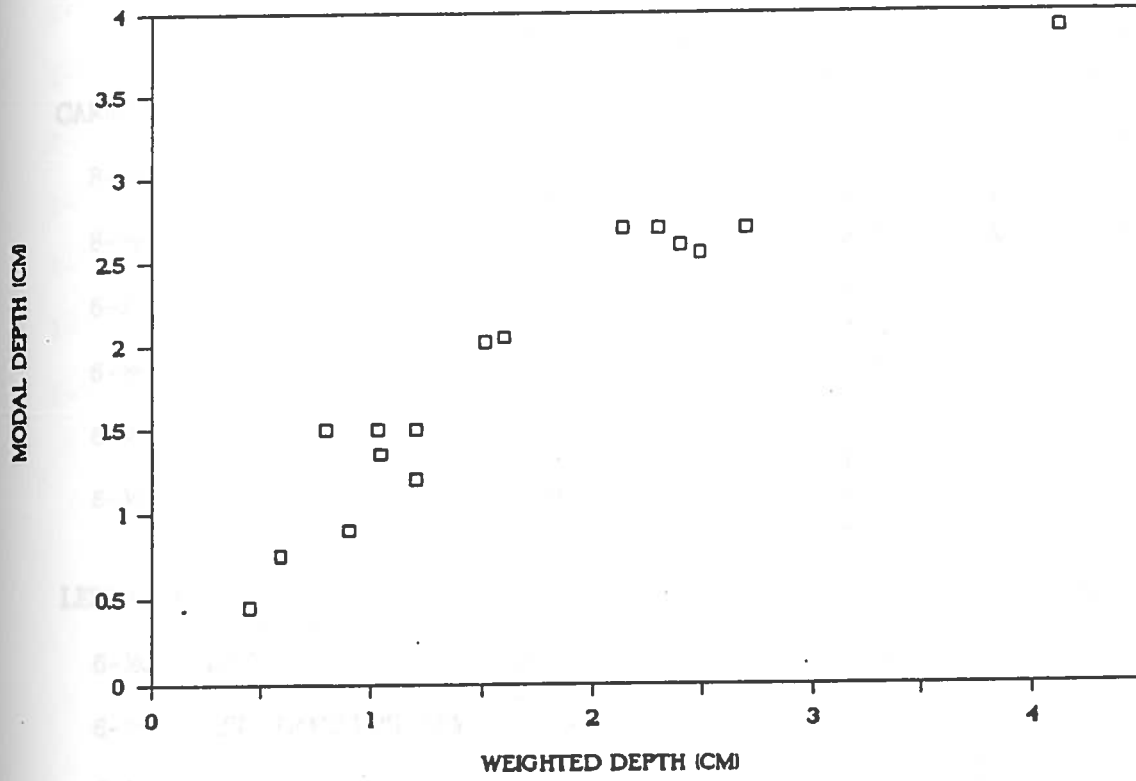


Table 5.5- Average sediment rates as determined by feldspar (AVG. CLAY).

MINERALS MANAGEMENT SERVICE STUDY

SITE	BINOM. DEPTH(MM)	MODE	BREAK PT.	CLASS	AVG.MODE AVG CLAY		
					DY SM	DY & SM (mm/yr)	
CAMERON							
	7/8/87					(mm/6 mo.)	
8-MO	CBN 1	11.8	7.5	7.5	IIA	5.6	2.6
		11.2	7.5	7.5	IIA		
8-MO	CBN-2-S	10.0	13.5	13.5	IIA	10.1	0.7
		9.7	13.5	13.5	IIA		
6-MO	CBNr 1	7.3	7.5	7.5	I	7.5	2.6
		7.3	7.5	7.5	I		
6-MO	CBNr 2	9.0	1.5	1.5	IIA	1.5	0.0
		8.7	1.5	1.5	IIA		
6-MO	CBC 1	9.1	1.5	1.5	IIA	1.5	0.0
		8.9	1.5	1.5	IIA		
6-MO	CBC 2	10.1	4.5	4.5	I	4.5	0.0
		9.8	4.5	4.5	I		
LEEVILLE							
	12/15/86					(mm/6 mo.)	
6-MO	LSC TRANS. (0-M)	N/A	1.5	1.5	I	1.5	
		N/A	1.5	1.5	I		
6-MO	LSC TRAN(BRG)15M	-	-	-	V	-	
		-	-	-	V		
6-MO	LSC TRAN(STRM)35	-	-	-	V	-	
		-	-	-	V		
6-MO	LSN 1	5.7	7.5	7.5	I	7.5	4.7
		6.2	7.5	7.5	I		
6-MO	LSN 2	8.5	10.5	10.5	IIA	10.5	5.1
		8.6	10.5	10.5	IIB		
6-MO	LSN 3	8.2	4.5	13.5	IIA	4.5	8.4
		8.6	4.5	4.5	IIA		
6-MO	LSCd 2	11.0	7.5	10.5	IIA	7.5	8.8
		11.3	7.5	7.5	IIA		
	5/13/87 & 6/11/87						
6-MO	LSN TRAN (0-M)JU	9.1	7.5	10.5	IIA	7.5	8.5
		9.1	7.5	10.5	IIA		
6-MO	LSN TRAN(10-M)JU	10.7	13.5	10.5	IIA	13.5	2.7
		10.7	13.5	10.5	IIA		
6-MO	LSN TRAN(30-M)JU	9.2	7.5	7.5	IIA	6.0	3.7
		10.3	4.5	4.5	IIB		
6-MO	LSN TRAN(50-M)JU	10.6	7.5	7.5	IIA	7.5	1.4
		7.0	7.5	7.5	IIA		
6-MO	LSCd 3 (50-M) JU	9.8	7.5	10.5	IIA	7.5	
		9.8	7.5	10.5	IIA		
6-MO	LSC 2 WEST MAY	7.5	7.5	-	IIA	7.5	5.7
		7.5	7.5	-	IIA		
6-MO	LSC 2 EAST MAY	4.6	4.5	4.5	I	4.5	

Table 5.5- Continued

SITE		MINERALS MANAGEMENT SERVICE STUDY					
		BINOM. DEPTH(MM)	MODE	BREAK PT.	CLASS	AVG. MODE	AVG CLAY
		DY SM	DY SM	DY SM	DY SM	DY & SM (mm/yr)	(mm)
1-YR	LSC TR(0-M)M CAN	N/A	16.5	16.5	III	16.5	9.0
1-YR	LSC TRAN(20-M)JU	9.9	16.5	10.5	IIA	16.5	13.4
1-YR	LSC TRAN(30-M)JU	9.2	16.5	7.5	IIB	15.0	17.3
1-YR	LSC TRAN(50-M)JU	10.3	16.5	10.5	I	16.5	11.7
1-YR	LSN 1 MAY	11.0	13.5	7.5	IIA	13.5	5.8
1-YR	LSN 2 MAY	5.9	7.5	7.5	IIA	7.5	9.8
1-YR	LSN 3 MAY	7.8	4.5	4.5	IIA	4.5	11.5
		7.9	4.5	4.5	IIA		

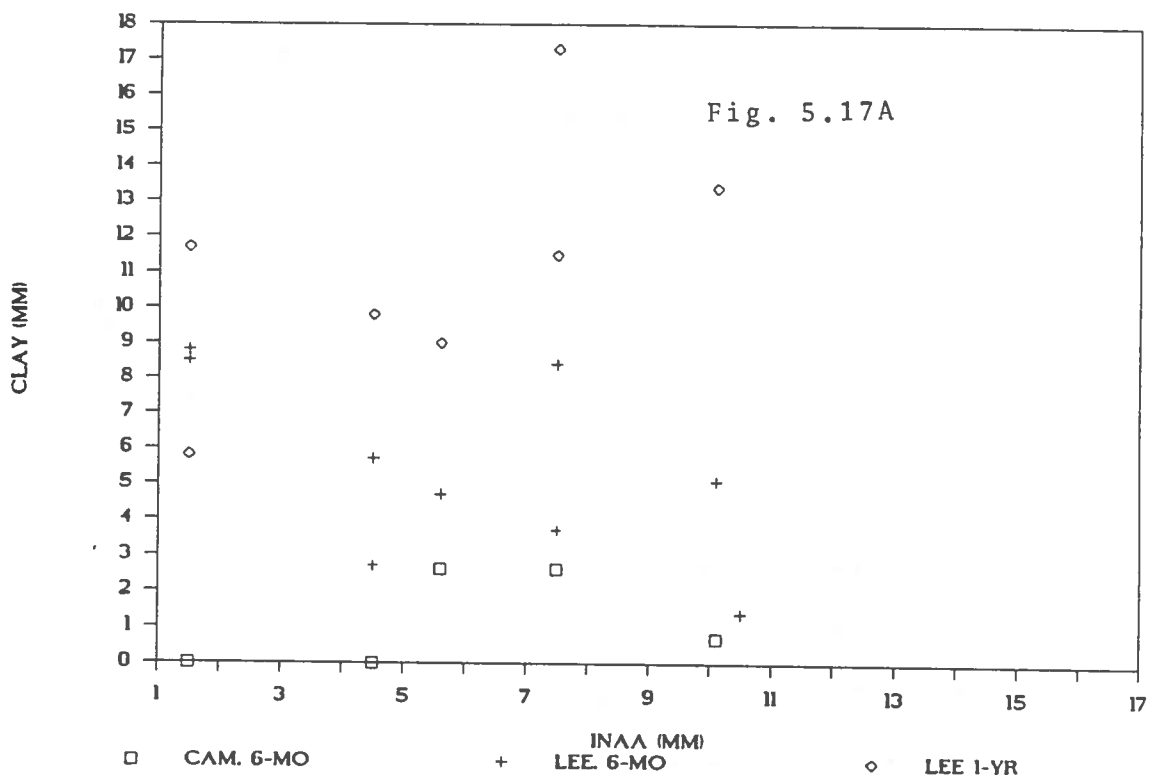
Comparison of INAA and clay marker methodology

Table 5.5 is a tabulation of accretion values as determined by the INAA technique (modal analysis) compared to accretion values as determined by the visible horizon methodology (clay). These are cases where samples were taken by both MMS working groups (Knaus and Van Gent; Cahoon and Turner) side-by-side at precisely the same times in plots that were established simultaneously. Figure 5.17A is a scattergram which depicts these data. The data appear to cluster in three distinct populations corresponding to sample site and sample date. Note that the 6-month Cameron data evidences the greatest bias between the two methodologies, the 6-month Leeville samples less, and the 1-year Leeville samples little if any. The INAA technique appears to yield larger accretion values as compared to the clay marker technique. Three unpaired *t*-tests were carried out to test the hypothesis that the 3 mean accretion values for Cameron 6-month data, Leeville 6-month data, and Leeville 1-year data as determined by the INAA technique are significantly greater than the three mean accretion values as determined by the clay marker technique (one-tailed test). The assumptions of equal variance, equal *n*, and independent samples were applied:

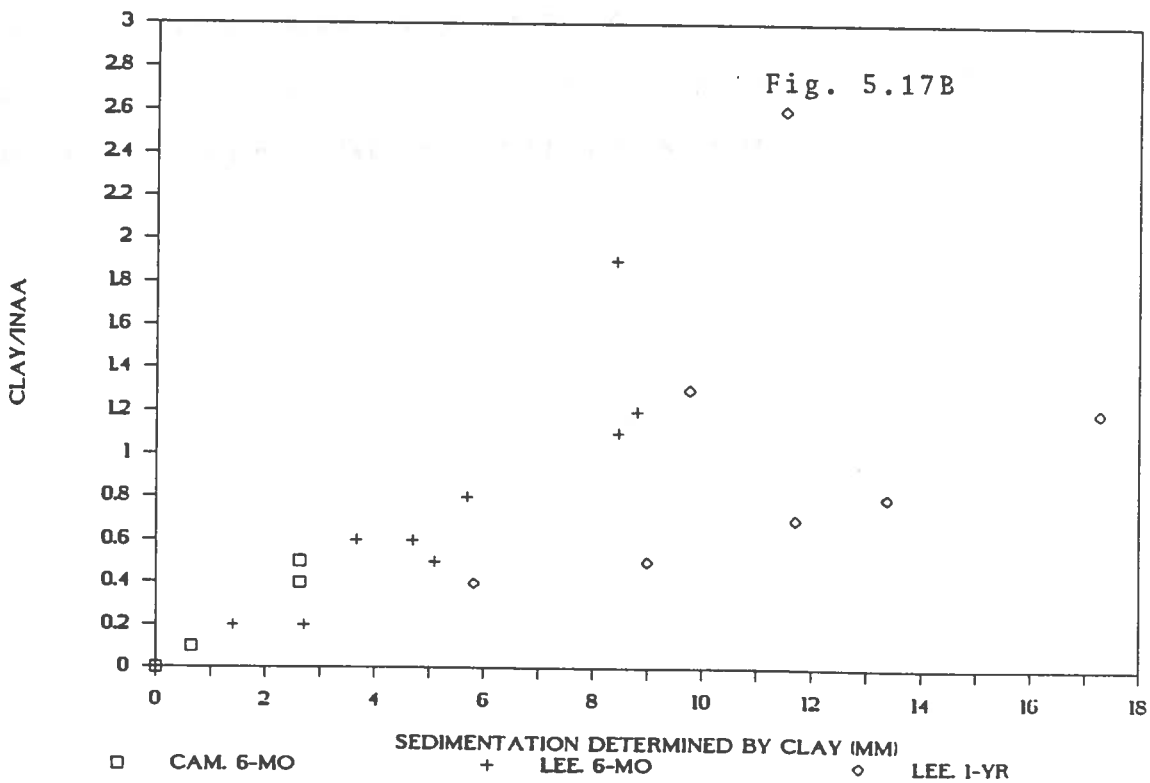
1. Cameron 6-month data- the INAA technique yielded a significantly higher mean accretion value than the clay marker technique ($p \leq 0.01$).

Figure 5.17A-B. Figure 5.16A depicts twenty-two accretion values as estimated by rare earth horizons using modal analysis (INAA) plotted against accretion values as estimated by the clay horizon method on the x-axis and y-axis, respectively. Figure 5.17B depicts the identical data as is shown in Figure 5.17A. The ratio of the individual accretion value determined by clay methodology and the individual accretion value determined by rare earth methodology (y-axis) is plotted against the individual accretion value determined by clay methodology (x-axis). Three of the data points in Figure 5.17B are at the origin (Cameron samples).

INAA vs. CLAY METHOD



CLAY/INAA RATIO vs. CLAY ONLY



2. Leeville 6-month data- the INAA technique yielded a significantly higher mean accretion value than the clay marker technique ($p \leq 0.05$).

3. Leeville 1-year data- the INAA technique did not yield a significantly higher mean value than the clay marker technique ($p \geq 0.24$)

Figure 5.17B depicts the same data represented in Figure 5.17A with the exception that the individual values on the y-axis are determined by taking the ratio of the accretion values as determined by both methods. The value as determined by the clay method was divided by the value as determined by the INAA method and then plotted against the clay value on the x-axis. This manipulation appears to indicate that the clay technique is the source of the bias between the two methods and that the magnitude of the bias is inversely proportional to the amount of sediment which has accumulated above the clay marker. There are a number of possible explanations for this observation which are discussed in Chapter 6 of this thesis.

CHAPTER 6

DISCUSSION

The *Results* section of this thesis (Chapter 5) presented the results of two possible interpretations applied to the problem of ascertaining the depth of accreted material as referenced against the observed rare-earth marker distributions found in the cryogenic cores. The first was *modal analysis* which is applied to the data with the primary assumption being that the point at which the highest concentration of marker occurs in the soil profile is indicative of the original position of the rare-earth marker and that point is the reference horizon from which accretion depth is measured.

The other possible interpretation was *dynamic analysis* with the primary assumption being that the weighted mean depth is the point at which the reference horizon is found. Because of the complexities involved in this type of analysis, it was applied only to data which closely matched the computer generated theoretical distributions.

Since the *modal analysis* scheme of data analysis was originally hypothesized to be the best method for accretion determination, all statistical analyses concerning effects of waterways on the wetland systems under observation during this study were carried out using values as determined by *modal analysis*. The results of *dynamic analysis* were presented for comparison and as a basis for future work.

Lafourche at Leeville

The grand mean of accretion for 6-month samples in the Lafourche at Leeville study area was 7.6 mm with a standard deviation of 2.6 mm and range of 4.5-13.5 mm. The grand mean for all 1-year data was 12.9 mm with a range of 4.5-16.5 mm. These means are inclusive of all waterway types, both natural and man made, and are probably representative of the Lafourche at Leeville study area. Testing for a significant difference between the natural treatment and the canal treatment revealed that there was no significant difference ($p \geq 0.41$) after 6 months had elapsed since plot establishment.

A test for a significant difference between waterway types after 1 year had elapsed revealed that the canal treatment showed significantly higher accretion ($p \leq 0.02$) as compared to the natural waterway treatment. This result was unexpected and should be viewed with caution since the major premise at the beginning of this study was that natural waterways should evidence the greatest accretion rates because of the increased resistance offered by natural waterways to the flow of sediment-laden water and the consequential greater sedimentation rates. If this statistical test is trustworthy, it may be possible that this effect traces to increased erosion and redeposition of eroded materials in canal waterways.

Terrebonne

The grand mean of accretion at the Terrebonne study area for all 6-month data was 15.3 mm with a standard deviation of 6.6 mm and a

range of 4.5-26.0 mm. The grand mean for all 1-year data is 29.7 mm with a standard deviation of 9.2 mm and a range of 19.5-47.5 mm. These means are probably representative of the Terrebonne study area.

A test for a significant difference between waterways (natural and canal distance transects) revealed significantly greater accretion ($p \leq 0.01$) at the natural transect after 1-year. This result was expected but should also be viewed with caution because of small sample size and the novelty of this technique in application to freshwater wetland systems. No other tests involving effects of waterways on accretion were possible.

Cameron

The grand mean of accretion at the Cameron study area for 6-month samples is 5.1 mm with a standard deviation of 3.4 mm and a range of 1.5-10.1 mm. 1-year samples were not taken in time for inclusion in this thesis. No statistical tests were attempted because of small sample size.

Other study areas

The study areas that were not included in the MMS study are mentioned here for purposes of reference and future study. Since no experimental design was applied to these areas, it is not possible to test for effects due to waterway type.

Cocodrie 6-month samples yielded a mean value of 9.5 mm with a standard deviation of 1.7 mm and a range of 7.5-10.5 mm.

Lafourche at Fourchon 6-month samples yielded a mean of 7.5 mm

with a standard deviation of 0.0 mm and no range. 1-year samples yielded a mean of 8.3 mm with a standard deviation of 1.1 mm and a range of 7.5 mm to 9.0 mm.

Lac Des Allemands 2-year samples yielded a mean of 50.5 mm with a standard deviation of 12.5 mm and a range of 32.5-62.5 mm.

Rockefeller Wildlife Refuge 2.5-year samples yielded a mean accretion of 17.5 mm with a standard deviation of 7.1 mm and a range of 12.5-22.5 mm at the Superior Canal location and a mean accretion of 17.5 mm with a standard deviation of 5.0 mm and a range of 12.5-22.5 mm at the Price Lake location.

Statistical resolving power

The results of this study have yielded estimates of the variance associated with accretion measurement by rare-earth horizon technique in saline and freshwater marshes. Consequently, it is possible to estimate the number of samples (cores) which must be taken in order to detect a given disparity in accretion between natural and canal waterways. Table 6-1 shows the results of the application of the following relationship to some of the data collected during this study:

$$n = \frac{t^2 \cdot s^2 \cdot 2}{d^2} \quad (\text{Eq. 6-1})$$

where n is the total number of cores required to detect a difference

Table 6.1- Total number of cores (n) required to detect a difference (d) of accretion between natural and canal waterways with 95% confidence.

Resolving power of INAA methodology

6-mo Leeville		1-yr Leeville		1-yr Terrebonne	
d (mm)	n	d (mm)	n	d (mm)	n
1	103.6454	1	115.0477	1	783.5161
2	25.91136	2	28.76194	2	195.8790
3	11.51616	3	12.78308	3	87.05735
4	6.477840	4	7.190485	4	48.96976
5	4.145817	5	4.601910	5	31.34064
6	2.879040	6	3.195771	6	21.76433
7	2.115213	7	2.347913	7	15.99012
8	1.619460	8	1.797621	8	12.24244
9	1.279573	9	1.420342	9	9.673039
10	1.036454	10	1.150477	10	7.835161

of magnitude d (mm) with 95% confidence, s^2 is the estimated pooled variance of both natural and canal waterways, and t is the Student's- t value for the required confidence level (95%) and available degrees of freedom (Steel and Torrie, 1980). The Lafourche at Leeville 6-month and 1-year samples were utilized for estimation of required sample size for saline marshes, and the 1-year Terrebonne data was used for estimation of required sample size for freshwater marshes. The 6-month and 1-year Leeville data yielded essentially identical results (Table 6.1). In order to detect a difference (d) of accretion of 3 mm between natural and canal waterways, approximately 6 cores must be taken from 6 separate natural plots, and 6 cores from 6 separate canal plots. It is apparent that in the Terrebonne freshwater marsh system, a more realistic statistically significant resolution would be 7 mm, which would require 8 cores each from natural and canal waterways, for a total of approximately 16 cores. It is implicit that each core must yield useful information. If the success rate is not 100%, the number of cores must be increased accordingly.

Modal analysis vs. dynamic analysis

In Chapter 5 of this thesis, it was demonstrated that measured accretion differed significantly between the two methods of modal and dynamic analysis. The y-intercept of Figure 5.16 departed significantly from 0.0 mm ($p \leq 0.01$) which suggests that a bias of an average of 3.6 mm exists between the two methods. If the dynamic analysis model does indeed conform more closely to reality than the modal analysis model, then the modal accretion determination may

actually yield accretion rates that are too high. However, this fact should not affect statistical hypotheses designed to test for significant differences of accretion between waterway types since the bias would be present in all measurements. However, the bias may be of importance if an accurate determination of short-term accretion rates (less than 1 year) is required. For instance, attempts to accurately assess absolute quantities such as subsidence, submergence, and sediment budgets could be seriously hindered. A bias of 3.6 mm is critical in areas that accrete at a rate of 10 mm per year, representing a possible error of 36%.

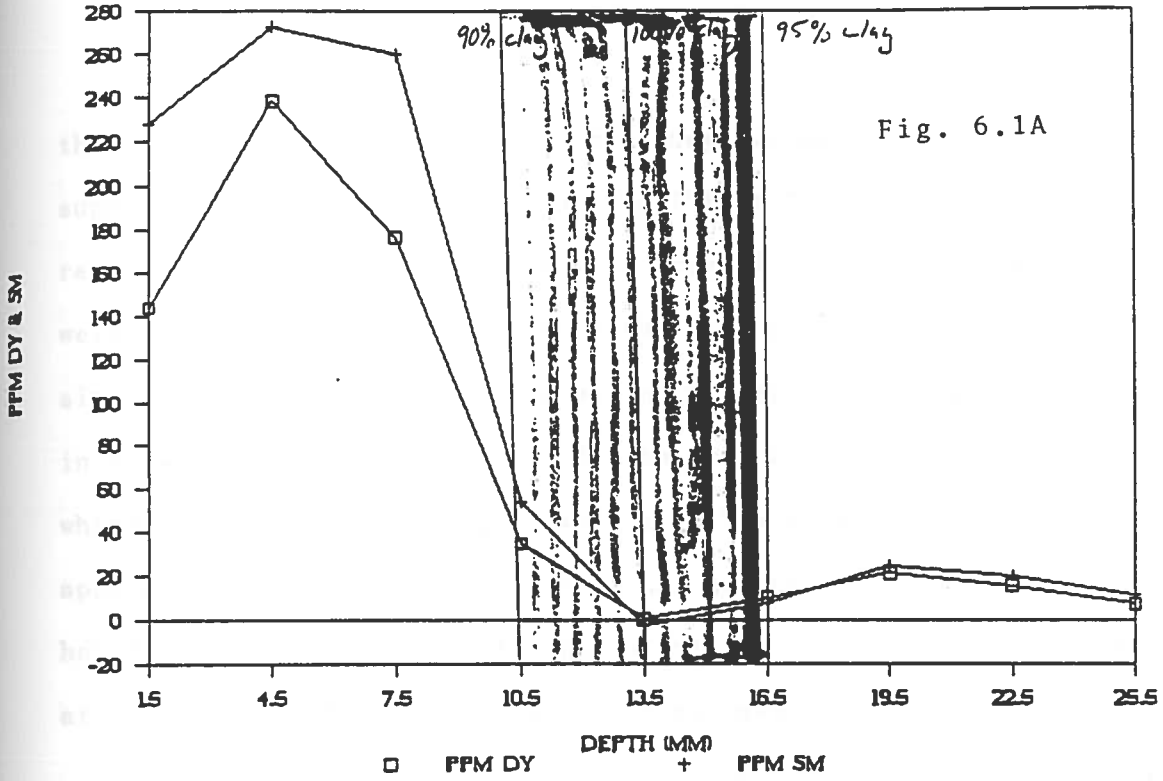
The *Dynamic analysis* model should not be considered to be complete as far as it was developed in this thesis. The assumption of a single mixing-layer is probably simplistic. The mixing-layer in nature is probably gradational (Guinasso and Schink, 1975). Additionally, sedimentation is not a continuous process but, rather, a series of discrete events, usually correlated with storm surges (Reed, 1987). However, it is likely that accretion is what is actually being measured by the INAA techniques. This study yielded evidence that accretion is a process which has a structural component and appears to occur uniformly over time, perhaps somewhat independent of short-term fluctuations in sediment supply. Lastly, a need exists to create a numerical method which will provide a best fit of the model to observed marker distributions. This is not a trivial optimization problem, and future work could be devoted to this concept.

INAA vs. Clay methodolgy

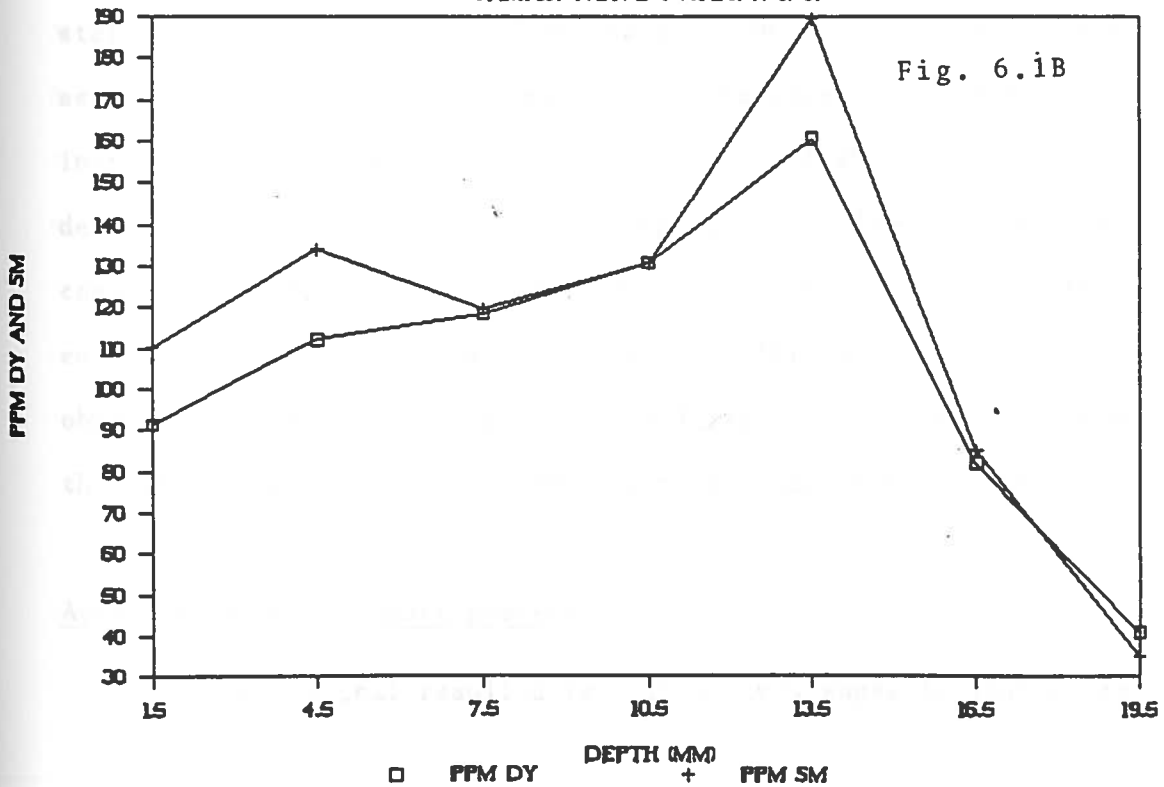
Figure 5.16A depicts the scattergram of accretion by INAA technique vs. accretion by the visible clay horizon. Only twenty-two samples were directly comparable in this way. Visual inspection of the scattergram reveals that there is similar variance in the clay data compared to that present in the INAA data. However, the data points cluster into three distinct populations directly related to area and sampling date. A Student's-*t* test applied to the means of each population revealed that the INAA technique yielded significantly higher accretion values for the Cameron 6-month population ($p \leq 0.01$) and the Leeville 6-month population ($p \leq 0.05$). Only at 1-year was this not the case ($p \geq 0.24$).

Figure 5.16B depicts the same data as that displayed in Figure 5.16A. The ratio between the individual data (clay/INAA), displayed on the y-axis, is plotted against the corresponding clay accretion value alone. This suggests that the clay method does not measure the same quantity as does the INAA method until a sediment layer of approximately 8 mm accumulates over the clay horizon. The most likely interpretation of this results is that the clay method provides an estimate of sedimentation while the INAA method provides an estimate of accretion, at least during short-term obsevation of less than 1 year. After 1 year, accretion measurements as determined by the 2 methodologies appears to converge, probably because the clay horizon presents a barrier to normal mixing of the incoming sediment with *in situ* organic materials. Additionally, the colonization of the incoming sediment with meio- and micro- fauna is possibly delayed by

Figure 6.1A-B. The marker distribution is shown for a cryogenic core which was inadvertently taken at the clay plot at the CBN 1 site at 1-year (Fig. 6.1A) The shaded region represents the actual boundaries of the clay layer. The marker distribution in the second figure shows a core taken at the same site at the 8-month sampling date (Fig. 6.1B) without clay. The implication is that the clay horizon acts as a barrier to normal soil processes.



DISTRIBUTION OF DY & SM
 CAMA87 (CBN-2-5 (CAN) 7/8/87



the clay barrier. Figure 6.1A-B provides evidence supporting this supposition. When the plot at Cameron (CBN-1) was established, rare-earth marker was applied to the exposed clay horizon surface as well as the rest of the plot which had been established simultaneously. Figure 6.1A shows the marker distribution at 6-months in this plot. Figure 6.1b depicts the core that was taken at 1-year which inadvertently overlapped with the clay horizon plot. It is apparent that the rare-earth marker has no affinity for the clay horizon, and furthermore, that normal mixing into the soil profile is at least partially prevented by the clay layer.

Alternate explanations for the bias between methods are possible. For instance, it is conceivable that the cryogenic coring device preserves the delicate flocculum presumably present at the surface early in the study while the clay method, which utilizes thin-walled aluminum beverage cans for the taking of cores, destroys the stratigraphy of the surface of the sample. However, this explanation seems unlikely because incoming sediment is usually more highly inorganic than the matrix it deposits into, and should thus be more dense and consolidated than underlying *in situ* sediments. A personal communication from Cahoon (1988) corroborated the supposition that the can-coring method is reliable and causes relatively little if any observable disturbance of surface stratigraphy. It is probable that the bias between the two methods traces to some other effect.

Accretion as a transport process

Information that resulted from this study suggests that accretion

is a dynamic process rather than a passive accumulation of sediment. Close agreement of observed data with the theoretical model of Guinasso and Schink (1975) lends support to the supposition that the upper centimeter or so of the marsh surface is a highly dynamic system, consisting of a biological mixing-layer. Quantitative estimates of biological mixing in this layer were determined, apparently for the first time. Rates of mixing (D) ranged from $0.03 \text{ cm}^2 \cdot \text{yr}^{-1}$ to $9.28 \text{ cm}^2 \cdot \text{yr}^{-1}$. These values are comparable in magnitude to mixing rates observed by others working with marine and lake benthic systems (Guinasso and Schink, 1975; Robbins, 1982). This type of mixing is presumably the result of Class II bioturbation as defined in Chapter 2 of this thesis.

If bioturbation is indeed an integral component of the wetland accretion process, then it is possible to construct a formalized framework for the description of accretion as a *transport process*. In technical terms, a transport process is one which involves a flow of matter or energy as a result of a force being applied to a given system (Eisenberg and Crothers, 1979). The net rate of motion in one direction is called the *transport velocity*. The flow of matter in this case is sediment, and the applied or driving force is gravitational. In order to define this transport process, the following assumptions are made:

1. The rare-earth marker "pulse" behaves in a manner which is exactly analogous to sediment particulate matter. It is therefore acting as a tracer which passively follows the movement and distribution of

particulate matter throughout the vertical soil profile. Thus, a pulse of tracer entering the soil system will behave exactly as a pulse of sediment entering the soil system.

2. The net vertical movement of sediment particles, both inorganic and organic, is in the downward (positive x direction).
3. The mixing effect in the upper boundary of the system can be described by a gaussian diffusion coefficient (D) as defined in Equation 4.6. All matter (sediment) entering the system must propagate through the upper mixing layer into a more consolidated non-mixing-layer beneath.

If the above assumptions are correct, the following formalizations result:

1. A discrete sediment pulse input into the upper boundary of the system will be distributed in the vertical soil profile in a probabilistic manner.
2. The probability of an individual particle of sediment being found at a depth x at some time t after initial input is a function of the gaussian diffusion coefficient (D), sedimentation velocity (V), mixing-layer thickness (L), and time (t). The probability density observed will range from gaussian to exponential and is described by Eq. 4.3.

Possible limitations of application of the theoretical model to observed data are:

1. Compaction is not accounted for in the theoretical model, although the model could be modified to compensate for compaction effects.
2. Sediment particles are not ultimately conserved in their original form. For example, organic carbon entering the system may be ultimately converted to methane.
3. The mixing-layer may not be completely uniform, but rather, gradational in nature, with decreased biological mixing with increasing depth.

The limitations listed above are unlikely to have a significant effect on the observed system over a short period of time (less than 1 year), so departures of the observed marker distributions from the theoretical model will most likely not be apparent until considerable time passes. It should be noted that in any case, the observed sediment (tracer) distributions are the *actual* probability distributions, so deviations from model predictions present no problem if the primary goal is to determine the stochastic sediment probability distribution for a given site. In fact, the stochastic probability distributions may be characteristic and indicative of site-specific processes. This specific distribution might be termed a "process signature". Recently, such observations have been made by Schaffner et al., 1987 in an estuarine system where the distribution of ^{137}Cs had been determined and classified according to site-specific characteristics such as erosion or dredging.

Figure 6.2A-D. This series of figures were selected from the available marker distribution graphs on the basis of apparent familial similarities demonstrating the "process signature" concept.

1 June 88



NUCLEAR SCIENCE CENTER

(12)

Thesis to: _____ Date 6-1-88

To _____

1 *Gene* mail { 1 Texas A&M } 2 Extra Copies
 1 OSU
 1 LUMCON

1 Don *campus mail*
 1 Gene *campus mail*

3 (Los Alamos, *Hand carry* Don, *Fancy* Parents)

2 for Dr. Knapp (*Hand carry* Bound)

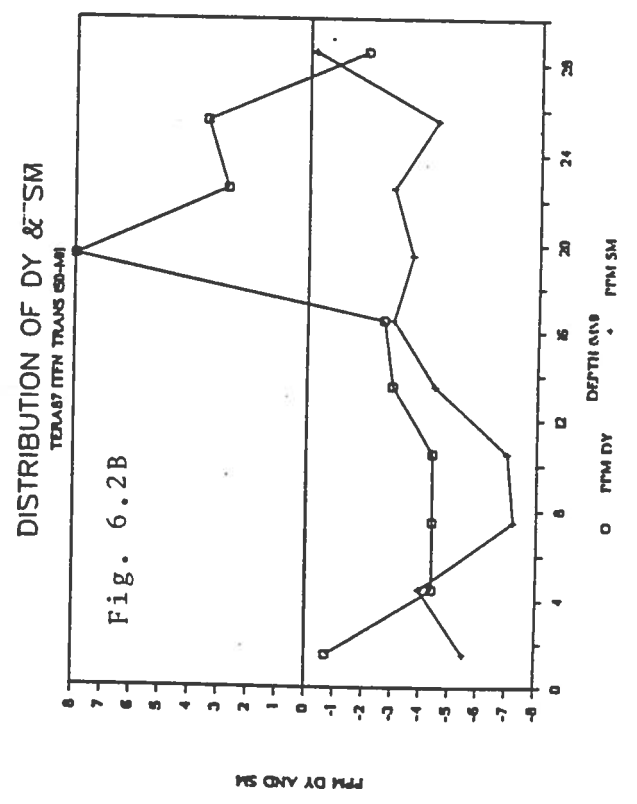
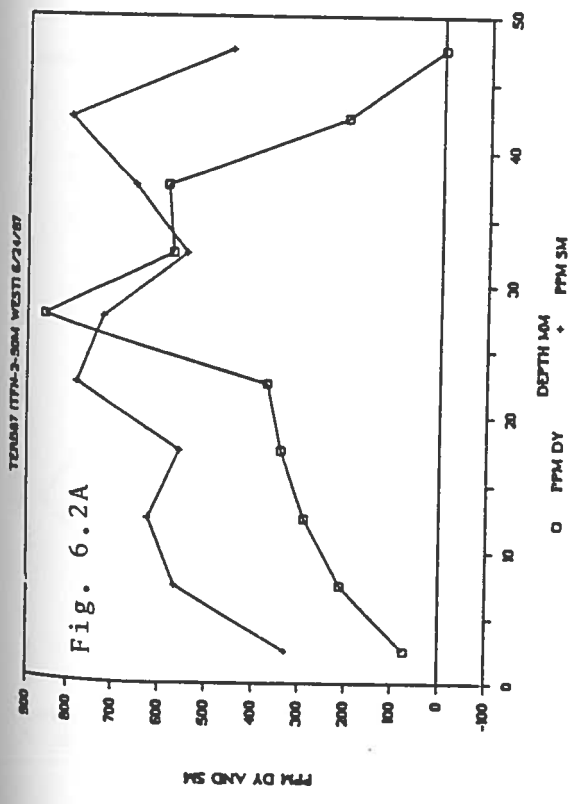
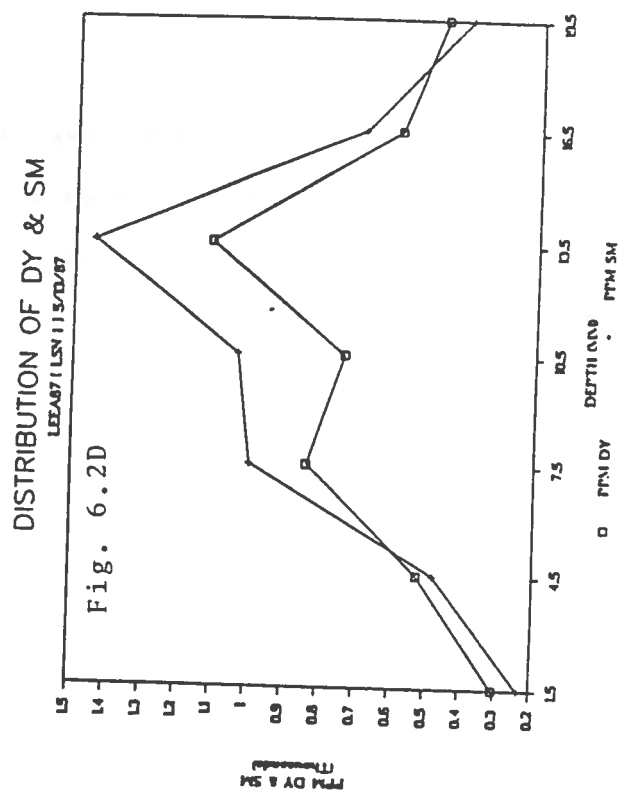
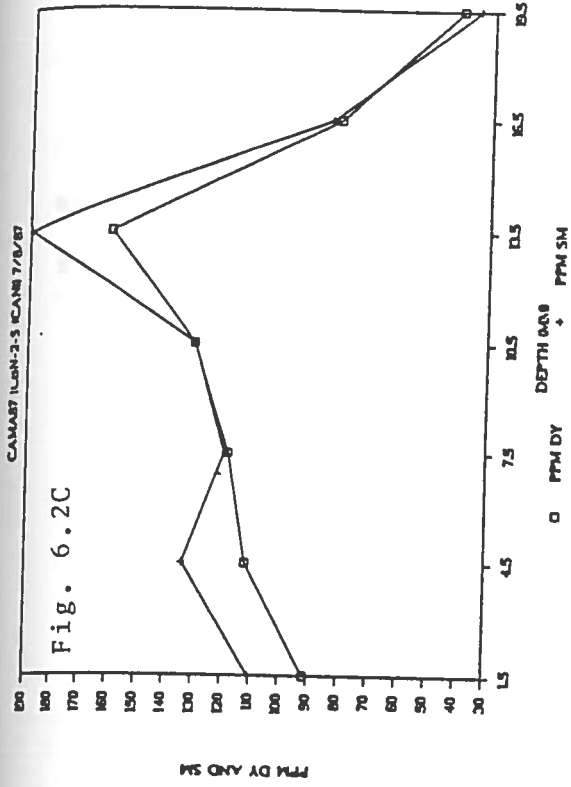
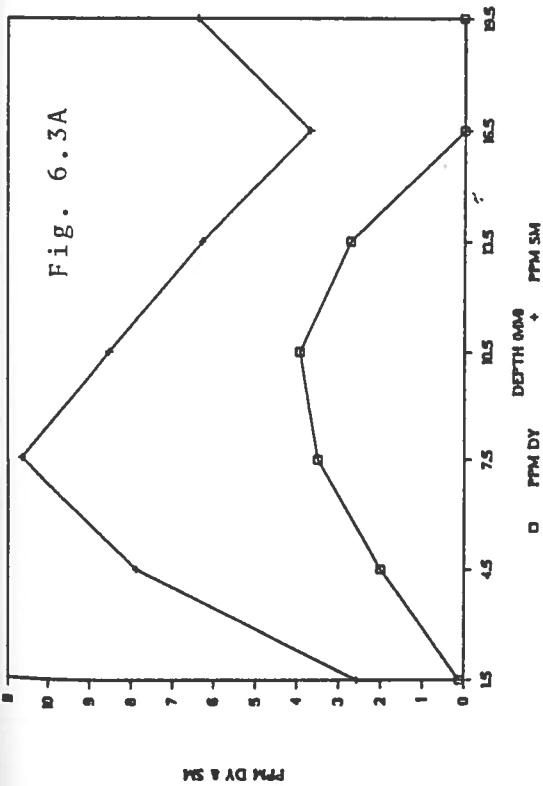
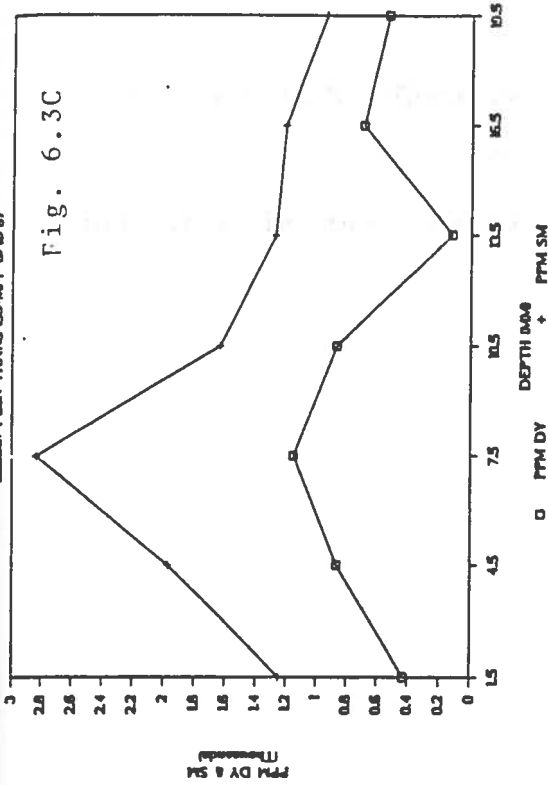


Figure 6.3A-D. This series of figures were selected from the available marker distributions graphs on the basis of familial similarities demonstrating the "process signature" concept.

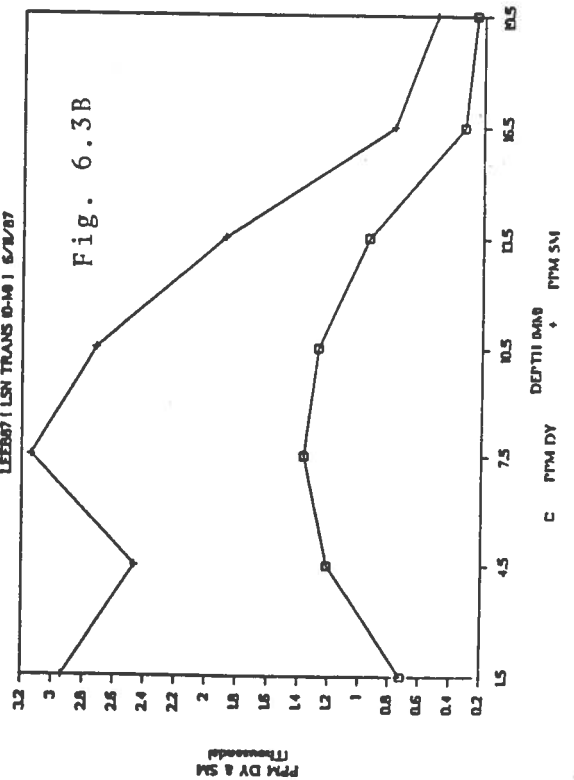
LEZERN7 IFCOURTEDO COL-20 5/13/87



LEZERN7 I LSN TRANS 80-10 1 6/18/87



DISTRIBUTION OF DY & SM
LEZERN7 I LSN TRANS 80-10 1 6/18/87



DISTRIBUTION OF DY & SM
COCARAS COCCOROT FLANK-70 11/18/86

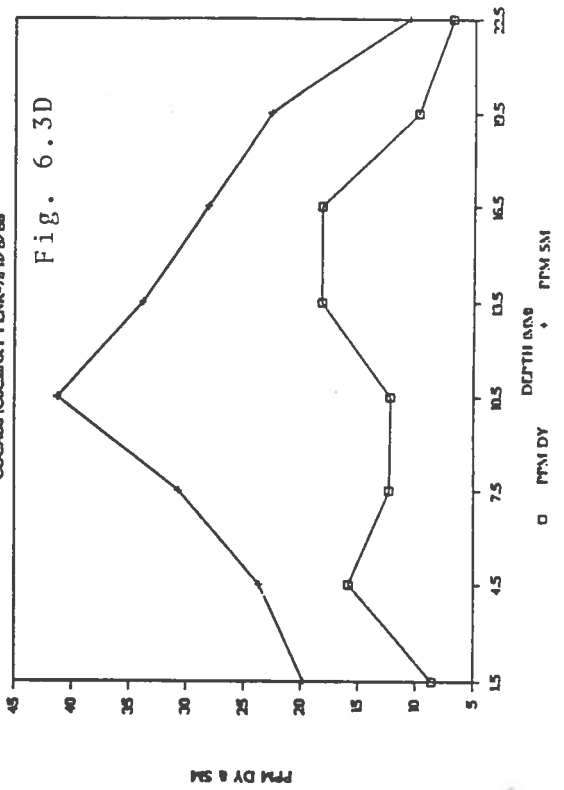
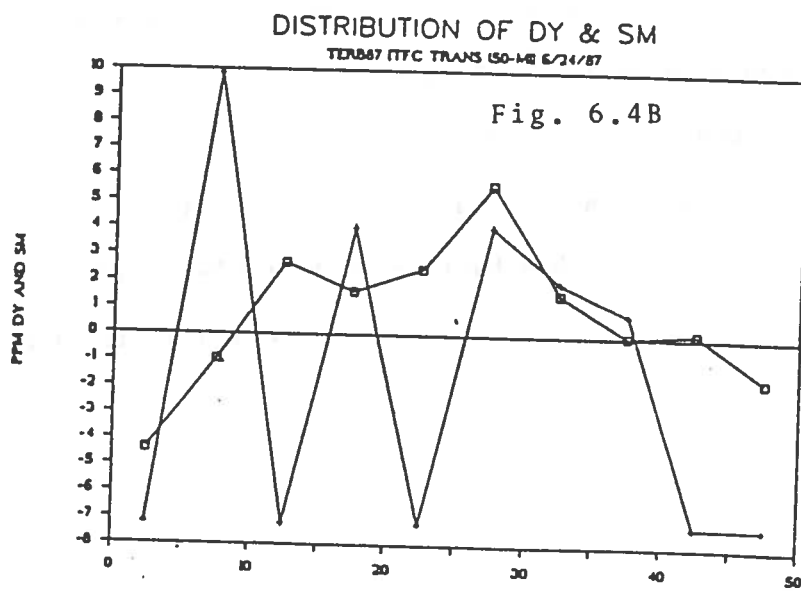
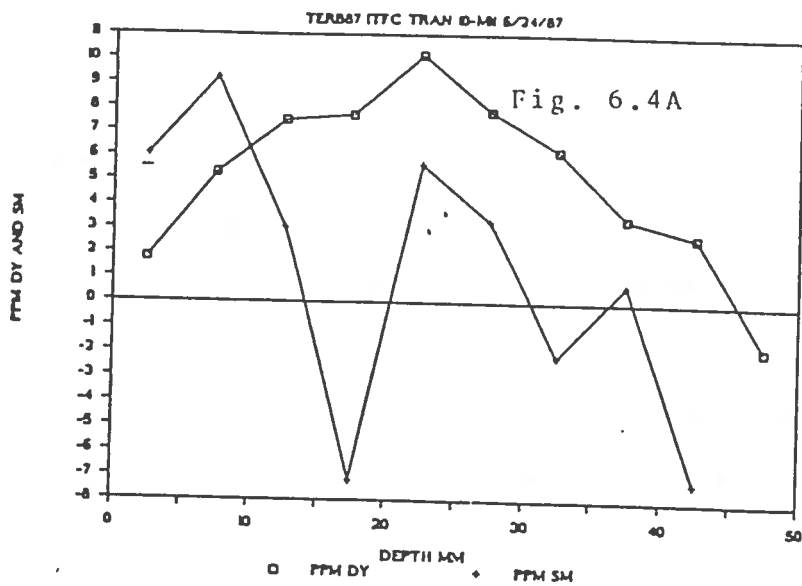


Figure 6.4A-B. These two figures were selected from the available marker distribution graphs on the basis of familial similarities in order to demonstrate the "process signature" concept.



Process signatures

A number of process signatures have been identified in the data collected during this study. Figures 6.2A-D, 6.3A-D, and 6.4A-B show some of those that have been identified. These examples are presented here for reference and speculation for further study. It may be possible to characterize an area or site by taking a number of cores and performing an autocorrelation which would result in a composite "signature" for that site. Association of the signature with status of the marsh (Chapter 1 of this thesis) may give rise to a technique whereby the status of a marsh system under consideration for restorative efforts could be gauged. This is only one of many possible utilities of the rare-earth tracer methodology as applied to wetland system processes. It is hoped that this discussion provides a basis for the development of refined and useful wetland assessment techniques in future work.

CHAPTER 7

CONCLUSION

The rare-earth soil horizon marker methodology successfully provided estimates of short-term accretion of the order of 6 months to 1 year. The method yielded meaningful results in nearly 90% of the cores taken (68). The methodology is unique in that it appeared to be applicable to freshwater wetland habitats (Terrebonne, Rockefeller, and Lac Des Allemands). This was apparently the first time that short-term accretion rates were successfully and consistently estimated in freshwater wetland systems. The reason for this success may be related to the sorption of the rare-earths to organic surfaces, as well as inorganic surface components. (The sorption of rare-earths to living root in flowing streams has previously been demonstrated [Knaus and Curry, 1979; Knaus, 1981; Knaus and El-Fawaris, 1981]). Macroscopic organic components, such as roots, are probably less mobile than the inorganic and decaying organic components during periodic episodes of intense waterflow which are characteristic of freshwater wetland systems (Baumann, 1980). For instance, if the marker sorbs to live roots in the soil matrix, it is likely to remain, while marked inorganic components and loose detrital material wash away.

The data strongly suggest that the rare-earths passively follow vertical sediment transport processes in the soil profile. In this respect, the rare-earths are behaving as tracers as well as providing an artificial horizon marker. Apparently, a layer of feldspar clay which is nearly as thick as the dynamic mixing layer (~ 1 cm) acts as

a physical barrier which interferes with normal mixing of incoming sediment pulses into the marsh soil system. On a short-term basis of 6 months or less, it appeared that accumulation as measured by feldspar clay more accurately reflects sedimentation as opposed to accretion rates. After 6 months, the feldspar clay and rare-earth horizons appear to yield comparable accretion values. This observation can best be explained by supposing that the incoming sediment which deposits onto the feldspar clay horizon is not initially of the same composition as the proximal undisturbed marsh surface. It is probable that some time must elapse before the deposited sediment mixes with *in situ* organic materials and is colonized by the indigenous meiofauna and micro flora and fauna.

Finally, there appears to be some bias introduced into accretion estimates by *modal analysis* as opposed to *dynamic analysis*. *Modal analysis* does not compensate for distortion of the original discrete marker pulse by biological mixing in the upper layers of the marsh surface.

Hopefully, future studies will directly address the ideas and hypotheses presented in this chapter. Currently, a study is in progress at the Cocodrie LUMCON site which will specifically test the hypothesis that feldspar clay horizon methodology does not accurately gauge accretion rates until a period of about 6 months has expired. At the same site, an experiment is in progress to determine if, indeed, the concept of "process signatures" is a useful index of marsh viability. If this proves to be so, the judicious application of stable tracer methodology to assessment of wetland status may

be of considerable value in future marsh management and restoration schemes.

REFERENCES CITED

- Basan, P. B., and R. W. Frey. 1977. Actual-palaeontology and neoichnology of salt marshes near Sapelo Island, Georgia. In T. P. Crimes and J. C. Harper (eds.). Trace Fossils 2. Geol. J. Spec. Issue 9.
- Baumann, R. H. 1980. Mechanisms of maintaining marsh elevation in a subsiding environment. A thesis. Department of Geography, Louisiana State University. 90 p.
- Baumann, R. H., J. W. Day Jr., and C. A. Miller. 1984. Mississippi deltaic wetland survival; Sedimentation versus coastal submergence. Science 224: 1093-1095.
- Berger, W. H. and G. Ross Heath. 1968. Vertical mixing in pelagic sediments. J. Mar. Res. 26: 134-143.
- Boesch, D. F., D. Levin, D. Nummedal, and K. Bowles. 1983. Subsidence in coastal Louisiana, causes, rates and effects on wetlands. U.S. Fish and Wildlife Service, FWS/OBS 83/26. Biological Service Program. 259 p.
- Cahoon, D. R. and R. E. Turner. 1987. Marsh Accretion, Mineral Sediment, and Organic Matter Accumulation: Clay Marker Horizon Technique. p. 259-275. In R. E. Turner and D. R. Cahoon (eds.). Causes of Wetland Loss in the Coastal Central Gulf of Mexico. Vol. 2. Final Report, Minerals Management Service, New Orleans, LA. Contract No. 14-12-0001-30252. OCS Study/MMS 87-0120.

- Cahoon, D. R., R. D. DeLaune, and R. M. Knaus. 1987. Marsh Accretion, Mineral Sediment Deposition, and Organic Matter Accumulation Along Man-Made Canals and Natural Waterways: Introduction, p. 233-243. *In* R. E. Turner and D. R. Cahoon (eds.). Causes of Wetland Loss in the Coastal Central Gulf of Mexico. Vol. 2. Final Report, Minerals Management Service, New Orleans, LA. Contract No. 14-12-0001-30252. OCS Study/MMS 87-0120.
- Christensen, E. R. 1982. A model for radionuclides in sediments influenced by mixing and compaction. *J. Geophys. Res.* 87: 566-572.
- Coleman, J. M., and S. Gagliano. 1964. Cyclic sedimentation in the Mississippi River deltaic plain. *Trans. Gulf Assoc. Geol. Soc.* 14: 67-80.
- Covell, D. F. 1959. Determination of gamma-ray abundance directly from the total absorption peak. *Anal. Chem.* 31: 1785-1790.
- Craig, N. J., R. E. Turner, and J. W. Day, Jr. 1979. Land loss in coastal Louisiana (U.S.A.). *Environmental Management* 3(2): 133-144.
- Cullen, D. J. 1973. Bioturbation of Superficial Marine Sediments by Interstitial Meiobenthos. *Nature.* 242: 323-324.
- Dapples, E. C. 1942. The effect of macro-organisms upon near-shore marine sediments. *J. Sediment. Petrology.* 12(3): 118-126.
- Darwin, C. R. 1881. The Formation of Vegetable Mold, Through the Action of Worms, With Observation of Their Habits. John Murray, London, (Reprinted by Faber and Faber, London, 1945).

- Davis, R. B. 1967. Pollen studies of the near surface sediments in Maine lakes. *Quaternary Paleocology*. Cushing, E. J., Wright, H. E., Eds., Yale University Press, New Haven (1967). p. 153-157.
- Delaune, R. D., W. H. Patrick, Jr., and R. J. Buresh. 1978. Sedimentation rates determined by ^{137}Cs dating in a rapidly accreting salt marsh. *Nature*. 275: 532-533.
- Eddington, D. N. and J. A. Robbins. 1977. Patterns of deposition of natural and fallout radionuclides in the sediments of Lake Michigan and their relationship to limnological processes. p. 705-719. *In* *Environmental Biogeochemistry*. V. 2. Ann Arbor Sci.
- Eisenberg, D. S. and D. Crothers. 1979. *Physical Chemistry*. p.700-705. The Benjamin/Cummings Publishing Company, Inc., Menlo Park, CA.
- Fleeger, J. W. 1985. Meiofaunal Densities and Copepod Species Composition in a Louisiana, U.S.A., Estuary. *Trans. Am. Microsc. Soc.*, 104(4): 321-332.
- Gagliano, S. M., K. J. Meyer-Arendt, and K. M. Wicker. 1981. Land loss in the Mississippi River Deltaic plain. *Trans. Gulf Coast Assoc. Geol. Soc.* 31: 295-300.
- Glass, B. P. 1969. Reworking Of Deep-Sea Sediments As Indicated By The Vertical Dispersion Of The Australian And Ivory Coast Microtektite Horizons. *Earth and Planetary Science Letters*, 6: 409-415.
- Goldberg, E. D., and M. Koide. 1962. Geochemical; studies of deep sea sediments by the thorium-ionium method. *Geochim. Cosmochim. Acta.* 26: 417-450.

- Guinasso, Jr., N. L., and D. R. Schink. 1975. Quantitative Estimates of Biological Mixing Rates in Abyssal Sediments. *J. Geophys. Res.* 80(21): 3032-3043.
- Harrison, E. Z., and A. L. Bloom. 1977. Sedimentation rates on tidal salt marshes in Connecticut. *J. Sed. Petrology* 47: 1484-1490.
- Hatton, R. S., R. D. DeLaune, and W. H. Patrick, Jr. 1983. Sedimentation accretion and subsidence in marshes of Barataria Basin, Louisiana. *Limnol. Oceanogr.* 28(3): 494-502.
- Kesel, R. H. 1987. Historical Sediment Discharge Trends for the Lower Mississippi River. p. 214-232. *In* R. E. Turner and D. R. Cahoon (eds.). *Causes of Wetland Loss in the Coastal Central Gulf of Mexico. Vol. 2. Final Report, Minerals Management Service, New Orleans, LA. Contract No. 14-12-0001-30252. OCS Study/MMS 87-0120.*
- Knaus, R. M. and L. R. Curry. 1979. Double Activation Analysis: A New Application of Established Techniques. *Bull. Environm. Contam. Toxicol.* 21: 388-391.
- Knaus, R. M. and A. H. El-Fawaris. 1981. A Biomonitor Of Trace Heavy Metals: Indium And Dysprosium In Red Alder Roots (*Alnus Rubra Bong.*) *Environmental and Experimental Botany*, Vol. 21, No. 2, p. 217-223.
- Knaus, R. M. 1986. A cryogenic coring device for sampling loose, unconsolidated sediments near the water-sediment interface. *J. Sed. Petrology* 56: 551-553.

- Knaus, R. M. 1987. Neutron activation of very recent sediment accumulations in wetlands bordering the northern Gulf of Mexico. American Chemical Society, Abstract Presented Before the Division of Environmental Chemistry, New Orleans, LA., August 1987.
- Knaus, R. M., and D. L. Van Gent. 1987. Marsh Accretion, Mineral Sediment Deposition and Organic Matter Accumulation: Rare Earth Stable Tracer Technique. *In* R. E. Turner and D. R. Cahoon (eds.). Causes of Wetland in the Coastal Central Gulf of Mexico. Vol. 2. Final Report, Minerals Management Service, New Orleans, LA. Contract No. 14-12-0001-30252. OCS Study/MMS 87-0120.
- Letzsch, W. S., and R. W. Frey. 1980. Deposition and erosion in a Holocene salt marsh, Sapelo Island, Georgia. *J. of Sed. Petrology* 50(2): 529-542.
- Miller, K. M., and M. Heit. 1986. A time resolution methodology for assessing the quality of lake sediment cores that are dated by ^{137}Cs . *Limnol. Oceanogr.* 31: 1292-1300.
- Moore, D. G., and P. C. Scruton. 1957. Minor internal structures of some recent unconsolidated sediments. *Amer. Ass. Petrol. Geol. Bull.* 41(12), 2723-2751.
- Reed, D. J. 1987. Short-term variability in salt marsh sedimentation, Terrebonne Bay, Louisiana. Brodtmann, N. V. (ed.). Fourth Water Quality and Wetlands Management Conference Proceedings, New Orleans, LA. p. 221-234.

- Richard, L. A. 1978. Seasonal and environmental variations in sediment accretion on a Long Island salt marsh. *Estuaries* 1(1): 29-35.
- Robbins, J. A., and D. N. Eddington. 1975. Determination of recent sedimentation rates in Lake Michigan using Pb-210 and Cs-137. *Geochimica et Cosmochimica Acta* 39: 285-304.
- Robbins, J. A., J. R. Krezoski and S. C. Mozley. 1977. Radioactivity in sediments of the Great Lakes: Post-depositional redistribution by deposit-feeding organisms. *Earth and Planetary Science Letters* 36: 325-333.
- Robbins, J. A. 1982. Stratigraphic and dynamic effects of sediment reworking by Great Lake zoobenthos. *Geobiologia* 92: 611-622.
- Schaffner, L. C., R. J. Diaz, C. R. Olsen and I. L. Larsen. 1987. Faunal Characteristics and Sediment Accumulation Processes in the James River Estuary, Virginia. *Estuarine, Coastal and Shelf Science* 25: 211-226.
- Skoog D. A., and D. M. West. 1969. *Fundamentals of Analytic Chemistry*. Holt, Rinehart and Winston, New York. 835 p.
- Stearns, L. A., and D. MacCreary. 1957. The case of the vanishing brick dust. *Mosquito News* 17: 303-304.
- Steel, R. G., and J. H. Torrie. 1980. *Principles and Procedures of Statistics, a Biometrical Approach*. 2nd ed. McGraw-Hill, New York. 633 p.
- Turner R. E. 1985. *Outer Continental Shelf Development and Potential Coastal Habitat Alteration. A proposal to the U.S. Department of Interior Minerals Management Service. Solicitation No. 3252.*

Turner, R. E. 1987. Executive Summary. *In* R. E. Turner and D. R.

Cahoon (eds.). Causes of Wetland Loss in the Coastal Central Gulf of Mexico. Vol. 1. Final Report, Minerals Management Service, New Orleans, LA. Contract No. 14-12-0001-30252. OCS Study/MMS 87-0120.

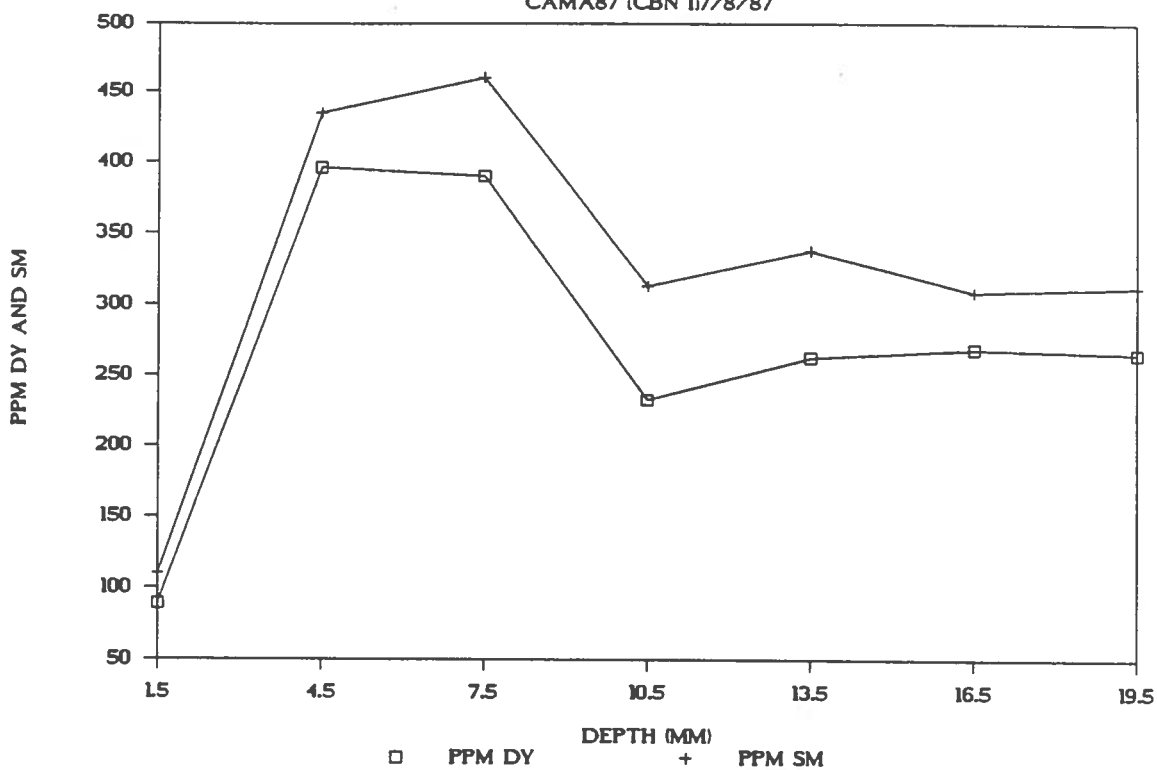
Wang, C. H., D. L. Willis and W. D. Loveland. 1975. Radiotracer Methodology in the Biological, Environmental, and Physical Sciences. Prentice-Hall, New Jersey. 480 p.

APPENDICES

APPENDIX A
MARKER DISTRIBUTION GRAPHS

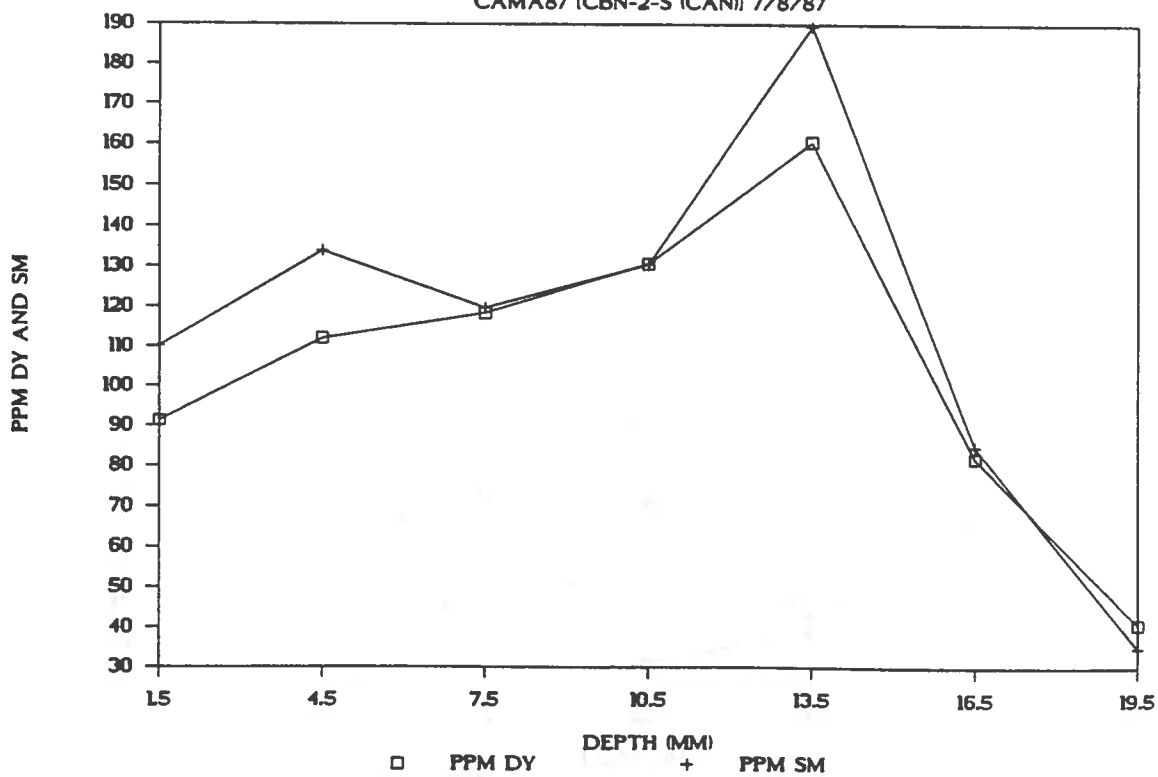
DISTRIBUTION OF DY & SM

CAMA87 (CBN 17/8/87)



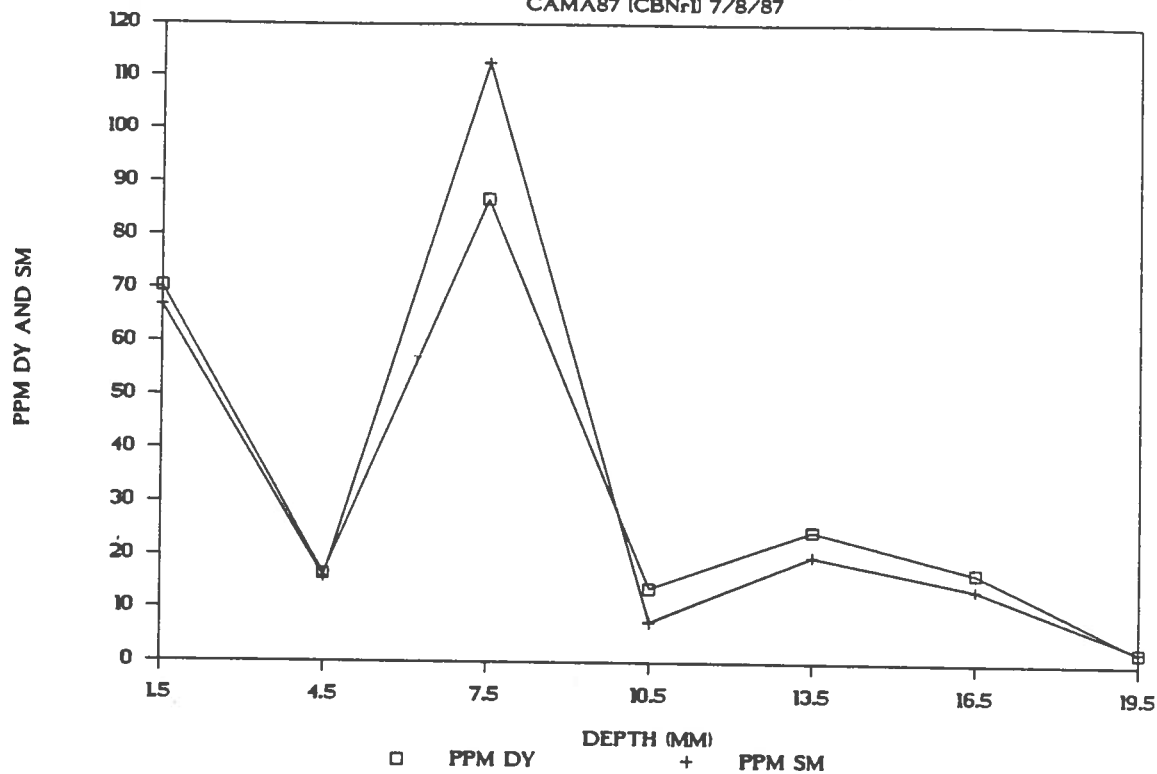
DISTRIBUTION OF DY & SM

CAMA87 (CBN-2-S (CAN)) 7/8/87



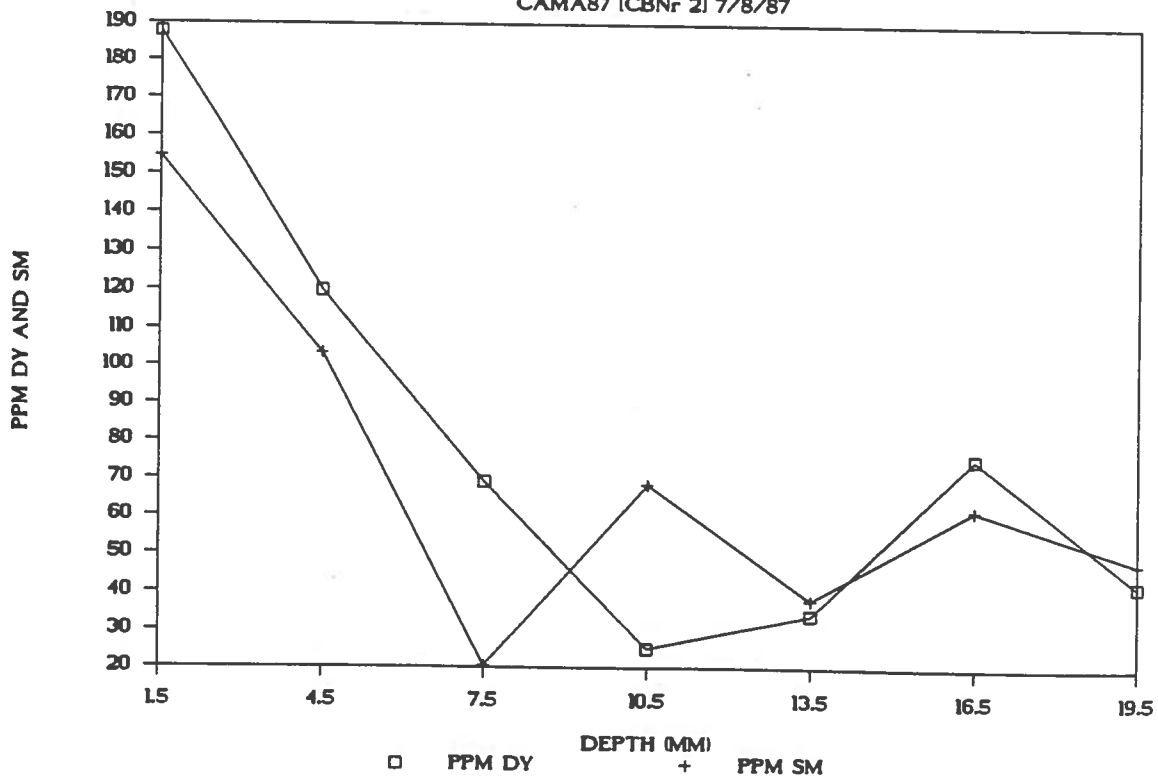
DISTRIBUTION OF DY & SM

CAMA87 (CBN#1) 7/8/87



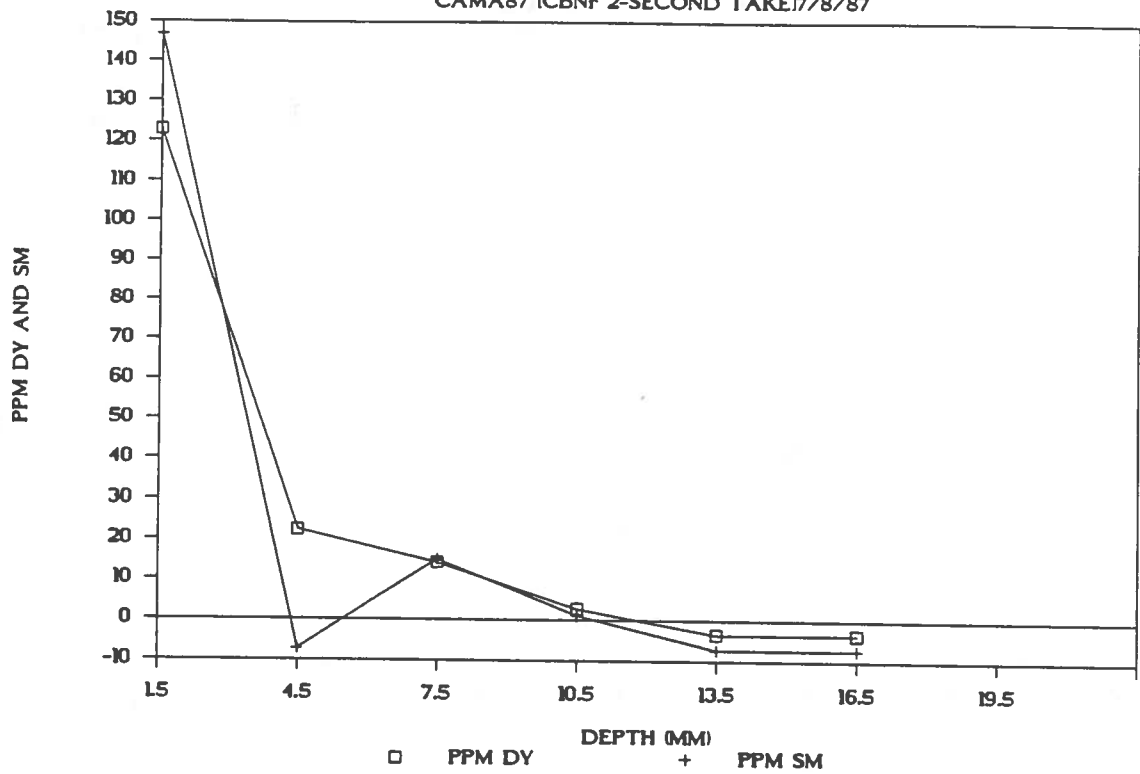
DISTRIBUTION OF DY & SM

CAMA87 (CBN# 2) 7/8/87



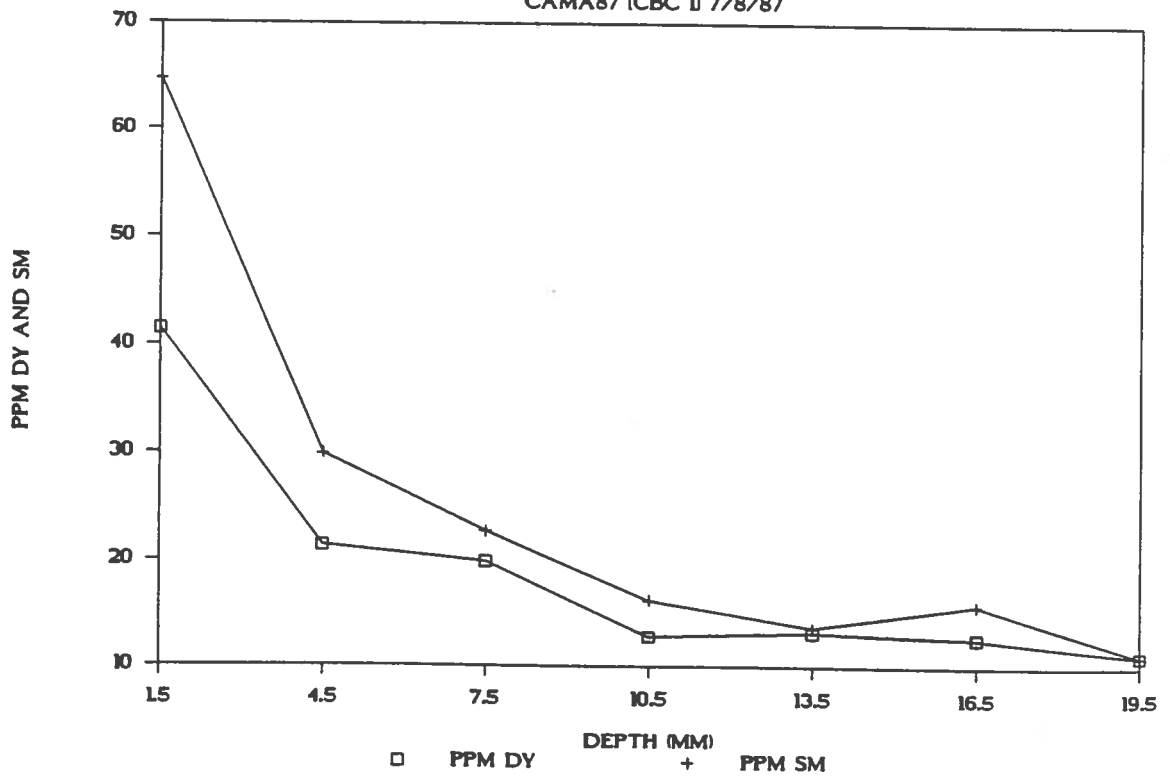
DISTRIBUTION OF DY & SM

CAMA87 ICBnr 2-SECOND TAKE 7/8/87



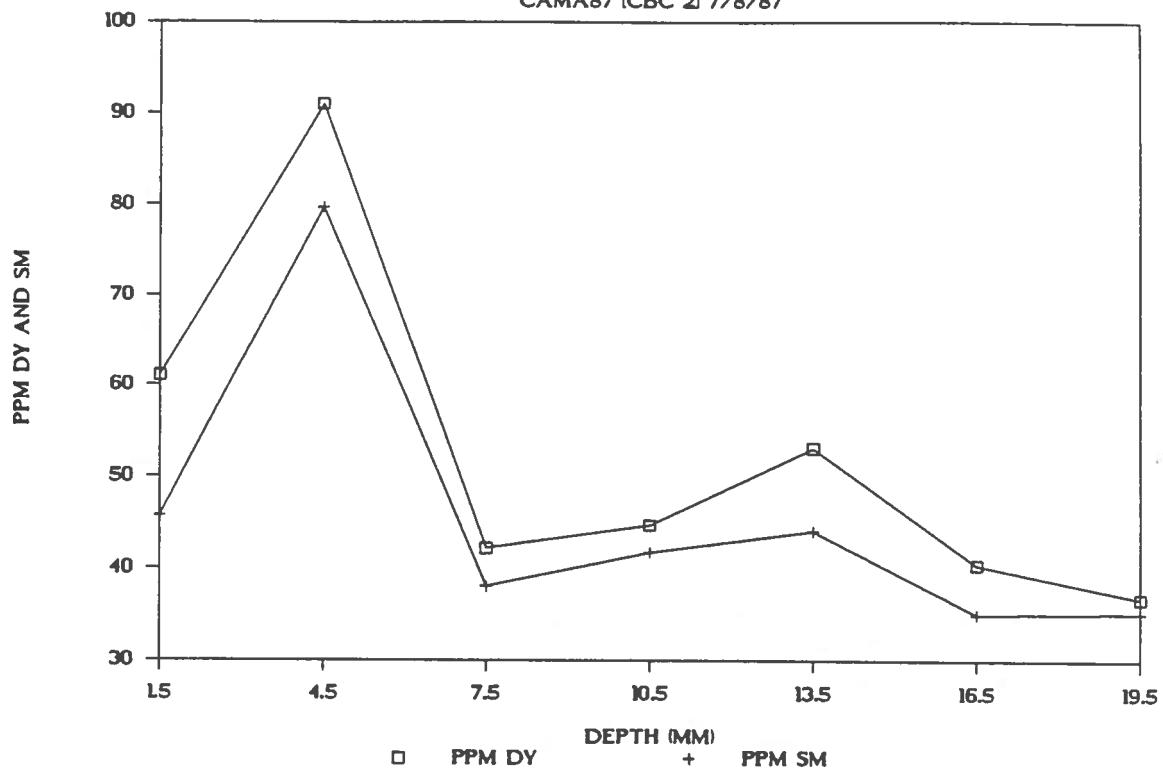
DISTRIBUTION OF DY & SM

CAMA87 ICB 11 7/8/87



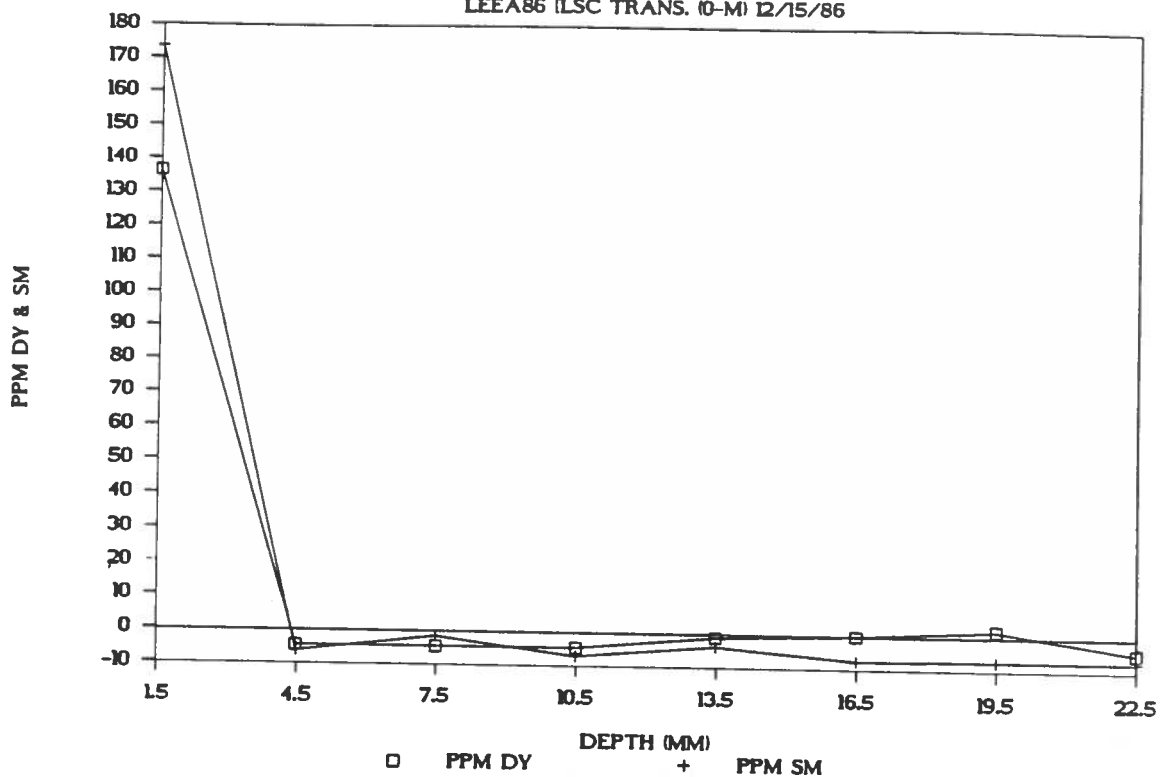
DISTRIBUTION OF DY & SM

CAMA87 (CBC 2) 7/8/87



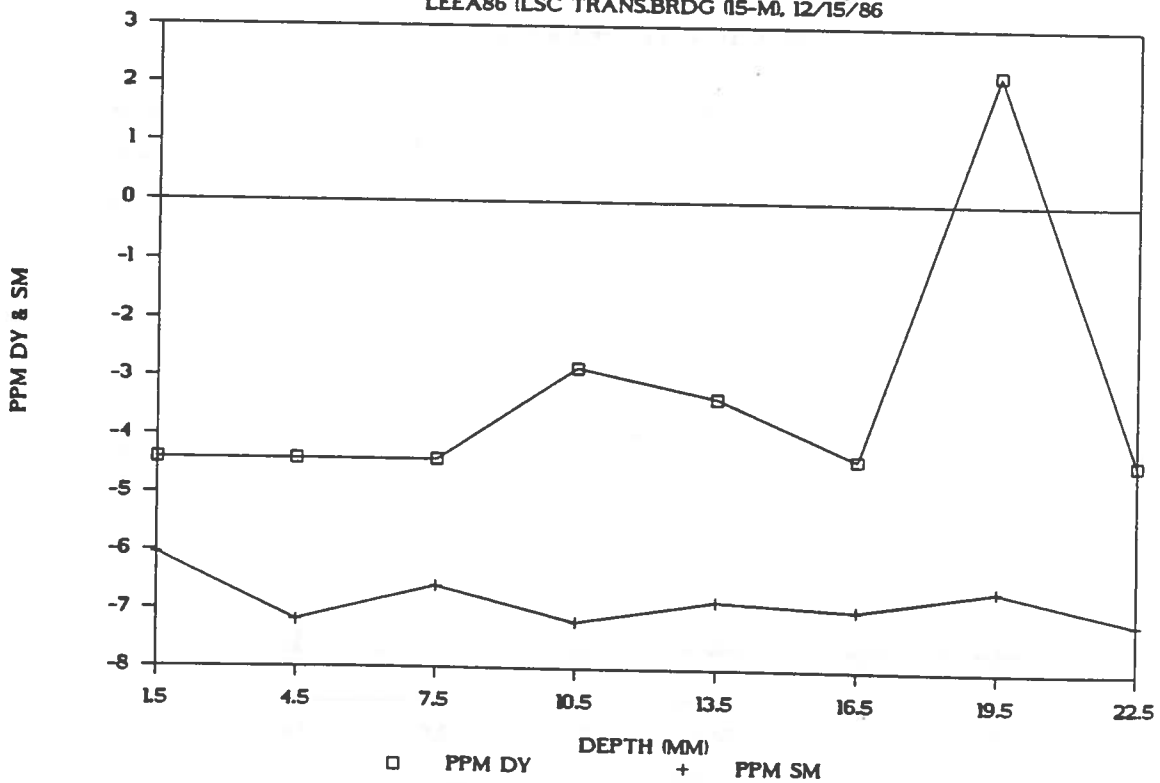
DISTRIBUTION OF DY & SM

LEE86 (LSC TRANS. 10-M) 12/15/86



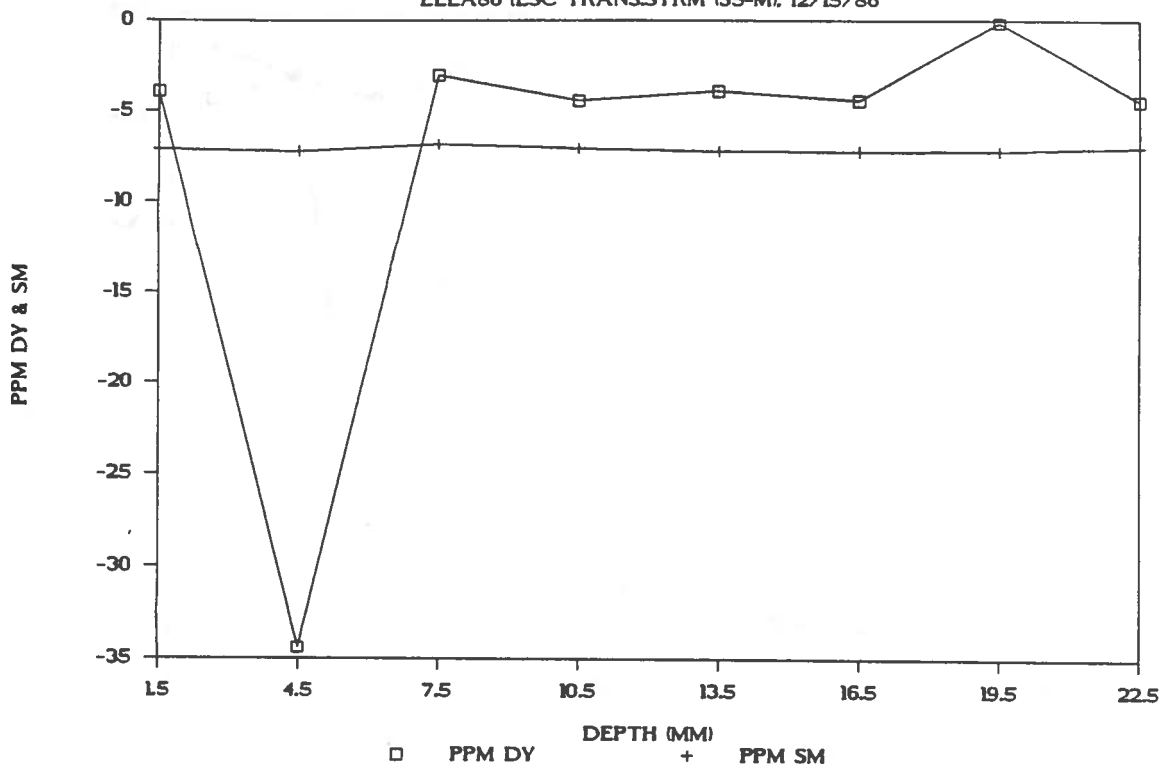
DISTRIBUTION OF DY & SM

LEE86 (LSC TRANS. BRDG (15-M), 12/15/86



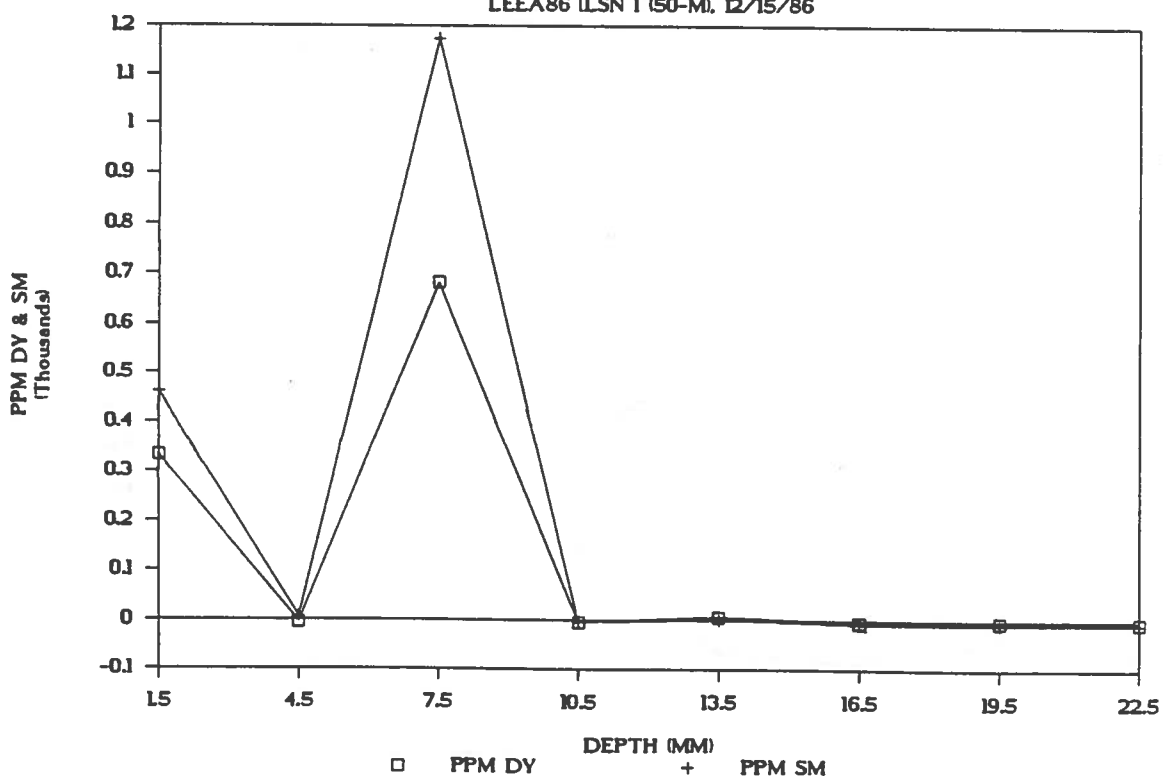
DISTRIBUTION OF DY & SM

LEEA86 (LSC TRANS.STRM (35-M), 12/15/86



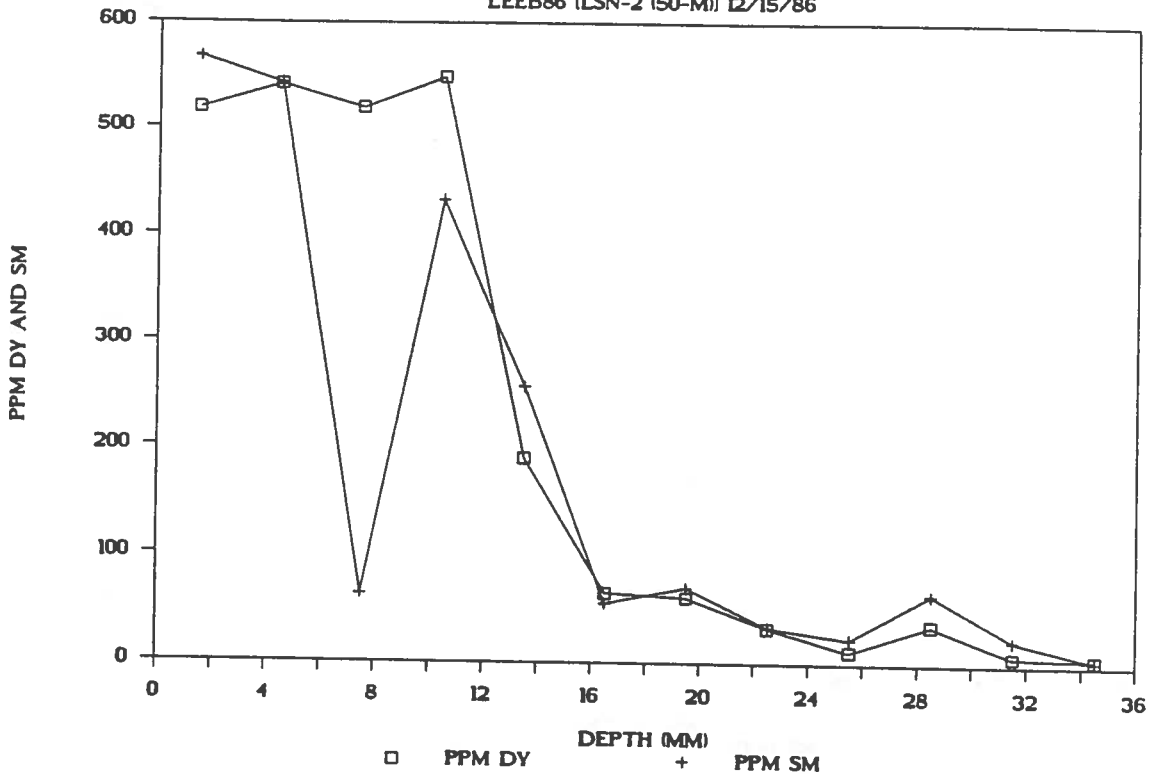
DISTRIBUTION OF DY & SM

LEEA86 (LSN 1 (50-M), 12/15/86



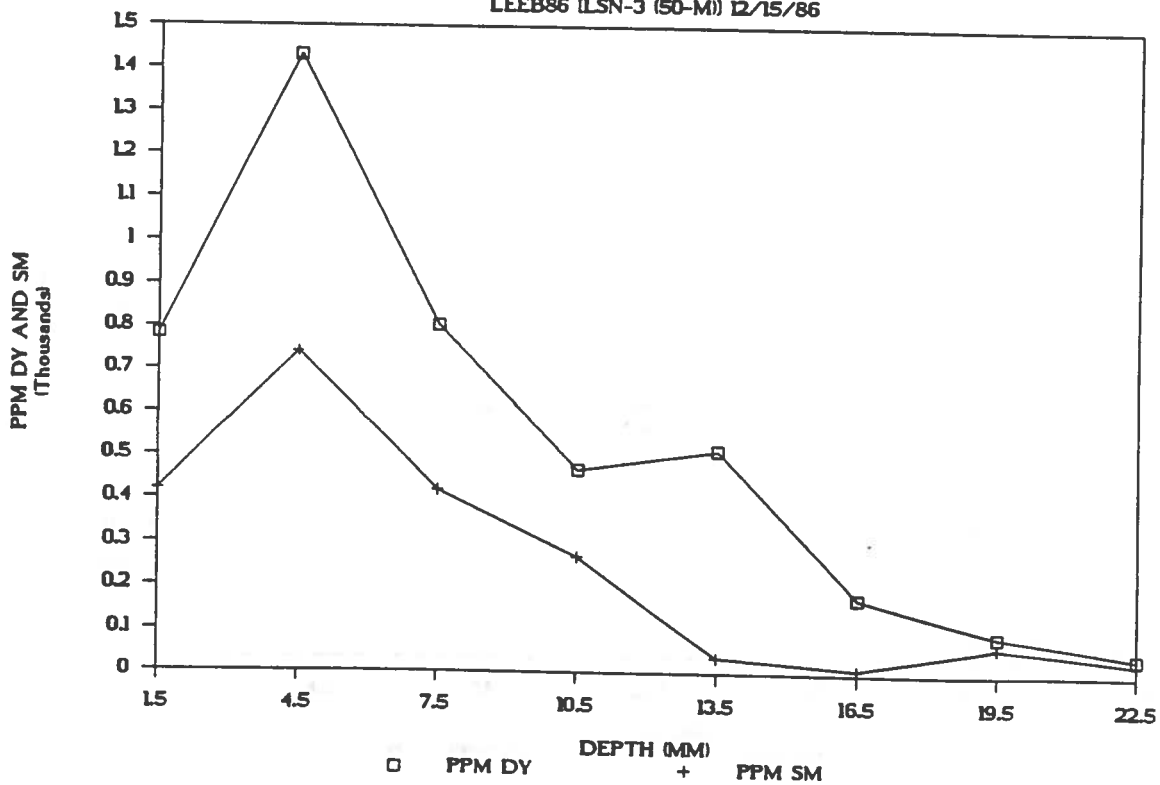
DISTRIBUTION OF DY & SM

LEEB86 (LSN-2 (50-M)) 12/15/86



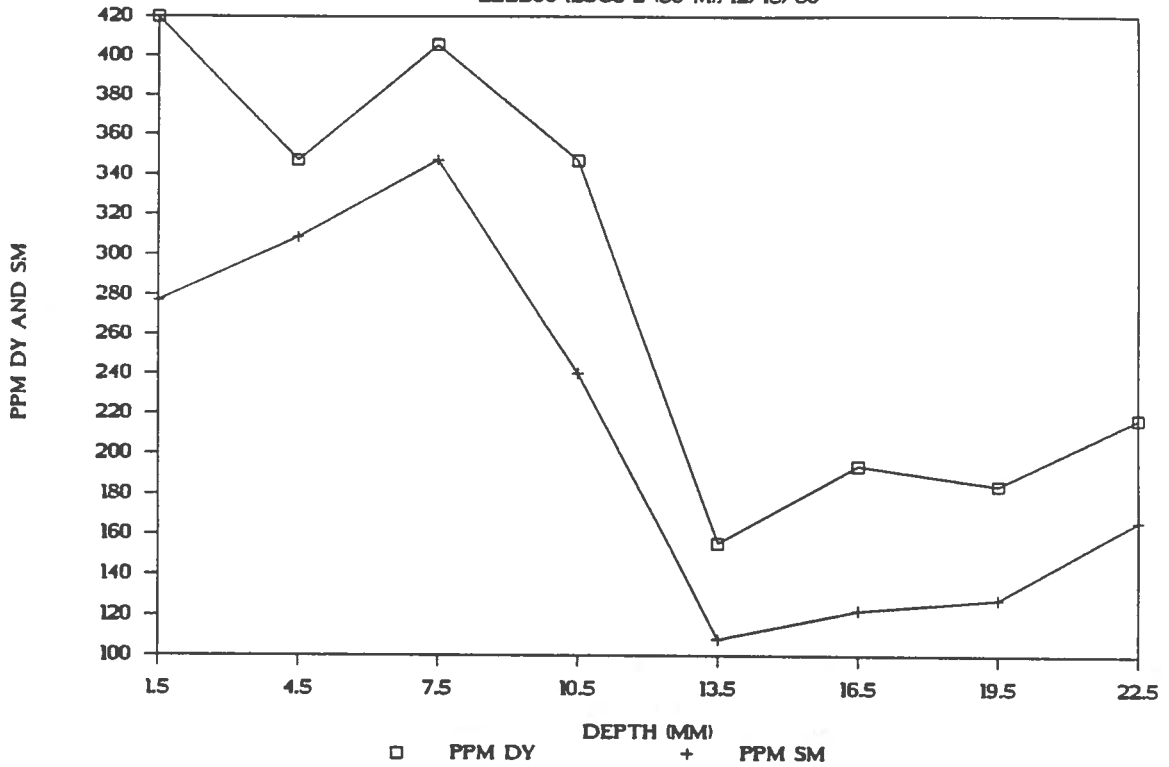
DISTRIBUTION OF DY & SM

LEEB86 (LSN-3 (50-M)) 12/15/86



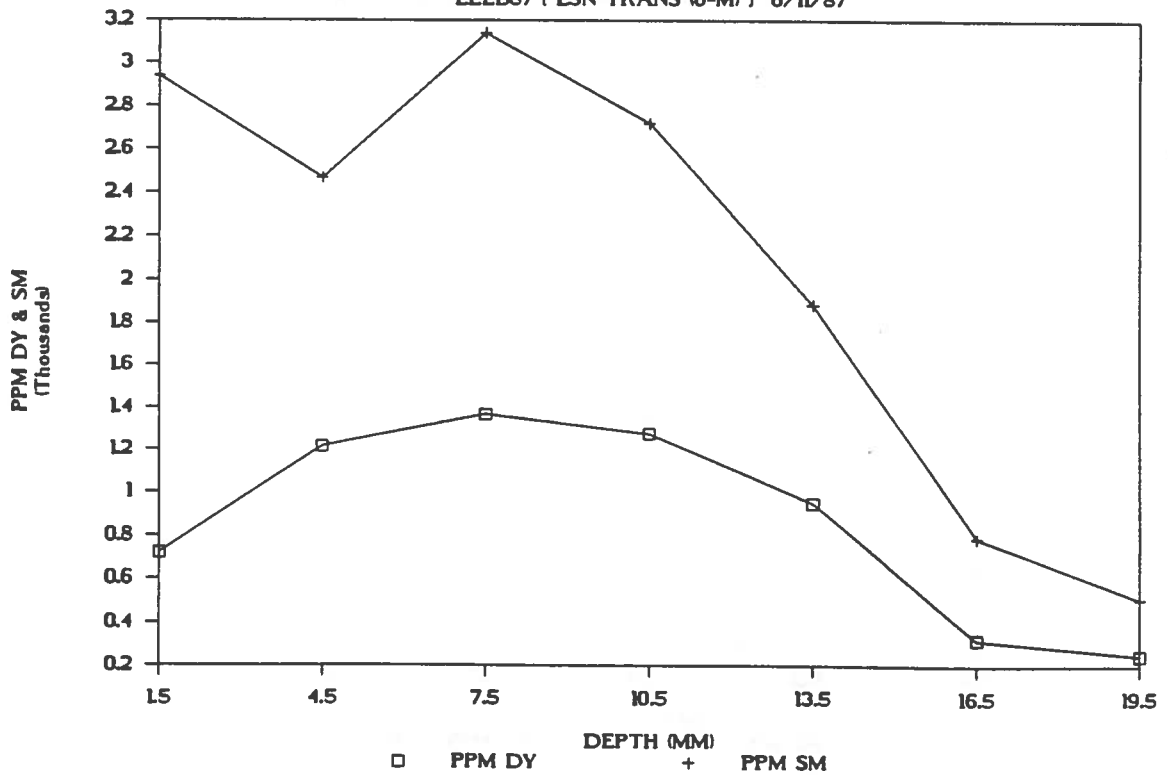
DISTRIBUTION OF DY & SM

LEEB86 (LSCd 2 (50-M)) 12/15/86



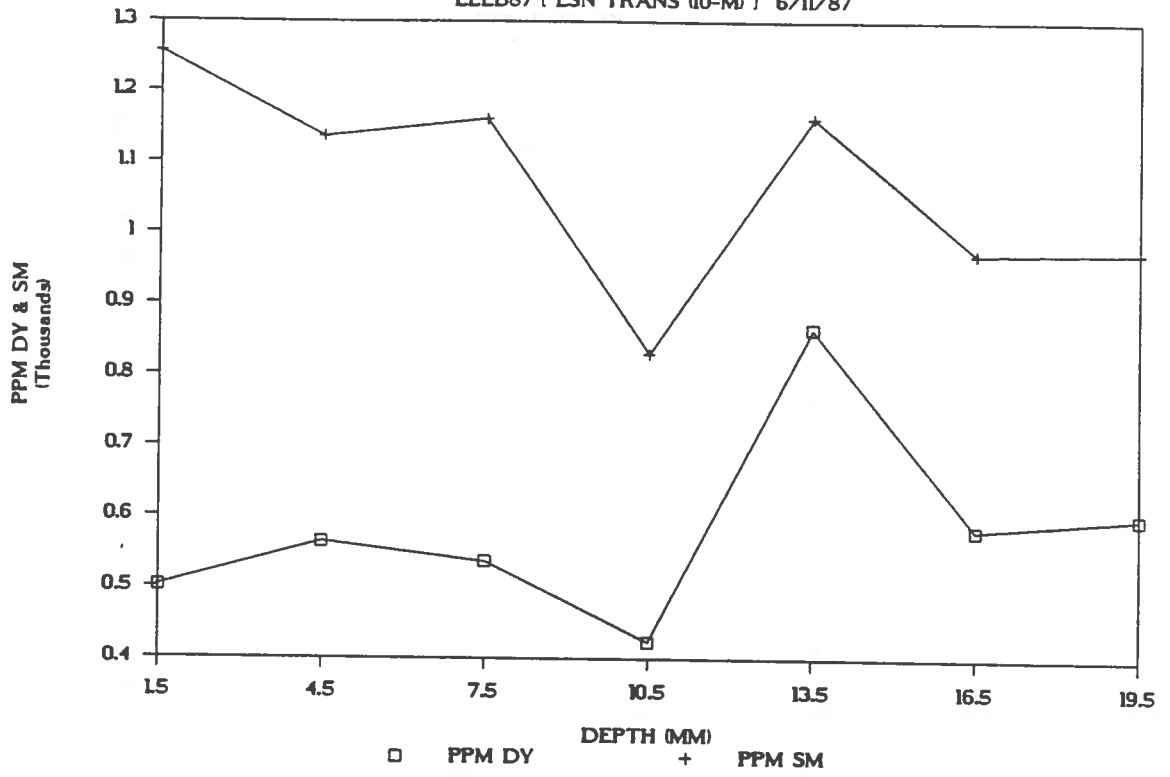
DISTRIBUTION OF DY & SM

LEEB87 (LSN TRANS (0-M)) 6/11/87



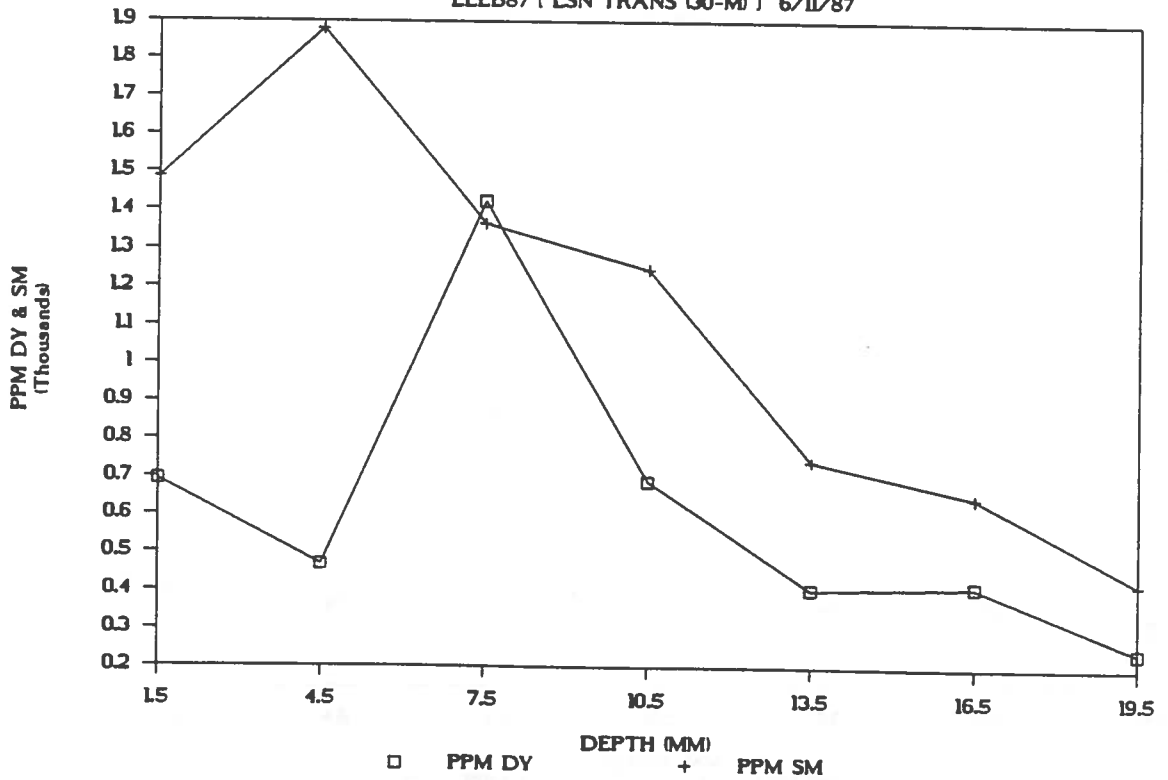
DISTRIBUTION OF DY & SM

LEEB87 (LSN TRANS (00-M)) 6/11/87



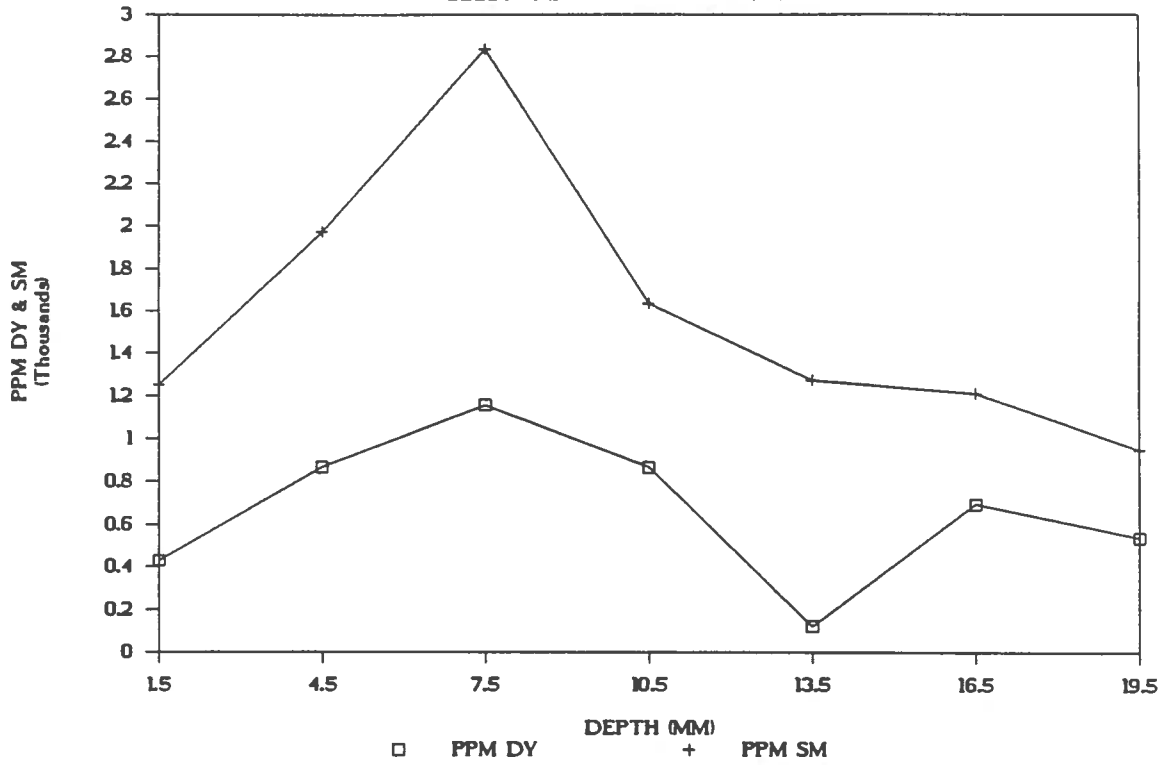
DISTRIBUTION OF DY & SM

LEEB87 (LSN TRANS (00-M)) 6/11/87



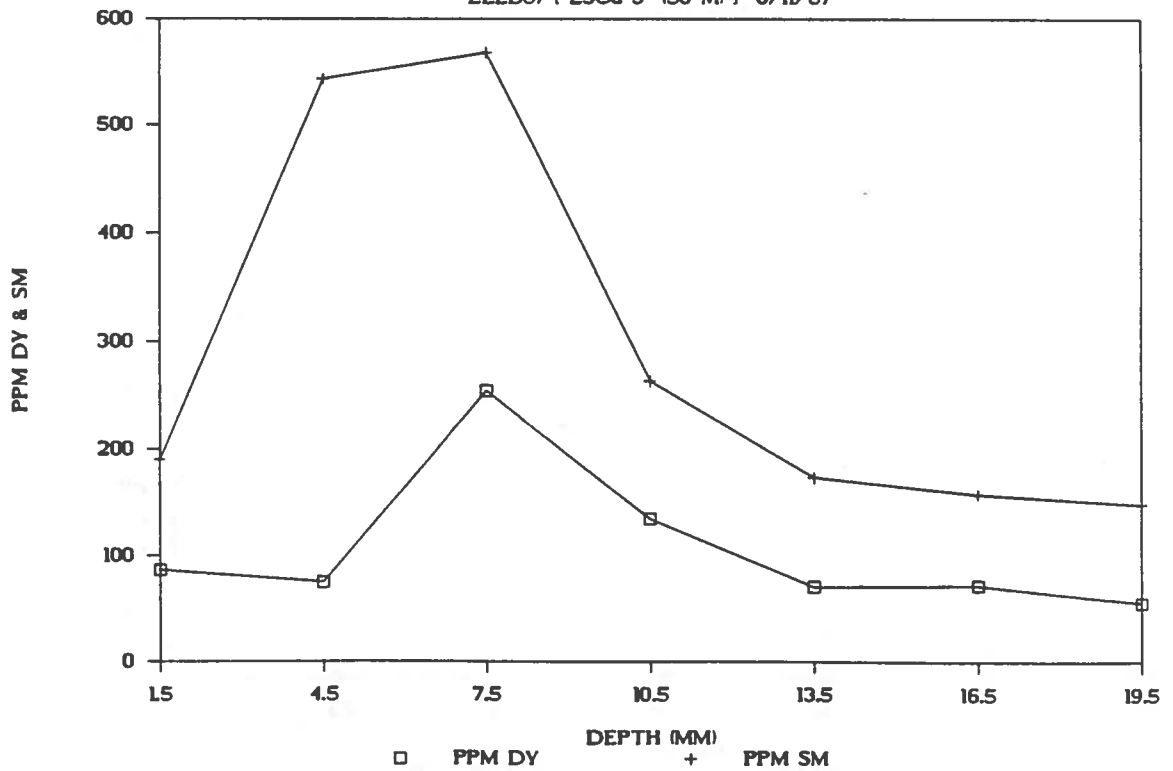
DISTRIBUTION OF DY & SM

LEEB87 (LSN TRANS (50-M)) 6/11/87



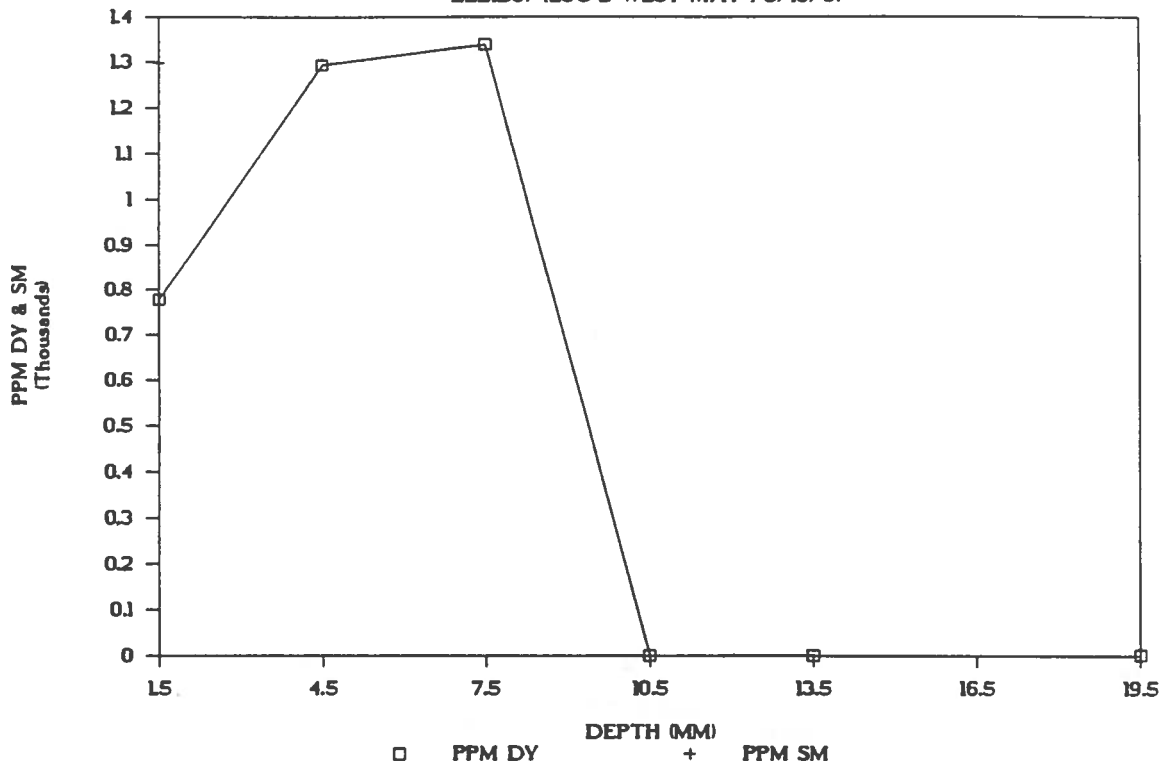
DISTRIBUTION OF DY & SM

LEEB87 (LSCd 3 (50-M)) 6/11/87



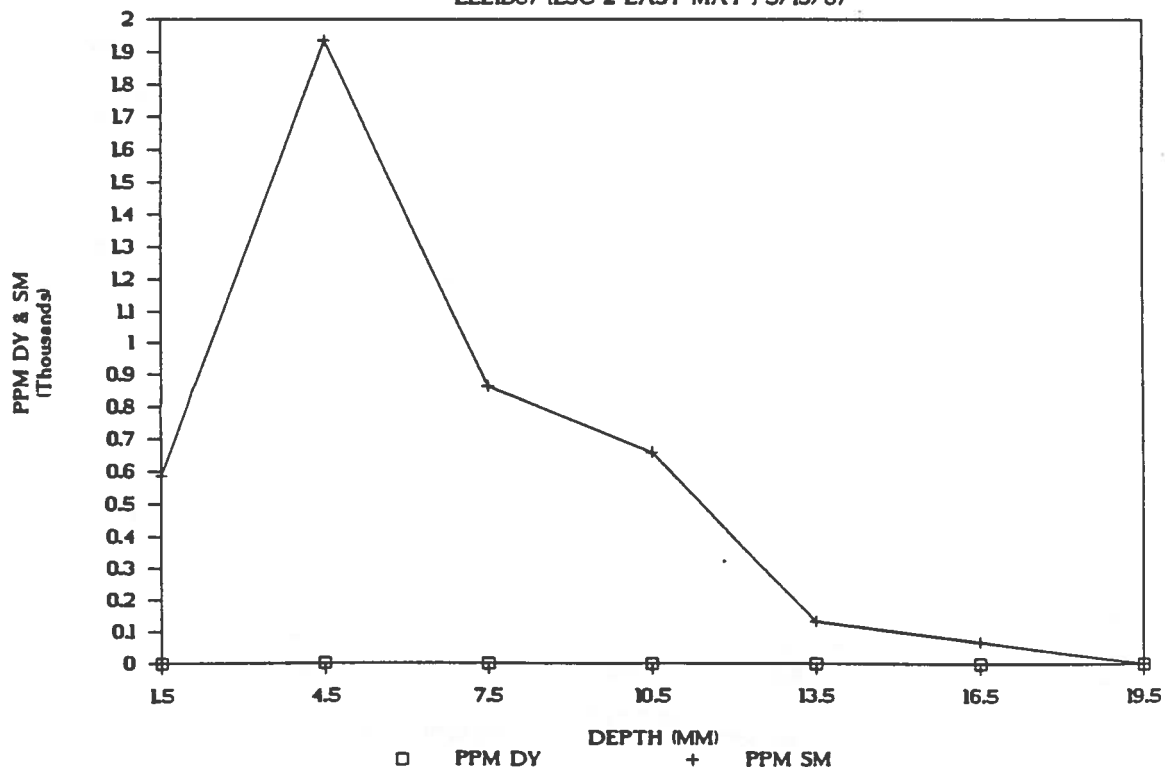
DISTRIBUTION OF DY & SM

LEEIB87 (LSC 2 WEST MAY) 5/13/87



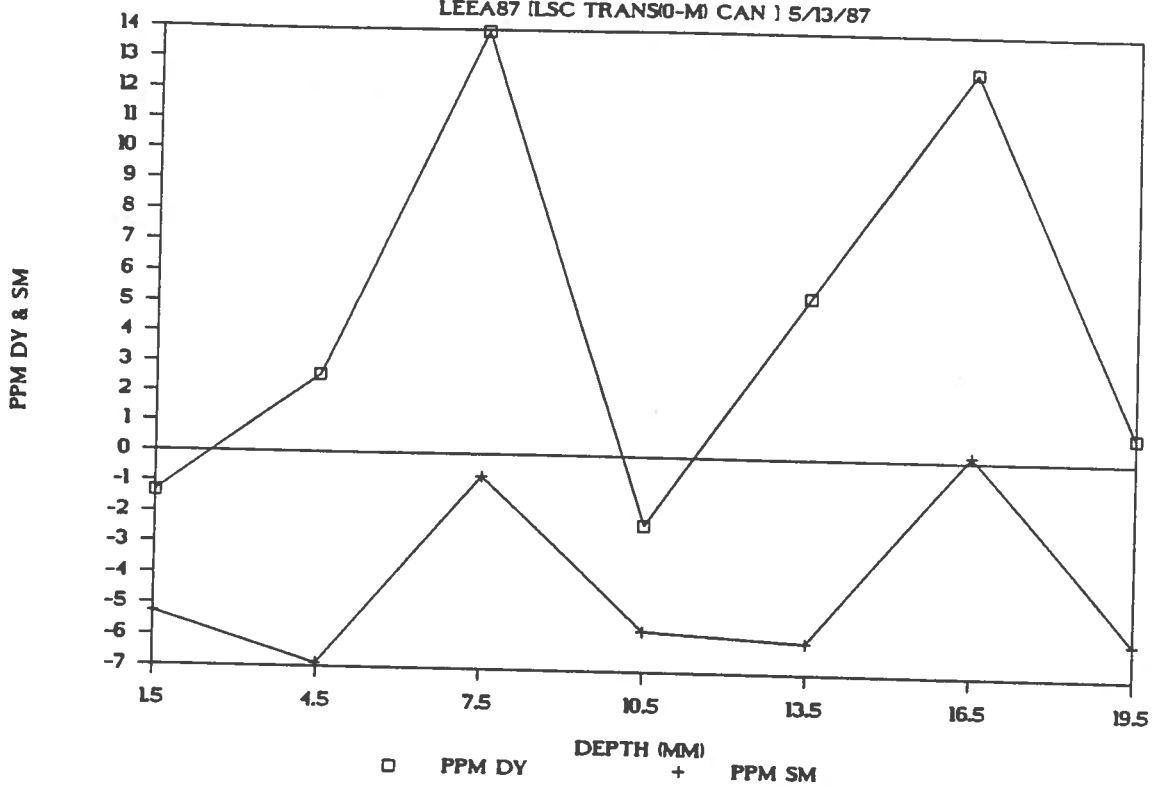
DISTRIBUTION OF DY & SM

LEEIB87 (LSC 2 EAST MAY) 5/13/87



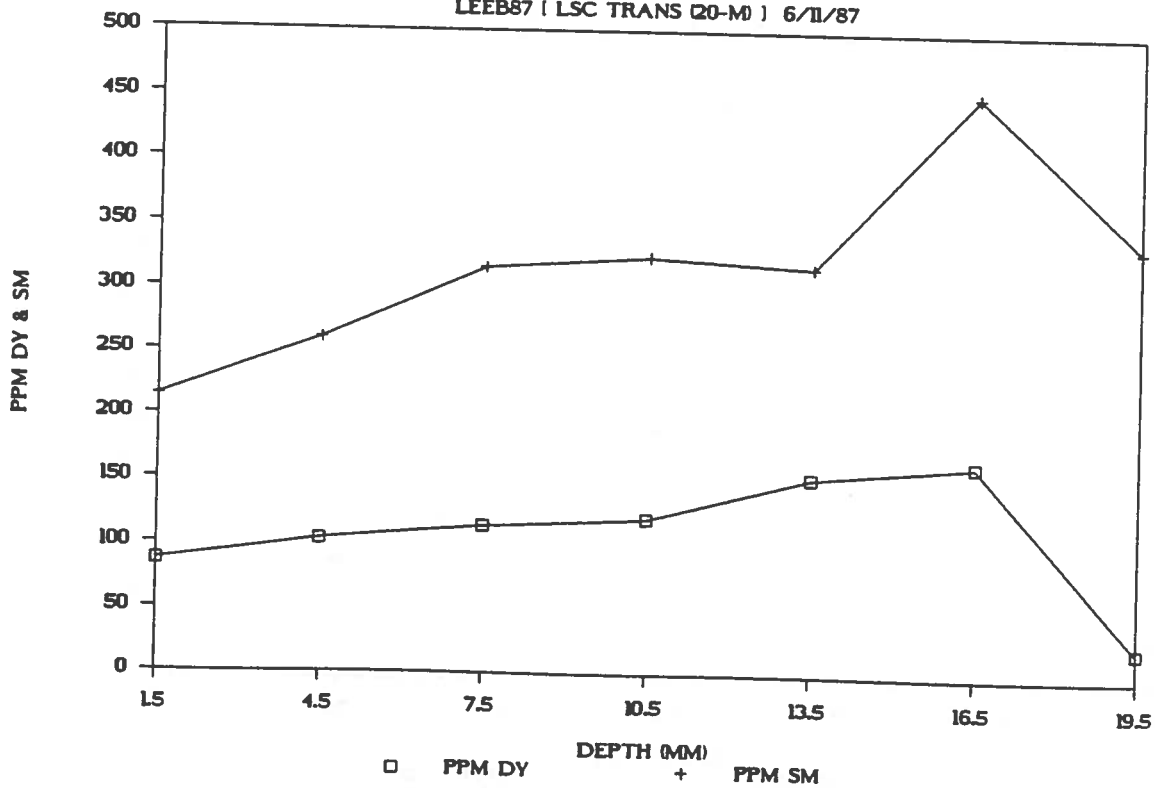
DISTRIBUTION OF DY & SM

LEEA87 (LSC TRANS10-M) CAN) 5/13/87



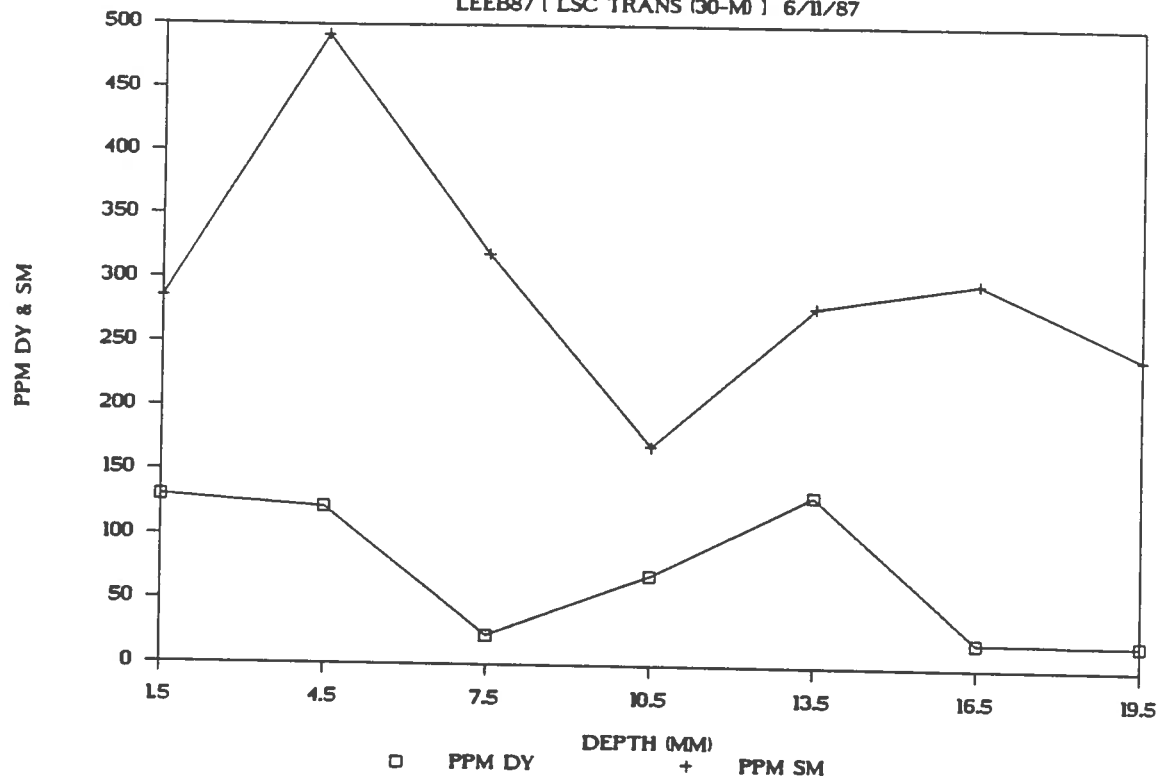
DISTRIBUTION OF DY & SM

LEEB87 (LSC TRANS 20-M)) 6/11/87



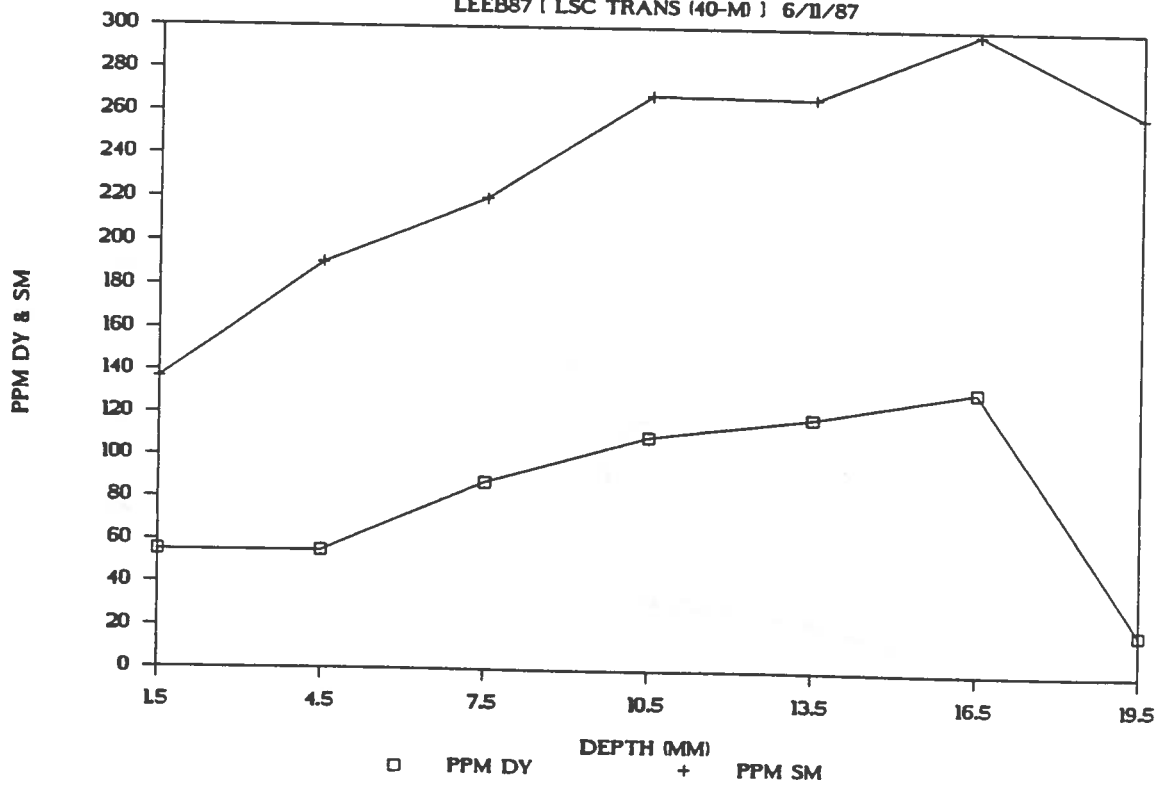
DISTRIBUTION OF DY & SM

LEEB87 (LSC TRANS (30-M)) 6/11/87



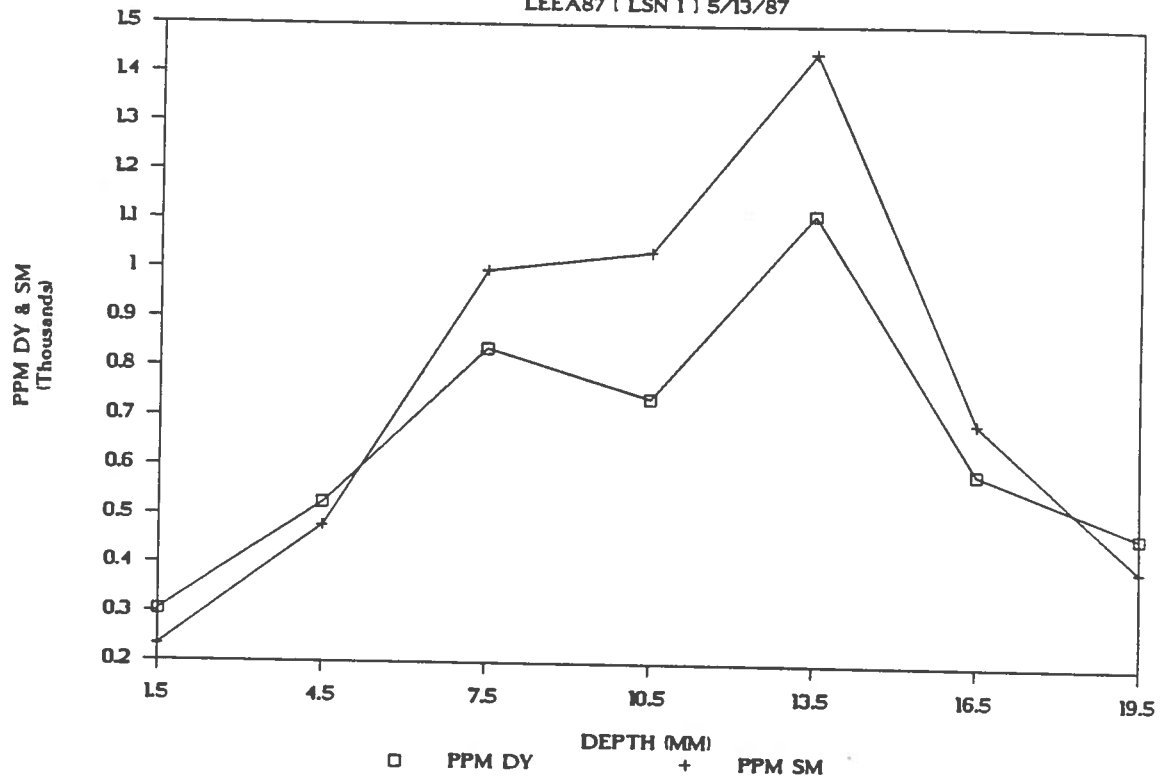
DISTRIBUTION OF DY & SM

LEEB87 (LSC TRANS (40-M)) 6/11/87



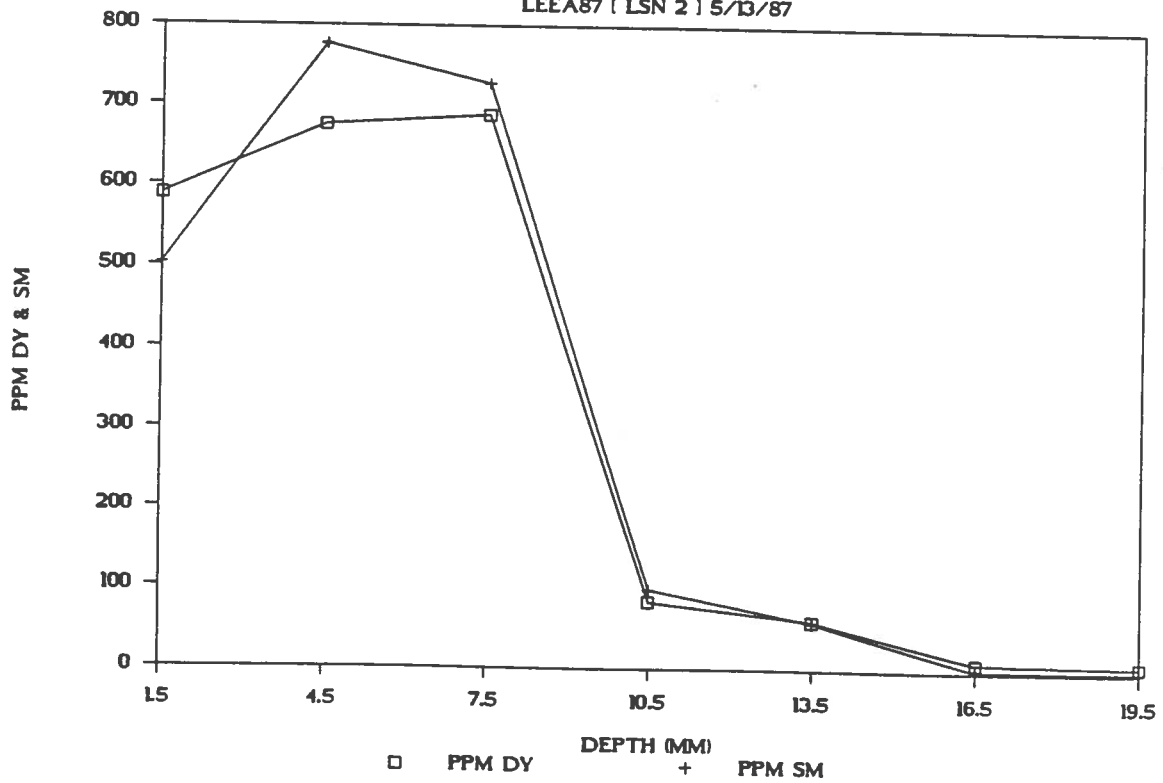
DISTRIBUTION OF DY & SM

LEEA87 (LSN 1) 5/13/87



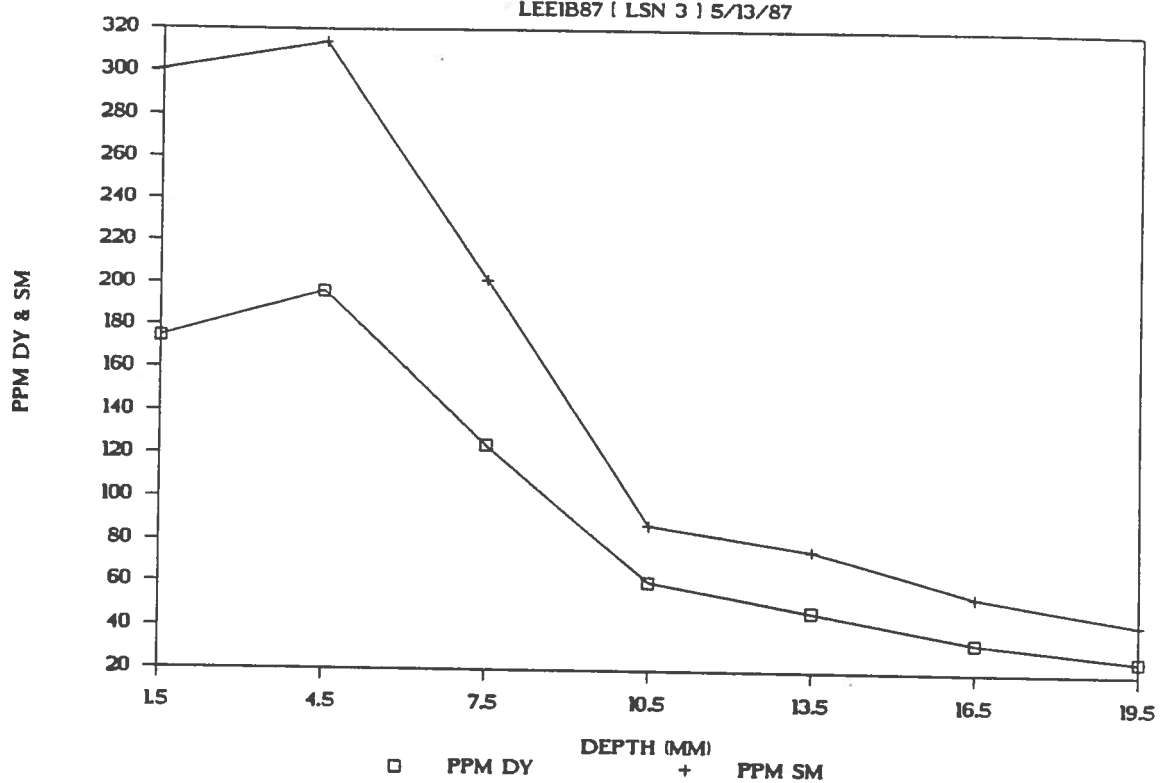
DISTRIBUTION OF DY & SM

LEEA87 (LSN 2) 5/13/87



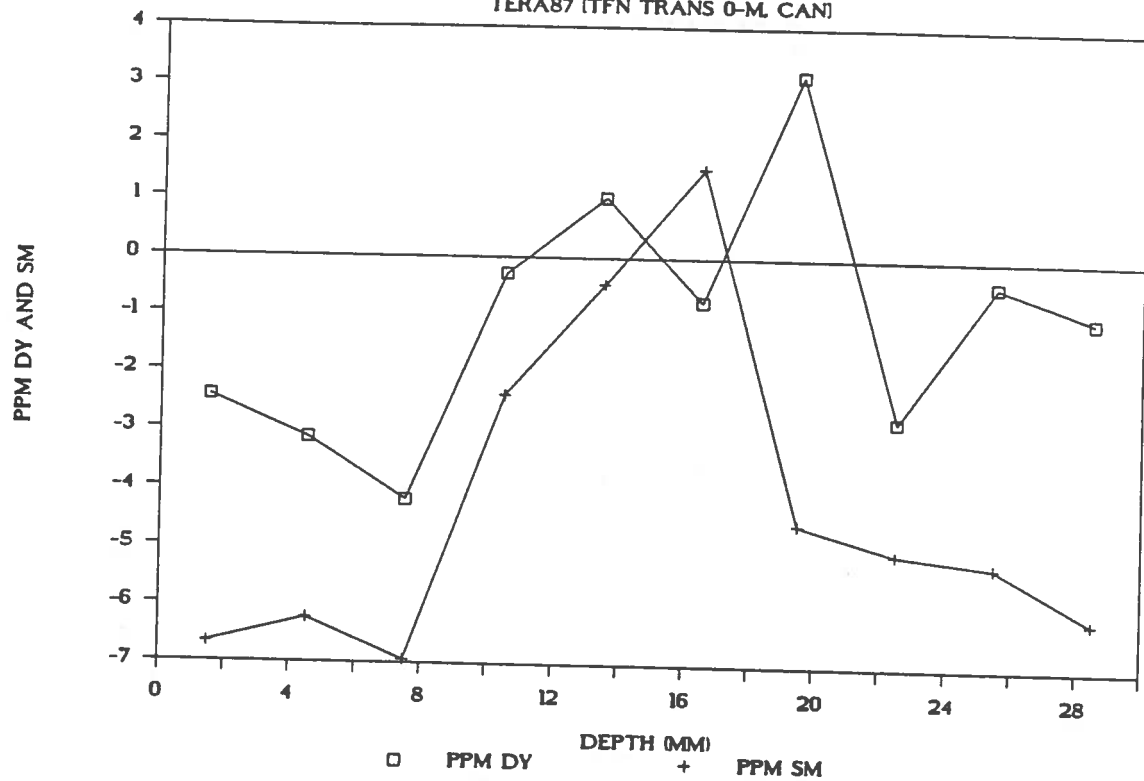
DISTRIBUTION OF DY & SM

LEE1B87 (LSN 3) 5/13/87



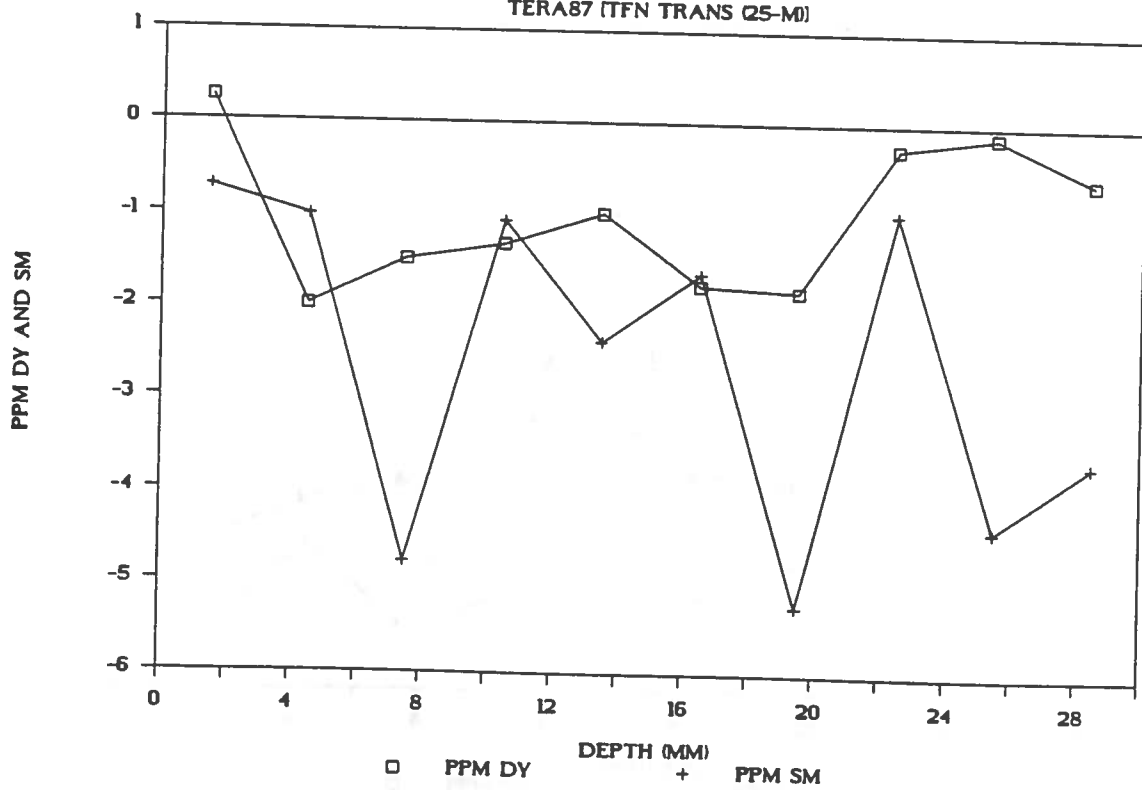
DISTRIBUTION OF DY & SM

TERA87 (TFN TRANS 0-M CAN)



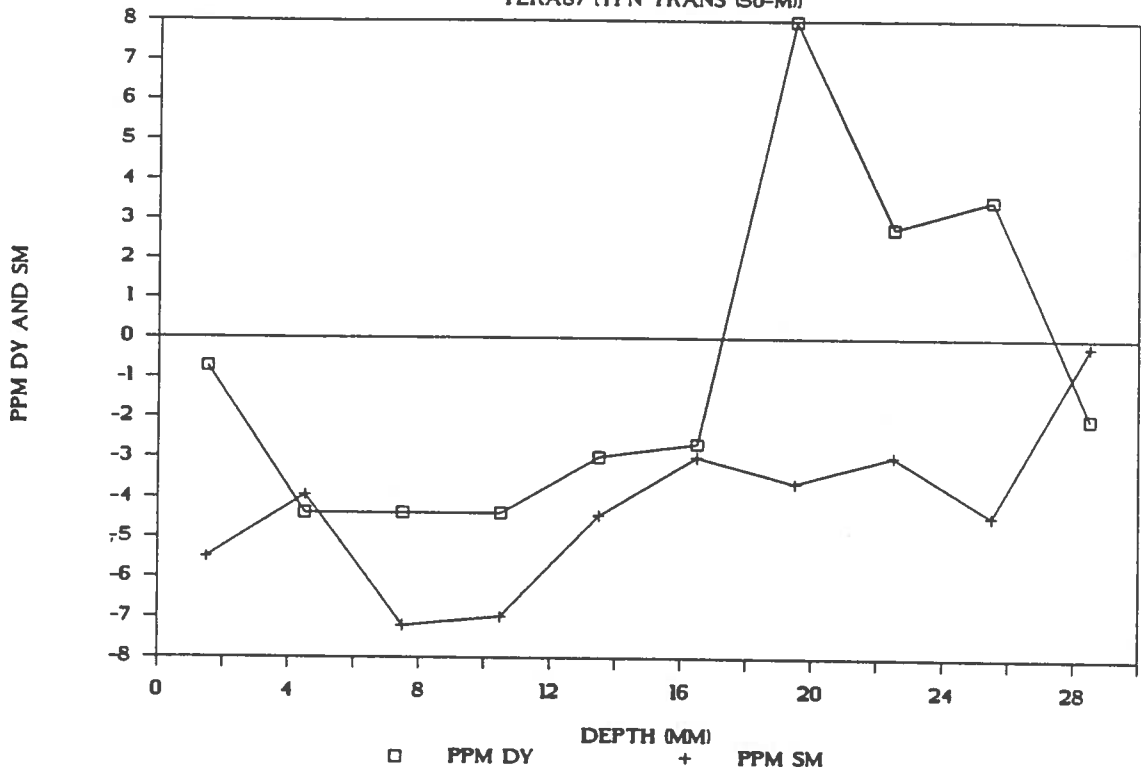
DISTRIBUTION OF DY & SM

TERA87 (TFN TRANS (25-M))



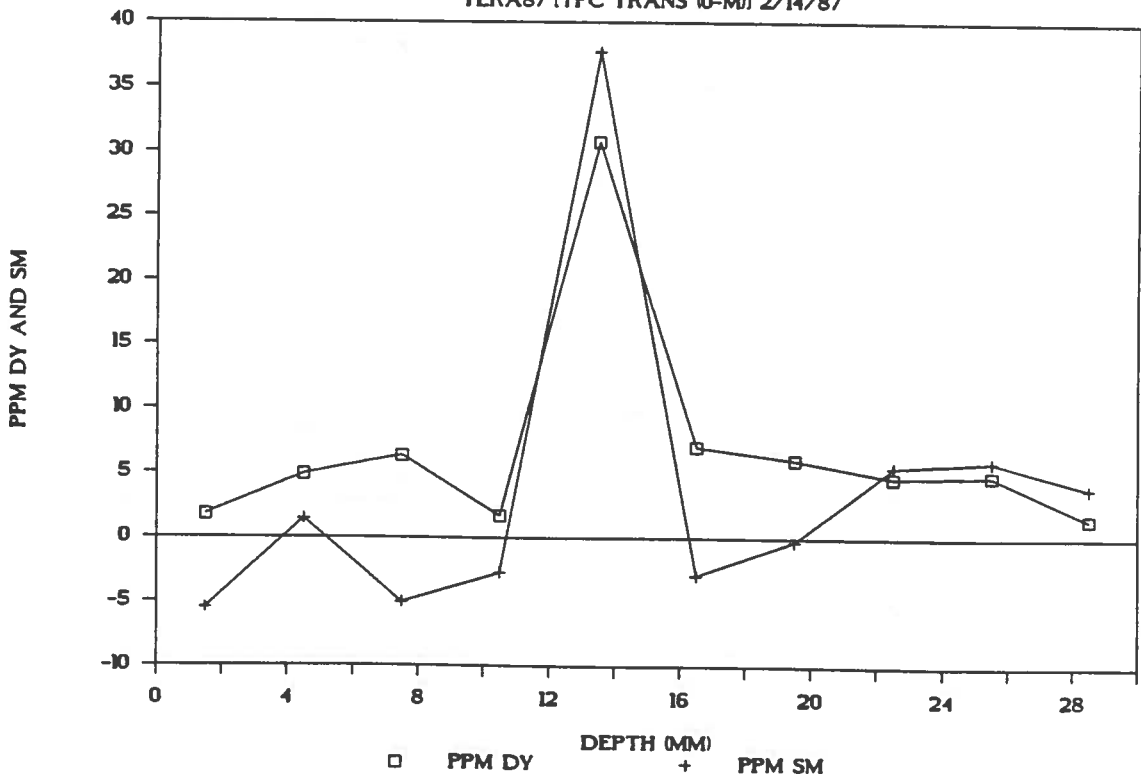
DISTRIBUTION OF DY & SM

TERA87 (TFN TRANS (50-M))



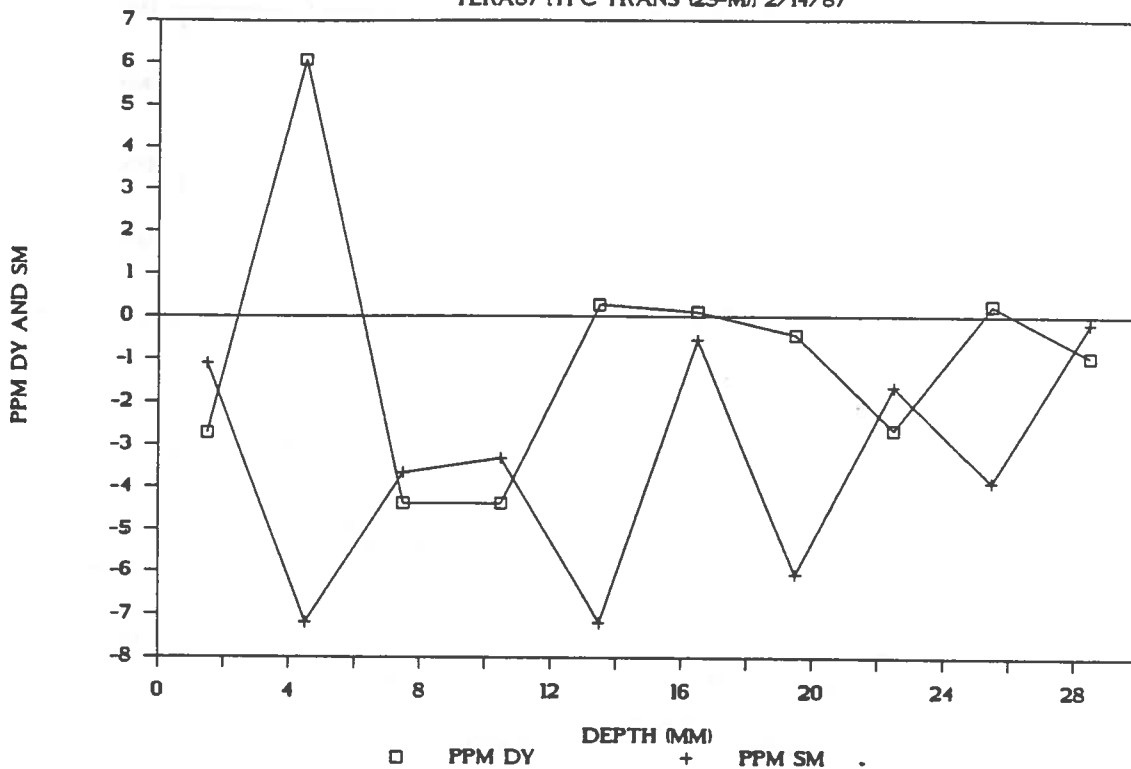
DISTRIBUTION OF DY & SM

TERA87 (TFC TRANS (10-M) 2/14/87)



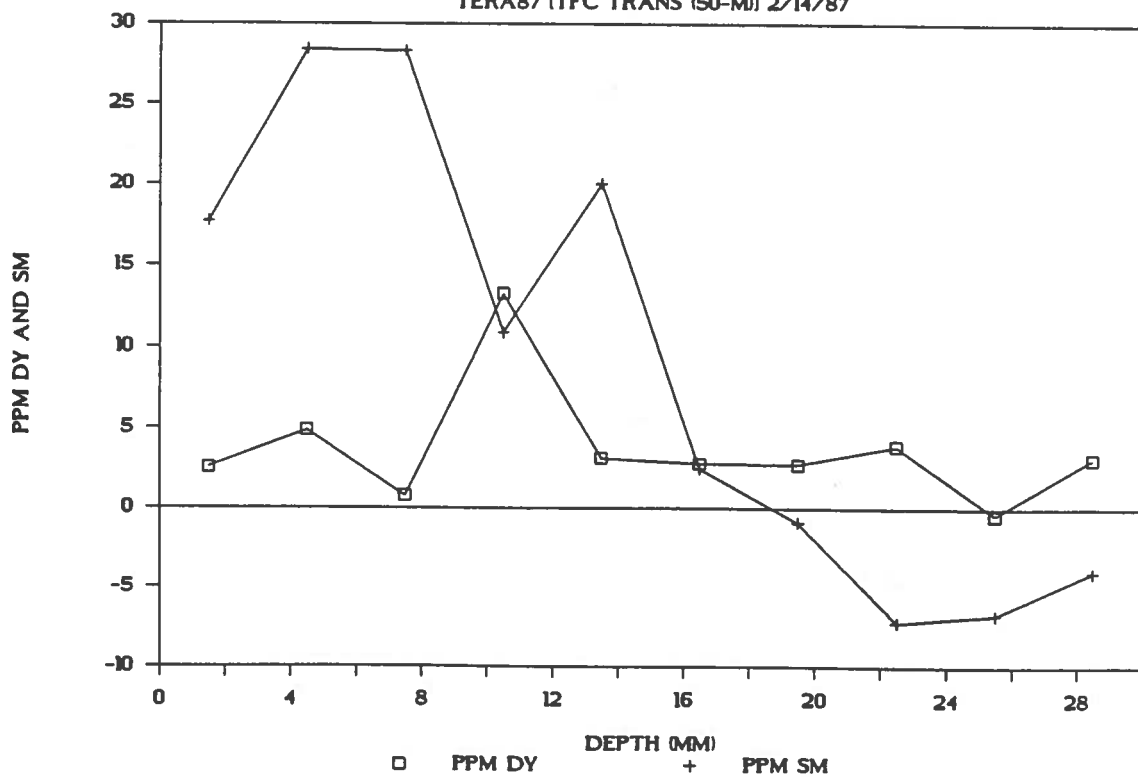
DISTRIBUTION OF DY & SM

TERA87 (TFC TRANS (25-M)) 2/14/87



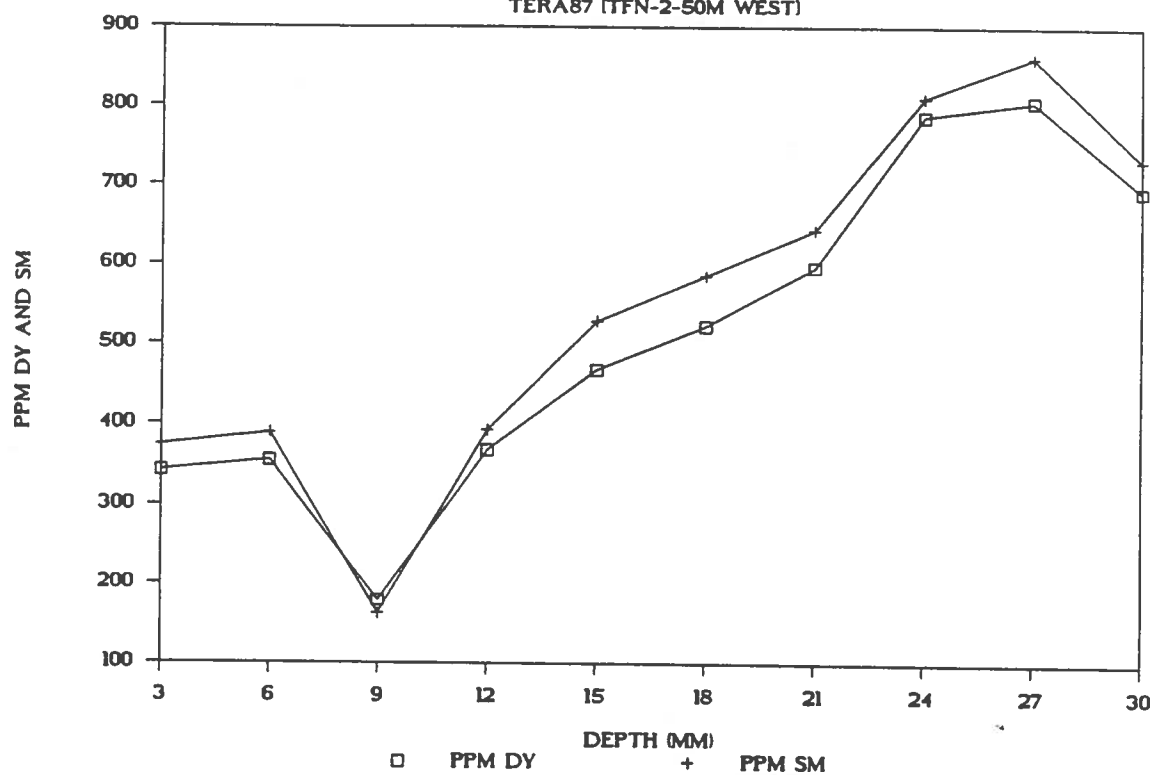
DISTRIBUTION OF DY & SM

TERA87 (TFC TRANS (50-M)) 2/14/87



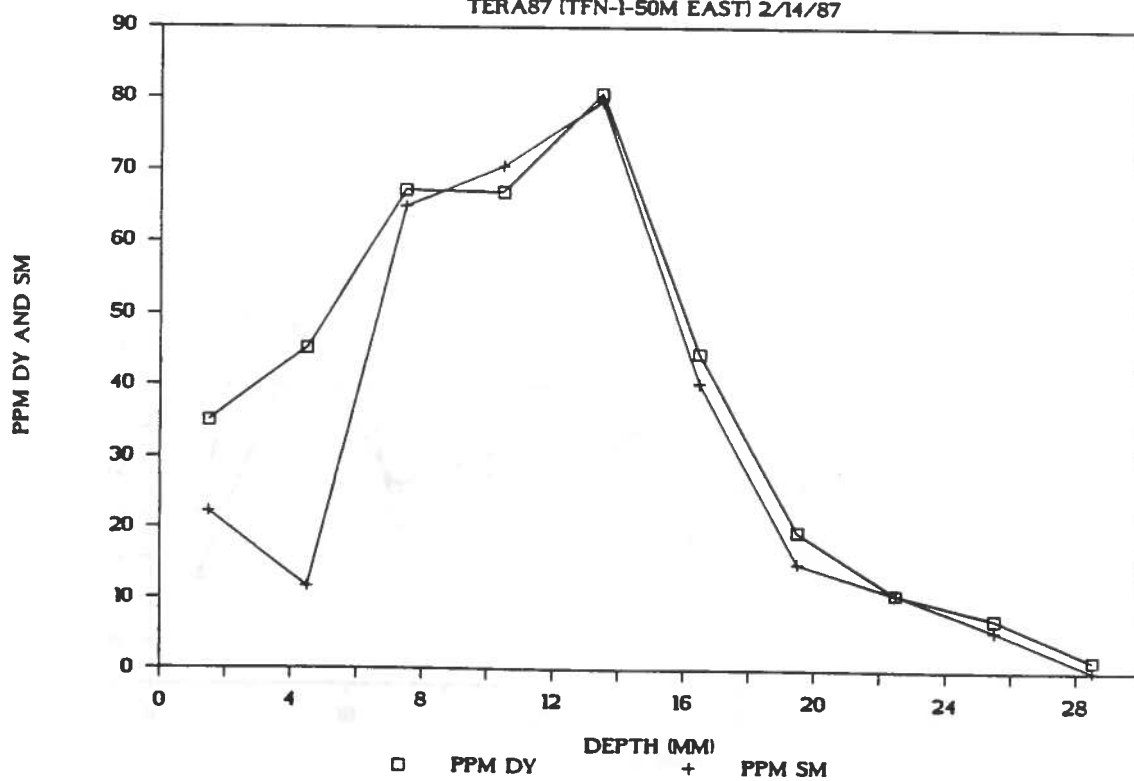
DISTRIBUTION OF DY & SM

TERA87 (TFN-2-50M WEST)



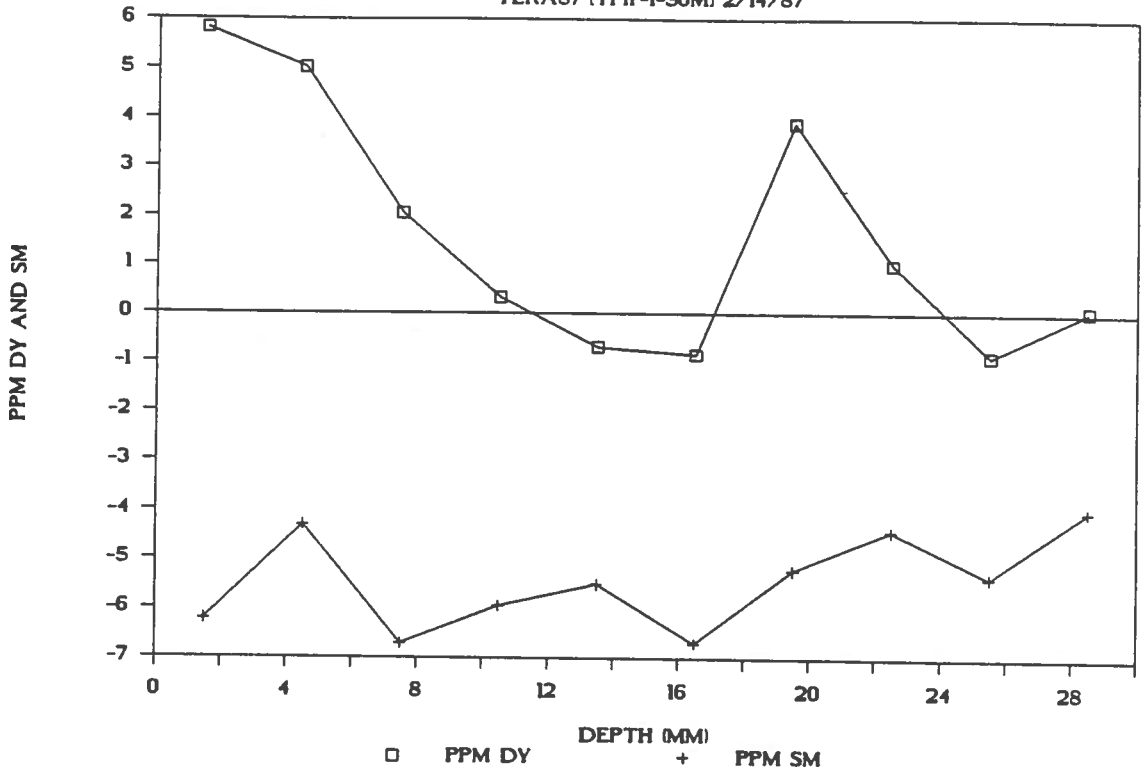
DISTRIBUTION OF DY & SM

TERA87 (TFN-1-50M EAST) 2/14/87



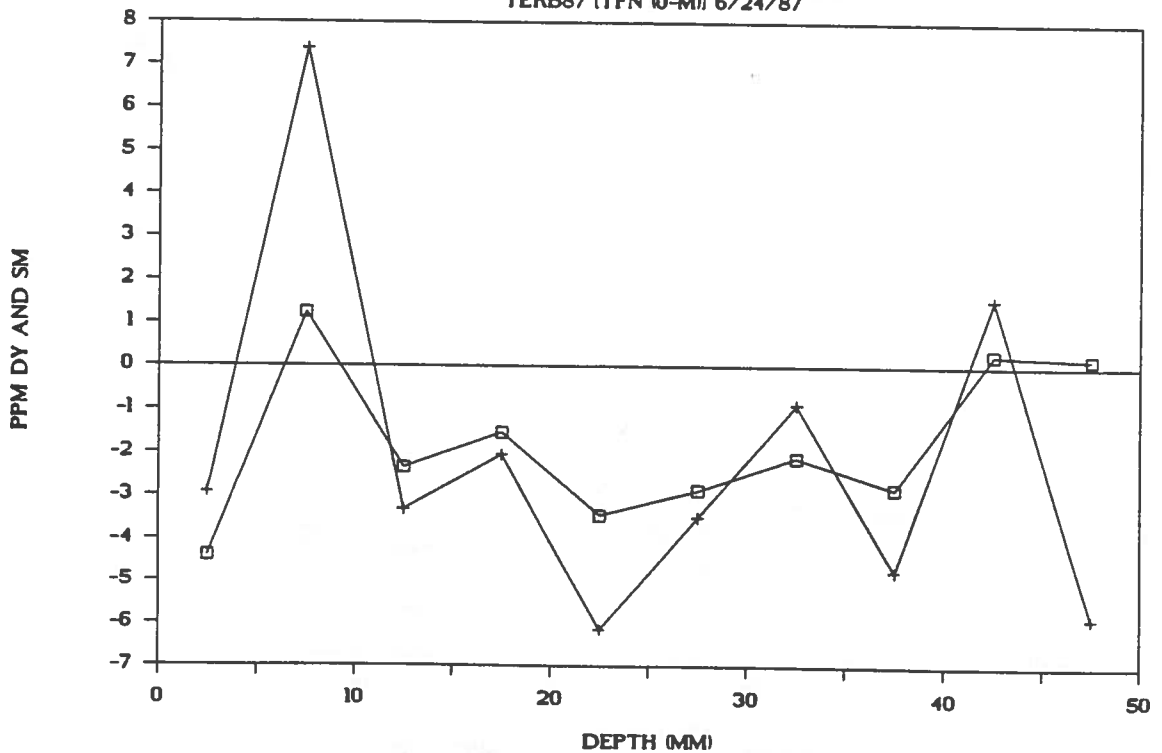
DISTRIBUTION OF DY & SM

TERA87 (TFIr-1-50M) 2/14/87



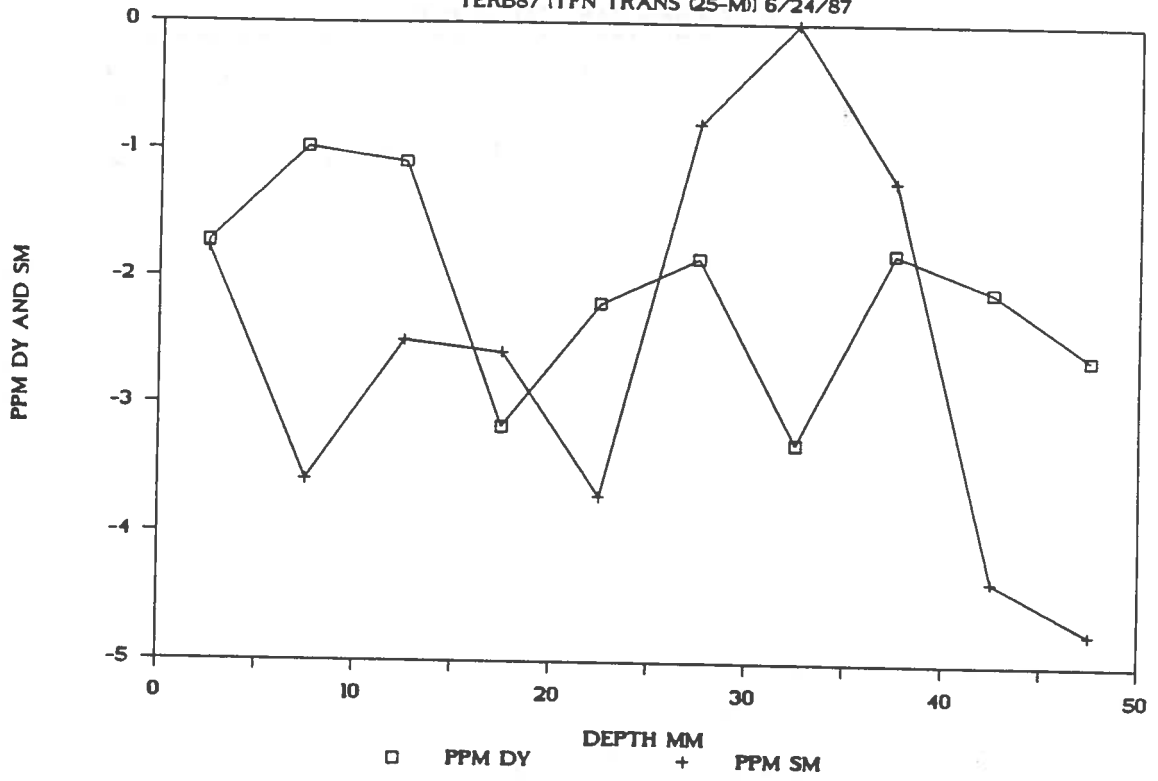
DISTRIBUTION OF DY & SM

TERB87 (TFN 10-M) 6/24/87



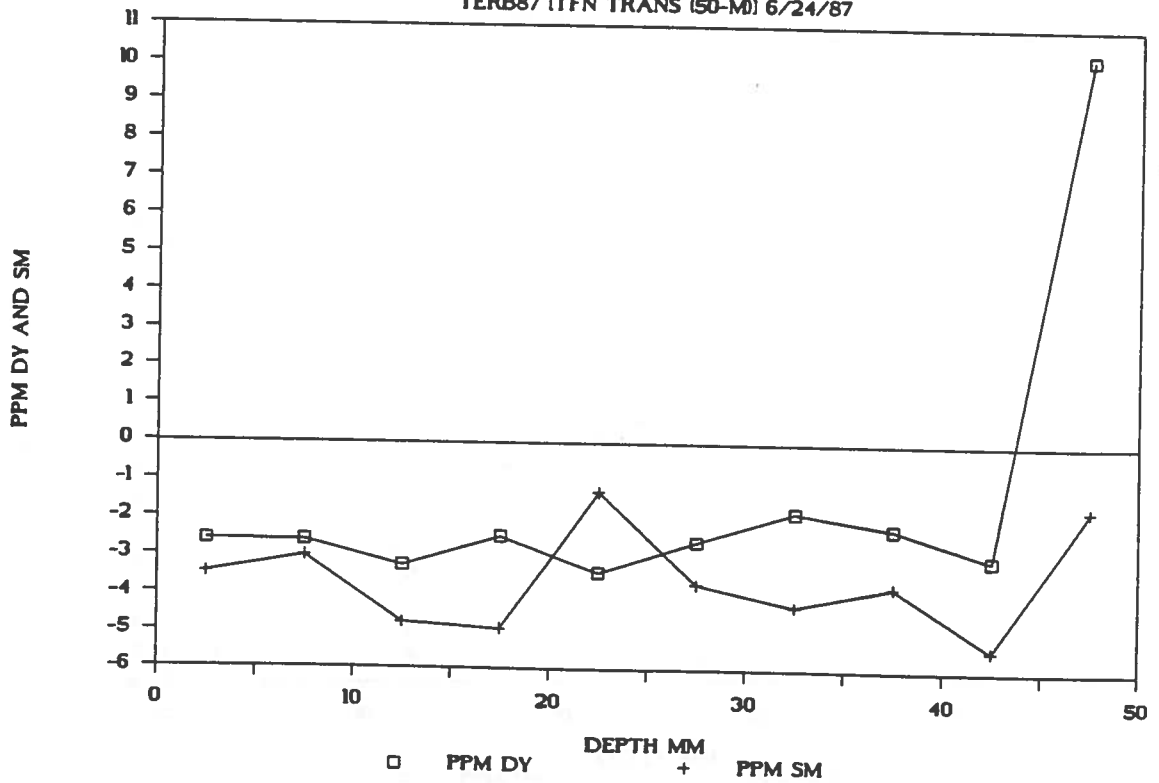
DISTRIBUTION OF DY & SM

TERB87 (TFN TRANS (25-M)) 6/24/87



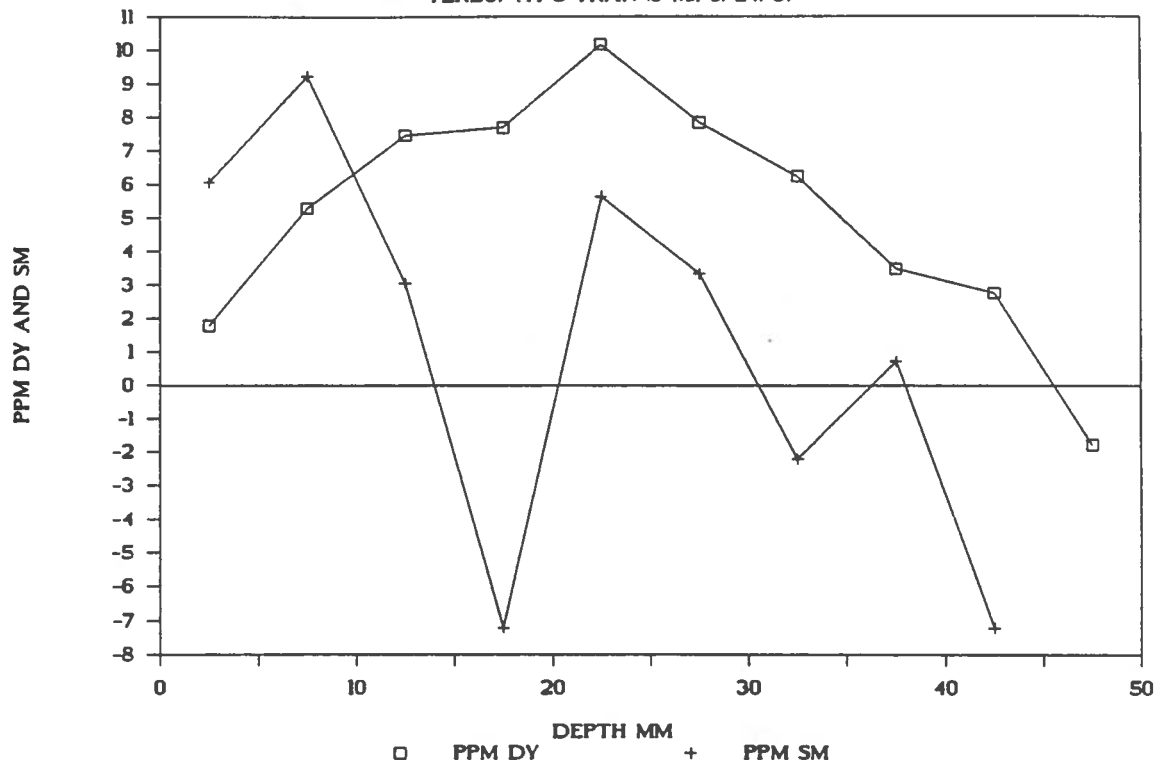
DISTRIBUTION OF DY & SM

TERB87 (TFN TRANS (50-M)) 6/24/87



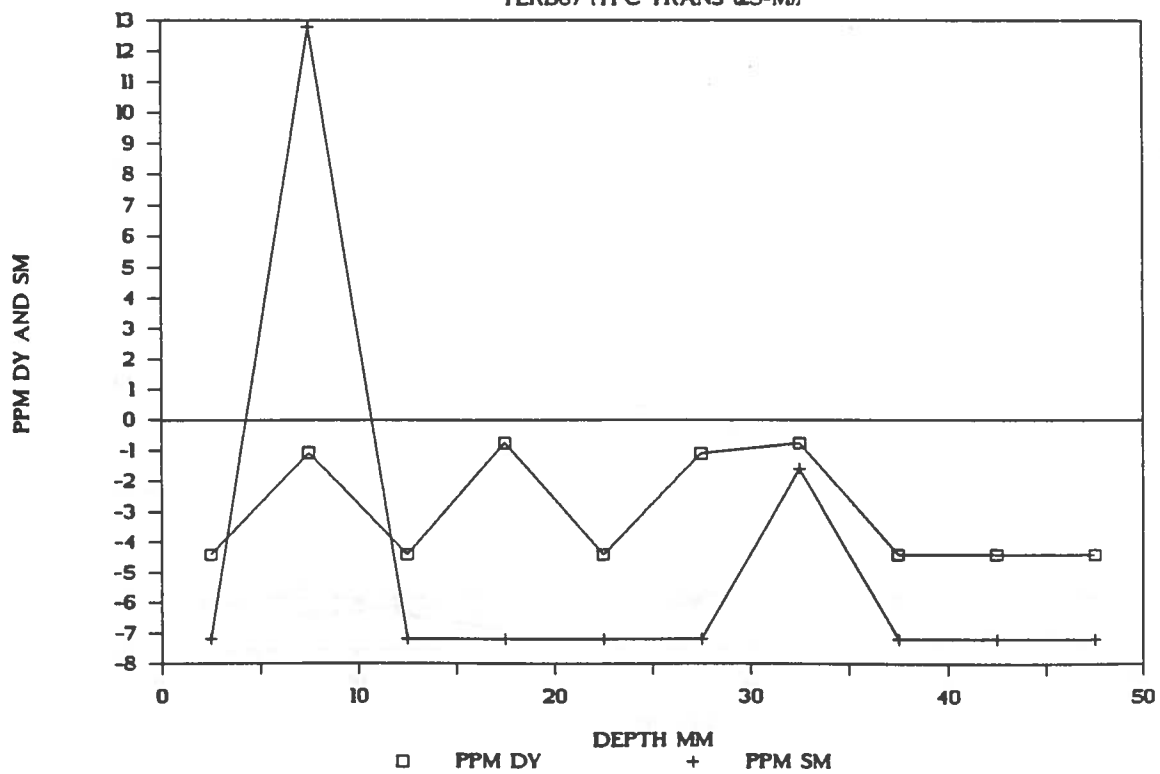
DISTRIBUTION OF DY & SM

TERB87 (TFC TRAN (0-M)) 6/24/87



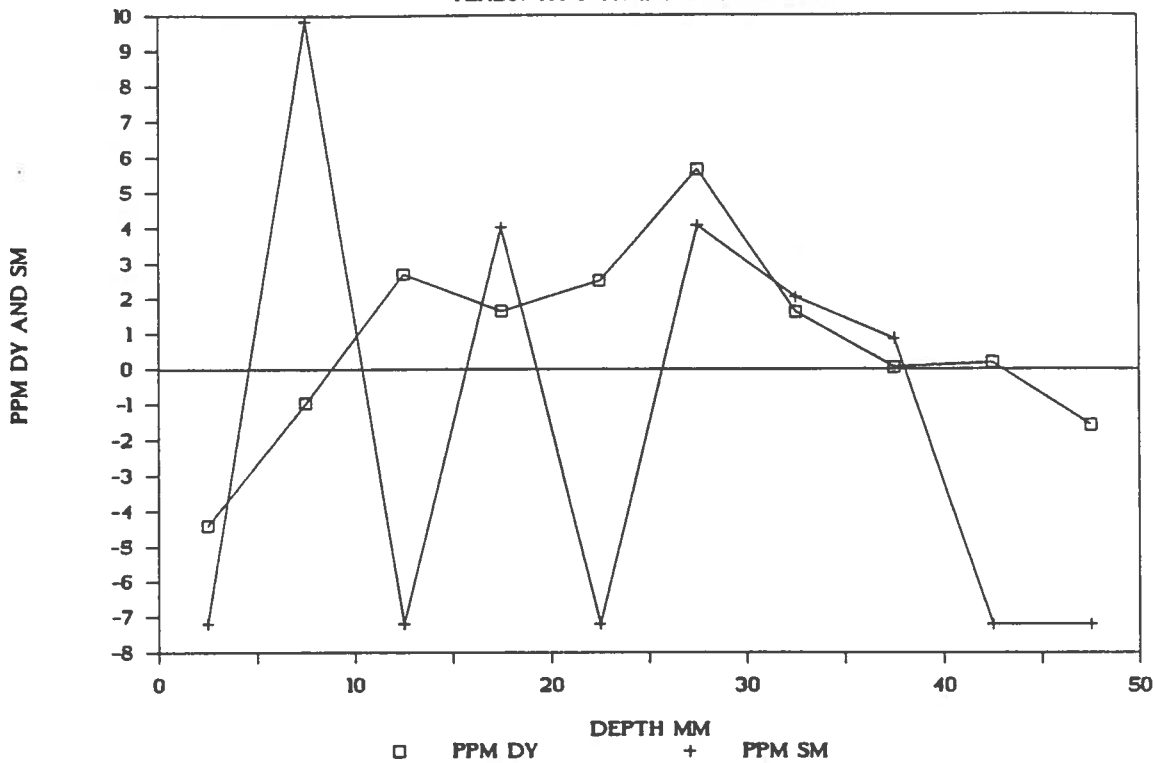
DISTRIBUTION OF DY & SM

TERB87 (TFC TRANS (25-M))



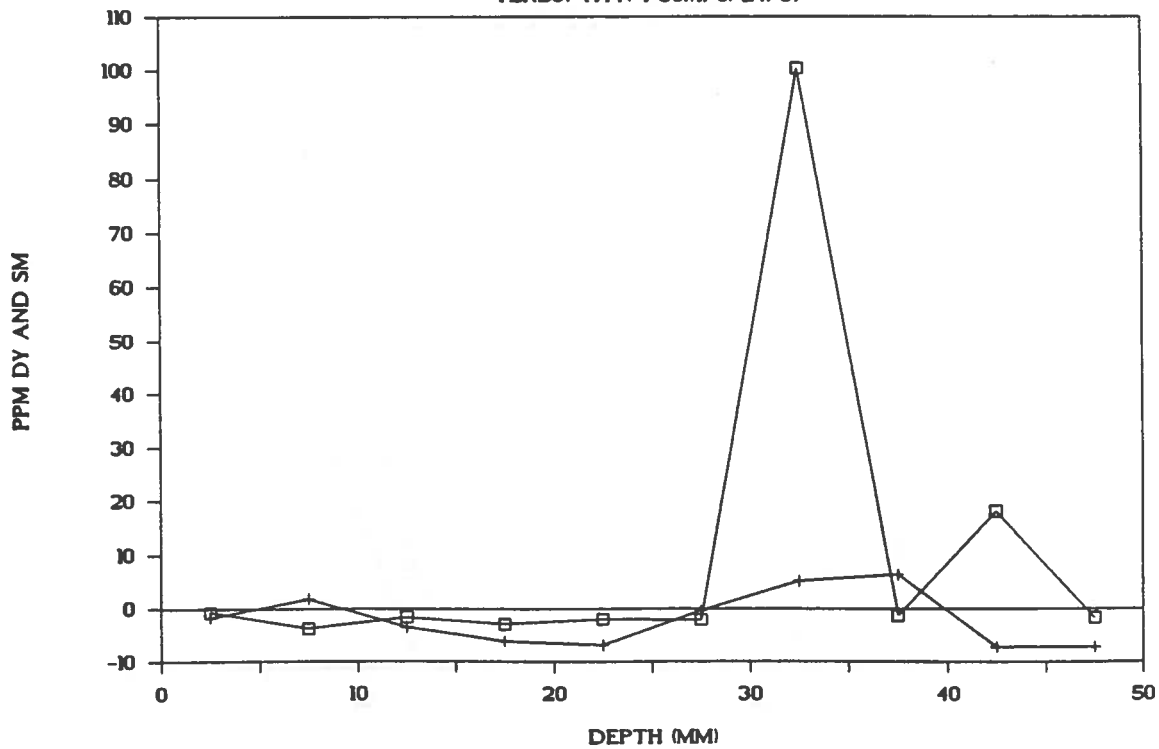
DISTRIBUTION OF DY & SM

TERB87 (TFC TRANS (50-M)) 6/24/87



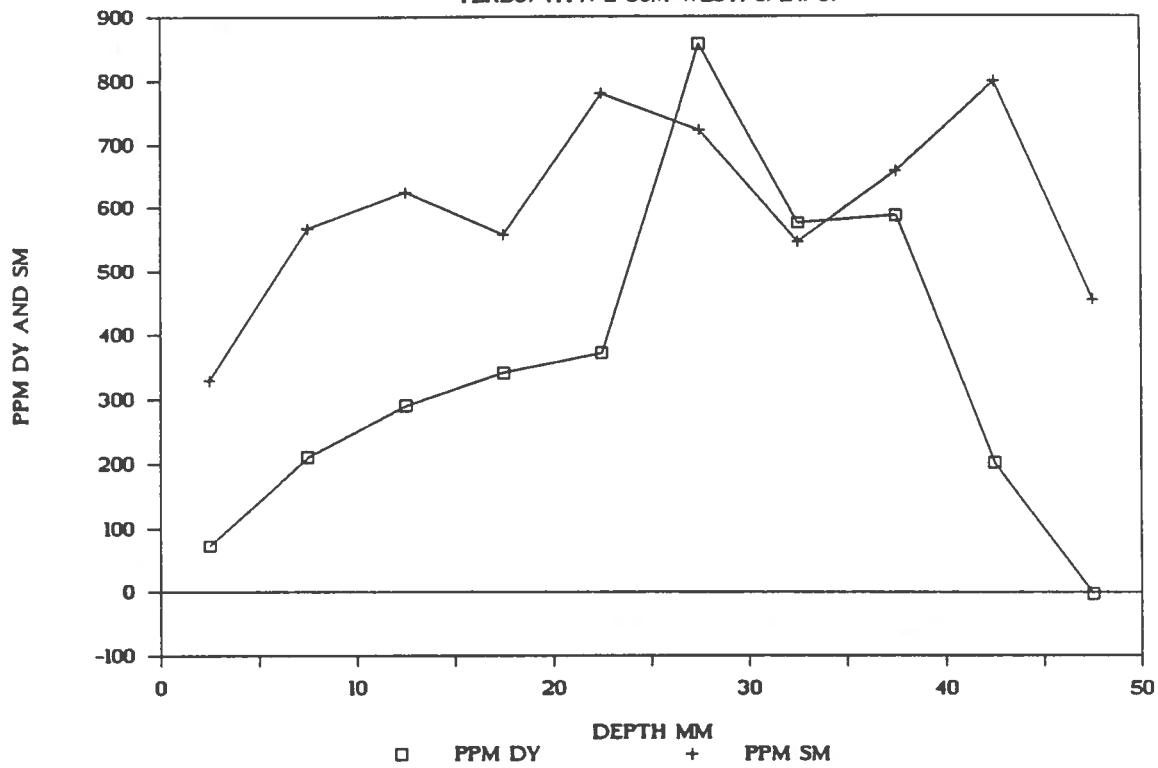
DISTRIBUTION OF DY & SM

TERB87 (TFN-1-50M) 6/24/87



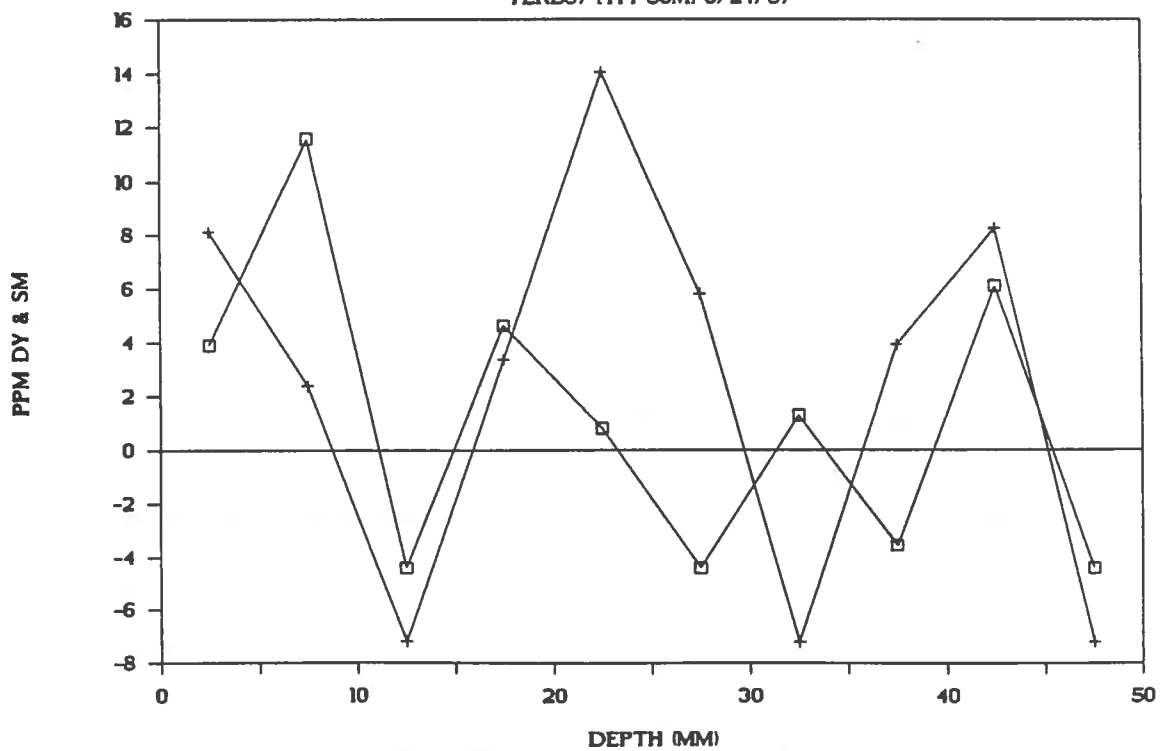
DISTRIBUTION OF DY & SM

TERB87 (TFN-2-50M WEST) 6/24/87



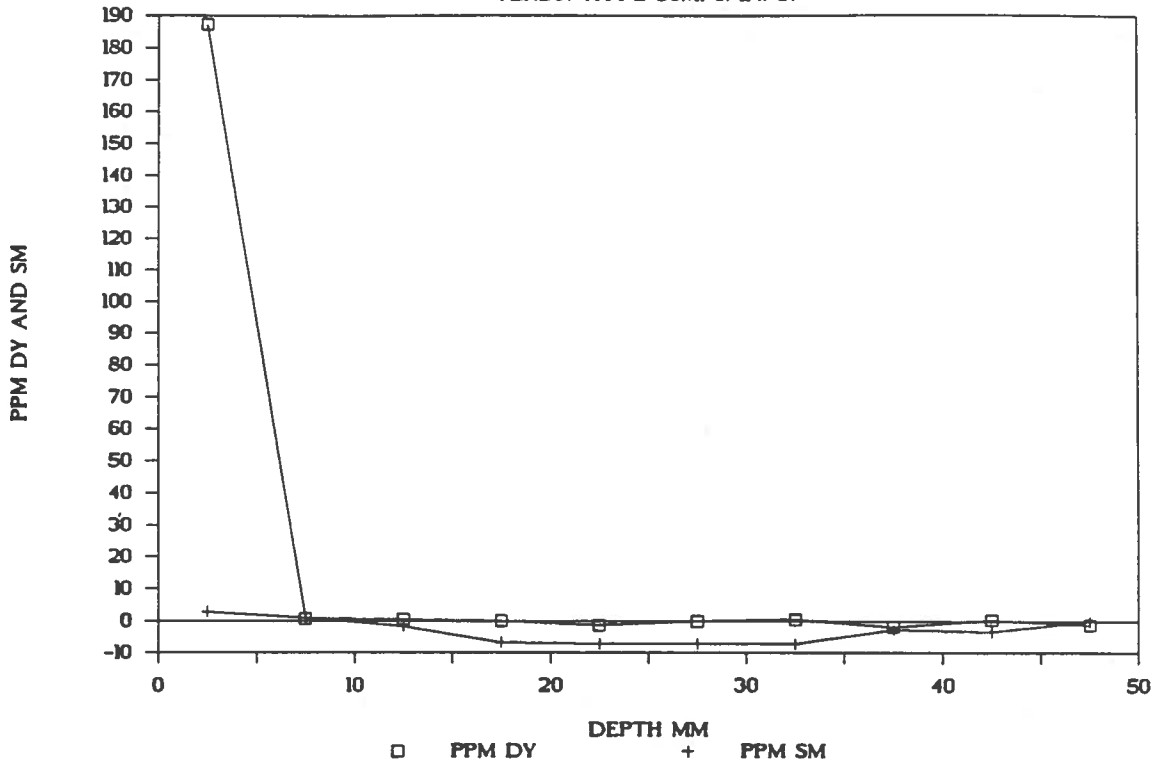
DISTRIBUTION OF DY & SM

TERB87 (TF1-50M) 6/24/87



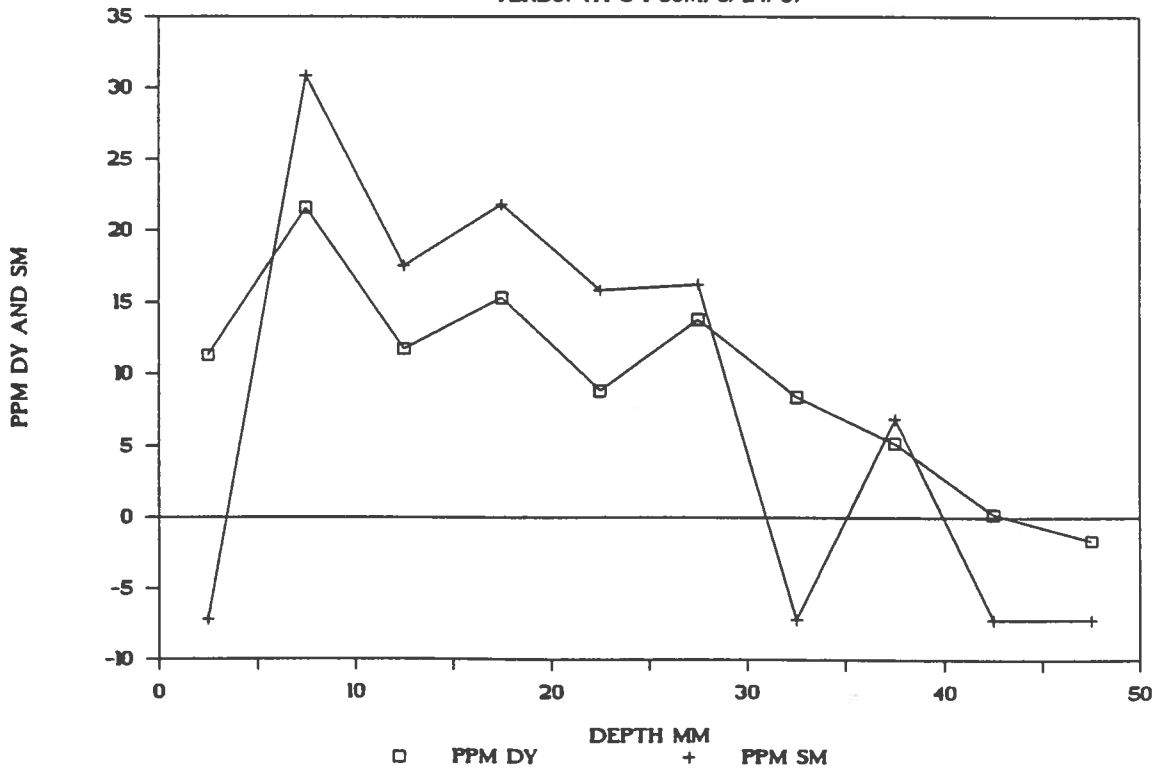
DISTRIBUTION OF DY & SM

TERB87 (TFI-2-50M) 6/24/87



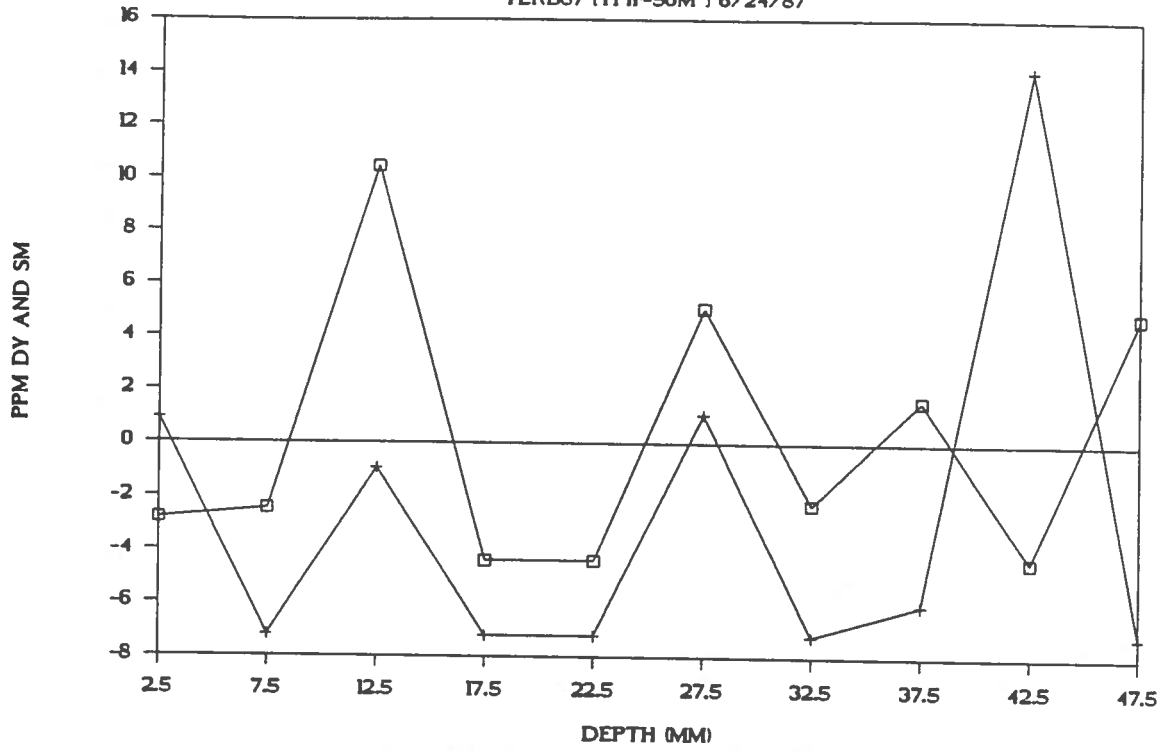
DISTRIBUTION OF DY & SM

TERB87 (TFC-1-50M) 6/24/87



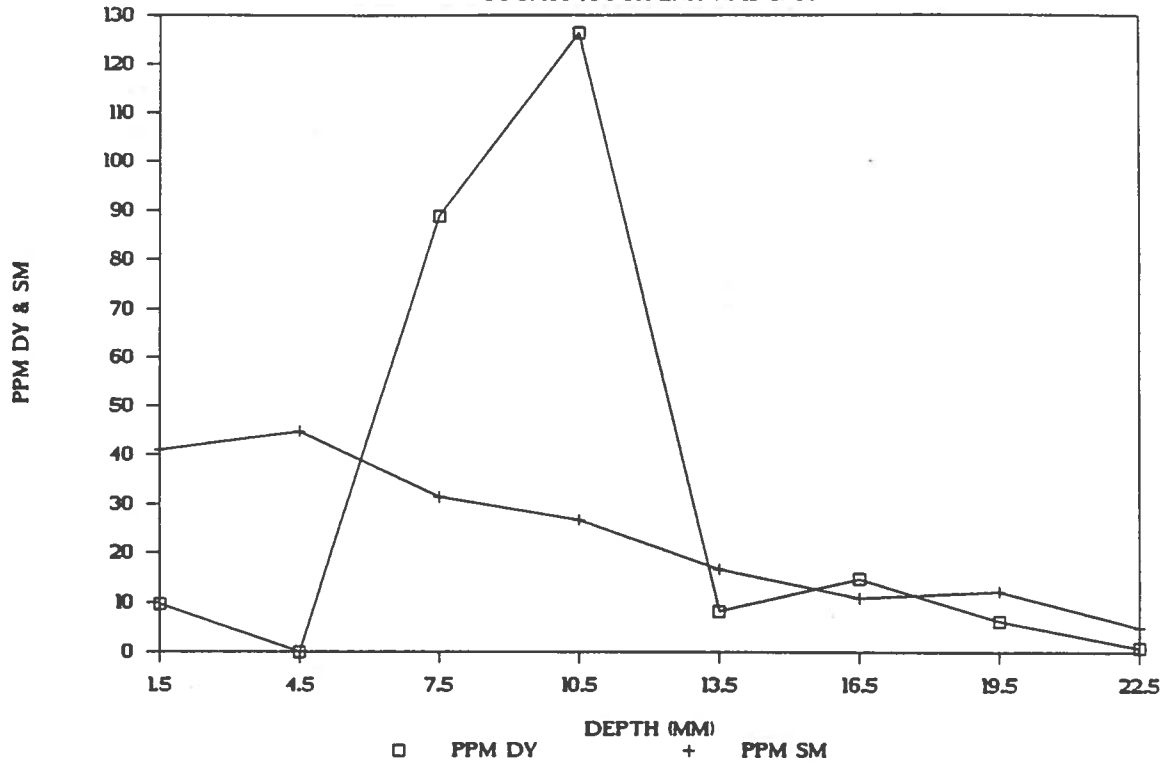
DISTRIBUTION OF DY & SM

TERB87 (TFir-50M) 6/24/87



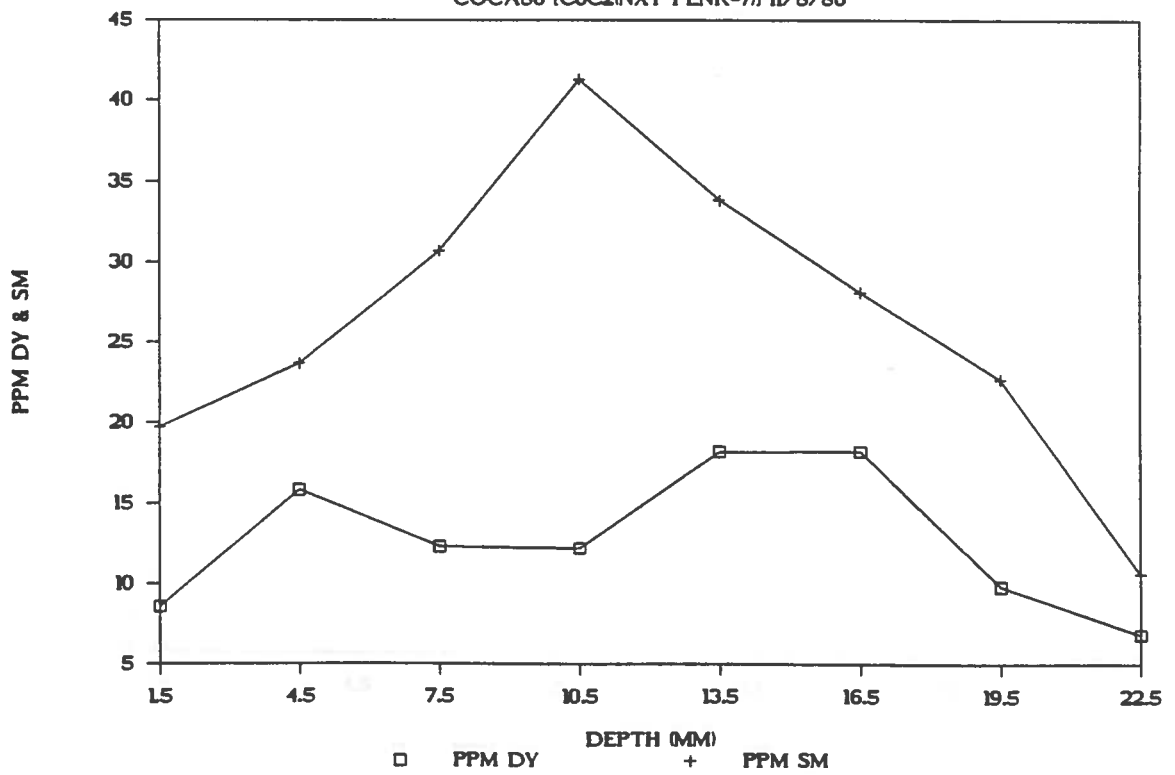
DISTRIBUTION OF DY & SM

COCA86 (COC1PLNK-7) 11/8/86



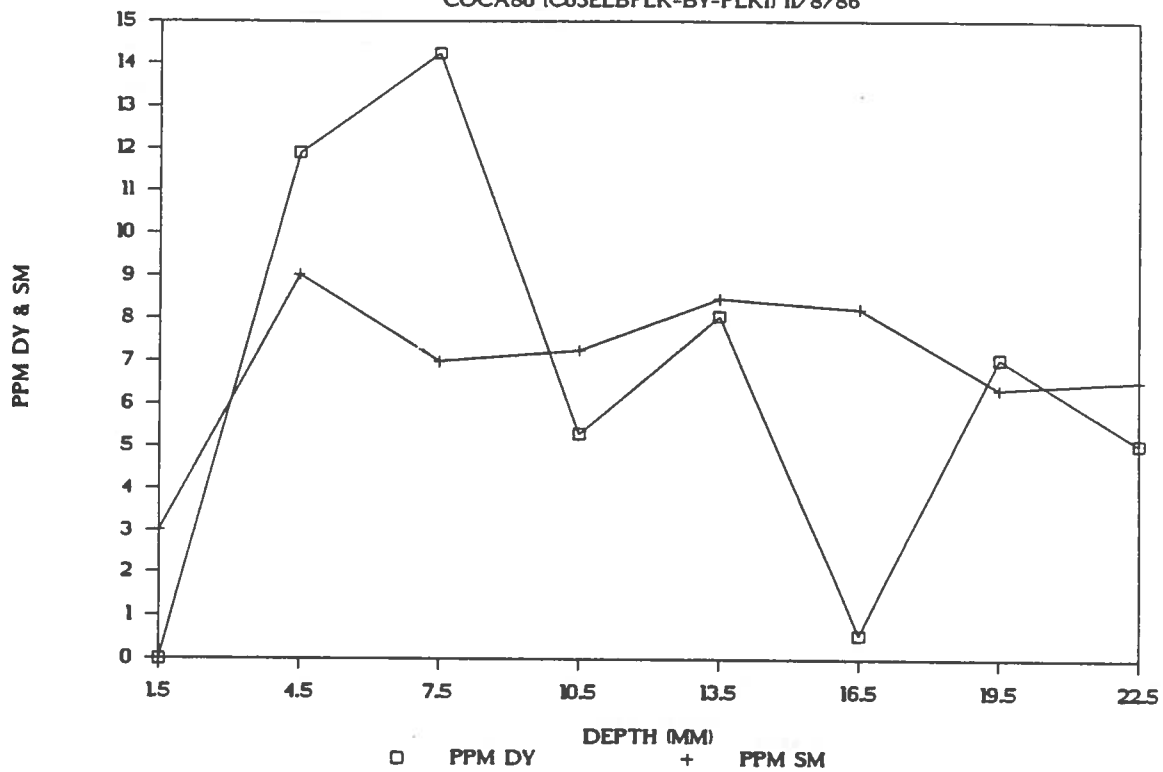
DISTRIBUTION OF DY & SM

COCA86 (COC2INXT PLNK-7) 11/8/86



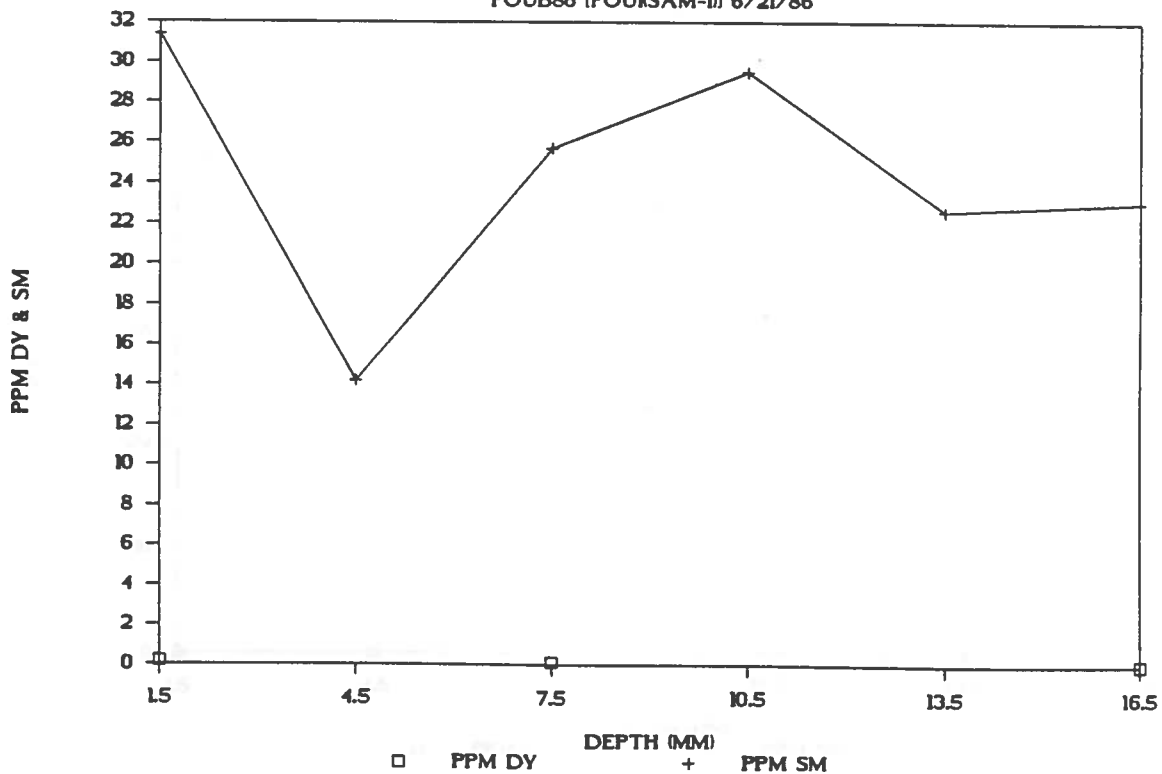
DISTRIBUTION OF DY & SM

COCA86 (C03ELBPLK-BY-PLK) 11/8/86



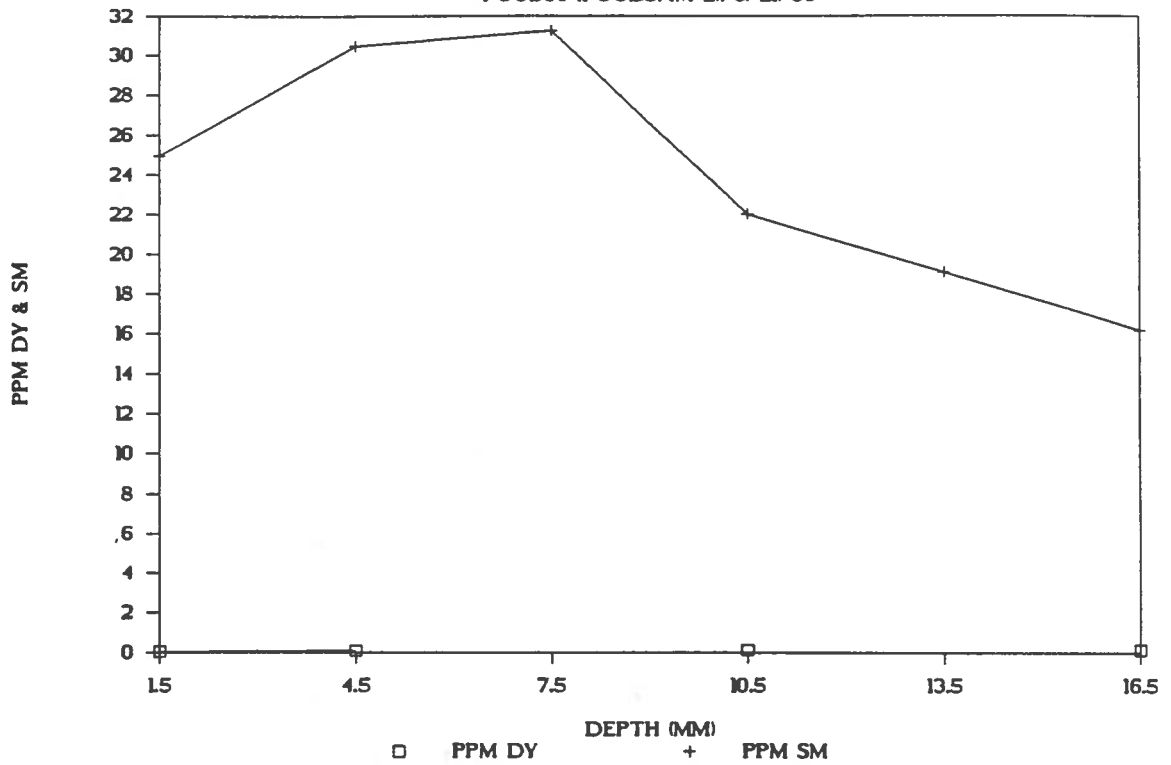
DISTRIBUTION OF DY & SM

FOUB86 (FOUKSAM-1) 6/21/86



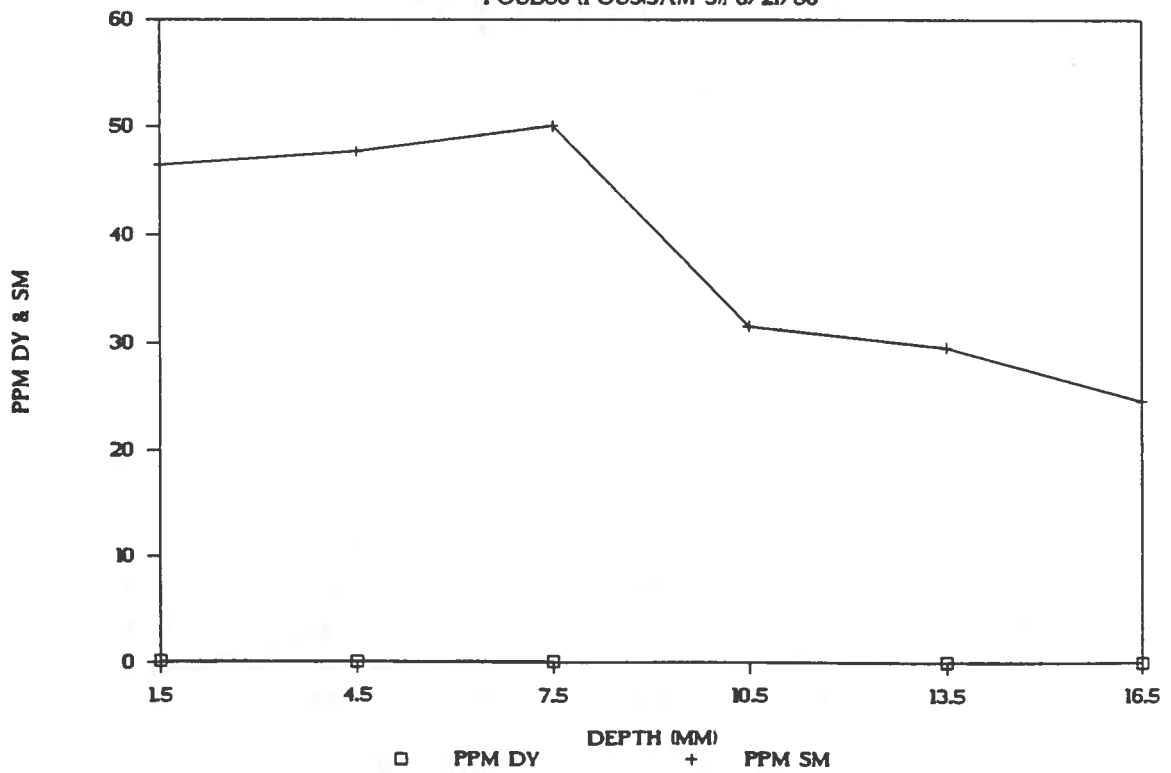
DISTRIBUTION OF DY & SM

FOUB86 (FOU2SAM-2) 6/21/86



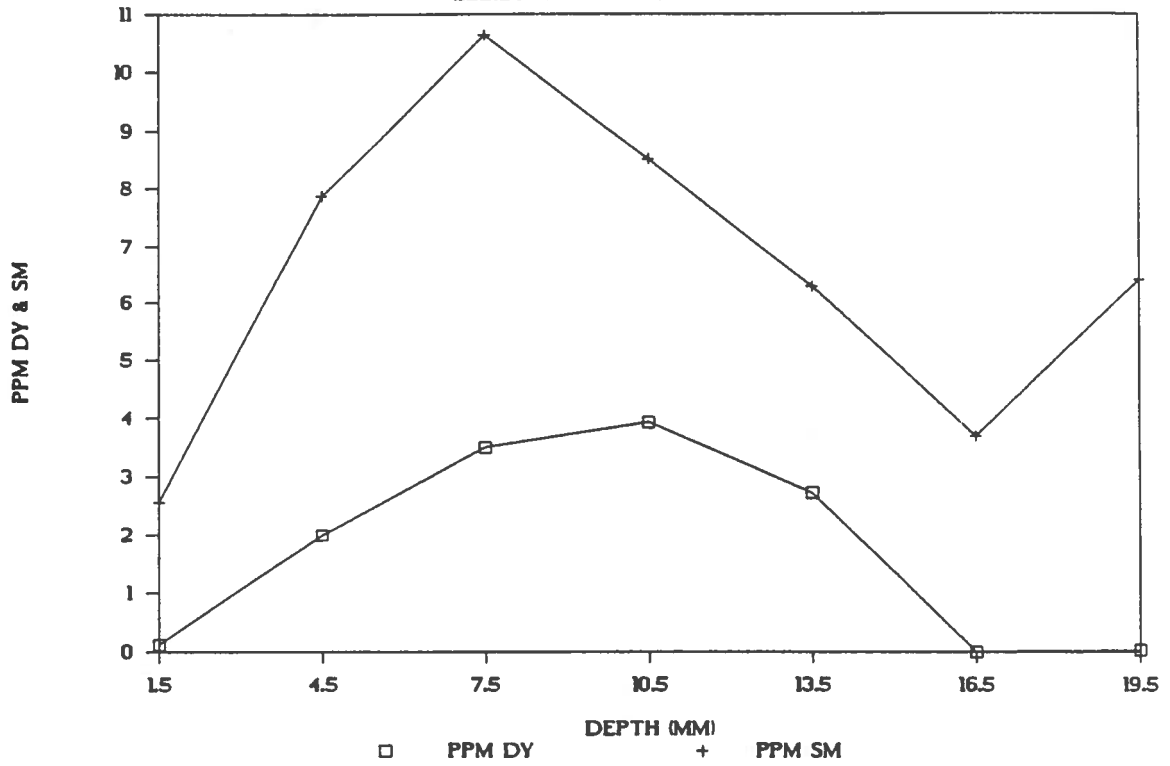
DISTRIBUTION OF DY & SM

FOUB86 (FOU3SAM-3) 6/21/86



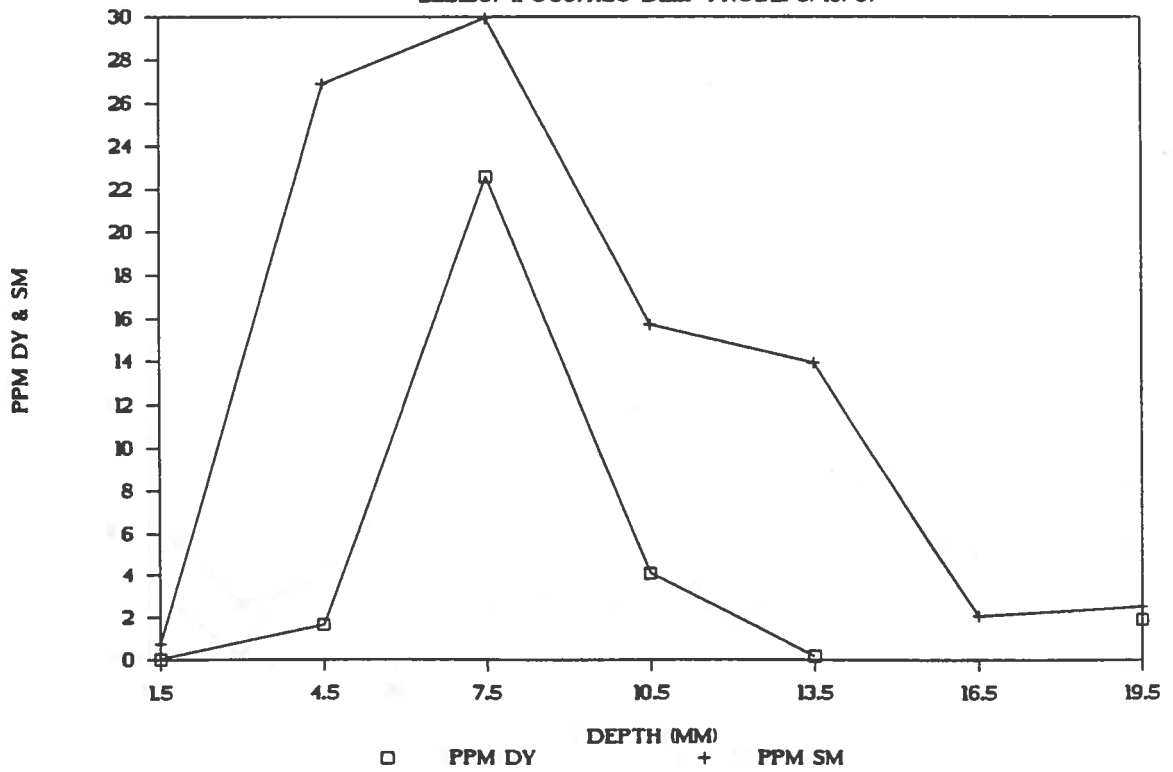
DISTRIBUTION OF DY & SM

LEE1B87 (FOU87EDG COL-2) 5/13/87



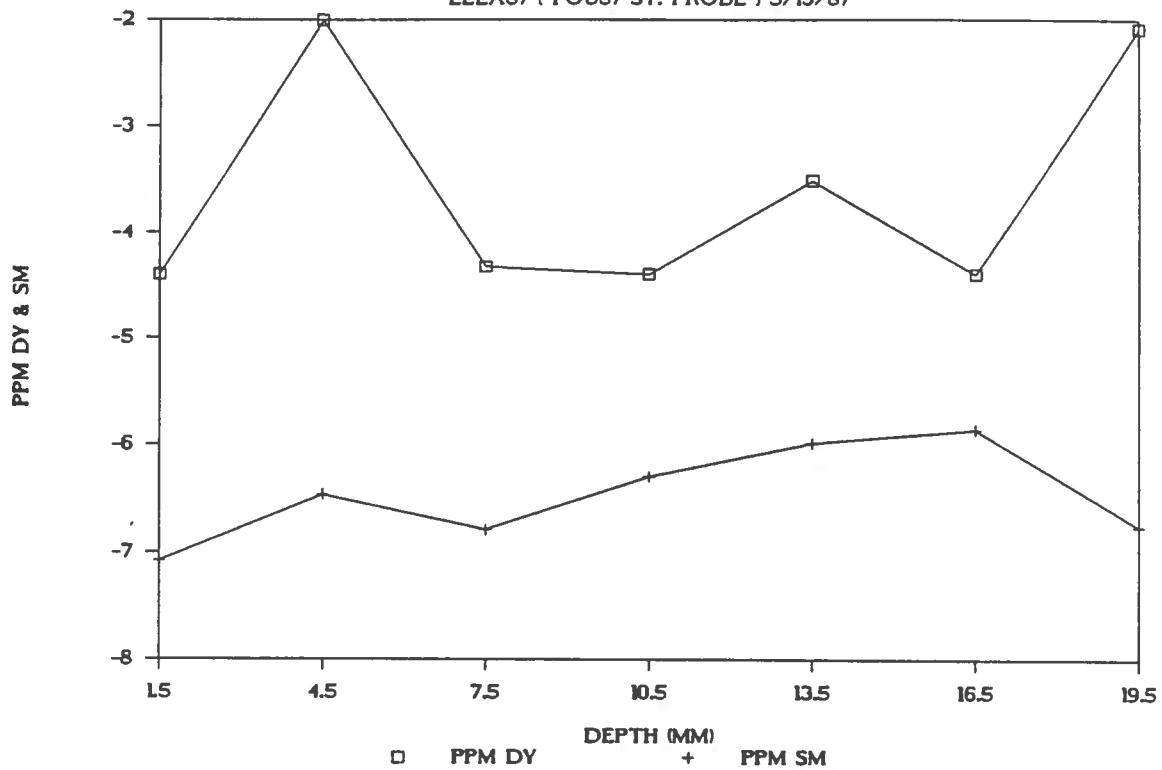
DISTRIBUTION OF DY & SM

LEE1B87 (FOU87H2O DEEP PROBE) 5/13/87



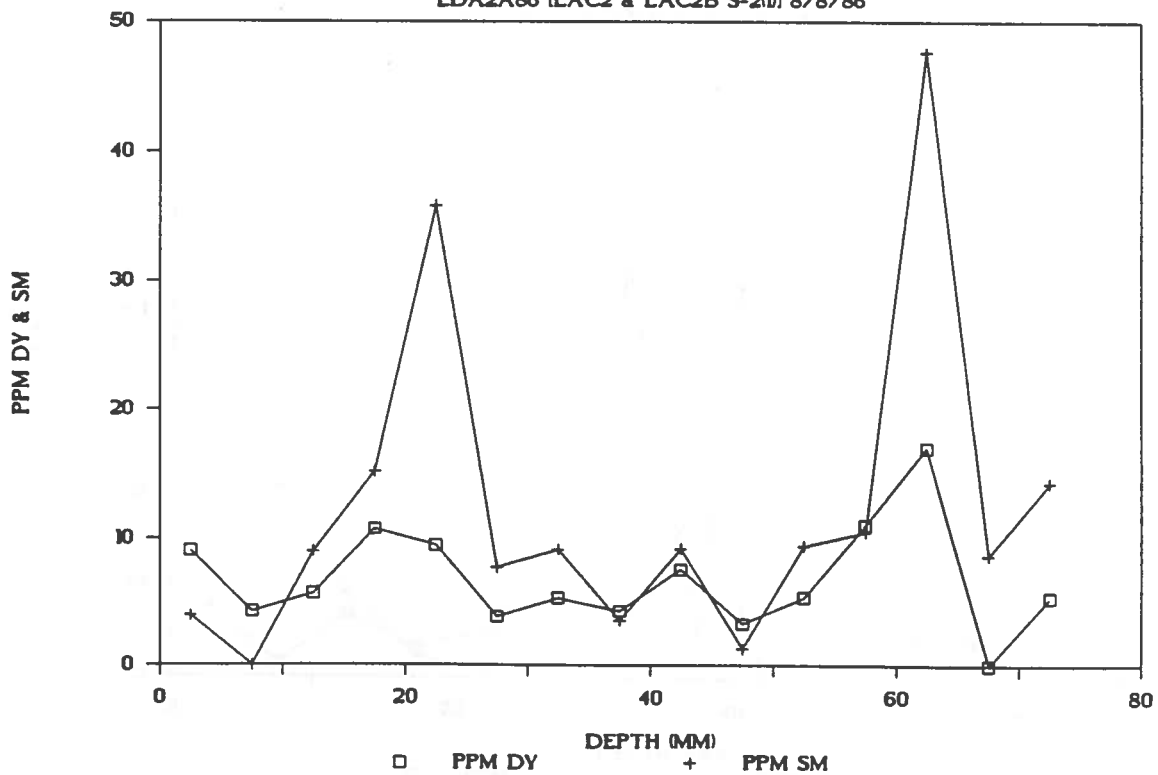
DISTRIBUTION OF DY & SM

LEEA87 (FOU87 ST. PROBE) 5/13/87



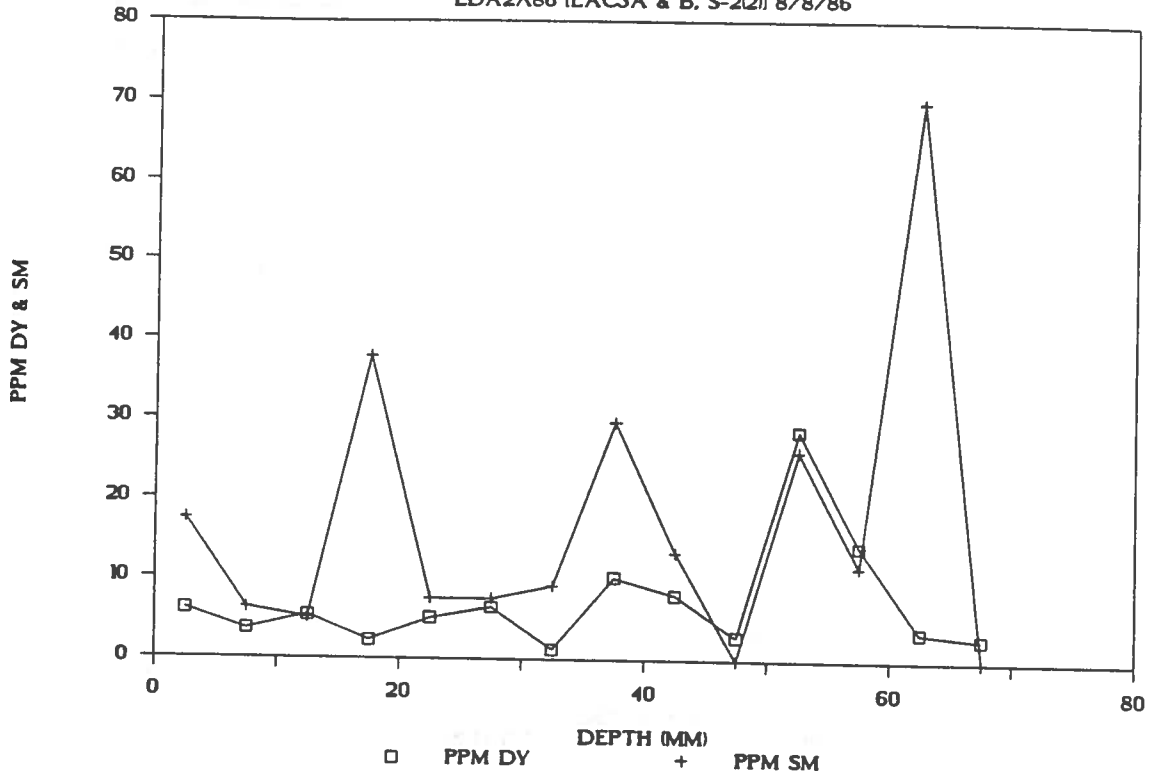
DISTRIBUTION OF DY & SM

LDA2A86 (LAC2 & LAC2B S-211) 8/8/86



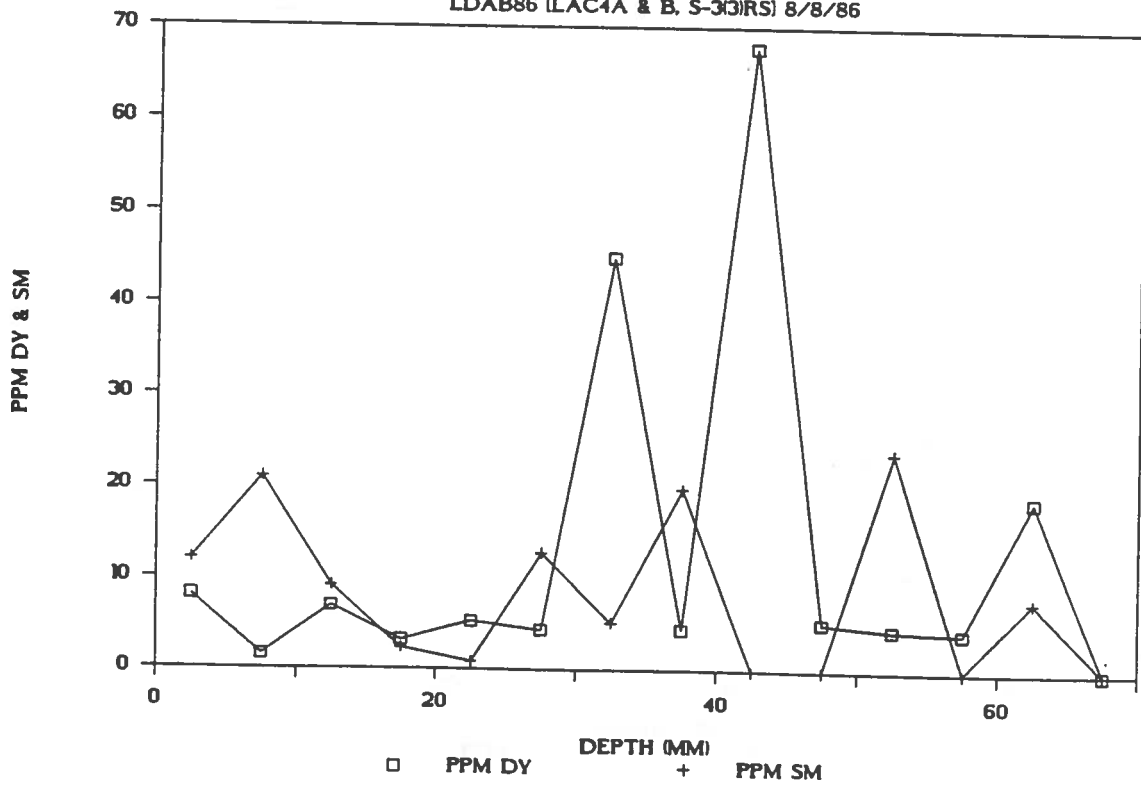
DISTRIBUTION OF DY & SM

LDA2A86 (LAC3A & B, S-22) 8/8/86



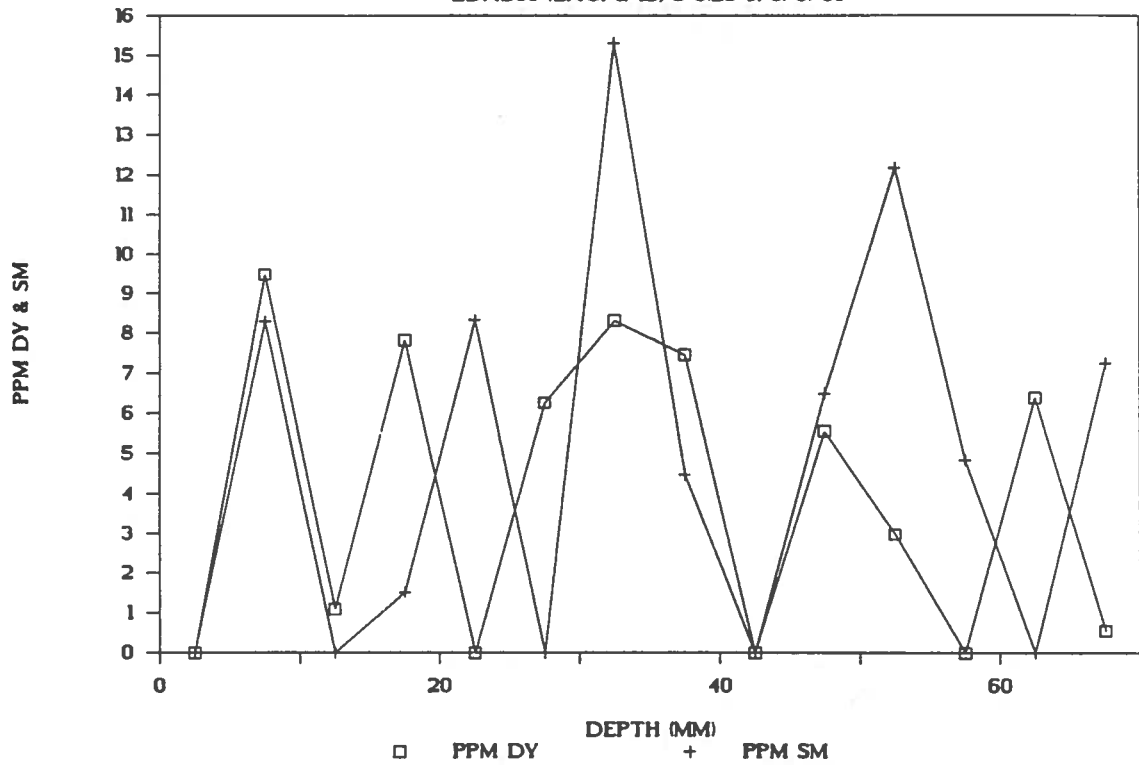
DISTRIBUTION OF DY & SM

LDAB86 (LAC4A & B, S-33RS) 8/8/86



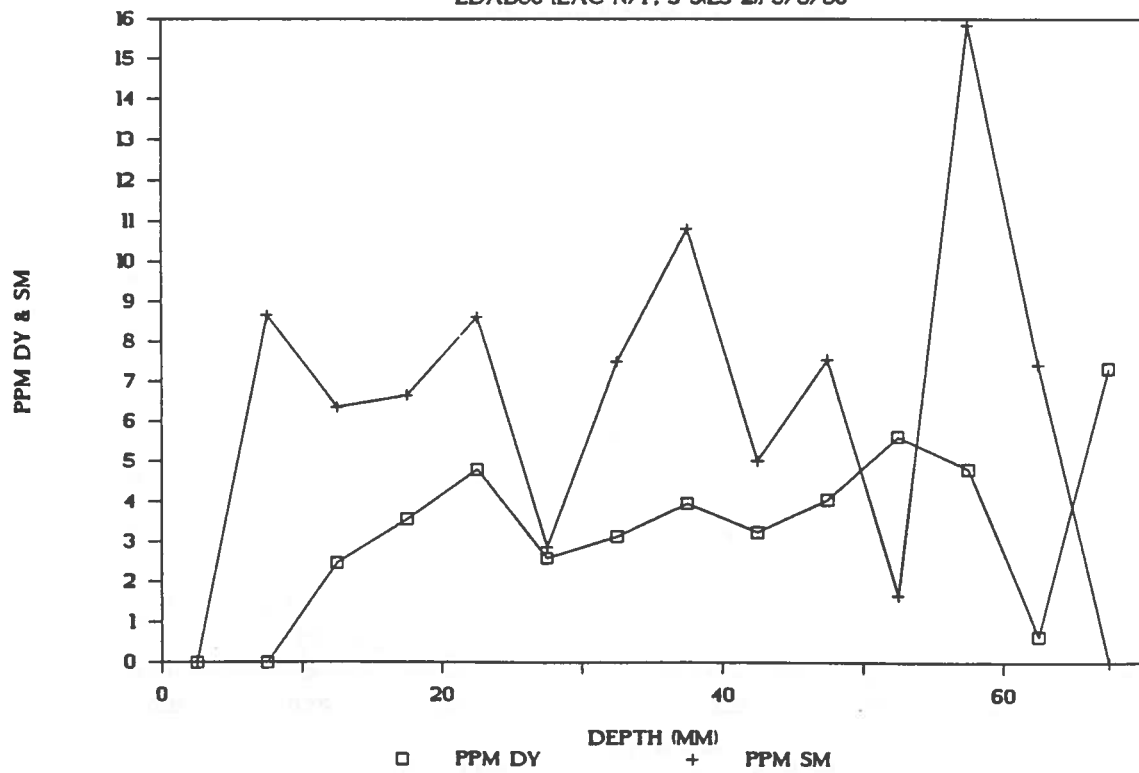
DISTRIBUTION OF DY & SM

LDAB86 (LAC1 & 1B, S-3(LS-1)) 8/8/86



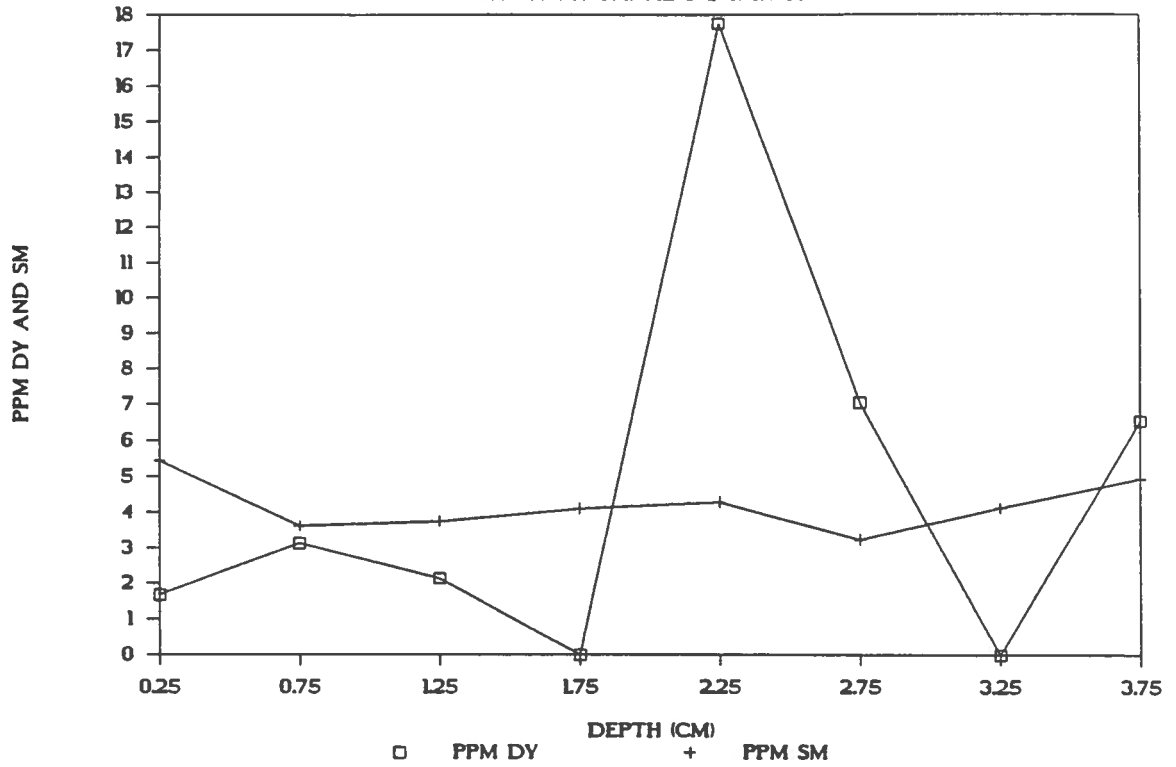
DISTRIBUTION OF DY & SM

LDAB86 (LAC N/F, S-3(LS-2)) 8/8/86



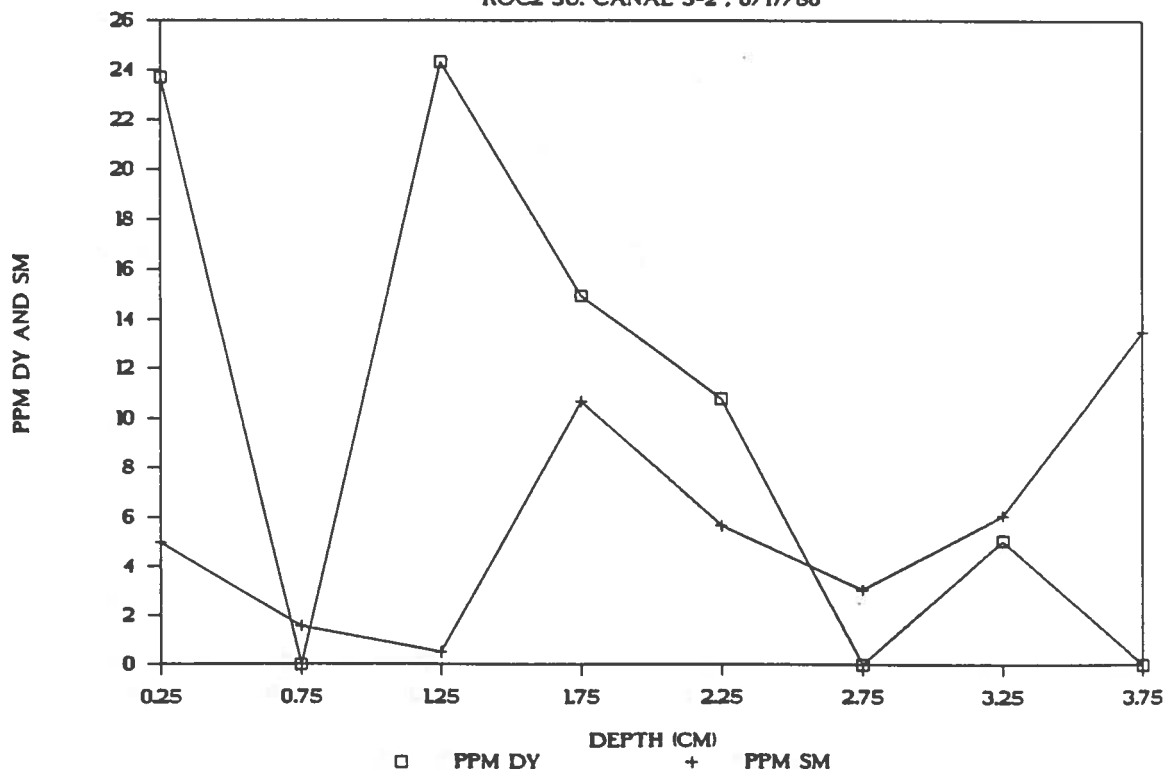
DISTRIBUTION OF DY & SM

ROC1 SU. CANAL S-1 6/17/86



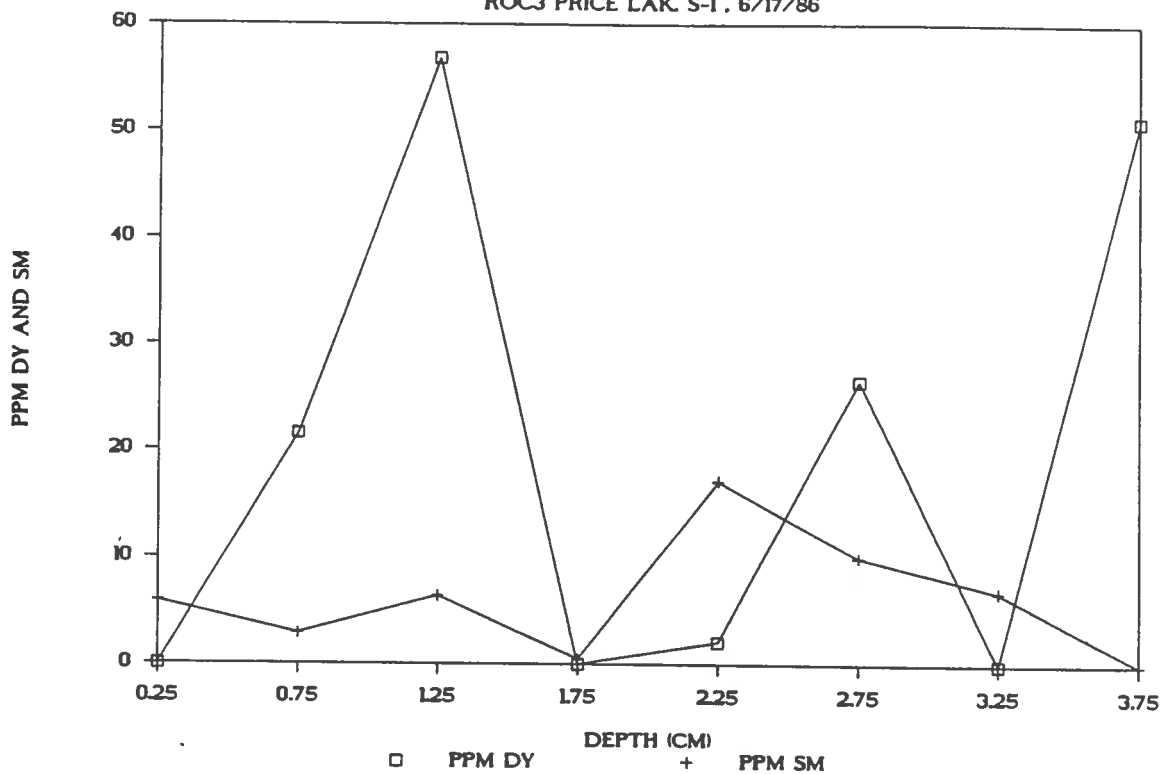
DISTRIBUTION OF DY & SM

ROC2 SU. CANAL S-2 . 6/17/86



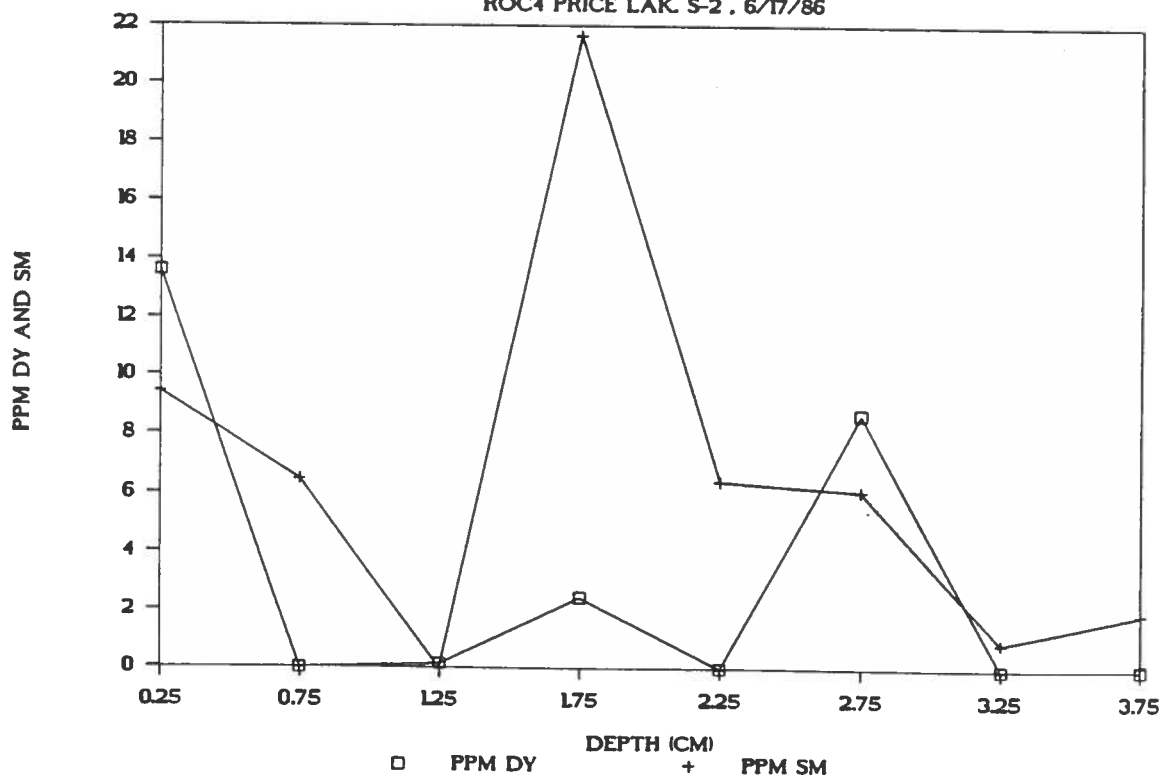
DISTRIBUTION OF DY & SM

ROC3 PRICE LAK. S-1 . 6/17/86

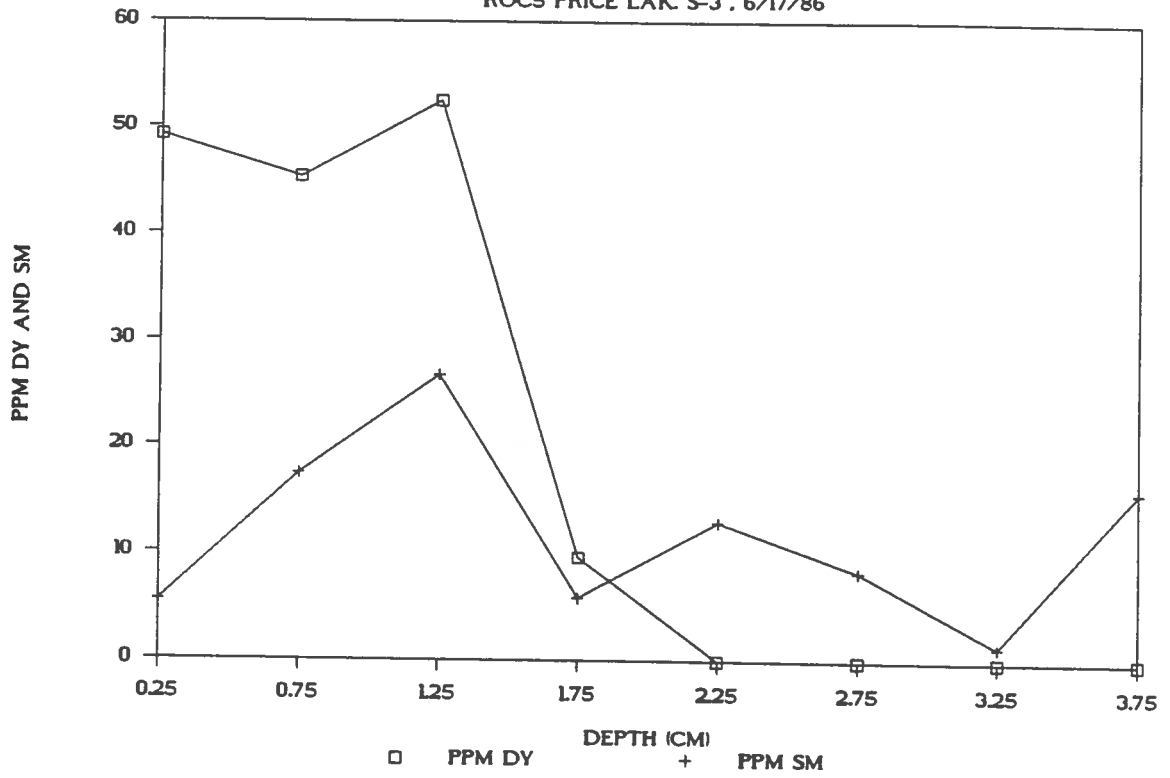


DISTRIBUTION OF DY & SM

ROC4 PRICE LAK. S-2 . 6/17/86



DISTRIBUTION OF DY & SM ROCS PRICE LAK. S-3, 6/17/86



APPENDIX B
COST ANALYSIS

Assuming that a plot size of 25 x 25 M is desired with a rare earth metal rate at 100 ug per square cm of both Dy and Sm, the total area covered would be 250,000 square cm and the amount of both rare earth oxides would be 50 gm each for a total of \$130.00 (1988). 80 ml of concentrated HCl @ \$1.00 would be required for dissolving both oxides. Assuming 35 polyvials (for neutron activation analysis) @ 20 cents apiece for a total of \$7.00 for ten samples (one core), and an average neutron activation analysis cost @ \$10.00 per sample, the grand total without labor is about \$238.00. Since the establishment of the site is a one-time expense, the cost of each core thereafter would be \$108.00. If reactor sharing is available, the researcher's funds are matched approximately 9:1 by the reactor sharing program. This would result in a cost per core of about \$11.00.

VITA

Daniel Lee Van Gent Jr., was born on August 9, 1956, in Scotia California, to Daniel L. Van Gent Sr., and Charolette Joy Van Gent. He attended highschool in Redding, California, and after graduation in 1974, enrolled in Shasta College in Redding, California, where he graduated with an A.A. Chemistry. He enrolled at U.C. Davis, California and graduated in 1980 with a B.S. Entomology. Daniel has worked with the U.S.D.A. as a Laboratory Technician II and with the University of California at Davis as a Research Assistant I. He is currently working at Los Alamos National Laboratory as a Staff Laboratory Research Assistant.

MASTER'S EXAMINATION AND THESIS REPORT


Candidate: Daniel L. Van Gent

Major Field: Nuclear Science

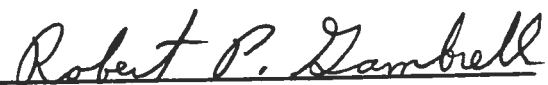
Title of Thesis: Rare-Earth Soil Horizon Markers to Determine the Short-Term Accretion in Louisiana Marshes

Approved:

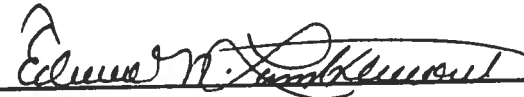

Major Professor and Chairman


Dean of the Graduate School

EXAMINING COMMITTEE:







Date of Examination:

April 12, 1988